Integrating Oxylipins into the 'Omics' Research Framework

by

Lucien GJ Cayer

A Thesis submitted to the Faculty of Graduate Studies of
The University of Manitoba
in partial fulfilment of the requirements of the degree of

Doctor of Philosophy

Department of Food and Human Nutritional Sciences
University of Manitoba
Winnipeg

Copyright © 2024 Lucien Cayer

Abstract

Oxylipins are a class of lipids encompassing the oxygenated metabolites of polyunsaturated fatty acids (PUFAs). As current biochemical analytical techniques have enabled the high-throughput quantification of whole profiles of oxylipins from biological samples, the interpretation of this data has posed a challenge to researchers. The studies presented here will consist of three different contexts in which oxylipin analysis was improved by integrating data layers from other *omics* analyses, clinical data, or oxylipins in other tissues. Specifically, multi-omics analysis of the hearts of rats orally exposed to the cardiotoxic food contaminant 2-monochloropropane-1,3-diol (2-MCPD) identified upregulation of immune response pathways and downregulation of energy metabolism and cardiac function. The inflammatory nature of 2-MCPD-induced cardiotoxicity included the suppression of anti-inflammatory docosahexaenoic acid (DHA)-derived oxylipins. The integration of the oxylipin data with transcriptomic data elucidated the suppression of DHA oxylipins by identifying dysregulation of secreted phospholipase A2, which has substrate preference for DHA. In another analysis rats were exposed to 2-MCPD with and without adequate dietary α-linolenic acid (ALA), the essential dietary n-3 PUFA. This study demonstrated that dietary ALA modulated oxylipins, enhancing n-3 PUFA-derived oxylipins in the heart, liver, kidney, and serum, while 2-MCPD exposure elevated pro-inflammatory arachidonic acid-derived oxylipins in heart and possibly liver. Adequate ALA revealed 2-MCPD exposure reduced cardiac DHA oxylipins, not apparent in the ALA-deficient diet. Integration of the oxylipin profiles across tissues identified 13-hydroxy-octadecatrienoic acid-γ (13-HOTrE-γ) as the top contributor to the distinct oxylipin profiles induced by 2-MCPD exposure, thus highlighting 13-HOTrE-γ's association with 2-MCPD exposure across tissues. The final study analyzed valvular and plasma oxylipins from patients with severe calcific aortic valve stenosis (AVS). Valvular oxylipins were found to be broadly increased with AVS severity. The integration of the oxylipin data with clinical data, which included AVS risk factors, made for a more robust model by controlling for these factors, and enabled the identification of specific associations of arachidonic acid derived prostanoids with AVS severity markers. These studies contribute to the molecular understanding of lipid

metabolism pathways altered by toxic exposure, diet, and disease, as well as providing a framework for integration of oxylipins into the *omics* framework.

Acknowledgements

I am deeply grateful to my supervisors: Dr. Aukema and Dr. Karakach, whose expertise, guidance, and devotion, were essential to this process. Their willingness to give their time so generously has been invaluable to my development as a researcher. Special thanks also to my committee members: Dr. Raju and Dr. Ravandi, for their insightful guidance and dedication to these projects.

I would also like to thank Tanja, our dedicated lab technician, whose expertise and assistance was always available. Additionally, I am grateful to my lab mates in both the Aukema and Karakach labs, whose camaraderie and feedback have enhanced my work as well as made it more enjoyable.

My appreciation extends to the support staff in the Department of Food and Human Nutritional Sciences, for their unwavering support and services over the years.

I am immensely thankful for the support of my family. Particularly, my parents who always encouraged me and instilled the values that enabled me to reach this point in my academic career. Most of all, my heartfelt thanks go to my wife, Ronna, whose love, support, and understanding have been essential during this challenging journey.

Thanks are also due to The University of Manitoba and NSERC for their financial support during my studies, and to St. Boniface Hospital Research for the access to their facilities and resources.

Dedication

To Glenn and Robin,

Although you will never read this, you were foundational in making this happen.

To Ben,

You are now the reason for everything I strive to achieve.

Thesis Outline

This thesis was prepared in a grouped manuscript format. The introduction, literature review, rationale, hypotheses, and objectives are followed by three chapters (Chapters 3-5) each comprised of separate manuscripts. Chapter 3 is **Study A: An integrated multi-omics analysis of the effects of the food processing-induced contaminant 2-monochloropropane-1,3-diol (2-MCPD) in rat heart**. Chapter 4 is **Study B: Increased cardiac oxylipins in response to 2-monochloropropane-1,3-diol exposure are partially ameliorated by dietary adequacy of the essential n-3 fatty acid, α-linolenic acid**. Chapter 5 is **Study C: Valvular prostaglandins are elevated in severe human aortic valve stenosis**. Finally, this thesis concludes with an overall discussion, then references, followed by the appendices which contain the supplemental materials for each manuscript.

Author Contributions

Lucien GJ Cayer was the primary author of this thesis. For the multi-authored papers presented below, each of the authors' contributions have been described below.

Study A: An integrated multi-omics analysis of the effects of the food processing-induced contaminant 2-monochloropropane-1,3-diol (2-MCPD) in rat heart.

Authors: Lucien GJ Cayer, Thorsten Buhrke, Katharina Sommerkorn, Anna Reinhold, Jennifer Roberts, Albert Braeuning, Jayadev Raju, Harold M Aukema, Tobias Karakach.

For this manuscript, the animal feeding, tissue collection, next generation RNA sequencing (RNA-seq), and quantitative polymerase chain reaction (qPCR) was conducted by Jayadev Raju and Jennifer Roberts from the Food Directorate, Health Canada. For additional documentation regarding the relationship with Health Canada see Appendix 1. The measurement of proteins by 2D-gel electrophoresis for by mass spectrometry (MS) was conducted by Thorsten Buhrke, Katharina Sommerkorn, Anna Reinhold, and Albert Braeuning. The oxylipin and oxidized phosphatidylcholine (OxPC) analysis was conducted by Lucien GJ Cayer and previously reported in (Cayer, 2019). Lucien GJ Cayer conceptualized the framework for the manuscript. From the data generated by each of these procedures, Lucien GJ Cayer performed all data analyses, with guidance from Tobias Karakach. The interpretation of the results was conducted by Lucien GJ Cayer. The manuscript was written primarily by Lucien GJ Cayer, with contributions from Thorsten Buhrke, Jayadev Raju, Harold M Aukema, and Tobias Karakach. The docosahexaenoic acid oxylipin synthesis diagram used to produce Figure 3.5 in Cytoscape was created from an original WikiPathways entry that Lucien GJ Cayer created. Not included in the manuscript are the other WikiPathways original contributions authored by Lucien GJ Cayer and intended for this project (see Appendix 2).

Study B: Increased cardiac oxylipins in response to 2-monochloropropane-1,3-diol exposure are partially ameliorated by dietary adequacy of the essential n-3 fatty acid, α-linolenic acid.

Authors: Lucien GJ Cayer, Tobias Karakach, Jennifer Roberts, Stephen PJ Brooks, Jayadev Raju, Harold M Aukema.

For this manuscript, the experimental groups included were a subset of the original experimental design primarily formulated by Jayadev Raju and Stephen PJ Brooks, with contributions regarding the ALA groups and the ALA diet formulations from Lucien GJ Cayer and Harold M Aukema. For additional documentation regarding the relationship with Health Canada see Appendix 1. The animal feeding and tissue collection was done by Jayadev Raju, Jennifer Roberts, and Stephen PJ Brooks. The oxylipin extraction and quantification of all tissues was performed by Lucien GJ Cayer. The oxylipin data analysis and interpretation was primarily done by Lucien GJ Cayer, with the guidance of Harold M Aukema and Tobias Karakach. The manuscript was primarily written by Lucien GJ Cayer, with contributions form Harold M Aukema, Tobias Karakach, and Jayadev Raju.

Study C: Valvular prostaglandins are elevated in severe human aortic valve stenosis.

Authors: Lucien GJ Cayer, Arun Surendran, Tobias Karakach, Harold M Aukema, Amir Ravandi.

For this manuscript, the design of the study and the attainment of samples was performed by Amir Ravandi and Arun Surendran. Lucien GJ Cayer conducted the method development to homogenize calcified aortic valves for oxylipin extraction, followed by the oxylipin extraction and quantification. The data analysis and manuscript writing were primarily conducted by Lucien GJ Cayer, with input from Amir Ravandi, Tobias Karakach, and Harold M Aukema.

Table of Contents

Abstract i
Acknowledgements iii
Dedication iv
Thesis Outline v
Author Contributions vi
Table of Contents viii
List of Tables xii
List of Figures xiv
List of Abbreviations xvi
Introduction 1
Chapter 1: Literature Review 5
1.1. Multivariate statistics 5
1.2. Web-based bioinformatics applications 6
1.3. Oxylipins 7
1.3.1. Oxylipins in health and disease 8
1.3.2. Analytical methodology 10
1.4. 2-MCPD toxicology 11
1.4.1. 2-MCPD exposure: Genetic and protein level changes 13
1.4.2. 2-MCPD exposure: Oxylipins and n-3 adequacy 14
1.4.3. New approach methodologies (NAMs) 16
1.5. Aortic Valve Stenosis 18
1.5.1. Aortic Valve Stenosis and oxylipins 19
1.6. References 22
Chapter 2: Rationale, Hypotheses, and Objectives 37
2.1. Rationale 37
2.2. Hypotheses 40
2.3. Objectives 41
2.4. Chapter Transition 42
Chapter 3: Study A: An integrated multi-omics analysis of the effects of the food processing-induced contaminant 2-monochloropropane-1,3-diol (2-MCPD) in rat heart 43

3.1. Abstract 44
3.2. Introduction 45
3.3. Materials and Methods 46
3.3.1. Animals and experimental design 46
3.3.2. Next-Generation RNA Sequencing 47
3.3.3. Quantitative PCR 47
3.3.4. Proteomic analysis 47
3.3.5. Targeted lipidomic analysis 48
3.3.6. Statistical analyses 48
3.4. Results 49
3.4.1. Transcriptomic analysis 49
3.4.2. Quantitative PCR panel 51
3.4.3. Proteomic analysis 54
3.4.4. Differential expression of oxylipin metabolism genes 56
3.4.5. Targeted lipidomic analysis 57
3.5. Discussion 59
3.6. Conclusions 63
3.7. Chapter Transition 64
Chapter 4: Study B: Increased cardiac oxylipins in response to 2-monochloropropane-1,3-diol exposure are partially ameliorated by dietary adequacy of the essential n-3 fatty acid, α-linolenic acid 65
4.1. Abstract 66
4.2. Introduction 67
4.3. Materials and Methods 68
4.3.1. Animals and experimental design 68
4.3.2. Oxylipin analyses 69
4.3.3. Statistical analyses 70
4.4. Results 71
4.4.1. Heart 71
4.4.2. Liver 73
4.4.3. Kidney 74

4.4.4. Serum 77
4.4.5. Multi-tissue analysis: P-integration 79
4.5. Discussion 81
4.6. Conclusion 83
4.7. Chapter Transition 84
Chapter 5: Study C: Valvular prostaglandins are elevated in severe human aortic valve stenosis 85
5.1. Abstract 86
5.2. Introduction 89
5.3. Methods 91
5.3.1. Human aortic valve tissue 91
5.3.2. Oxylipin extraction and quantification 91
5.3.3. Data analyses 92
5.4. Results 93
5.4.1. Patient characteristics 93
5.4.2. Valvular oxylipins 97
5.4.3. Valvular oxylipins and clinical parameters 102
5.4.4. Plasma oxylipins 106
5.5. Discussion 108
5.6. Article Information 113
5.6.1. Acknowledgements 113
5.6.2. Sources of Funding 114
Chapter 6: Discussion 115
6.1. Overall Discussion 115
6.2. Strengths & Limitations 118
Chapter 7: References 124
Appendices 148
1. Linkage to Health Canada's Projects on 2-Monochloro-1-3, propanediol (2-MCPD) 149
2. Oxylipin Synthesis Pathway Diagrams 151
3. Study A: Supplemental Tables 156
4. Study A: Supplemental Figures 188

5. Study B: Supplemental Tables 204
6. Study C: Supplemental Tables 228
LLOD and ULOD values were determined using 40 µL on the column of standards in 236
7. Study C: Supplemental Figures 259

List of Tables

Table 3.1. Comparison of qPCR array and RNA-seq results on genes with FDR < 0.05 in either analysis, sorted by qPCR LFC. 53
Table 3.2. Oxylipin metabolism DEGs from RNA-seq analysis of rat heart. 57
Table 3.3. List of differentially expressed oxylipins in the male rat heart exposed to 2-MCPD for 90-days. 58
Table 5.1. Patient characteristics for AV oxylipin analysis 94
Table 5.2. Shared Patient Characteristics for Plasma Analysis 96
Table 5.3. Effect of Clinical Parameters and Oxylipins on Aortic Valve Mean Transvalvular Gradient 105
Study A: Supplemental Table 1. RNA-seq rat heart DEGs with 40 mg/kg BW/d 2-MCPD exposure. 156
Study A: Supplemental Table 2. Gene set enrichment analysis: Gene Ontology top activated and suppressed biological processes in rat heart with 40 mg/kg BW/d 2-MCPD exposure. 168
Study A: Supplemental Table 3. Gene set enrichment analysis: Gene Ontology fibroblast related biological processes in rat heart with 40 mg/kg BW/d 2-MCPD exposure. 170
Study A: Supplemental Table 4. Rat heart oxidative stress qPCR panel. 171
Study A: Supplemental Table 5. Identified rat heart proteins expression. 174
Study A: Supplemental Table 6. Oxylipin metabolism related genes. 181
Study A: Supplemental Table 7. Rat heart oxylipin expression with 40 mg/kg BW/d 2-MCPD exposure. 183
Study A: Supplemental Table 8. Rat heart oxidized phosphatidylcholine expression with 40 mg/kg BW/d 2-MCPD exposure. 187
Study B: Supplemental Table 1. Rat heart oxylipins by diet group. 204
Study B: Supplemental Table 2. Rat liver oxylipins by diet group. 209
Study B: Supplemental Table 3. Rat kidney oxylipins by diet group. 215
Study B: Supplemental Table 4. Rat serum oxylipins by diet group. 222
Study C: Supplemental Table 1. Characteristics of healthy control patients included in the plasma oxylipins analysis. 228
Study C: Supplemental Table 2. The complete list of deuterated internal standards and oxylipins scanned for. 230

Study C: Supplemental Table 3. Aortic valve leaflet oxylipins by aortic valve stenosis severity group determined by patient transvalvular mean pressure gradient. 237
Study C: Supplemental Table 4. Aortic Valve Oxylipins by patient ASA use..... 242
Study C: Supplemental Table 5. Plasma oxylipins by aortic valve stenosis severity determined by patient transvalvular mean pressure gradient. 247
Study C: Supplemental Table 6. Aortic valve leaflet oxylipins grouped by patient aortic valve stenosis severity (transvalvular mean pressure gradient) and sex. 251
Study C: Supplemental Table 7. Plasma oxylipins grouped by patient aortic valve stenosis severity (transvalvular mean pressure gradient) and sex. 256

List of Figures

Figure 1.1 Oxylipin biosynthesis diagram. 8
Figure 3.1. Comparison of rat heart transcriptomic profiles between control and treatment. 49
Figure 3.2. Gene set enrichment analysis of Gene Ontology biological processes. 51
Figure 3.3. Comparison of rat heart proteomic profiles between control and treatment. 54
Figure 3.4. Matched rat heart gene-protein pairs differentially expressed with 2-MCPD treatment. 55
Figure 3.5 Volcano plot comparison of rat heart oxylipins between control and treatment. 58
Figure 3.6. DHA oxylipin synthesis via LOX and CYP ω-hydrolase pathways. 59
Figure 4.1 Experimental design. 69
Figure 4.2. Rat heart oxylipin profile and individual oxylipins compared between experimental groups. 72
Figure 4.3. Rat liver oxylipin profile and individual oxylipins compared between experimental groups. 74
Figure 4.4. Rat kidney oxylipin profile and individual oxylipins compared between experimental groups. 76
Figure 4.5. Rat serum oxylipin profile and individual oxylipins compared between experimental groups. 78
Figure 4.6. Multivariate Integration-Partial Least Squares-Discriminant Analysis of cardiac, hepatic, renal, and serum oxylipins. 80
Figure 5.1. Correlation of oxylipins with severity of aortic valve stenosis. 97
Figure 5.2. Heatmap of aortic valve oxylipins by mean transvalvular pressure gradient (MPG) severity. 98
Figure 5.3. Aortic valve oxylipins totaled by fatty acid precursor. 100
Figure 5.4. Aortic valve oxylipins totaled by enzymatic pathway. 101
Figure 5.5. Pearson correlations of valvular oxylipins and clinical parameters. 103
Figure 5.6. Patient characteristics and valvular oxylipins modeled by principal component (PC) analysis. 105
Figure 5.7. Plasma oxylipins of control and mean transvalvular pressure gradient (MPG)-severe patients. 107

Figure 5.8. Patient characteristics and plasma oxylipins modeled by principal component analysis. 108
Appendix Figure 1. Docosahexaenoic acid oxylipin metabolism (WP5154) 152
Appendix Figure 2. ALA oxylipin metabolism (WP5136) 153
Appendix Figure 3. Arachidonic acid (AA, ARA) oxylipin metabolism (WP5155) 154
Appendix Figure 4. Linoleic acid oxylipin metabolism (WP5137) 155
Study A: Supplemental Figure 1. rno04062 “Chemokine signalling pathway” 189
Study A: Supplemental Figure 2. rno04210 “Apoptosis” 190
Study A: Supplemental Figure 3. rno04514 “Cell adhesion molecules” 191
Study A: Supplemental Figure 4. rno04650 “Natural killer cell mediated cytotoxicity” 192
Study A: Supplemental Figure 5. rno04657 “IL-17 signalling pathway” 193
Study A: Supplemental Figure 6. rno04659 “Th17 cell differentiation” 194
Study A: Supplemental Figure 7. rno04662 “B cell receptor signalling pathway” 195
Study A: Supplemental Figure 8. rno04666 “FcγR-mediated phagocytosis” 196
Study A: Supplemental Figure 9. rno04668 “TNF signalling pathway” 197
Study A: Supplemental Figure 10. rno04670 “Leukocyte transendothelial migration” 198
Study A: Supplemental Figure 11. rno00010 “Glycolysis / gluconeogenesis” 199
Study A: Supplemental Figure 12. rno00071 “Fatty acid degradation” 200
Study A: Supplemental Figure 13. rno00190 “Oxidative phosphorylation” 201
Study A: Supplemental Figure 14. rno00640 “Propanoate metabolism” 202
Study A: Supplemental Figure 15. rno04260 “Cardiac muscle contraction” 203
Study C: Supplemental Figure 1. Example chromatograms of oxylipin peak selection. 259

List of Abbreviations

2-MCPD	2-monochloropropane-1,3-diol
3-MCPD	3-monochloropropane-1,2-diol
A	Adequate ALA group
A2M	Adequate ALA with 2-MCPD group
AA	Arachidonic acid
AVS	Aortic valve stenosis
COX	Cyclooxygenase
CP	Chlorinated propanol
CYP	Cytochrome P450
CYPe	Cytochrome P450-epoxygenase
D	Deficient ALA group
D2M	Deficient ALA with 2-MCPD group
DEG	Differentially expressed gene
DEP	Differentially expressed protein
DGLA	Dihomo-γ-linolenic acid
DiHDoPE	Dihydroxy-docosapentaenoic acid
DiHETrE	Dihydroxy-eicosatrienoic acid
EDA	Exploratory data analysis
EpETrE	Epoxy-eicosatrienoic acid
FDR	Benjamini-Hochberg false discovery rate
GO	Gene Ontology
GSEA	Gene set enrichment analysis
HDoHE	Hydroxy-docosahexaenoic acids
HEPE	Hydroxy-eicosapentaenoic acids
HETE	Hydroxy-eicosatetraenoic acids
HETrE	Hydroxy-eicosatrienoic acid
HOTrE	Hydroxy-octadecatrienoic acids
HPLC-MS/MS	High-performance liquid chromatography tandem mass spectrometry
KEGG	Kyoto Encyclopedia of Genes and Genomes
LA	Linoleic acid

LDL	Low-density lipoprotein
LFC	Log_2 fold change
LOX	Lipoxygenase
LT	Leukotrienes
m/z	Mass to charge ratio
MPG	mean transvalvular pressure gradient
MS	Mass spectrometry
MSM	Multivariate statistical methods
NAMs	New approach methodologies
OxPC	Oxidized phosphatidylcholine
PC	Principal component
PCA	Principal component analysis
PG	Prostaglandin
PG	Prostaglandin
PLA2	Phospholipase A2
PLS-DA	Partial least squares discriminant analysis
qPCR	Quantitative polymerase chain reaction
RNA-seq	Next generation RNA sequencing
sEH	Soluble epoxide hydrolase
sPLA2	Secreted phospholipase A2
SPM	Specialized pro-resolving mediator
TDI	Tolerable daily intake
t_R	Retention time
TX	Thromboxane
VIC	Valvular interstitial cell
ΣALA_{Ox}	Sum of ALA oxylipins
$\Sigma DGLA_{Ox}$	Sum of DGLA oxylipins
ΣDHA_{Ox}	Sum of DHA oxylipins
ΣEPA_{Ox}	Sum of EPA oxylipins

Introduction

This thesis will focus on the application of new computational methods for analyzing large-scale bio-analytical data with a focus on oxylipins. These data will be derived from molecular level measurements of eukaryotic (more precisely mammalian) cellular responses to xenobiotics, dietary modification, and disease. Large-scale molecular-level bioanalytical data are commonly referred to as *omics* data and arise from high throughput measurements of molecules that comprise a living organism. These molecules include genomic DNA, gene transcripts (RNA), proteins, lipids, and metabolites, and have been shown to individually exhibit some causal relationships with diseases, xenobiotics, or the organism's environment.

The term *omics* derives from the sub-disciplines that study high throughput measurements of the basic biological molecular classes: DNA, RNA, proteins, lipids, and metabolites. For example, lipidomics refers to the high throughput comprehensive measurement of lipids in a living organism with a view to identifying and quantifying their concentrations and activities under a set of standard or perturbed conditions. Definitions for metabolomics, transcriptomics, genomics, and proteomics can be derived similarly by replacing the term "lipids" for metabolites, gene transcripts, genes, or proteins, respectively. These analyses are termed "untargeted" when they scan for all molecules of a given class, and "targeted" when a relevant subset of the molecular class is focused on.

Bioanalytical technology platforms popularly used for acquiring these high throughput measurements include next-generation sequencing for genomics and transcriptomics, and high-performance liquid chromatography tandem mass spectrometry (HPLC-MS/MS) for metabolomics, proteomics, and lipidomics—including oxylipins. Characteristically, the output from these instruments is complex. For example, in HPLC-MS/MS, sample complexity is first resolved through a separation front-end that measures the retention time (t_R) of each analyte which is then sent to the mass analyzer where its intensity at every mass to charge ratio (m/z) is recorded. Thus, each sample will have measurements that correspond to its t_R and m/z, over a range of time and mass fragments. The data become complex and special methods are required to integrate the information imbedded in them in order to visualize differences and develop calibration models. In a targeted analysis matched isotope-labelled internal standards are utilized to quantification a defined set of analytes, offering improved precision at the expense of scope. The data from the three studies presented in this thesis will have a two-way structure represented

in a matrix $\mathbf{X}_{n \times p}$, where *n* represents the number of samples and *p* is the number of variables. For example, the oxylipin data will comprise, for each sample, of a concentration value for each variable (oxylipin), which will be calculated from the intensity reading for mass fragments at each t_R-m/z pair relative to that of known standards. The *n*'s will vary based on the study design and *p*'s will vary by the bioanalytical technique used, the biological molecular class analyzed, and the tissue analyzed.

So, while technological advancements have made it easier to generate large datasets of biomolecular information, the challenge of interpreting that data still looms large. For more well-studied fields, such as genomics and proteomics, bioinformatics software exists which can be used to assess networks of molecules and determine potential pathway activation/inhibition from omics data. In more nascent fields, for which there are no ready computational solutions to infer biological information in the data, statistical analyses are left up to the researcher.

In classical applications, statistical methods exist for inferring the relationships between an experimental condition and an individual variable that is assumed to exclusively characterize that condition. Such approaches are referred to as univariate statistical methods since the effect of one variable is modelled at a time. These approaches have previously been sufficient to determine differences in study groups when fewer variables where measured. In practice biological systems are characterized by complex networks of biochemical signals that are highly interconnected making it difficult to rationalize the use of univariate approaches to comprehensively characterise such systems. An alternative approach that has quickly gained traction in the biological sciences, but which has been prevalent in the physical sciences for a number of decades (Massart et al., 1997), is the so called multivariate statistical methods (MSM).

In contrast to univariate approaches, MSM of data analysis allow the modelling of more than one independent variable, loosening the assumption that an experimental condition can be fully described by measuring one variable. Such methods allow multiple correlated variables, which describe a biological system, to be modelled simultaneously enabling interconnections between variables to be inferred and enabling analyses more suited to interpret the biological reality.

One disadvantage of high throughput bioanalytical analyses that generate numerous variable measurements per sample is that it is difficult to integrate sample correlations by the human eye. For this reason, the initial application of MSM to large datasets, often referred to as

exploratory data analysis (EDA), enables the data to be analyzed in a manner that allows independent variables to be defined and represented graphically, facilitating visual interpretation, and providing a comprehensive overview of the dataset. EDA was utilized in the three studies described below to analyze data generated from HPLC-MS/MS, next generation RNA sequencing (RNA-seq), and 2-D gel electrophoresis coupled to mass spectrometry (MS). This approach significantly enhanced the interpretation of these complex datasets.

Oxylipins are oxygenated metabolites of polyunsaturated fatty acids (PUFAs) with an array of bioactive properties. This thesis will cover three studies in which targeted lipidomic analyses of oxylipins were employed in three different contexts and demonstrate how the interpretation and presentation of this data can be achieved, particularly by the utilization of MSM.

Two of the projects presented in this thesis will be investigations of how the processing induced chemical food contaminant 2-monochloropropane-1,3-diol (2-MCPD) impacts biomolecules, including oxylipins in both studies. The detection of 2-MCPD in the food system is recent, and the toxicological impact of 2-MCPD on humans is yet to be elucidated. Rodent toxicity models have shown cardiotoxic effects to be the primary outcome with other organs affected to a lesser extent (Cayer, 2019; European Food Safety Authority, 2016; Raju et al., 2019, 2016; Schultrich et al., 2017). However, there is limited data regarding the mechanisms of action of 2-MCPD-induced harm. The first study presented elucidated molecular mechanisms of action of 2-MCPD in a 90-day sub-chronic dietary exposure rodent model. The study employed a multi-omics analysis that integrated the transcriptome, proteome, and targeted lipidome of the rat heart. The second study followed up the first by addressing the influence of dietary ALA adequacy on heart, liver, kidney, and serum oxylipins in rodents acutely exposed to oral 2-MCPD.

The third study is focussed on the most common valvular disease in the developed world, aortic valve stenosis (AVS) (Coffey et al., 2021). AVS involves the progressive calcification of the aortic valve (AV), which impairs functions, and ultimately leads to heart failure if left untreated. Currently, there are no pharmacological treatments or dietary interventions that are known to slow AVS progression; there are only surgical options available. The lack of treatment options is due to the gaps in our understanding of the underlying mechanisms of AVS. Studies have pointed to a role for oxylipins in AVS (Artiach et al., 2020; Nagy et al., 2011; Suzuki et al.,

2014). Thus, the study surveyed the oxylipins of the valves and plasma of AVS patients and determine which oxylipins or subclasses of oxylipins are related to AVS progression.

Chapter 1: Literature Review

1.1. Multivariate statistics

Advances in bio-analytical technologies are increasingly enabling the quantification of whole classes of biological molecules. The premise for most omics studies is that under different physical and/or biochemical conditions, it is possible to classify samples based on measured signals that characterize biomolecules. This classification is achieved using MSM that allow visualization of sample differences and determine the molecules that are responsible for such differences. Principal component analysis (PCA) and partial least squares discriminant analysis (PLS-DA) are *de facto* MSM employed in these studies. PCA and PLS-DA and are often implemented, respectively, using singular value decomposition, nonlinear iterative partial least squares, or the simple implementation of the partial least squares method (Massart et al., 1997). These methods reduce the dimensionality of the dataset in a way that includes all variables by plotting each sample virtually with each variable as orthogonal axes, the first principal component (PC) is created as a line through the virtual point swarm such that it accounts for the maximum amount of the variance in the data, thus representing the dominant linear trend. Subsequent PCs are determined such that they are orthogonal to PC1 and account for the maximum amount of the remaining variance (Kenkel, 2006). Because the proportion of the total variance explained decreases with subsequent PCs, a small number of the PCs can summarize most of the dataset. The dimension reduction then occurs by selecting the first few PCs, as these are typically representative of the majority of the variance underlying the dataset. Using the first two or three PCs as scatter plot axes the entire dataset can be graphically represented in two or three dimensions, which address the problem of visually representing large datasets. The clustering of data points will be an indication of how similar (in terms of all the variables) samples are. The variables can also be plotted as weighted values (eigenvectors) to illustrate how each variable related to the PC and samples (Kenkel, 2006). An advantage to using a PC to represent multiple variables is that it avoids issue of multicollinearity and can be highly representative of the aggregated variables.

PLS-DA is a similar method to PCA because it also reduces the dimensionality of a dataset and can be represented in graphical form. The main difference between the two methods is that the PCA algorithm does not consider group labels, while PLS-DA algorithm does (Ruiz-

Perez and Narasimhan, 2017; Worley and Powers, 2013). PCA is thus termed an unsupervised method, while PLS-DA is termed supervised. As a result of its consideration of group labels, PLS-DA is a less conservative analysis that is more prone to overfitting (Ruiz-Perez and Narasimhan, 2017). A benefit of PLS-DA, however, is that a greater emphasis is put on group separation, so it can be more suitable for assigning group affiliation once a model has been constructed (Farrés et al., 2015).

PCA and PLS both use variance in their algorithm, a limitation of this is the susceptibility to outliers. Other MSM use parameters other than variance such as non-metric multidimensional scaling which uses pairwise distances (Taguchi and Oono, 2005). There are multiple other machine-learning methods like artificial neural networks, random forests, or projection pursuit which can similarly be used to interpret multivariate data (Grear et al., 2021; Qi, 2012; Yu et al., 2019). Ultimately the MSM selection should be influenced by what is appropriate for the data and the research question.

1.2. Web-based bioinformatics applications

One example of how oxylipins are currently inadequately integrated into the omics framework is the lack of pathway mapping that has been done for the various PUFA and their metabolites. These pathways can be found in the literature (Gabbs et al., 2015), but are not well-integrated to bioinformatics platforms. For instance, the widely used Kyoto Encyclopedia of Genes and Genomes (KEGG) Pathway Database currently contains pathway diagrams for AA and linoleic acid (LA) metabolism with annotations for the genes involved in each reaction (https://www.genome.jp/pathway/map00590; https://www.kegg.jp/pathway/ko00591), but the other oxylipin producing PUFA are not available. Also, the oxylipins in these pathways are not annotated, thus software that utilizes KEGG, such as Ingenuity Pathway Analysis (IPA) or R packages including clusterProfiler, cannot be used to connect experimental data to predict expression of pathway-adjacent metabolites and enzymes. The gene set enrichment analysis (GSEA) used by clusterProfiler of RNA-seq data is a technique that has achieved wide-spread adoption (Xie et al., 2021). It is fundamentally a MSM in that its algorithm produces enrichment scores by combining expression values of the genes associated with a given pathway or process, termed “gene sets” (Subramanian et al., 2005). Unfortunately, the equivalent of gene sets for oxylipins do not yet exist.

1.3. Oxylipins

Oxylipins are a class of bioactive lipid which consists of the oxygenated metabolites of 18-22 carbon polyunsaturated fatty acids (PUFAs). In biological systems, oxylipins mediate an array of homeostatic functions acting as local hormones (Gabbs et al., 2015). To do so, free oxylipins are produced enzymatically or non-enzymatically through various pathways which all begin with the liberation of PUFAs from phospholipids in the cellular membrane by phospholipase A2 (PLA2) (Dennis et al., 2011). The free PUFA can then undergo a series of reactions to produce oxygenated metabolites, termed oxylipins.

The enzymatic biosynthesis of oxylipins, summarized in Figure 1, can be categorized into three main pathways: cyclooxygenase (COX), cytochrome P450 (CYP), or lipoxygenase (LOX). The COX pathway will induce a cyclization of the PUFA forming an oxygenated 5-carbon ring, producing prostanoids [prostaglandins (PGs) and thromboxanes (TXs)] (Buczynski et al., 2009; Funk CD, 2001). The CYP pathway has two major activities regarding PUFA metabolism: ω-hydroxylase activity producing terminal hydroxy-PUFAs, and epoxygenase activity producing epoxy-PUFAs that can be hydrolyzed to dihydroxy-PUFAs by soluble epoxide hydrolase (sEH) (Buczynski et al., 2009). Lastly, the LOX pathway produces hydroxy-PUFAs which can be subsequently metabolized to produce various other oxylipins [e.g. oxo-PUFAs, leukotrienes (LTs), and resolvins (Rvs)] (Kuhn et al., 2015).

The structure of the oxylipins produced will also depend on their precursor PUFA, both the carbon chain length and the degree of unsaturation in that chain will influence what end products are synthesized. The oxylipins can then influence biological functions intercellularly by binding to G-protein coupled receptors or intracellularly by binding nuclear membrane peroxisome proliferator-activated receptors (Gabbs et al., 2015), as shown in Figure 1.

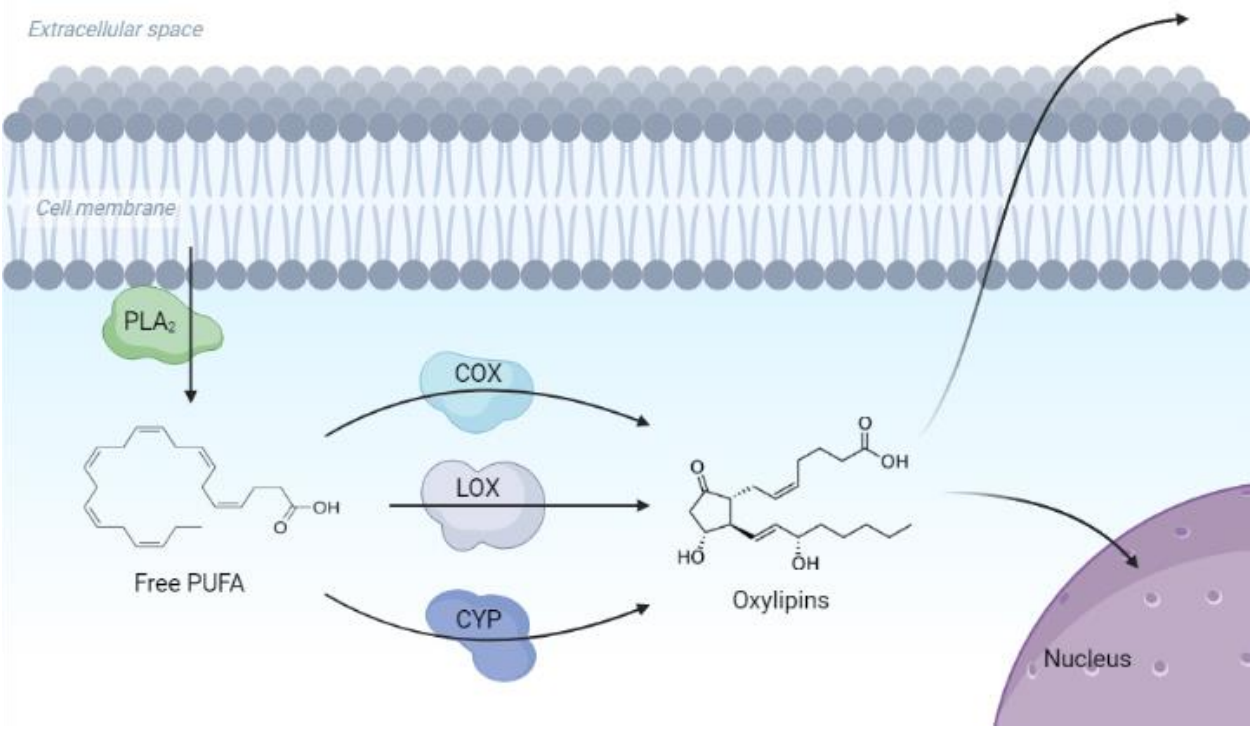

Figure 1.1 Oxylipin biosynthesis diagram.
Phospholipid PUFAs in the cell membrane are liberated by PLA2. The free PUFAs are available for metabolism by the COX, LOX, and CYP enzymatic pathways, which produce oxylipins that go on to bind nuclear receptors or membrane receptors.

The bioactive properties of oxylipins tend to have variable potency or opposing function dependent upon the precursor PUFA and the enzymatic pathway from which they were derived (Gabbs et al., 2015). Thus, in order to elucidate the influence of an experimental intervention or other perturbance from homeostasis, it is crucial to measure the array of oxylipins present in the tissue of interest, in order to comprehensively assess the effects of these lipids.

1.3.1. Oxylipins in health and disease

Oxylipins, as bioactive lipids, play critical roles in various physiological and pathological processes. These molecules are involved in maintaining homeostasis with their dysregulation often linked to the development of diseases. Throughout this thesis, the roles of oxylipins as mediators of inflammation and immune responses are addressed. PGs, TXs, and LTs, produced via the COX and LOX pathways, are among the most studied oxylipins. These molecules can have pro-inflammatory or anti-inflammatory effects depending on their structure and the context

of their production (Gabbs et al., 2015). For instance, PGE2, derived from AA through the COX pathway, has been shown to have both pro-inflammatory and immunomodulatory effects, influencing fever, pain, and vasodilation (Funk CD, 2001; Yao and Narumiya, 2019).

Oxylipins also play significant roles in specific diseases. For instance, in cardiovascular health, epoxy-eicosatrienoic acids (EpETrEs), produced via the CYP pathway from AA, have vasodilatory and anti-inflammatory properties, contributing to the maintenance of blood pressure and protecting against ischemic injury (Caligiuri et al., 2017; Imig et al., 2012). Conversely, elevated levels of certain oxylipins, such as those produced by the COX pathway, have been implicated in cardiovascular diseases. For instance, increased levels of TXA2 are associated with platelet aggregation and vasoconstriction, contributing to the pathology of atherosclerosis and thrombosis (Caligiuri et al., 2017; Ricciotti and Fitzgerald, 2011).

The role of oxylipins in toxicology is an emerging field of interest, as these molecules can be significantly altered by exposure to environmental toxins, drugs, and other chemical agents. Oxylipins mediate various cellular responses to toxic insults, including inflammation, oxidative stress, and apoptosis. As the utilization of oxylipin analyses in the field of toxicology is expanding, so too is the identification of exposures to toxicants which disrupt oxylipin pathways (Anwar-Mohamed et al., 2014, 2013, 2012; Dai et al., 2023; Huang et al., 2020; Wu et al., 2023, 2016). In toxicological studies, oxylipin analyses can identify novel biomarkers for exposure and can provide insights into underlying the mechanisms of toxicity.

Notably, oxylipins are modifiable by diet. The levels of oxylipins can be altered by dietary PUFA intake, with variable effects by tissue. For instance, in the Sprague-Dawley rat heart, high dietary ALA (3.43 g/100g diet) elevated ALA and EPA oxylipins, while lowering AA oxylipins compared to a control diet (0.27 g/100g diet) (Ferdouse et al., 2019). However, in the kidneys of the same animals, high dietary ALA not only elevated ALA and EPA oxylipins while reducing AA oxylipins, but also increased DHA oxylipins (Leng et al., 2018a). Thus, the specific tissue of interest needs to be analyzed to know how modifying dietary PUFA will alter the oxylipin profile of said tissue. As the functions of oxylipins and interpretation of changes to whole oxylipin profiles are elucidated, the ability to make dietary recommendations based on the desired oxylipin profiles will be enhanced.

1.3.2. Analytical methodology

HPLC-MS/MS is the premier analytical technique in the field of lipidomics. For oxylipins, specifically reversed-phase high-performance liquid chromatography coupled to triple-quadrupole MS in the negative mode with electrospray ionization allows for sensitive, high-throughput quantification ideal for detecting oxylipins in biological samples where they may be present at very low concentrations.

In this method, high-performance liquid chromatography separates molecules based on their chemical characteristics, with reversed-phase columns referring to a non-polar stationary phase and polar mobile phase (Hall and Murphy, 1998; Žuvela et al., 2019). Following separation, tandem MS enables further resolution, detection, and quantification. For this process, molecules are first ionized by high voltage, in the case of triple-quadruple, parent ions are first filtered by m/z, then fragmented into daughter ions, which are filtered again by m/z, and finally the signal intensities are measured. Using multiple reaction monitoring, selecting specific transitions of father-daughter pairs, coupled with t_R data from the high-performance liquid chromatography, oxylipin identities can be inferred and quantified with high sensitivity (Hall and Murphy, 1998; Yost and Enke, 1979). Additionally, HPLC-MS/MS is a high-throughput technique that can quantify multiple oxylipins in a single run. This capacity offers a comprehensive profiling of oxylipins within a given sample.

Despite its advantages, HPLC-MS/MS for oxylipin analysis faces several challenges throughout the entire process from sample collection to oxylipin quantification. At the initial stage of sample collection, various factors can introduce variability in oxylipin levels, including the method of euthanasia, timing of sample collection, postmortem changes, cell damage, or contamination by other tissues (Aukema and Ravandi, 2023). Furthermore, oxylipins are highly susceptible to rapid degradation and oxidation, which necessitates stringent sample handling and processing protocols to maintain their integrity. Immediate freezing of samples is crucial to the prevention of sample degradation. To ensure the stability of oxylipins, samples must be stored at -80°C, which has been shown to preserve oxylipin integrity for at least 2.5 years. In contrast, storage at -20°C has been demonstrated to introduce significant variability in oxylipin profiles (Gladine et al., 2019).

The analytical process itself can be affected by matrix and batch effects, which can influence the accuracy of oxylipin quantification. To mitigate these effects, robust sample

preparation techniques such as solid phase extraction and the use of stable-isotope internal standards are essential. Solid phase extraction has proven superior to traditional liquid-liquid extraction for isolating oxylipins effectively. While different protocols offer varied extraction efficiencies by oxylipin, the use of water and n-hexane rinses improve the removal of matrix prior to elution (Ostermann et al., 2015). Furthermore, the use of stable isotope internal standards can control for oxylipin extraction efficiency and enables robust quantification of oxylipins. However, a limitation arises from the lack of primary standards for all oxylipins, which restricts the quantification capabilities for those molecules not covered by available standards.

Another current analytical challenge is the resolution of enantiomers. The chirality of oxylipins can provide valuable information regarding their synthesis by enzymatic pathway or autooxidation. Recent advances in liquid chromatography methods have started to improve the resolution of enantiomers, potentially allowing for more precise determination of oxylipin pathways; however, these methods can sometimes compromise mass spectrometry sensitivity, presenting a trade-off between resolution and detection efficiency. (Blum et al., 2019; Cebo et al., 2020; Mazaleuskaya et al., 2018; Oliveira et al., 2021).

1.4. 2-MCPD toxicology

Two of the studies in this thesis seek to elucidate molecular alterations induced by 2-MCPD exposure. 2-MCPD is a chlorinated propanol (CP) isomer for which there is uncertainty regarding the toxic hazard to humans. CPs are processing induced food contaminants that can occur in a variety of food products. There are three methods by which CPs are produced. The first is as by-products in the production of the flavour enhancer hydrolyzed vegetable protein, and is found in various ‘Asian sauces’ which contain hydrolyzed vegetable protein (Fu et al., 2007; van Bergen et al., 1992). CP-fatty acid esters are also formed as by-products of the refining and cooking of vegetable oils, and thus occur in the plethora of foods that contain processed oils (Baer et al., 2010; Hamlet et al., 2002; Šmidrkal et al., 2016). One such food of particular concern is infant formula, as exclusively formula-fed children can be among the highest per bodyweight consumers (European Food Safety Authority, 2016; Schneider et al., 2022). CPs have also been shown to be imparted into foods through water-resistant paper products, such as paper cups or Styrofoam trays (Becalski et al., 2016).

The majority of the toxicological research into CPs has focussed on 3-monochloropropane-1,2-diol (3-MCPD), as it is typically the most abundant CP isomer formed

and has been categorized by the International Agency for Research on Cancer as a possible human carcinogen (Group 2B) (International Agency for Research on Cancer, 2013), with a tolerable daily intake (TDI) ranging from 2-4 µg/kg BW, depending on the regulatory body (European Food Safety Authority, 2018; Joint FAO/WHO Expert Committee on Food Additives, 2017). Of particular concern is the potential exposure to children under 2-years as the highest per BW consumers can potentially consume 3-MCPD in excess of its TDI (Joint FAO/WHO Expert Committee on Food Additives, 2017).

Investigation into 2-MCPD is, however, also warranted as it has been shown to be formed concomitantly at approximately 50% of 3-MCPD, in refined oils (Kuhlmann, 2016; Wöhrlin et al., 2015; Zelinková et al., 2006), and has unique toxicological activity (Buhrke et al., 2017; Schilter et al., 2011; Schultrich et al., 2017). The data on 2-MCPD toxicity in animals is currently limited, but the few sub-acute and sub-chronic 2-MCPD rodent toxicity studies that have been conducted have all identified cardiotoxicity as a primary outcome (European Food Safety Authority, 2016; Raju et al., 2019, 2016; Schilter et al., 2011). Raju et al. (2019) specifically described heart lesions characterized by inflammation, vacuolation, fibrosis, and immune cell infiltration. Secondary target organs have had some discrepancy between studies, with the kidney, skeletal muscle, liver, thymus, and spleen only being affected in some studies (European Food Safety Authority, 2016; Raju et al., 2019, 2016; Schilter et al., 2011). The data for 2-MCPD carcinogenicity is also limited, although some studies have shown 2-MCPD to not be genotoxic *in vitro* and *in vivo* (Frei and Würgler, 1997; Schilter et al., 2011). There is also insufficient data for a TDI of 2-MCPD to be established. Thus, there is need for further toxicological investigation of the effects dietary 2-MCPD in animals to strengthen the literature and enable risk assessment.

There is notable evidence of rodent strain-related differences in sensitivity to 2-MCPD exposure. In weanling Sprague-Dawley rats (outbred), 2-MCPD exposure of 30 mg/kg body weight (BW)/day induced heart failure at 8-23 days treatment (European Food Safety Authority, 2016). In contrast, weanling F344 (inbred) rats exposed to 50 mg/kg BW/day for 28 days and 40mg/kg BW/day for 90 days developed myocardial necrosis and vacuolation but did not experience fatalities (Raju et al., 2019, 2016). Both strains are commonly used in toxicological models; however, the reasons behind these differences in response to 2-MCPD remain unclear.

Free 2-MCPD was selected for this research as the foundational data for assessing 2-MCPD toxicity must first elucidate the effects of pure 2-MCPD. It has been demonstrated that CP-esters are readily digested in the gut by lipases (Kaze et al., 2016), and free 2-MCPD, but not its mono-esters, can cross an *in vitro* model of the human intestinal barrier consisting of Caco-2 cells (Buhrke et al., 2015). Furthermore, proteomic analysis of rodent heart exposed to non-toxic doses of 2-MCPD showed strong similarities between free 2-MCPD and esterified 2-MCPD (2-MCPD-dipalmitate) (Schultrich et al., 2017). Moreover, the oral bioavailability of 3-MCPD diester was found to be 86% that of free 3-MCPD, in a rodent model, and 3-MCPD esters were not detected in the blood with a limit of quantification of 0.25 μg/ml (Abraham et al., 2013). This suggests that the relative oral bioavailability of free 2-MCPD compared to its esters would be at least as high as for 3-MCPD because the sn-1 and sn-3 positions of the fatty acid esters on esterified 2-MCPD are more readily digested by pancreatic lipase than the sn-2 ester of a 3-MCPD diester (Kaze et al., 2016). Thus, decision to use free 2-MCPD in these studies is supported by the literature regarding the intestinal absorption of CPs, which suggests the choice model is highly applicable to human exposure, because the toxic effects of 2-MCPD can be assumed to be imparted by the free form which is readily cleaved of esterified fatty acids before absorption in the gut.

1.4.1. 2-MCPD exposure: Genetic and protein level changes

In addition to the sparse data regarding the mode of action of 2-MCPD toxicity, data on the mechanism of action are also limited, which further precludes toxic hazard assessment (European Food Safety Authority, 2016). Molecular analyses are also being utilized to investigate 2-MCPD in a way that can provide insight towards the toxic mechanism of action. Sub-toxic doses of 2-MCPD induce dysregulation of various metabolic and structural proteins in the rodent heart (Schultrich et al., 2017). In the kidney and liver transcriptomic data, also using a sub-toxic 2-MCPD model, showed dysregulation of genes related to structure and transporters (Buhrke et al., 2017). Sub-acute and sub-chronic rodent bioassays of oral 2-MCPD show multiple genes are dysregulated in the heart and kidney (Raju et al., 2019, 2016). In the heart, these genes were related to oxidative stress response, inflammatory response, and tissue repair. Similarly, in the kidney, the altered genes were related to oxidative stress response.

Following the central dogma of molecular biology, that genetic information is stored in DNA and transcribed in mRNA and translated into protein, it was previously assumed that

protein expression would closely correlate to mRNA expression. However, we now understand that the reality is more complex. For instance, transcriptional regulation, post-translation modifications, and half-life differences can occur, and when measured many transcript-protein pairs turn out to only be moderately correlated (Hasin et al., 2017). Also, RNA has been shown to have functional roles beyond its classically understood role as an intermediate between DNA and protein (Knoll et al., 2015). Thus, analysis which includes both the transcriptome and proteome will provide a more robust analysis to help us better understand the mechanisms of 2-MCPD toxicity.

1.4.2. 2-MCPD exposure: Oxylipins and n-3 adequacy

In our previous work, a targeted lipidomic profiling of heart, kidney, muscle, and serum from F344 rats sub-chronically exposed to oral 2-MCPD for 90 days, was conducted (Cayer et al., 2019). These analyses targeted oxylipins and OxPCs. The rationale to look at oxylipins in this toxicological context was that studies of other chemical hazards have shown the expression and activity of oxylipin producing enzymes (PLA2, CYP, sEH, COX, and LOX) to be altered by exposure to other toxins (Anwar-Mohamed et al., 2014, 2013, 2012; Wu et al., 2016). Also, oxylipins are known to mediate functions that had been identified to occur due to 2-MCPD exposure in previous toxicogenomic analysis, such as inflammation (PGs, LTs, and SPMs), apoptosis [PGs, hydroxy-eicosatetraenoic acids (HETEs), and EpETrEs], and cell proliferation [HETEs, oxo-eicosatetraenoic acids, EpETrEs, hydroxy-docosahexaenoic acids (HDoHE)] (Gabbs et al., 2015; Raju et al., 2019, 2016; Serhan, 2014). More recently, studies have confirmed that oxylipins are perturbed in response to various chemical hazards, with multiple studies reporting elevated AA-COX derived PGs and increased dihydroxy-eicosatrienoic acid (DiHETrE):EpETrE ratios, both of which indicate pro-inflammatory states (Dai et al., 2023; Huang et al., 2020; Wu et al., 2023).

The results of our previous oxylipin analysis in the 2-MCPD exposed rodent heart identified a pronounced decrease in the DHA derived oxylipins with 2-MCPD exposure (Cayer, 2019). While the functions of many DHA oxylipins are not established in cardiac tissue, they have demonstrated anti-inflammatory properties through inhibition of immune cell aggregation and cytokine production (Gabbs et al., 2015; Serhan, 2014). This raised the question of the mechanism by which DHA oxylipins were suppressed in the 2-MCPD exposed heart. As well as whether the oxylipin changes were just a decrease to the DHA oxylipins, or a broad decrease to

the n-3 PUFA derived oxylipins, was not clear (Cayer et al., 2019). Too few ALA and EPA oxylipins were above the LOQ in the treatment and control group for a distinction between a DHA-effect or an n-3-effect to be made. From a lipid perspective, a limitation to the study was the use of corn oil in the AIN-93G rodent diets (Cayer, 2019). Corn oil was selected in this study for diets to conform with previous toxicological literature; however, corn oil is regarded to be deficient in essential dietary n-3 PUFA, which is why soybean oil is typically used in the AIN-93 diets, such that the total diet contains 0.5% ALA (Lien et al., 2001; Reeves et al., 1993). When the control group heart oxylipins from the Cayer et al. (2019) data were compared to another heart oxylipin profiling from Sprague-Dawley rats fed AIN-93G with 10% soybean oil, it is apparent that the corn oil diet rodent hearts had lower levels of n-3 oxylipins, particularly from ALA and EPA (Ferdouse et al., 2019).

It is not yet known how the oxylipins of 2-MCPD-exposed rodent heart are affected when sufficient dietary n-3 PUFA is provided, but it is possible that rodents fed adequate n-3 PUFA will have a cardioprotective effect in the presence of 2-MCPD for multiple reasons. Firstly, deficient dietary ALA can quicken rodent mortality due to a toxic exposure, as shown in an acute triethyltin intraperitoneal injection (Bourre et al., 1989). Secondly, n-3 PUFA and their oxylipin metabolites have cardiovascular benefits, such as improving blood pressure, inhibiting platelet aggregation, and inflammation resolution (Caligiuri et al., 2017). Thirdly, from the data that showed DHA oxylipins were reduced in the 2-MCPD-exposed heart concurrent with cardiac lesions, it is likely that a higher n-3 diet would mitigate this effect, as dietary n-3 PUFA has been shown to increase n-3 oxylipins in the heart (Ferdouse et al., 2019). Lastly, there is potential for detrimental effects on cardiovascular health due high dietary LA, which is the major PUFA in corn oil. High dietary LA can increase LA derived oxylipins in the heart (Ferdouse et al., 2019). The hydroxylated and di-hydroxylated metabolites of LA can mediate detrimental cardiovascular effects (Caligiuri et al., 2017; Honn et al., 1992; Theken et al., 2012). Thus, there is a need for analysis of the 2-MCPD-exposed rodent heart under conditions of adequate dietary n-3 PUFA.

To a lesser extent than cardiotoxicity, nephrotoxicity has also been identified to be induced by 2-MCPD exposure. Two 28-day sub-acute studies using 0-30 and 0-50 mg/kg BW 2-MCPD found nephrotoxic effects (Raju et al., 2016; Schilter et al., 2011). While a 90-day sub-chronic study using 0-40 mg/kg BW 2-MCPD did not detect histological changes, elevated kidney weight still occurred (Raju et al., 2019). The kidney is a common site for toxicity of

water-soluble toxins because they can be concentrated there (Hodgson, 2004), but the mechanism of action for 2-MCPD in the kidney has received little attention.

The oxylipin profiling of the kidney in our previous study identified 8 out of 64 oxylipins quantified were significantly altered from control (Cayer, 2019). These changes to renal oxylipins occurred while the toxicological assessment of the kidney determined the exposure to be sub-toxic. Therefore, oxylipins are potential markers of the early effects of 2-MCPD exposure. In order to build foundational literature on the toxic mechanism of action of 2-MCPD nephrotoxicity, further oxylipin analysis of the 2-MCPD-exposed kidney is also needed.

1.4.3. New approach methodologies (NAMs)

The 2-MCPD-related studies presented in this thesis align well with the paradigm shift toward new approach methodologies (NAMs) in regulatory toxicology, as endorsed by regulatory bodies such as the OECD, EPA, and Health Canada (EPA, 2024; Health Canada, 2023; OECD, 2023). NAMs is an innovative science-based advancement of hazard identification of chemicals for regulatory human health risk assessment. It encompasses modern precision-aimed technologies, in combination with human cell-based assays, and computational/bioinformatic-based methodologies to generate mechanistic-based adverse health outcomes of chemicals. Importantly, NAMs aims to provide high specificity and biological relevance to human health, where data derived from traditional animal-based hazard identification processes will persist as a critical limitation. Guided by the '3R principle' (replace, reduce, refine), NAMs offers an ethical alternative that minimizes the use of experimental animals in scientific research., where possible (Cattaneo et al., 2023).

To evaluate the adverse effects of chemicals, NAMs includes *in silico* models, such as quantitative structure-activity relationship models and physiologically based pharmacokinetic models, high-throughput screenings of potential toxins, and *in vitro* models that use isolated cells to study chemical effects (Hartung, 2009; OECD, 2017). Additionally, NAMs can involve permissible *in vivo* models of toxicity testing and hazard identification conducted in vertebrate animals. Ethical considerations drive the principles of replacement, reduction, and refinement in these approaches. For instance, omics studies efficiently generate substantial data from the animals used, reducing the need for separate studies and ultimately minimizing the total number of animals required. Omics research is essential for uncovering the mechanisms underlying toxic effects, identifying safe exposure levels, and characterizing cellular responses to chemicals.

These insights are crucial for developing NAMs that do not rely on animal testing (Health Canada, 2023; Li et al., 2023).

The development and validation of screening opportunities will lead to the reliance on animal testing to be reduced to only those chemicals that need further detailed hazard data. For example, certain cell- and tissue-based assays have provided total replacement of animal testing (eg. skin toxicity assays) (Cattaneo et al., 2023; Health Canada, 2023). However, some endpoints cannot yet be replaced, and reliance on hazard data from vertebrate animal testing is maintained, with provisions for refinements and reduction.

Mammalian models closest to humans, particularly laboratory rodents, continue to be required to ascertain complex biological processes such as carcinogenicity or developmental and reproductive toxicity (Yang et al., 2019). Additionally, there are no alternatives to comprehensively address the fate of chemicals when exposed through complex matrices, such as the oral ingestion route. For instance, the fate of chemicals exposed through the diet matrix is influenced by nutrient composition (e.g. dietary fats, carbohydrates, protein, fibre, etc.). Furthermore, food-borne chemicals are exposed to dynamic physiological processes in the gastrointestinal tract, leading to sequential alterations from the primary matrix (e.g. diet) to secondary matrices (e.g. stomach contents, intestinal digesta and feces). These processes can potentially lead to physicochemical modifications of chemicals, affecting systemic uptake (Mackie et al., 2020).

Developing robust methodologies to simulate these sequential and differential processes *in vitro* or *in silico* is challenging; especially considering interactions with the gut microbiome, for which reliable simulation tools are still lacking (Waclawiková et al., 2022). Consequently, completely reducing reliance on vertebrate animal testing for this purpose is not currently feasible. Integrating NAMs data with data derived from traditional hazard identification methods of vertebrate animal testing to elucidate the toxic mechanisms of action of chemical hazards, while adding to the weight of evidence for risk assessment, however, remains a key area of development (Bal-Price et al., 2015; Cattaneo et al., 2023; Coecke et al., 2013). NAMs is developing at a fast pace in its formative stage are at an early stage on the trajectory to completely replace animal testing.

1.5. Aortic Valve Stenosis

The third study of this thesis will investigate the role of oxylipins in AVS. AVS is the third most common cardiovascular disease, the most common valvular heart disease, and a major cause of heart failure and cardiovascular mortality in the North America and Europe (Iung et al., 2003; Nathaniel et al., 2010; Nkomo et al., 2006). Age is a major risk factor for AVS, hence the prevalence in Western nations. The symptoms of severe stage AVS include syncope, angina, and heart failure, and if left untreated the one-year event-free survival rate for severe AVS is below 40% (Baumgartner et al., 2018). The progression of AVS is characterized by calcific remodelling of the AV leaflets and cardiomyocyte hypertrophy which result in diminished valvular function and a narrowing of the valve opening (Dweck et al., 2012). The pathophysiology of AVS is being elucidated, but an effective pharmacological treatment for AVS is not available, and surgical valve replacement or transcatheter AV implantation are the current best treatment methods. Unfortunately, for patients with severe comorbidities, which are often present in older adults, surgery may not be an option (Baumgartner et al., 2017). Thus, there is a need to better understand the pathophysiology of AVS to enable the development of novel medical treatments or dietary recommendations, both to reduce the requirement for surgery and for those unable to receive it.

AVS was previously thought to be a passive disease associated with aging and wear-and-tear of the valve, but what is now known of AVS is that it is an active process with many similarities to atherosclerosis. For instance, many of the risk factors for cardiovascular disease are shared with AVS, such as elevated low-density lipoprotein (LDL), smoking history, hypertension, and diabetes (Messika-Zeitoun et al., 2007; Mohler et al., 2001; Stewart et al., 1997). AVS progression involves the transformation of valvular interstitial cells (VICs) into an osteoblast-like phenotype, driven by the infiltration of immune cells and the presence of oxidized lipoproteins (Grim et al., 2020). The process is initiated at points of mechanical stress on the valve leaflets; where the infiltration of immune cells (T cells and monocytes which differentiate into macrophages) and lipoproteins first occurs (Bouchareb et al., 2019; Dweck et al., 2012; Zheng et al., 2020). The accumulating lipoproteins, primarily LDL and Lp(a), become cytotoxic upon oxidation, exacerbating local inflammation which in turn triggers the release of inflammatory cytokines, including tumour necrosis factor alpha, tumour growth factor beta, C-reactive protein, and interleukin-1β. These cytokines not only stimulate the fibrosis process but

also initiate the calcification pathway by promoting the differentiation of myofibroblasts into osteoblast-like cells (Grim et al., 2020; Hulin et al., 2018). As these cells differentiate, they begin producing calcification-regulating proteins such as osteopontin, osteocalcin, osteonectin, and bone morphogenetic proteins 2 and 4. The presence of these proteins facilitates the deposition of minerals into the extracellular matrix, leading to the formation of bone-like structures within the valve supported by angiogenesis (Dweck et al., 2012; Mohler et al., 2001; Nathaniel et al., 2010; Rosenhek and Baumgartner, 2008; Yamazato et al., 2012).

From this understanding of AVS progression, it would be thought that lipid lowering drugs would reduce the risk of AVS, similarly to atherosclerosis. A rabbit model with genetic hypercholesterolemia showed beneficial results with Atorvastatin (Rajamannan et al., 2005). However, large-scale prospective randomized control clinical trials have failed to show beneficial results from multiple intensive statin-therapies (Chan et al., 2010; Cowell et al., 2005; Rossebø et al., 2008; Van Der Linde et al., 2011). The one exception was a post hoc analysis of the simvastatin and ezetimibe in aortic stenosis (SEAS) trial that revealed a potential benefit of statin therapy, particularly in patients with mild AVS and elevated LDL levels (Greve et al., 2019). This finding suggests that early intervention with lipid-lowering treatments could have a role in managing certain subgroups of AVS patients. One hypothesis for the general lack of benefit in such trials was the disease progression may have been too far at the onset of statin-therapy. This hypothesis is refuted by the trial by Van Der Linde et al. (2011), which specifically used younger patients to address this critique; this study also found statin-therapy to be ineffective. So, there is currently no effective medical treatment to address the progression of AVS, until the severe stage is reached and surgical AV replacement, or transcatheter AV implantation, becomes necessary.

1.5.1. Aortic Valve Stenosis and oxylipins

To develop novel treatments for AVS, further elucidation of the mechanism is needed, and studies have pointed to a role for oxylipins. The progression of AVS is driven by inflammation or may be thought of as improper tissue repair. In general, oxylipins produced from AA, such as the COX derived prostanoids and the LOX derived LT, mediate proinflammatory cellular processes; while oxylipins from n-3 PUFA (primarily from EPA and DHA), which include the SPM, mediate anti-inflammatory and tissue repair processes (Gabbs et al., 2015; Serhan, 2014). It has now been shown that enzymes involved in oxylipin production,

namely PLA2, COX-1, COX-2, and 5-LOX, are elevated in AVS leaflet tissue (Nagy et al., 2011; Suzuki et al., 2014; Wirrig et al., 2015). In a *klotho*-deficient mouse model for AVS, pharmacological inhibition of COX-2 reduced AV calcification (Wirrig et al., 2015). However, in humans the use of the selective COX-2 inhibitor Celecoxib has recently been associated with increased incidence of AVS and increased calcification of interstitial cells *in vitro* (Bowler et al., 2019).

It was recently found that in the calcified regions of the AVS leaflet, levels of two SPMs were reduced: the EPA derived RvE1 ($P < 0.05$), and the DHA derived RvD3 showed a trend towards reduction ($P = 0.06$). Conversely, the AA derived LTB4 was significantly elevated ($P < 0.001$), suggesting a shift in oxylipins that would favour pro-inflammatory processes in these regions (Artiach et al., 2020). However, it is important to consider that if the oxylipin profile of the leaflet resembles that of the whole heart, these three oxylipins (RvE1, RvD3, and LTB4) are just a few among many others identified in such tissues (Cayer, 2019; Ferdouse et al., 2019). Oxylipins often exhibit antagonistic functions or varying potencies in mediating specific cellular processes, which are largely influenced by the PUFAs from which they are derived. For instance, the 5-series LT, which are derived from EPA via 5-LOX, can inhibit the production of their AA derived isomers, be less potent neutrophil aggregators, or decrease interleukin-1β induced prostanoid production (Ait-Said et al., 2003; Leitch et al., 1984; Nathaniel et al., 1985; Terano et al., 1984).

Furthermore, there are many oxylipins that mediate cellular functions particularly relevant to AVS. PGs are well-known to be mediators of inflammation (Cattan et al., 2000; Dorris and Stokes Peebles Jr, 2012; Ricciotti and Fitzgerald, 2011), but also have roles in bone homeostasis and remodelling. For instance, PGD2, PGE2, and PGE3 mediate bone formation and absorption (Koshihara and Kawamura, 1989; Kruger et al., 2010). PGE2 presents complex effects on bone dynamics; studies indicate it inhibits osteoclast development (Take et al., 2005), enhances osteoclast differentiation (Kobayashi et al., 2005) and inhibits osteoblast differentiation (Choudhary et al., 2013). Moreover, PGE2 receptor agonists have been shown to improve bone repair (Tanaka et al., 2004). PGI2 may possess osteogenic properties. PGI2 synthase knockout mice exhibited increased bone formation, resorption, and overall bone mass (Nakalekha et al., 2010). Additionally, the stable PGI2 analog, Iloprost, increased osteogenesis in vitro (Wendler et al., 2019). Also, the AA and DHA epoxides have opposing function in promoting and inhibiting

angiogenesis, respectively (Pozzi et al., 2005; Zhang et al., 2013). Thus, there is a need for comprehensive profiling of oxylipin alteration with AVS severity in order to elucidate the underlying mechanism of this disease.

1.6. References

Abraham, K., Appel, K.E., Berger-Preiss, E., Apel, E., Gerling, S., Mielke, H., Creutzenberg, O., Lampen, A., 2013. Relative oral bioavailability of 3-MCPD from 3-MCPD fatty acid esters in rats. Arch. Toxicol. 87, 649–659. https://doi.org/10.1007/s00204-012-0970-8

Ait-Said, F., Elalamy, I., Werts, C., Gomard, M.T., Jacquemin, C., Couetil, J.P., Hatmi, M., 2003. Inhibition by eicosapentaenoic acid of IL-1β-induced PGHS-2 expression in human microvascular endothelial cells: Involvement of lipoxygenase-derived metabolites and p38 MAPK pathway. Biochim. Biophys. Acta - Mol. Cell Biol. Lipids 1631, 77–84. https://doi.org/10.1016/S1388-1981(02)00358-X

Anwar-Mohamed, A., El-Sherbeni, A., Hee Kim, S., Elshenawy, O.H., Althurwi, H.N., M Zordoky, B.N., S El-Kadi, A.O., 2013. Acute arsenic treatment alters cytochrome P450 expression and arachidonic acid metabolism in lung, liver and kidney of C57Bl/6 mice. Xenobiotica 43, 1366–5928. https://doi.org/10.3109/00498254.2012.754113

Anwar-Mohamed, A., El-Sherbeni, A.A., Kim, S.H., Althurwi, H.N., Zordoky, B.N.M., El-Kadi, A.O.S., 2012. Acute arsenic toxicity alters cytochrome P450 and soluble epoxide hydrolase and their associated arachidonic acid metabolism in C57Bl/6 mouse heart. Xenobiotica 42, 1235–1247. https://doi.org/10.3109/00498254.2012.693971

Anwar-Mohamed, A., Elshenawy, O.H., El-Sherbeni, A.A., Abdelrady, M., El-Kadi, A.O.S., 2014. Acute arsenic treatment alters arachidonic acid and its associated metabolite levels in the brain of C57Bl/6 mice. Can. J. Physiol. Pharmacol. 92, 693–702. https://doi.org/10.1139/cjpp-2014-0136

Artiach, G., Carracedo, M., Plunde, O., Wheelock, C.E., Thul, S., Sjövall, P., Franco-Cereceda, A., Laguna-Fernandez, A., Arnardottir, H., Bäck, M., 2020. Omega-3 Polyunsaturated Fatty Acids Decrease Aortic Valve Disease Through the Resolvin E1 and ChemR23 Axis. Circulation 142, 776–789. https://doi.org/10.1161/CIRCULATIONAHA.119.041868

Aukema, H.M., Ravandi, A., 2023. Factors affecting variability in free oxylipins in mammalian tissues. Curr. Opin. Clin. Nutr. Metab. Care 26, 91–98. https://doi.org/10.1097/MCO.0000000000000892

Baer, I., de la Calle, B., Taylor, P., 2010. 3-MCPD in food other than soy sauce or hydrolysed vegetable protein (HVP). Anal. Bioanal. Chem. 396, 443–456. https://doi.org/10.1007/s00216-009-3177-y

Bal-Price, A., Crofton, K.M., Leist, M., Allen, S., Arand, M., Buetler, T., Delrue, N., FitzGerald, R.E., Hartung, T., Heinonen, T., Hogberg, H., Bennekou, S.H., Lichtensteiger, W., Oggier, D., Paparella, M., Axelstad, M., Piersma, A., Rached, E., Schilter, B., Schmuck, G., Stoppini, L., Tongiorgi, E., Tiramani, M., Monnet-Tschudi, F., Wilks, M.F., Ylikomi, T., Fritsche, E., 2015. International STakeholder NETwork (ISTNET): creating a developmental neurotoxicity (DNT) testing road map for regulatory purposes. Arch. Toxicol. 89, 269–287. https://doi.org/10.1007/S00204-015-1464-2/TABLES/2

Baumgartner, H., Falk, V., Bax, J.J., De Bonis, M., Hamm, C., Holm, P.J., Iung, B., Lancellotti, P., Lansac, E., Muñoz, D.R., Rosenhek, R., Sjögren, J., Tornos Mas, P., Vahanian, A., Walther, T., Wendler, O., Windecker, S., Zamorano, J.L., Roffi, M., Alfieri, O., Agewall, S., Ahlsson, A., Barbato, E., Bueno, H., Collet, J.P., Coman, I.M., Czerny, M., Delgado, V., Fitzsimons, D., Folliguet, T., Gaemperli, O., Habib, G., Harringer, W., Haude, M., Hindricks, G., Katus, H.A., Knuuti, J., Kolh, P., Leclercq, C., McDonagh, T.A., Piepoli, M.F., Pierard, L.A., Ponikowski, P., Rosano, G.M.C., Ruschitzka, F., Shlyakhto, E., Simpson, I.A., Sousa-Uva, M., Stepinska, J., Tarantini, G., Tche, D., Aboyans, V., Kzhdryan, H.K., Mascherbauer, J., Samadov, F., Shumavets, V., Van Camp, G., Loncar, D., Lovric, D., Georgiou, G.M., Linhartova, K., Ihlemann, N., Abdelhamid, M., Pern, T., Turpeinen, A., Srbinovska-Kostovska, E., Cohen, A., Bakhutashvili, Z., Ince, H., Vavuranakis, M., Temesvari, A., Gudnason, T., Mylotte, D., Kuperstein, R., Indolfi, C., Pya, Y., Bajraktari, G., Kerimkulova, A., Rudzitis, A., Mizariene, V., Lebrun, F., Demarco, D.C., Oukerraj, L., Bouma, B.J., Steigen, T.K., Komar, M., De Moura Branco, L.M., Popescu, B.A., Uspenskiy, V., Foscoli, M., Jovovic, L., Simkova, I., Bunc, M., de Prada, J.A.V., Stagmo, M., Kaufmann, B.A., Mahdhaoui, A., Bozkurt, E., Nesukay, E., Brecker, S.J.D., 2017. 2017 ESC/EACTS Guidelines for the management of valvular heart disease. Eur. Heart J. 38, 2739–2786. https://doi.org/10.1093/eurheartj/ehx391

Baumgartner, H., Walther, T., Camm, A.J., Lüscher, T.F., Maurer, G., Serruys, P.W., 2018. ESC CardioMed, 3rd ed, ESC CardioMed. https://doi.org/10.1093/med/9780198784906.001.0001

Becalski, A., Zhao, T., Breton, F., Kuhlmann, J., 2016. 2- and 3-Monochloropropanediols in paper products and their transfer to foods. Food Addit. Contam. Part A 33, 1499–1508. https://doi.org/10.1080/19440049.2016.1223353

Blum, M., Dogan, I., Karber, M., Rothe, M., Schunck, W.H., 2019. Chiral lipidomics of monoepoxy and monohydroxy metabolites derived from long-chain polyunsaturated fatty acids. J. Lipid Res. 60, 135–148. https://doi.org/10.1194/JLR.M089755

Bouchareb, R., Boulanger, M.C., Tastet, L., Mkannez, G., Nsaibia, M.J., Hadji, F., Dahou, A., Messadeq, Y., Arsenault, B.J., Pibarot, P., Bossé, Y., Marette, A., Mathieu, P., 2019. Activated platelets promote an osteogenic programme and the progression of calcific aortic valve stenosis. Eur. Heart J. 40, 1362–1373. https://doi.org/10.1093/EURHEARTJ/EHY696

Bourre, J.M., Francois, M., Youyou, A., Dumont, O., Piciotti, M., Pascal, G., Durand, G., 1989. The effects of dietary α-linolenic acid on the composition of nerve membranes, enzymatic activity, amplitude of electrophysiological parameters, resistance to poisons and performance of learning tasks in rats. J. Nutr. 119, 1880–1892. https://doi.org/10.1093/jn/119.12.1880

Bowler, M.A., Raddatz, M.A., Johnson, C.L., Lindman, B.R., Merryman, W.D., 2019. Celecoxib Is Associated With Dystrophic Calcification and Aortic Valve Stenosis. JACC Basic to Transl. Sci. 4, 135–143. https://doi.org/10.1016/J.JACBTS.2018.12.003

Buczynski, M.W., Dumlao, D.S., Dennis, E.A., 2009. Thematic Review Series: Proteomics. An integrated omics analysis of eicosanoid biology1[S]. J. Lipid Res. 50, 1015–1038. https://doi.org/10.1194/JLR.R900004-JLR200

Buhrke, T., Frenzel, F., Kuhlmann, J., Lampen, A., 2015. 2-Chloro-1,3-propanediol (2-MCPD) and its fatty acid esters: cytotoxicity, metabolism, and transport by human intestinal Caco-2 cells. Arch. Toxicol. 89, 2243–2251. https://doi.org/10.1007/s00204-014-1395-3

Buhrke, T., Schultrich, K., Braeuning, A., Lampen, A., 2017. Comparative analysis of transcriptomic responses to repeated-dose exposure to 2-MCPD and 3-MCPD in rat kidney, liver and testis. Food Chem. Toxicol. 106, 36–46. https://doi.org/10.1016/j.fct.2017.05.028

Caligiuri, S.P.B., Parikh, M., Stamenkovic, A., Pierce, G.N., Aukema, H.M., 2017. Dietary modulation of oxylipins in cardiovascular disease and aging. Am. J. Physiol. - Hear. Circ. Physiol. 313, H903–H918. https://doi.org/10.1152/ajpheart.00201.2017

Cattan, N., Mary, D., Peleraux, A., Mari, B., Aussel, C., Rossi, B., 2000. Prostaglandin B2 delivers a co-stimulatory signal leading to T cell activation. Eur. Cytokine Netw. 11, 293–300.

Cattaneo, I., Astuto, M.C., Binaglia, M., Devos, Y., Dorne, J.L.C.M., Fernandez Agudo, A.,

Fernandez Dumont, A., Garcia-Vello, P., Kass, G.E.N., Lanzoni, A., Liem, A.K.D., Panzarea, M., Paraskevopulos, K., Parra Morte, J.M., Tarazona, J. V., Terron, A., 2023. Implementing New Approach Methodologies (NAMs) in food safety assessments: Strategic objectives and actions taken by the European Food Safety Authority. Trends Food Sci. Technol. 133, 277–290. https://doi.org/10.1016/J.TIFS.2023.02.006

Cayer, L.G.J., 2019. Effects of sub-chronic dietary 2-monochloro-1,3-propanediol on oxidized lipids in rat heart, kidney, serum, and skeletal muscle. University of Manitoba.

Cebo, M., Fu, X., Gawaz, M., Chatterjee, M., Lämmerhofer, M., 2020. Enantioselective ultra-high performance liquid chromatography-tandem mass spectrometry method based on sub-2μm particle polysaccharide column for chiral separation of oxylipins and its application for the analysis of autoxidized fatty acids and platelet releasates. J. Chromatogr. A 1624, 461206. https://doi.org/10.1016/J.CHROMA.2020.461206

Chan, K.L., Teo, K., Dumesnil, J.G., Ni, A., Tam, J., 2010. Effect of lipid lowering with rosuvastatin on progression of aortic stenosis: Results of the aortic stenosis progression observation: Measuring effects of rosuvastatin (Astronomer) trial. Circulation 121, 306–314. https://doi.org/10.1161/CIRCULATIONAHA.109.900027

Choudhary, S., Blackwell, K., Voznesensky, O., Roy, D., Pilbeam, C., Deb Roy, A., Pilbeam, C., 2013. Prostaglandin E2 acts via bone marrow macrophages to block PTH-stimulated osteoblast differentiation in vitro. Bone 56, 31–41. https://doi.org/10.1016/j.bone.2013.04.017

Coecke, S., Pelkonen, O., Leite, S.B., Bernauer, U., Bessems, J.G.M., Bois, F.Y., Gundert-Remy, U., Loizou, G., Testai, E., Zaldívar, J.M., 2013. Toxicokinetics as a key to the integrated toxicity risk assessment based primarily on non-animal approaches. Toxicol. In Vitro 27, 1570–1577. https://doi.org/10.1016/J.TIV.2012.06.012

Coffey, S., Roberts-Thomson, R., Brown, A., Carapetis, J., Chen, M., Enriquez-Sarano, M., Zühlke, L., Prendergast, B.D., 2021. Global epidemiology of valvular heart disease. Nat. Rev. Cardiol. https://doi.org/10.1038/s41569-021-00570-z

Cowell, S.J., Newby, D.E., Prescott, R.J., Bloomfield, P., Reid, J., Northridge, D.B., Boon, N.A., 2005. A Randomized Trial of Intensive Lipid-Lowering Therapy in Calcific Aortic Stenosis. N. Engl. J. Med. 352, 2389–2397. https://doi.org/10.1056/nejmoa043876

Dai, Y., Cheng, Z., Zeng, Z., Hylkema, M.N., Faas, M.M., Huo, X., 2023. A Targeted Lipidomic

Reveals CYP450-Derived Oxylipin Linked to the Inflammatory Response by Polycyclic Aromatic Hydrocarbon Exposure in Children. Expo. Heal. 15, 455–466. https://doi.org/10.1007/S12403-022-00503-2/FIGURES/4

Dennis, E.A., Cao, J., Hsu, Y.H., Magrioti, V., Kokotos, G., 2011. Phospholipase A2 Enzymes: Physical Structure, Biological Function, Disease Implication, Chemical Inhibition, and Therapeutic Intervention. Chem. Rev. 111, 6130. https://doi.org/10.1021/CR200085W

Dorris, S.L., Stokes Peebles Jr, R., 2012. PGI 2 as a Regulator of Inflammatory Diseases. Mediators Inflamm. 2012. https://doi.org/10.1155/2012/926968

Dweck, M.R., Boon, N.A., Newby, D.E., 2012. Calcific aortic stenosis: A disease of the valve and the myocardium. J. Am. Coll. Cardiol. 60, 1854–1863. https://doi.org/10.1016/j.jacc.2012.02.093

EPA, 2024. EPA Releases Updated New Approach Methodologies (NAMs) Work Plan [WWW Document]. URL https://www.epa.gov/sciencematters/epa-releases-updated-new-approach-methodologies-nams-work-plan

European Food Safety Authority, 2018. Update of the risk assessment on 3-monochloropropane diol and its fatty acid esters. EFSA J. https://doi.org/10.2903/j.efsa.2018.5083

European Food Safety Authority, 2016. Risks for human health related to the presence of 3- and 2-monochloropropanediol (MCPD), and their fatty acid esters, and glycidyl fatty acid esters in food. EFSA J. 14, e04426. https://doi.org/10.2903/j.efsa.2016.4426

Farrés, M., Platikanov, S., Tsakovski, S., Tauler, R., 2015. Comparison of the variable importance in projection (VIP) and of the selectivity ratio (SR) methods for variable selection and interpretation. J. Chemom. 29, 528–536. https://doi.org/10.1002/cem.2736

Ferdouse, A., Leng, S., Winter, T., Aukema, H.M., 2019. Dietary n-6 and n-3 PUFA alter the free oxylipin profile differently in male and female rat hearts. Br. J. Nutr. 122, 252–261. https://doi.org/10.1017/S0007114519001211

Frei, H., Würgler, F.E., 1997. The vicinal chloroalcohols 1,3-dichloro-2-propanol (DC2P), 3-chloro-1,2-propanediol (3CPD) and 2-chloro-1,3-propanediol (2CPD) are not genotoxic in vivo in the wing spot test of Drosophila melanogaster. Mutat. Res. Toxicol. Environ. Mutagen. 394, 59–68. https://doi.org/10.1016/S1383-5718(97)00125-3

Fu, W.S., Zhao, Y., Zhang, G., Zhang, L., Li, J.G., Tang, C.D., Miao, H., Bo, J., Zhang, Q., Wu, Y.N., 2007. Occurrence of chloropropanols in soy sauce and other foods in China between

2002 and 2004. Food Addit. Contam. 24, 812–819. https://doi.org/10.1080/02652030701246039

Funk CD, 2001. Prostaglandins and leukotrienes: advances in eicosanoid biology. Science (80-.). 294, 1871–1875.

Gabbs, M., Leng, S., Devassy, J.G., Monirujjaman, M.M., Aukema, H.M., Leng, S., Gabbs, M., 2015. Advances in Our Understanding of Oxylipins Derived from Dietary PUFAs. Adv. Nutr. An Int. Rev. J. 6, 513–540. https://doi.org/10.3945/an.114.007732

Gladine, C., Ostermann, A.I., Newman, J.W., Schebb, N.H., 2019. MS-based targeted metabolomics of eicosanoids and other oxylipins: Analytical and inter-individual variabilities. Free Radic. Biol. Med. 144, 72–89. https://doi.org/10.1016/J.FREERADBIOMED.2019.05.012

Grear, T., Avery, C., Patterson, J., Jacobs, D.J., 2021. Molecular function recognition by supervised projection pursuit machine learning. Sci. Rep. 11, 4247. https://doi.org/10.1038/s41598-021-83269-y

Grim, J.C., Aguado, B.A., Vogt, B.J., Batan, D., Andrichik, C.L., Schroeder, M.E., Gonzalez-Rodriguez, A., Yavitt, F.M., Weiss, R.M., Anseth, K.S., 2020. Secreted Factors From Proinflammatory Macrophages Promote an Osteoblast-Like Phenotype in Valvular Interstitial Cells. Arterioscler. Thromb. Vasc. Biol. 40, E296–E308. https://doi.org/10.1161/ATVBAHA.120.315261

Hall, L.M., Murphy, R.C., 1998. Electrospray mass spectrometric analysis of 5-hydroperoxy and 5-hydroxyeicosatetraenoic acids generated by lipid peroxidation of red blood cell ghost phospholipids. J. Am. Soc. Mass Spectrom. 9, 527–532. https://doi.org/10.1016/S1044-0305(98)00013-0

Hamlet, C.G., Sadd, P.A., Crews, C., Velíšek, J., Baxter, D.E., 2002. Occurrence of 3-chloro-propane-1,2-diol (3-MCPD) and related compounds in foods: A review. Food Addit. Contam. 19, 619–631. https://doi.org/10.1080/02652030210132391

Hartung, T., 2009. Toxicology for the twenty-first century. Nat. 2009 4607252 460, 208–212. https://doi.org/10.1038/460208A

Hasin, Y., Seldin, M., Lusis, A., 2017. Multi-omics approaches to disease. Genome Biol. https://doi.org/10.1186/s13059-017-1215-1

Health Canada, 2023. Use of new approach methods (NAMs) in risk assessment [WWW

Document]. URL https://www.canada.ca/en/health-canada/services/chemical-substances/fact-sheets/use-new-approach-methods-risk-assessment.html

Hodgson, E., 2004. A Textbook of Modern Toxicology, Third. ed. John Wiley & Sons, Inc., Hoboken, New Jersey. https://doi.org/DOI:10.1002/0471646776

Honn, K. V., Nelson, K.K., Renaud, C., Bazaz, R., Diglio, C.A., Timar, J., 1992. Fatty acid modulation of tumor cell adhesion to microvessel endothelium and experimental metastasis. Prostaglandins 44, 413–429. https://doi.org/10.1016/0090-6980(92)90137-I

Huang, Y., Rajput, I.R., Sanganyado, E., Yajing, S., Yu, F., Liang, B., Liu, W., 2020. Immune stimulation effect of PBDEs via prostaglandin pathway in pantropical spotted dolphin: An in vitro study. Chemosphere 254, 126717. https://doi.org/10.1016/j.chemosphere.2020.126717

Hulin, A., Hego, A., Lancellotti, P., Oury, C., 2018. Advances in Pathophysiology of Calcific Aortic Valve Disease Propose Novel Molecular Therapeutic Targets. Front. Cardiovasc. Med. https://doi.org/10.3389/fcvm.2018.00021

Imig, J.D., Walsh, K.A., Khan, M.A.H., Nagasawa, T., Cherian-Shaw, M., Shaw, S.M., Hammock, B.D., 2012. Soluble epoxide hydrolase inhibition and peroxisome proliferator activated receptor γ agonist improve vascular function and decrease renal injury in hypertensive obese rats. https://doi.org/10.1258/ebm.2012.012225 237, 1402–1412. https://doi.org/10.1258/EBM.2012.012225

International Agency for Research on Cancer, 2013. Some chemicals present in industrial and consumer products, food and drinking-water. IARC Monogr. Eval. Carcinog. Risks Hum.

Iung, B., Baron, G., Butchart, E.G., Delahaye, F., Gohlke-Bärwolf, C., Levang, O.W., Tornos, P., Vanoverschelde, J.L., Vermeer, F., Boersma, E., Ravaud, P., Vahanian, A., 2003. A prospective survey of patients with valvular heart disease in Europe: The Euro Heart Survey on valvular heart disease. Eur. Heart J. 24, 1231–1243. https://doi.org/10.1016/S0195-668X(03)00201-X

Joint FAO/WHO Expert Committee on Food Additives, 2017. Evaluation of certain contaminants in food, WHO Technical Report Series.

Kaze, N., Watanabe, Y., Sato, H., Murota, K., Kotaniguchi, M., Yamamoto, H., Inui, H., Kitamura, S., 2016. Estimation of the Intestinal Absorption and Metabolism Behaviors of 2- and 3-Monochloropropanediol Esters. Lipids 51, 913–922. https://doi.org/10.1007/s11745-

016-4143-z

Kenkel, N.C., 2006. On selecting an appropriate multivariate analysis. Can. J. Plant Sci. 86, 663–676. https://doi.org/10.4141/P05-164

Knoll, M., Lodish, H.F., Sun, L., 2015. Long non-coding RNAs as regulators of the endocrine system. Nat. Rev. Endocrinol. https://doi.org/10.1038/nrendo.2014.229

Kobayashi, Y., Mizoguchi, T., Take, I., Kurihara, S., Udagawa, N., Takahashi, N., 2005. Prostaglandin E2 enhances osteoclastic differentiation of precursor cells through protein kinase A-dependent phosphorylation of TAK1. J. Biol. Chem. 280, 11395–11403. https://doi.org/10.1074/jbc.M411189200

Koshihara, Y., Kawamura, M., 1989. Prostaglandin D2 stimulates calcification of human osteoblastic cells. Biochem. Biophys. Res. Commun. 159, 1206–1212. https://doi.org/10.1016/0006-291X(89)92238-9

Kruger, M.C., Coetzee, M., Haag, M., Weiler, H., 2010. Long-chain polyunsaturated fatty acids: Selected mechanisms of action on bone. Prog. Lipid Res. 49, 438–449. https://doi.org/10.1016/j.plipres.2010.06.002

Kuhlmann, J., 2016. Analysis and occurrence of dichloropropanol fatty acid esters and related process-induced contaminants in edible oils and fats. Eur. J. Lipid Sci. Technol. 118, 382–395. https://doi.org/10.1002/ejlt.201400518

Kuhn, H., Banthiya, S., Van Leyen, K., 2015. Mammalian lipoxygenases and their biological relevance. Biochim. Biophys. Acta - Mol. Cell Biol. Lipids 1851, 308–330. https://doi.org/10.1016/J.BBALIP.2014.10.002

Leitch, A.G., Lee, T.H., Ringel, E.W., Prickett, J.D., Robinson, D.R., Pyne, S.G., Corey, E.J., Drazen, J.M., Austen, K.F., Lewis, R.A., 1984. Immunologically induced generation of tetraene and pentaene leukotrienes in the peritoneal cavities of menhaden-fed rats. J. Immunol. 132.

Leng, S., Winter, T., Aukema, H.M., 2018. Dietary ALA, EPA and DHA have distinct effects on oxylipin profiles in female and male rat kidney, liver and serum. J. Nutr. Biochem. 57, 228–237. https://doi.org/10.1016/J.JNUTBIO.2018.04.002

Li, Y., Zhang, Z., Jiang, S., Xu, F., Tulum, L., Li, K., Liu, S., Li, S., Chang, L., Liddell, M., Tu, F., Gu, X., Carmichael, P.L., White, A., Peng, S., Zhang, Q., Li, J., Zuo, T., Kukic, P., Xu, P., 2023. Using transcriptomics, proteomics and phosphoproteomics as new approach

methodology (NAM) to define biological responses for chemical safety assessment. Chemosphere 313, 137359. https://doi.org/10.1016/J.CHEMOSPHERE.2022.137359

Lien, E.L., Boyle, F.G., Wrenn, J.M., Perry, R.W., Thompson, C.A., Borzelleca, J.F., 2001. Comparison of AIN-76A and AIN-93G diets: A 13-week study in rats. Food Chem. Toxicol. 39, 385–392. https://doi.org/10.1016/S0278-6915(00)00142-3

Mackie, A., Mulet-Cabero, A.I., Torcello-Gomez, A., 2020. Simulating human digestion: developing our knowledge to create healthier and more sustainable foods. Food Funct. 11, 9397–9431. https://doi.org/10.1039/D0FO01981J

Massart, D.L., Vandeginste, B.G.M., Buydens, L.M.C., DeJong, S., Lewi, P.J., Smeyers-Verbeke, J., 1997. Handbook of Chemometrics and Qualimetrics: Part A, 1st ed. Elsevier, Amsterdam.

Mazaleuskaya, L.L., Salamatipour, A., Sarantopoulou, D., Weng, L., FitzGerald, G.A., Blair, I.A., Mesaros, C., 2018. Analysis of HETEs in human whole blood by chiral UHPLC-ECAPCI/HRMS. J. Lipid Res. 59, 564–575. https://doi.org/10.1194/jlr.D081414

Messika-Zeitoun, D., Bielak, L.F., Peyser, P.A., Sheedy, P.F., Turner, S.T., Nkomo, V.T., Breen, J.F., Maalouf, J., Scott, C., Tajik, A.J., Enriquez-Sarano, M., 2007. Aortic valve calcification: Determinants and progression in the population. Arterioscler. Thromb. Vasc. Biol. 27, 642–648. https://doi.org/10.1161/01.ATV.0000255952.47980.c2

Mohler, E.R., Gannon, F., Reynolds, C., Zimmerman, R., Keane, M.G., Kaplan, F.S., 2001. Bone formation and inflammation in cardiac valves. Circulation 103, 1522–1528. https://doi.org/10.1161/01.CIR.103.11.1522

Nagy, E., Andersson, D.C., Caidahl, K., Eriksson, M.J., Eriksson, P., Franco-Cereceda, A., Hansson, G.K., Bäck, M., 2011. Upregulation of the 5-lipoxygenase pathway in human aortic valves correlates with severity of stenosis and leads to leukotriene-induced effects on valvular myofibroblasts. Circulation 123, 1316–1325. https://doi.org/10.1161/CIRCULATIONAHA.110.966846

Nakalekha, C., Yokoyama, C., Miura, H., Alles, N., Aoki, K., Ohya, K., Morita, I., 2010. Increased bone mass in adult prostacyclin-deficient mice. J. Endocrinol. 204, 125–133. https://doi.org/10.1677/JOE-09-0376

Nathaniel, D.J., Evans, J.F., Leblanc, Y., Léveillé, C., Fitzsimmons, B.J., Ford-Hutchinson, A.W., 1985. Leukotriene A5 is a substrate and an inhibitor of rat and human neutrophil

LTA4 hydrolase. Biochem. Biophys. Res. Commun. 131, 827–835. https://doi.org/10.1016/0006-291X(85)91314-2

Nathaniel, S., Saligram, S., Innasimthu, A.L., 2010. Aortic stenosis: An update. World J. Cardiol. 2, 135–139. https://doi.org/10.4330/wjc.v2.i6.135

Nkomo, V.T., Gardin, J.M., Skelton, T.N., Gottdiener, J.S., Scott, C.G., Enriquez-Sarano, M., 2006. Burden of valvular heart diseases: a population-based study. Lancet 368, 1005–1011. https://doi.org/10.1016/S0140-6736(06)69208-8

OECD, 2023. OECD Releases new Test Guidelines for NAMs in 2023 [WWW Document]. URL https://www.icapo.org/news/oecd-releases-new-test-guidelines-nams-2023

OECD, 2017. Guidance Document for the Use of Adverse Outcome Pathways in Developing Integrated Approaches to Testing and Assessment (IATA), OECD Series on Testing and Assessment. OECD Publishing, Paris. https://doi.org/10.1787/44bb06c1-en

Oliveira, R. V, Valéria, A., Simionato, C., Cass, Q.B., Tiritan, E., Pinto, M., Sofia, C., Fernandes, G., 2021. Enantioselectivity Effects in Clinical Metabolomics and Lipidomics. Mol. 2021, Vol. 26, Page 5231 26, 5231. https://doi.org/10.3390/MOLECULES26175231

Ostermann, A.I., Willenberg, I., Schebb, N.H., 2015. Comparison of sample preparation methods for the quantitative analysis of eicosanoids and other oxylipins in plasma by means of LC-MS/MS. Anal. Bioanal. Chem. 407, 1403–1414. https://doi.org/10.1007/S00216-014-8377-4/FIGURES/3

Pozzi, A., Macias-Perez, I., Abair, T., Wei, S., Su, Y., Zent, R., Falck, J.R., Capdevila, J.H., 2005. Characterization of 5,6- and 8,9-epoxyeicosatrienoic acids (5,6- and 8,9-EET) as potent in vivo angiogenic lipids. J. Biol. Chem. 280, 27138–27146. https://doi.org/10.1074/jbc.M501730200

Qi, Y., 2012. Random Forest for Bioinformatics, in: Ensemble Machine Learning. Springer US, pp. 307–323. https://doi.org/10.1007/978-1-4419-9326-7_11

Rajamannan, N.M., Subramaniam, M., Caira, F., Stock, S.R., Spelsberg, T.C., 2005. Atorvastatin inhibits hypercholesterolemia-induced calcification in the aortic valves via the Lrp5 receptor pathway. Circulation 112. https://doi.org/10.1161/01.CIRCULATIONAHA.104.524306

Raju, J., Roberts, J., Kocmarek, A.L., Fine, J., 2016. Toxicology of 2-monochloro-1,3-propanediol (2-MCPD) in F344 rats: 28-days dietary study.

Raju, J., Roberts, J., Patry, D., Caldwell, D., Curran, I., Mehta, R., 2019. Toxicology of 2-monochloro-1-3, propanediol (2-MCPD) in F344 rats: 90-days sub-chronic exposure study.

Reeves, P.G., Nielsen, F.H., Fahey, G.C., 1993. AIN-93 Purified Diets for Laboratory Rodents: Final Report of the American Institute of Nutrition Ad Hoc Writing Committee on the Reformulation of the AIN-76A Rodent Diet. J. Nutr. 123, 1939–1951. https://doi.org/10.1093/jn/123.11.1939

Ricciotti, E., Fitzgerald, G.A., 2011. Prostaglandins and Inflammation. Arterioscler. Thromb. Vasc. Biol. 31, 986–1000. https://doi.org/10.1161/ATVBAHA.110.207449

Rosenhek, R., Baumgartner, H., 2008. Aortic sclerosis, aortic stenosis and lipid-lowering therapy. Expert Rev. Cardiovasc. Ther. https://doi.org/10.1586/14779072.6.3.385

Rossebø, A.B., Pedersen, T.R., Boman, K., Brudi, P., Chambers, J.B., Egstrup, K., Gerdts, E., Gohlke-Bärwolf, C., Holme, I., Kesäniemi, Y.A., Malbecq, W., Nienaber, C.A., Ray, S., Skjærpe, T., Wachtell, K., Willenheimer, R., 2008. Intensive Lipid Lowering with Simvastatin and Ezetimibe in Aortic Stenosis. N. Engl. J. Med. 359, 1343–1356. https://doi.org/10.1056/NEJMoa0804602

Ruiz-Perez, D., Narasimhan, G., 2017. So you think you can PLS-DA? bioRxiv. https://doi.org/https://doi.org/10.1101/207225

Schilter, B., Scholz, G., Seefelder, W., 2011. Fatty acid esters of chloropropanols and related compounds in food: Toxicological aspects. Eur. J. Lipid Sci. Technol. 113, 309–313. https://doi.org/10.1002/ejlt.201000311

Schneider, J.F., Becalski, A., Zhao, T., Chen, F., Liao, Y., Rawn, D.F.K., 2022. Occurrence of 2- and 3-monochloropropanediol esters (MCPDE) in infant formula products on the Canadian market between 2015 and 2019. Food Addit. Contam. - Part A 39, 1663–1673. https://doi.org/10.1080/19440049.2022.2104934

Schultrich, K., Frenzel, F., Oberemm, A., Buhrke, T., Braeuning, A., Lampen, A., 2017. Comparative proteomic analysis of 2-MCPD- and 3-MCPD-induced heart toxicity in the rat. Arch. Toxicol. 91, 3145–3155. https://doi.org/10.1007/s00204-016-1927-0

Serhan, C.N., 2014. Pro-resolving lipid mediators are leads for resolution physiology. Nature 510, 92–101. https://doi.org/10.1038/nature13479

Šmidrkal, J., Tesařová, M., Hrádková, I., Berčíková, M., Adamčíková, A., Filip, V., 2016. Mechanism of formation of 3-chloropropan-1,2-diol (3-MCPD) esters under conditions of

the vegetable oil refining. Food Chem. 211, 124–129. https://doi.org/10.1016/j.foodchem.2016.05.039

Stewart, B.F., Siscovick, D., Lind, B.K., Gardin, J.M., Gottdiener, J.S., Smith, V.E., Kitzman, D.W., Otto, C.M., 1997. Clinical factors associated with calcific aortic valve disease. J. Am. Coll. Cardiol. 29, 630–634. https://doi.org/10.1016/S0735-1097(96)00563-3

Subramanian, A., Tamayo, P., Mootha, V.K., Mukherjee, S., Ebert, B.L., Gillette, M.A., Paulovich, A., Pomeroy, S.L., Golub, T.R., Lander, E.S., Mesirov, J.P., 2005. Gene set enrichment analysis: A knowledge-based approach for interpreting genome-wide expression profiles. Proc. Natl. Acad. Sci. U. S. A. 102, 15545–15550. https://doi.org/10.1073/pnas.0506580102

Suzuki, K., Takahashi, S., Watanabe, K., Fujioka, D., Nakamura, T., Obata, J.-E.E., Kawabata, K.-I.I., Katoh, R., Matsumoto, M., Kugiyama, K., 2014. The expression of groups IIE and V phospholipase A2 is associated with an increased expression of osteogenic molecules in human calcified aortic valves. J. Atheroscler. Thromb. 21, 1308–1325. https://doi.org/10.5551/jat.24273

Taguchi, Y. -h., Oono, Y., 2005. Relational patterns of gene expression via non-metric multidimensional scaling analysis. Bioinformatics 21, 730–740. https://doi.org/10.1093/bioinformatics/bti067

Take, I., Kobayashi, Y., Yamamoto, Y., Tsuboi, H., Ochi, T., Uematsu, S., Okafuji, N., Kurihara, S., Udagawa, N., Takahashi, N., 2005. Prostaglandin E2 Strongly Inhibits Human Osteoclast Formation. Endocrinology 146, 5204–5214. https://doi.org/10.1210/EN.2005-0451

Tanaka, M., Sakai, A., Uchida, S., Tanaka, S., Nagashima, M., Katayama, T., Yamaguchi, K., Nakamura, T., 2004. Prostaglandin E2 receptor (EP4) selective agonist (ONO-4819.CD) accelerates bone repair of femoral cortex after drill-hole injury associated with local upregulation of bone turnover in mature rats. Bone 34, 940–948. https://doi.org/10.1016/J.BONE.2004.01.002

Terano, T., Salmon, J.A., Moncada, S., 1984. Biosynthesis and biological activity of leukotriene B5. Prostaglandins 27, 217–232. https://doi.org/10.1016/0090-6980(84)90075-3

Theken, K.N., Schuck, R.N., Edin, M.L., Tran, B., Ellis, K., Bass, A., Lih, F.B., Tomer, K.B., Poloyac, S.M., Wu, M.C., Hinderliter, A.L., Zeldin, D.C., Stouffer, G.A., Lee, C.R., 2012.

Evaluation of cytochrome P450-derived eicosanoids in humans with stable atherosclerotic cardiovascular disease. Atherosclerosis 222, 530–536. https://doi.org/10.1016/j.atherosclerosis.2012.03.022

van Bergen, C.A., Collier, P.D., Lucas, R.A., Preston, H.D., Sissons, D.J., 1992. Determination of chloropropanols in protein hydrolysates. J. Chromatogr. A 589, 109–119. https://doi.org/10.1016/0021-9673(92)80011-I

Van Der Linde, D., Yap, S.C., Van Dijk, A.P.J., Budts, W., Pieper, P.G., Van Der Burgh, P.H., Mulder, B.J.M., Witsenburg, M., Cuypers, J.A.A.E., Lindemans, J., Takkenberg, J.J.M., Roos-Hesselink, J.W., 2011. Effects of rosuvastatin on progression of stenosis in adult patients with congenital aortic stenosis (PROCAS Trial). Am. J. Cardiol. 108, 265–271. https://doi.org/10.1016/j.amjcard.2011.03.032

Waclawiková, B., Codutti, A., Alim, K., El Aidy, S., 2022. Gut microbiota-motility interregulation: insights from in vivo, ex vivo and in silico studies. Gut Microbes 14. https://doi.org/10.1080/19490976.2021.1997296

Wendler, S., Schlundt, C., Bucher, C.H., Birkigt, J., Schipp, C.J., Volk, H.D., Duda, G.N., Schmidt-Bleek, K., 2019. Immune modulation to enhance bone healing-a new concept to induce bone using prostacyclin to locally modulate immunity. Front. Immunol. 10, 713. https://doi.org/10.3389/FIMMU.2019.00713/BIBTEX

Wirrig, E.E., Gomez, M.V., Hinton, R.B., Yutzey, K.E., 2015. COX2 inhibition reduces aortic valve calcification in vivo. Arterioscler. Thromb. Vasc. Biol. 35, 938–947. https://doi.org/10.1161/ATVBAHA.114.305159

Wöhrlin, F., Fry, H., Lahrssen-Wiederholt, M., Preiß-Weigert, A., 2015. Occurrence of fatty acid esters of 3-MCPD, 2-MCPD and glycidol in infant formula. Food Addit. Contam. Part A 32, 1810–1822. https://doi.org/10.1080/19440049.2015.1071497

Worley, B., Powers, R., 2013. Multivariate Analysis in Metabolomics. Curr. Metabolomics 1, 92–107. https://doi.org/10.2174/2213235x11301010092

Wu, S., Zhou, X., Qin, W., An, X., Wang, F., Lv, L., Tang, T., Liu, X., He, Y., 2023. Prostaglandin Metabolome Profiles in Zebrafish (Danio rerio) Exposed to Acetochlor and Butachlor. Int. J. Mol. Sci. 24, 3488. https://doi.org/10.3390/IJMS24043488/S1

Wu, X., Yang, J., Morisseau, C., Robertson, L.W., Hammock, B., Lehmler, H.J., 2016. 3,3’,4,4’,5-pentachlorobiphenyl (PCB 126) decreases hepatic and systemic ratios of epoxide

to diol metabolites of unsaturated fatty acids in male rats. Toxicol. Sci. 152, 309–322. https://doi.org/10.1093/toxsci/kfw084

Xie, C., Jauhari, S., Mora, A., 2021. Popularity and performance of bioinformatics software: the case of gene set analysis. BMC Bioinformatics 22, 1–16. https://doi.org/10.1186/S12859-021-04124-5/FIGURES/2

Yamazato, R., Yamamoto, H., Tadehara, F., Teragawa, H., Kurisu, S., Dohi, Y., Ishibashi, K., Kunita, E., Utsunomiya, H., Oka, T., Kihara, Y., 2012. Association between aortic valve calcification and myocardial ischemia, especially in asymptomatic patients. J. Nucl. Med. 53, 1216–1221. https://doi.org/10.2967/jnumed.111.099275

Yang, Y., Wu, W., Wu, A., 2019. Toxicity Evaluation Using Animal and Cell Models, in: Food Safety & Mycotoxins. Springer Singapore, Singapore, pp. 33–64. https://doi.org/10.1007/978-981-32-9038-9_3

Yao, C., Narumiya, S., 2019. Prostaglandin-cytokine crosstalk in chronic inflammation. Br. J. Pharmacol. 176, 337–354. https://doi.org/10.1111/BPH.14530

Yost, R.A., Enke, C.G., 1979. Triple quadrupole mass spectrometry for direct mixture analysis and structure elucidation. Anal. Chem. 51, 1251–1264. https://doi.org/10.1021/ac50048a002

Yu, H., Samuels, D.C., Zhao, Y. yong, Guo, Y., 2019. Architectures and accuracy of artificial neural network for disease classification from omics data. BMC Genomics 20, 1–12. https://doi.org/10.1186/s12864-019-5546-z

Zelinková, Z., Svejkovská, B., Velíšek, J., Doležal, M., Zelinkov, Z., Svejkovsk, B., Vel, J., Ek, Š., Dolež Al, M., 2006. Fatty acid esters of 3-chloropropane-1,2-diol in edible oils. Food Addit. Contam. 2312, 1290–1298. https://doi.org/10.1080/02652030600887628

Zhang, G., Panigrahy, D., Mahakian, L.M., Yang, J., Liu, J.Y., Lee, K.S.S., Wettersten, H.I., Ulu, A., Hu, X., Tam, S., Hwang, S.H., Ingham, E.S., Kieran, M.W., Weiss, R.H., Ferrara, K.W., Hammock, B.D., 2013. Epoxy metabolites of docosahexaenoic acid (DHA) inhibit angiogenesis, tumor growth, and metastasis. Proc. Natl. Acad. Sci. U. S. A. 110, 6530–6535. https://doi.org/10.1073/pnas.1304321110

Zheng, K.H., Tzolos, E., Dweck, M.R., 2020. Pathophysiology of Aortic Stenosis and Future Perspectives for Medical Therapy. Cardiol. Clin. 38, 1–12. https://doi.org/10.1016/j.ccl.2019.09.010

Žuvela, P., Skoczylas, M., Jay Liu, J., Bączek, T., Kaliszan, R., Wong, M.W., Buszewski, B., 2019. Column Characterization and Selection Systems in Reversed-Phase High-Performance Liquid Chromatography. Chem. Rev. 119, 3674–3729.

Chapter 2: Rationale, Hypotheses, and Objectives

2.1. Rationale

The overall rationale for this thesis is based in the need to enhance our understanding of complex biological systems, particularly through the use of oxylipin analyses. The field of oxylipin research explores a class of lipid molecules with diverse bioactivities, presenting a unique opportunity to uncover novel insights into an array of homeostatic processes and pathological states. The ability to comprehensively profile oxylipins, however, presents challenges regarding the analysis of the vast data produced. Thus, there is a need for effective data analysis in order to make valuable contributions to the research landscape.

This thesis demonstrates how the interpretation of omics data can be enhanced through the integration of oxylipin data with other data layers. Despite significant advancements in omics technologies, the integration of lipidomics with genomics, proteomics, and clinical data is not yet standard practice. This thesis posits that a comprehensive, integrative approach, which utilizes MSM, can yield deeper insights into how oxylipins influence disease mechanisms and responses to treatments.

The individual studies presented in this thesis have their own specific rationales. For Study A, there is a need to characterize the biological effects of 2-MCPD toxicity. The mechanisms of action of 2-MCPD are poorly understood, thus it is crucial to fill this data gap and enable effective regulatory chemical hazard assessments. The analysis of multiple biological layers using transcriptomics, proteomics, and targeted lipidomics was selected to capture a broad spectrum of biological alterations induced by 2-MCPD exposure, enabling the identification of disrupted pathways and biomolecular interactions. While transcriptomics and proteomics are well-established methodologies in toxicology that can provide valuable insights into gene and protein changes, the inclusion of oxylipin analysis was desired because previous studies have now identified oxylipins and the enzymes that produce them to be altered by other toxic exposures (Anwar-Mohamed et al., 2014, 2013, 2012; Dai et al., 2023; Huang et al., 2020; Wu et al., 2023, 2016), and oxylipins mediate multiple cellular function relevant to 2-MCPD toxicity, including inflammation and fibrosis (Gabbs et al., 2015; Li et al., 2021). The integration of the data layers collected enabled a robust analysis, with findings from each layer providing valuable

results but also enriching the interpretations of the other layers, ultimately providing important data for future hazard assessment of 2-MCPD.

For Study B, the rationale largely centers on following-up from our previous oxylipin analysis that showed a significant decrease in DHA-derived oxylipins in the 2-MCPD-exposed rodent heart (Cayer, 2019). The use of corn oil in the rodent diet, which is deficient in essential n-3 PUFA, likely contributed to overall low levels of n-3 oxylipins because dietary n-3 PUFA has been shown to modulate cardiac oxylipins (Ferdouse et al., 2019). Given the known cardiovascular benefits of n-3 PUFA and their oxylipins (Caligiuri et al., 2017), there is a need to investigate whether adequate dietary n-3 PUFA can mitigate the cardiotoxic effects of 2-MCPD. Thus, the rationale for Study A of elucidating the mechanisms of action of 2-MCPD also applies to Study B. Study B aimed to explore these effects under different conditions, specifically by employing a different rodent strain and a shorter treatment duration. This approach was taken to investigate the impact of more acute exposure to 2-MCPD, thereby providing insights into the immediate biological responses and alterations in oxylipin profiles triggered by short-term exposure. Additionally, Study B was designed to address limitations identified in Study A concerning dietary influences on oxylipin dynamics. The inclusion of dietary alpha-linolenic acid (ALA) adequacy in the experimental design was specifically intended to assess how dietary ALA, an essential n-3 polyunsaturated fatty acid, affects the oxylipin milieu in the context of 2-MCPD exposure. The focus on dietary intervention reflects a growing interest in understanding how nutrition can modulate the body's response to environmental toxins and contribute to protective mechanisms at a molecular level.

The rationale for Study C is based in the growing body of evidence suggesting that oxylipins may play crucial roles in the pathophysiology of AVS. Given the prevalence of AVS, there is a critical need to identify reliable biomarkers and develop targeted therapeutic interventions to reduce the suffering of patients and burden on healthcare systems. Oxylipin producing enzymes and some oxylipins have been identified as being perturbed in calcified AV tissue (Artiach et al., 2020; Nagy et al., 2011; Suzuki et al., 2014; Wirrig et al., 2015). Furthermore, oxylipins mediate various pathological processes involved in AVS, such as inflammation, calcification, and fibrosis (Gabbs et al., 2015; Koshihara and Kawamura, 1989; Kruger et al., 2010; Quarles et al., 1993; Sato et al., 2003; Yao and Narumiya, 2019). Thus,

oxylipins are apt candidates for exploration given that there is a significant clinical interest in identifying new biomarkers and therapeutic targets of AVS.

2.2. Hypotheses

The general hypotheses which underpin these three studies are that:

- Whole profiles of the target molecules will be distinguishable between experimental groups.
- The integration of data from different molecular classes, different tissues, or clinical patient data will provide additional interpretive capabilities to these studies.

The individual studies also have specific hypotheses. For Study A, it was hypothesized that:

- Transcriptomic, proteomic, and oxylipin alterations will occur in the 2-MCPD exposed rodent heart.
- The cardiac genes, proteins, and oxylipin alterations will be related to upregulated inflammation, vacuolation, fibrosis, and necrosis.

For Study B, it was hypothesized that:

- Dietary 2-MCPD exposure will induce alterations to oxylipins in the rodent heart, but the effects will be less pronounced with adequate dietary ALA compared to an ALA deficient diet.
- Heart oxylipins will be altered by dietary 2-MCPD exposure, such that the exposed rodent hearts will have lower levels of n-3 PUFA derived oxylipins.
- Heart oxylipin profiles will differ between diet groups, such that those fed adequate ALA will have higher levels of n-3 derived oxylipins compared to those fed an ALA deficient diet.
- Regardless of whether nephrotoxic effects are manifested at the dose provided, oxylipin alterations related to oxidative stress response will be detected.

For Study C, it is hypothesized that:

- AV leaflet oxylipin profiles will differ with AVS severity.
- Pro-inflammatory oxylipins will be elevated and anti-inflammatory oxylipins will be decreased with AVS severity.
- Pro-calcific oxylipins prostanoids will increase with AVS severity.

2.3. Objectives

The overarching objectives of the thesis are to:

- Utilize MSM to compare omics data between experimental groups or between disease severity.
- Enhance the statistical analysis of oxylipin data by integrating data from other molecular classes, oxylipin data from other tissues, and clinical data.

For Study A, the specific objectives are to:

- Determine alterations in cardiac transcriptomic, proteomic, and oxylipin data from F344 rats sub-chronically exposed to 2-MCPD.
- Integrate the transcriptomic, proteomic, and oxylipin data using MSM to identify physiological pathways altered by 2-MCPD exposure.

For Study B, the specific objectives are to:

- Quantify heart, kidney, liver, and serum oxylipins of rats fed experimental diets with and without acute 2-MCPD exposure and with and without adequate dietary ALA.
- Systematically compare oxylipin profiles and individual oxylipins to determine differences between experimental groups to identify the key oxylipins or sub-classes of oxylipins altered by the experimental treatments.

For Study C, the specific objectives are to:

- Quantify and compare human AV leaflet and plasma oxylipins by AVS severity.
- Identifying the individual oxylipins or subclasses that correlate with AVS severity.
- Combine oxylipin data with clinical data to strengthen the model and identify novel associations.

2.4. Chapter Transition

From the rationale, hypotheses, and objectives that underpin this thesis, we now transition to the first study, which leveraged the integration of multiple layers of biomolecular data using MSM to achieve robust data analysis.

Study A was designed to elucidate the molecular alterations underlying 2-MCPD cardiotoxicity. The study utilized a multi-omics approach, that integrated transcriptomics, proteomics, and a targeted lipidomics of oxylipins to provide an extensive characterization of the alterations from homeostasis induced by 2-MCPD exposure. This comprehensive methodology not only provided valuable data for future hazard assessment of 2-MCPD but also demonstrated the utility of including oxylipin analyses into multi-omics study designs.

Chapter 3: Study A: An integrated multi-omics analysis of the effects of the food processing-induced contaminant 2-monochloropropane-1,3-diol (2-MCPD) in rat heart

Authors: Lucien GJ Cayer[1,2], Thorsten Buhrke[3], Katharina Sommerkorn[3], Anna Reinhold[3], Jennifer Roberts[4], Albert Braeuning[3], Jayadev Raju[1,4], Harold M Aukema[1,2], Tobias Karakach[1,5]

[1]Food and Human Nutritional Sciences, University of Manitoba, Winnipeg, MB, Canada;
[2]Canadian Centre for Agri-Food Research in Health and Medicine, St Boniface Hospital Albrechtsen Research Centre, Winnipeg, MB, Canada;
[3]German Federal Institute for Risk Assessment, Department of Food Safety, Berlin, Germany;
[4]Health Canada, Bureau of Chemical Safety, Ottawa, Canada;
[5]Pharmacology, Dalhousie University, Halifax, NS, Canada.

Manuscript submission to *Archives of Toxicology*, June 2024 (see Appendix 1).

3.1. Abstract

Many foods including edible oils contain 2-MCPD, a processing-induced chemical contaminant. Cardiotoxic effects have been shown to result from oral 2-MCPD exposure in rodents, but the underlying mechanisms-of-action remain poorly understood. We undertook a comprehensive multi-omics approach to assess changes at the transcriptomic, proteomic, and oxylipin levels in heart tissues from male F344 rats exposed to 0 or 40 mg/kg BW/day of 2-MCPD in the diet for 90 days, in a regulatory compliant rodent bioassay. Heart tissues were collected for RNA sequencing, quantitative PCR analysis, proteomic analysis via two-dimensional gel electrophoresis and mass spectrometry, and targeted lipidomic profiling of oxylipins and OxPCs by high-performance liquid chromatography-tandem mass spectrometry (HPLC-MS/MS). Transcriptomic and proteomic data analyses revealed upregulation of immune/inflammatory response processes and downregulation of energy metabolism and cardiac structure and functions. Among differentially expressed gene-protein pairs, coronin-1A, a key leukocyte regulating protein, emerged as markedly upregulated. Oxylipin profiling highlighted a selective suppression of docosahexaenoic acid-derived metabolites, suggesting a disruption in cardioprotective lipid pathways. These findings suggest that 2-MCPD disrupts homeostasis through inflammatory activation and suppression of metabolic and cardiac function. This research provides insights into 2-MCPD's cardiotoxicity, emphasizing the need for further studies to support hazard characterization.

Keywords: 2-MCPD, cardiotoxicity, multi-omics, transcriptome, proteome, oxylipin

3.2. Introduction

2-MCPD is a processing-induced chemical contaminant of which there is uncertainty concerning the health risks of dietary exposure. Despite the identification of 2-MCPD fatty acid esters in food products that contain refined edible oils (Andres et al., 2013; Schneider et al., 2022; Wöhrlin et al., 2015), there is currently insufficient data for toxicological hazard assessment. The few rodent toxicity studies that have been conducted have identified cardiotoxicity as a primary outcome of 2-MCPD-exposure (European Food Safety Authority, 2016; Raju et al., 2022; Schilter et al., 2011). However, the underlying molecular mechanisms of 2-MCPD-induced cardiotoxicity remain to be elucidated.

The majority of the toxicological research into chloropropanols has focused on 3-MCPD, as it is typically the most abundant chloropropanol isomer occurring in edible oils and the foods which contain them (Cui et al., 2021; European Food Safety Authority, 2016; Schneider et al., 2022). 3-MCPD has been categorized by the International Agency for Research on Cancer (IARC) as a possible human carcinogen (Group 2B) with the kidneys and testis as primary target organs (IARC, 2013). Based on data from animal studies, several food safety authorities have established TDIs for 3-MCPD equivalents ranging from 2-4 µg/kg BW/day (European Food Safety Authority, 2018; Joint FAO/WHO Expert Committee on Food Additives, 2017).

Far less is known about 2-MCPD; it has not been evaluated by the IARC, and no toxicity reference values for risk assessment have been established. However, it is formed concomitantly with 3-MCPD at approximately 2:1 (3-MCPD:2-MCPD) in refined oils (Kuhlmann, 2016; Wöhrlin et al., 2015; Zelinková et al., 2006), and crucially has unique toxicological activities (Buhrke et al., 2017; Schilter et al., 2011; Schultrich et al., 2017). Previous rodent studies have determined the heart is a primary target organ for 2-MCPD toxicity. Reported effects include non-neoplastic lesion development in the myocardium as well as evidence of elevated oxidative stress response (Buhrke et al., 2018; European Food Safety Authority, 2016; Raju et al., 2022, 2016; Schilter et al., 2011). However, the molecular mechanisms underpinning 2-MCPD's impact on cardiac health remain unclear, thus there is a need to fill this knowledge gap.

This is particularly significant considering the prevalence of 2-MCPD in foods containing processed oils, notably infant formula. Children under two-years were identified as having the highest exposure to 2-MCPD on a per kilogram basis (European Food Safety Authority, 2016),

representing a potentially vulnerable population. This risk profile, combined with the sparse toxicological data on 2-MCPD, presents a clear need for comprehensive investigation.

In this study, we evaluated the biological processes underlying 2-MCPD-induced cardiotoxicity by analyzing heart tissues from weanling F344 rats exposed to oral 0 and 40 mg/kg BW/day 2-MCPD for 90 days; the treatment group was previously shown to have increased heart weights and displayed cardiac lesions characterized by inflammatory cell infiltrate, fibrosis, necrosis, and vacuolation (Raju et al., 2019). To the best of our knowledge, this study represents the first attempt to measure changes at the transcriptomic, proteomic, and targeted lipidomic levels, a multi-omics approach that captures the complex molecular landscape of 2-MCPD-induced cardiotoxicity. RNA sequencing data provided information regarding the biological processes associated with the gene expression changes. Proteomic data were utilized in determining concomitant protein expression to ascertain the pipeline of gene transcription to protein translation. The lipidomic analysis targeted oxylipins, which are the oxygenated metabolites of PUFAs such as AA and DHA. When PUFA are released from cell membranes by PLA2 activity, oxylipins can be synthesized enzymatically by CYP, COX, or LOX pathways. Oxylipins have vital roles as mediators of cellular processes including inflammation, apoptosis, and fibrosis, and can have variable effects depending on their precursor PUFA (Aukema and Ravandi, 2023; Gabbs et al., 2015; Li et al., 2021; Serhan et al., 2015). The enzymes which synthesize oxylipins also contribute to xenobiotic metabolism and exhibit varied substrate preferences by isoform (Hodgson, 2004). Additionally, the lipidomic analysis also included OxPCs, which are induced by oxidative stress and implicated in atherosclerotic lesions development with roles in inflammation and apoptosis (Allen et al., 2013; Loidl et al., 2003). The integration of these biological layers enabled a comprehensive characterization of the molecular underpinnings of 2-MCPD's cardiotoxicity.

3.3. Materials and Methods

3.3.1. Animals and experimental design

Whole hearts were collected from male F344 rats exposed to dietary 2-MCPD at 0 (control) or 40 mg/kg BW/day (n = 6/group). 8-week-old rats received the treatment for 90 days, after which whole hearts were collected, flash-frozen, and pulverized into a homogeneous

powder for subsequent molecular analyses. These animals were from the control and highest dose group of an OECD 408 guideline-compliant rodent bioassay that provided F344 rats sub-chronic 2-MCPD oral exposure for 90 days, for which 40 mg/kg BW/day was the lowest observed adverse effect level for heart lesions. Detailed descriptions of the animal care conditions and histopathology results are reported in (Raju et al., 2019).

3.3.2. Next-Generation RNA Sequencing

Total RNA was extracted from 25 mg of pulverized frozen and powdered hearts using the miRNEasy RNA extraction kit (Qiagen). RNA-seq libraries (3′) were prepared from 400 ng of total RNA per sample using the Lexogen QuantSeq 3′-mRNA-Seq Library Prep Kit FWD for Illumina (Greenland, NH, USA). The resulting libraries were quantified using the Qubit 3.0 Fluorometer - High Sensitivity dsDNA assay (Thermo Fisher Scientific) and validated using the Agilent 2100 Bioanalyzer High Sensitivity DNA chip (Agilent, Mississauga, Canada). Libraries were normalized, pooled, and subsequently loaded onto an Illumina NextSeq 500 sequencing system using a NextSeq® 500/550 High Output Kit v2 (75 cycles) flow cell (Illumina, San Diego, CA, USA). After sequencing the libraries, the raw files were pre-processed following standard QC workflows that include demultiplexing, adaptor sequences removal and trimming. These were subsequently mapped to the *Rattus norvegicus* reference genome assembly mRATBN7.2 using STAR, with the --quantMode GeneCounts option which yielded read counts per gene while mapping (Dobin and Gingeras, 2015).

3.3.3. Quantitative PCR

For validation of RNA-seq findings, quantitative polymerase chain reaction (qPCR) was conducted on mRNA extracted from heart tissues. The TaqMan Low Density Array cards (Life Technologies) targeting oxidative stress-related genes were employed. Relative gene expression was calculated using the ΔΔCt method, normalized to 18S rRNA (Schmittgen and Livak, 2008).

3.3.4. Proteomic analysis

The proteomic analysis was performed using methodology previously described in (Sawada et al., 2016, 2015). Briefly, total proteins were extracted from heart tissue and subjected to two-dimensional gel electrophoresis for separation. The gels were stained using Ruthenium II for protein visualization, and images were captured with a VersaDoc Imaging system (Bio-Rad,

Munich, Germany). Differentially expressed proteins (DEPs) were identified through spot intensity comparison using ProteinMine software (version 1.6.1, BioImagene). Spots of interest were excised using a SpotXpress HT Spot Picking Robot (Proteome Factory AG, Berlin, Germany), digested with trypsin, and the peptides were analyzed by MALDI-TOF MS (Ultraflex II, Bruker). Protein identification was performed against the Mascot database (Perkins et al., 1999), with significance determined by a P value < 0.05.

3.3.5. Targeted lipidomic analysis

The oxylipin and OxPC data presented here have been previously reported in (Cayer, 2019); the methods used were adapted from (Monirujjaman et al., 2017). Briefly, heart tissues were prepared in Tyrode's solution with an added mixture of deuterated internal standards. Oxylipins and OxPCs were extracted using solid-phase extraction (Phenomenex, CA, USA) and quantified by high-performance liquid chromatography-tandem MS (Shimadzu Nexera XR coupled to a QTRAP 6500; Sciex, ON, Canada) using a method modified from (Deems et al., 2007) and described in (Aukema et al., 2016; Leng et al., 2017).

3.3.6. Statistical analyses

All statistical analyses were performed using R (version 4.3.2). RNA-seq and protein expression data were processed using the edgeR and limma packages to determine differential expression. Briefly, the data was filtered for lowly expressed genes and normalized by the trimmed mean of M-values method (Robinson and Oshlack, 2010), transformed via voom (Law et al., 2014), and differential expression analysis was determined by an empirical Bayes method (Robinson et al., 2010). GSEA was performed using the clusterProfiler package to identify enriched biological processes and pathways (Subramanian et al., 2005). The GSEA utilized the t-scores of all genes included in the differential expression analysis. qPCR and lipidomic data were analyzed by t-test when the assumptions of normal distribution and homogeneous variance were met, otherwise values were transformed by Tukey's power ladder to achieve assumptions, and if assumptions were still not met the Wilcoxon test was used.

3.4. Results

3.4.1. Transcriptomic analysis

To evaluate the impact of 2-MCPD on the cardiac transcriptome, we conducted a comprehensive RNA-seq analysis on rat hearts from 2-MCPD-treated animals. After removal of lowly expressed genes, 10853 genes were included in the analysis and displayed distinct transcriptomic profiles between the control and 2-MCPD-treated group, when modelled by PCA (Figure 1A). Differential gene expression analysis, with differentially expressed genes (DEGs) defined as $|\log_2$ fold change (LFC)| > 1 and Benjamini-Hochberg false discovery rate (FDR) < 0.05, revealed more upregulation (300 genes) than downregulation (41 genes) (Figure 1B, listed in Supplemental Table 1). Higher Pearson correlation coefficients between sample DEG expression profiles from the same group (r = 0.90 – 0.96) than between groups (r = 0.80-0.92) confirmed the consistency and reliability of these expression patterns (Figure 1C). These dysregulations highlight the considerable transcription level response to 2-MCPD exposure.

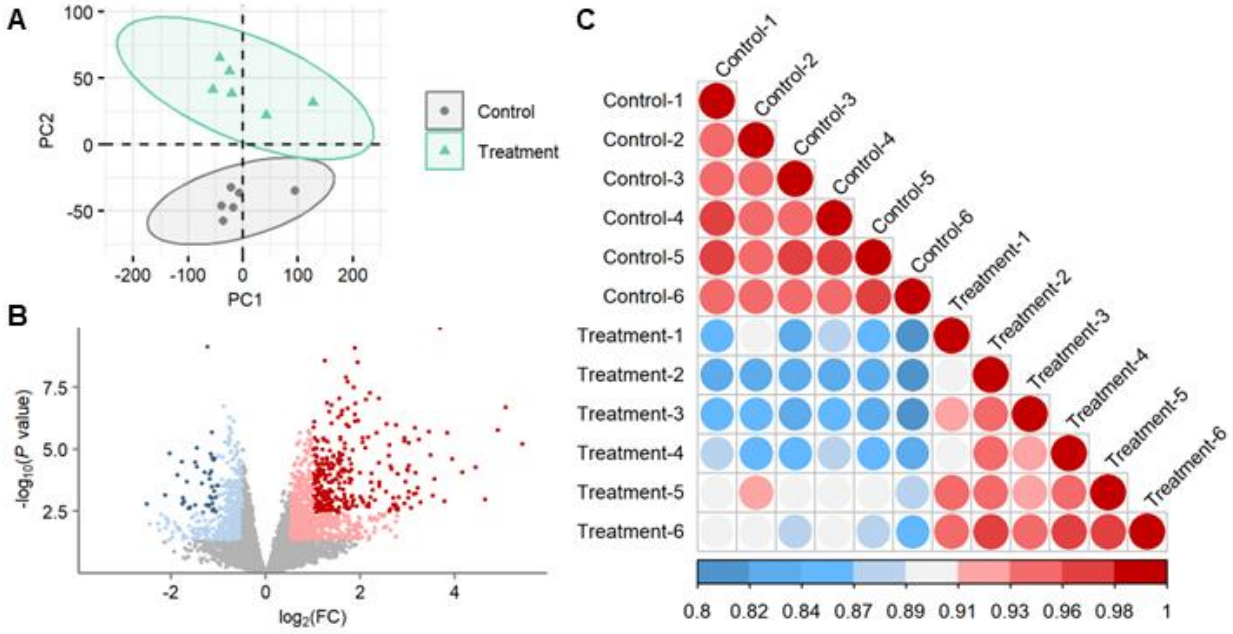

Figure 3.1. Comparison of rat heart transcriptomic profiles between control and treatment. **A)** PCA scores plot of rat heart transcripts. Colour overlayed by group. Ellipses illustrate 95% confidence intervals. **B)** Volcano plot of rat heart transcripts. Dark blue, LFC < -1 and FDR <

0.05; light blue, LFC < -0.5 and $P < 0.05$; grey, no change; pink, LFC > 0.5 and $P < 0.05$; red, LFC > 1 and FDR < 0.05. **C)** Correlation plot of sample DEG profiles. Colours represent Pearson correlation coefficients.

GSEA using the Gene Ontology (GO) database provided insights into the biological processes most associated with the gene expression changes in response to 2-MCPD exposure. The positively enriched (activated) GO terms were predominantly related to immune response processes, with the top 49 terms by FDR exclusively immunological, demonstrating the significant extent to which immune response processes are upregulated (Figure 2A, Supplemental Table 2A). The analysis also identified decreased mitochondrial function as gene sets related to energy metabolism related processes were most negatively enriched (suppressed) (Figure 2B, Supplemental Table 2B). A network analysis of this GSEA result revealed three clusters (Figure 2C). The largest cluster included the immune response related processes, further emphasizing the inflammatory impact of 2-MCPD on cardiac tissue. Another cluster contained energy metabolism related processes, and the third contained cardiac processes. The significantly altered cardiac processes were all suppressed indicating decreased cardiovascular function (Figure 2D, Supplemental Table 2B). From the histopathology results reported in (Raju et al., 2019), we also had interest in fibrotic processes, and identified 7 enriched processes related to fibroblast migration and proliferation (Supplemental Table 3). GSEA using the KEGG corroborated these findings, illustrating activation of numerous immune pathways, particularly those involving leukocyte functions such as chemokine signalling, cytotoxicity, phagocytosis, and migration, alongside signalling processes in apoptosis, inflammation, and cell differentiation. Conversely, energy metabolism pathways, including oxidative phosphorylation and propanoate metabolism, along with the cardiac muscle contraction pathway, were identified as downregulated (Supplementary Figures 1-15).

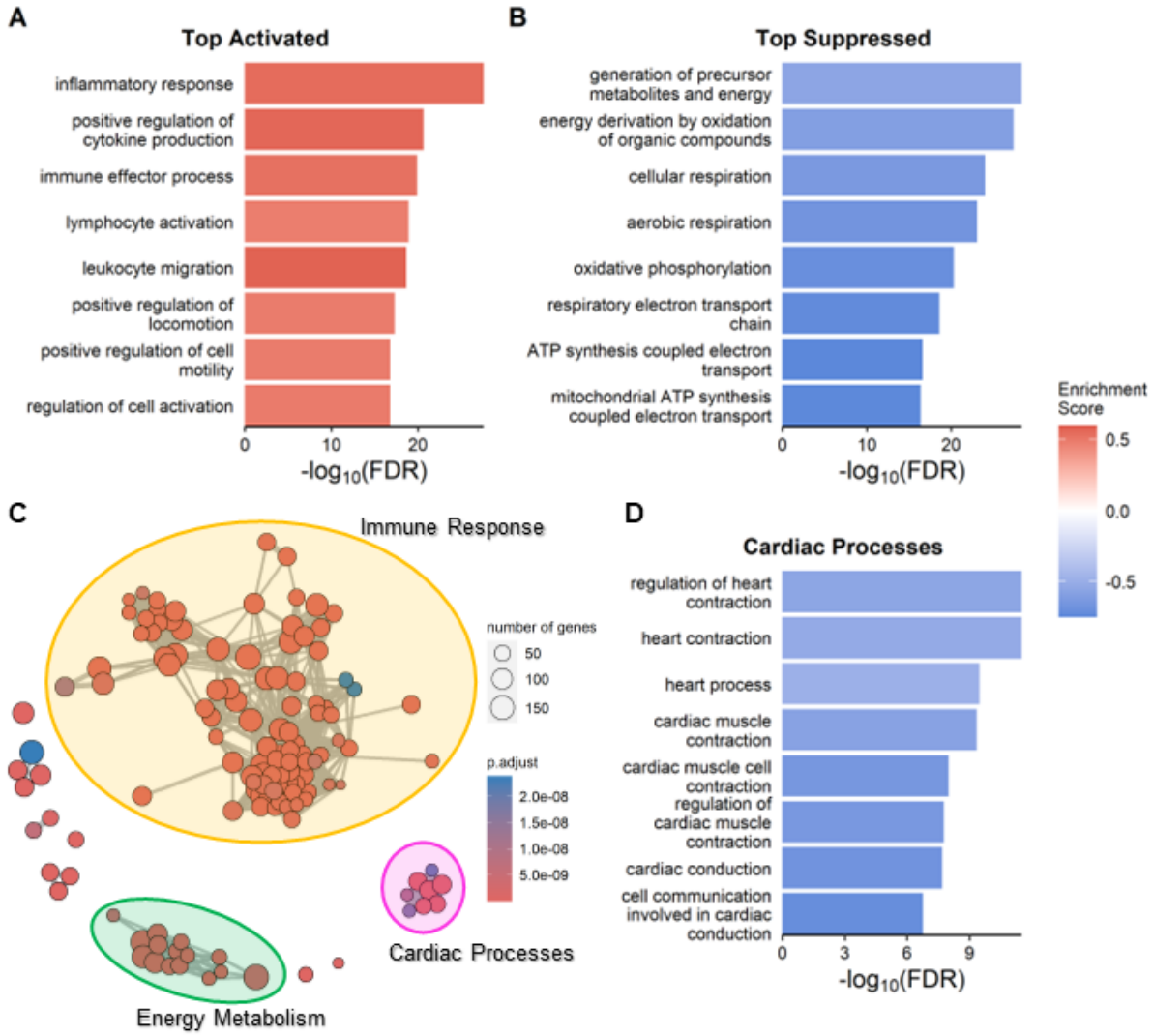

Figure 3.2. Gene set enrichment analysis of Gene Ontology biological processes.

A) Positively enriched GO terms by top FDR. **B)** Negatively enriched GO terms by top FDR. **C)** Network of enriched processes with nodes as GO terms. Edge length inversely related to the number of similar genes in the connected sets. **D)** Enriched cardiac processes by FDR. All processes altered were suppressed.

3.4.2. Quantitative PCR panel

Investigation into oxidative stress responses and validation of the RNA-seq data was conducted via a qPCR assay. Six out of the 91 genes measured in the oxidative stress panel (*Actb, Apoe, Ncf2, Ptgs2, Srxn1, Txnrd1*) were considered DEGs (|LFC| > 1 and FDR < 0.05), all

of which were upregulated from control values, suggesting a modest increase to oxidative stress response (Supplemental Table 4). Notably, *Ptgs2* emerged as the most upregulated gene in the panel. As the gene encoding COX-2, the rate-limiting enzyme in prostaglandin synthesis, *Ptgs2* is strongly associated with inflammation and linked to cardiac fibrosis, conditions associated with chronic oxidative stress (Aragno et al., 2008; Li et al., 2021; Maulik and Kumar, 2012; Ricciotti and Fitzgerald, 2011).

Importantly, the RNA-seq data were in good concordance with the qPCR results. The set of matched qPCR and RNA-seq genes with FDR < 0.05 from either analysis is displayed in Table 1. It revealed all genes to have LFCs in the same direction, except for *Atr* which had $P > 0.05$ in the RNA-seq analysis.

Table 3.1. Comparison of qPCR array and RNA-seq results on genes with FDR < 0.05 in either analysis, sorted by qPCR LFC.

	qPCR		RNA-seq	
Gene	LFC	*P* value	LFC	*P* value
Ptgs2	3.24	0.002	2.37	0.007
Actb	1.22	<0.001	0.902	<0.001
Apoe	1.03	<0.001	0.791	0.005
Txnrd1	1.02	0.002	0.813	0.003
Gpx7	0.831	<0.001	0.393	0.068
Gpx8	0.814	<0.001	0.928	<0.001
Gusb	0.768	0.004	0.593	0.020
Prdx4	0.764	<0.001	0.494	0.033
Cygb	0.735	<0.001	0.561	0.017
Ctsb	0.670	0.001	0.597	<0.001
Vim	0.662	0.011	0.687	<0.001
Atr	0.625	0.002	-0.207	0.537
Ptgs1	0.581	0.005	0.496	0.043
Nox4	0.574	<0.001	0.058	0.843
Ppp1r15b	0.524	0.002	0.239	0.510
Rplp0	0.502	0.009	0.349	0.001
Gsr	0.452	0.004	0.00	0.999
Idh1	0.438	0.003	0.259	0.136
Aqr	0.322	0.010	0.117	0.631
Gstk1	-0.262	0.086	-0.597	0.003
Slc41a3	-0.287	0.175	-0.536	<0.001
Ucp3	-0.412	0.057	-0.704	<0.001

3.4.3. Proteomic analysis

A proteomic analysis was conducted to provide a more comprehensive understanding of examine the impact of 2-MCPD in rat heart at the protein level. The proteomic profiles included 1341 protein spot intensities. A PCA model which included all measured proteins revealed distinct groupings of the control and treatment groups (Figure 3A). Differential expression analysis identified 20 DEPs, with 8 downregulated and 12 upregulated, that were induced by 2-MCPD treatment (Figure 3B). Stronger correlations (r = 0.92-0.96) between the DEP expression values of samples from the same group than between groups (r = 0.76-0.89) indicated reliable data and consistent treatment effects occurred (Figure 3C).

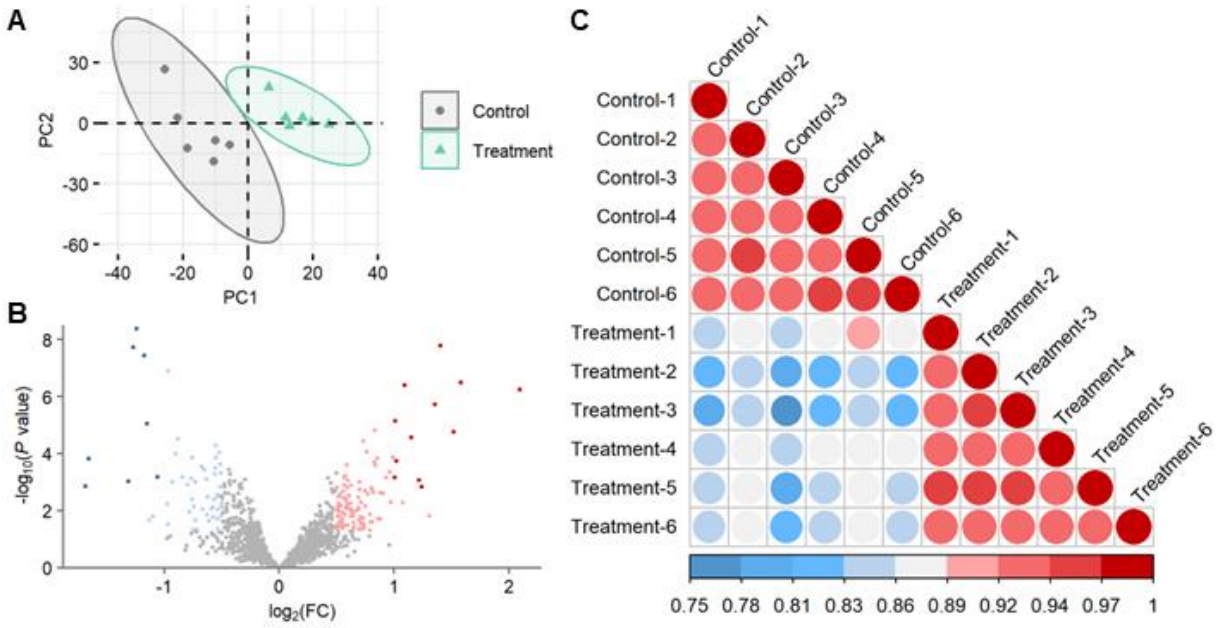

Figure 3.3. Comparison of rat heart proteomic profiles between control and treatment. **A)** PCA scores plot of rat heart proteins. Colour overlayed by group. Ellipses illustrate 95% confidence intervals. **B)** Volcano plot of rat heart proteins. Dark blue, LFC < -1 and FDR < 0.05; light blue, LFC < -0.5 and *P* < 0.05; grey, no change; pink, LFC > 0.5 and *P* < 0.05; red, LFC > 1 and FDR < 0.05. **C)** Correlation plot of sample DEG profiles. Colours represent Pearson correlation coefficients.

Of the protein spot intensities measured, a subset of 203 were identified by MS and are listed in Supplemental Table 5. The identified proteins were matched with their corresponding

genes from the RNA-seq analysis and plotted by expression when both gene and protein were significantly altered ($P < 0.05$) in Figure 4A. The DEG-DEP pair *Coro1a*-COR1A was concomitantly up-regulated with the strictest cutoffs of |LFC| > 1 and FDR < 0.05, thus identifying the corresponding coronin-1A as a protein of particular interest in 2-MCPD-exposure. An additional 4 downregulated (ACSF2, ATPA, ECSIT, and ENOB) and 9 upregulated (ACTA, ACTN1, CAPG, CRYM, GUAD, TBA1A, TRFE, and VIME) gene-protein pairs of interest were identified when the correlation analysis was expanded to include expression of |LFC| > 0.5 and FDR < 0.1 (Figure 4B). The downregulated gene-protein pairs were each involved in energy metabolism whereas the upregulated gene-protein pairs were predominantly related to inflammation or structural proteins.

A

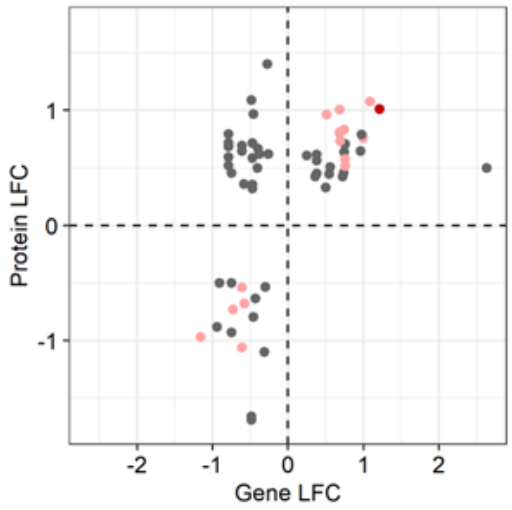

B

Gene	LFC	FDR	Protein	LFC	FDR
Coro1a	1.22	<0.001	COR1A	1.01	<0.001
Actn1	1.09	0.003	ACTN1	1.07	0.060
Capg	0.997	0.011	CAPG	0.759	0.006
Acta2	0.755	0.089	ACTA	0.517	0.061
				0.576	0.073
Gda	0.744	0.006	GUAD	0.832	0.002
Tf	0.739	0.027	TRFE	0.714	0.058
Crym	0.695	0.011	CRYM	0.732	0.003
Vim	0.687	0.015	VIME	0.809	0.031
				1.00	0.020
Tuba1a	0.516	0.009	TBA1A	0.963	0.016
Ecsit	-0.578	0.010	ECSIT	-0.677	0.012
Atp5f1a	-0.607	0.027	ATPA	-1.06	0.020
				-0.539	0.043
Acsf2	-0.728	<0.001	ACSF2	-0.731	0.023
Eno3	-1.16	0.002	ENOB	-0.968	<0.001

Immune response | Structural | Energy metabolism | Other

Figure 3.4. Matched rat heart gene-protein pairs differentially expressed with 2-MCPD treatment.

A) Scatter plot of matched significantly altered ($P < 0.05$) genes and proteins by expression in LFC. Red, gene and protein expression |LFC| > 1 and FDR < 0.05; pink, gene and protein expression |LFC| > 0.5 and FDR < 0.1; grey, gene and/or protein not differentially expressed.
B) DEG-DEP expression values.

3.4.4. Differential expression of oxylipin metabolism genes

The oxylipins of the 2-MCPD-exposed rat heart were of interest due to the dysregulation of oxylipin production genes. This particularly accounts for *Ptgs2* (COX-2) due to its function in the rate-limiting step of PG synthesis and their association with cardiac fibrosis and inflammation (Li et al., 2021; Ricciotti and Fitzgerald, 2011). The mRNA expression data was filtered for oxylipin metabolism-related genes, of which 13 genes exhibited differential expression of $|LFC| > 0.5$ and $P < 0.05$ (Table 2, for full list see Supplemental Table 6). In addition to *Ptgs2*, two other genes (*Ptgis* and *Txbas1*) from the COX pathway were upregulated, suggesting prostanoid synthesis would be upregulated. Three CYP genes were altered, two downregulated (*Cyp2e1* and *Cyp4b1*) and one upregulated (*Cyp1b1*), suggesting expected decreases in the epoxy-PUFA, dihydroxy-PUFA, and hydroxy-PUFA produced by the corresponding CYP enzymes. Additionally, sEH (*Ephx2*) was downregulated, suggesting suppressed conversion of epoxy-PUFA to dihydroxy-PUFA. Three PLA2 genes involved in the liberation of PUFA from the cell membrane were altered with two downregulated (*Pla2g2a* and *Pla2g5*) and one upregulated (*Pla2g2d*). Each of these genes belong to the secreted PLA2 (sPLA2) subfamily, which have selective substrate preference for DHA (Manson et al., 2023), thus a general decrease in DHA oxylipins could be expected. From the proteomic analysis, glutathione peroxidase 1 was the only oxylipin-metabolizing enzyme identified, and it was not significantly altered ($P = 0.212$).

Table 3.2. Oxylipin metabolism DEGs from RNA-seq analysis of rat heart.

Pathway	Gene	LFC	*P* value
COX	*Ptgis*	0.737	0.014
	Ptgs2	2.37	0.007
	Tbxas1	0.761	0.040
CYP	*Cyp1b1*	1.95	<0.001
	Cyp2e1	-1.77	<0.001
	Cyp4b1	-0.918	<0.001
	Ephx2	-0.528	0.012
LOX	*Gpx8*	0.928	<0.001
	Ltc4s	-0.961	0.014
PLA2	*Pla2g2a*	-0.759	0.019
	Pla2g2d	0.760	0.006
	Pla2g5	-0.959	0.002

3.4.5. Targeted lipidomic analysis

Despite the alterations in expression of genes regulating various oxylipin producing pathways, the oxylipin analysis revealed a specific effect of suppression of DHA derived oxylipins from both LOX and CYP pathways. Of the 53 oxylipins quantified, 5 were differentially expressed ($|LFC| > 0.5$ & $P < 0.05$; Figure 5), all 5 of which were DHA metabolites (Table 3 & Supplemental Table 7). In total, 6 DHA oxylipins were quantified, thus 5/6 were differentially expressed (Figure 6), and the total DHA oxylipin mass was reduced ($P = 0.002$, Supplemental Table 6). Notably, DHA and its metabolites are associated with cardioprotective properties, shedding light on the molecular perturbances of 2-MCPD treatment.

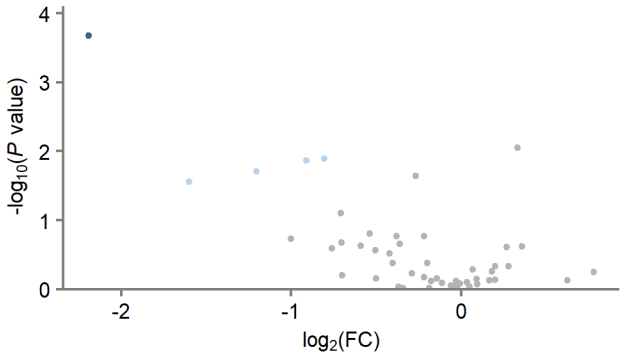

Figure 3.5 Volcano plot comparison of rat heart oxylipins between control and treatment. Dark blue, LFC < -1 and FDR < 0.05; light blue, LFC < -0.5 and P < 0.05; grey, no change.

Table 3.3. List of differentially expressed oxylipins in the male rat heart exposed to 2-MCPD for 90-days.

Precursor	Enzyme Pathway	Oxylipin	LFC	*P* value	FDR
DHA	LOX	4-HDoHE	-2.19	<0.001	0.011
	LOX	14-HDoHE	-0.909	0.014	0.181
	LOX	16-HDoHE	-1.60	0.028	0.210
	LOX	17-HDoHE	-0.806	0.013	0.181
	CYP	20-HDoHE	-1.20	0.019	0.203

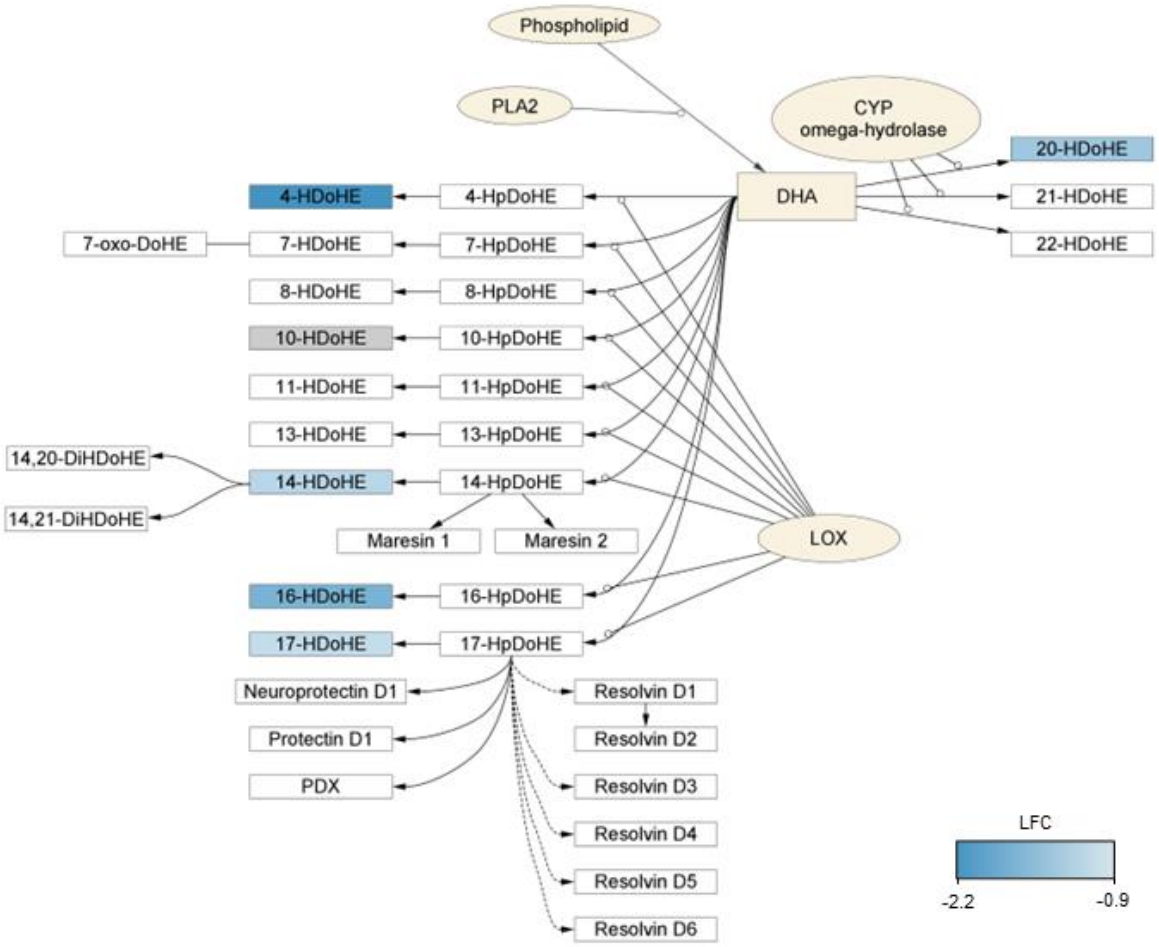

Figure 3.6. DHA oxylipin synthesis via LOX and CYP ω-hydrolase pathways.
Quantified oxylipins coloured in shades of blue if differentially expressed or grey if not altered. White, Oxylipins < LOQ; khaki, enzymes and non-oxylipin lipids.

OxPCs were also of interest, particularly as markers of oxidative stress. Of the 3 OxPCs measured, none were significantly altered ($P < 0.05$), indicating oxidative stress did not influence oxidized lipid expression between groups (Supplemental Table 8).

3.5. Discussion

This study elucidated molecular processes underlying cardiotoxic effects of 2-MCPD exposure in male F344 rats, by integrating the alterations in transcriptomic, proteomic, and targeted lipidomic profiles. Our findings revealed a multi-omic disruption of cardiac homeostatic processes, characterized by activated immune responses and suppression of mitochondrial

function and associated energy production, as well as suppressed cardiac muscle contraction and conduction. Transcriptomic analysis highlighted a pronounced response to 2-MCPD exposure, with immune response genes markedly upregulated, indicating an active inflammatory state within the heart tissue. Concurrently, downregulated genes involved in energy metabolism and cardiac function reveal 2-MCPD disrupted cardiac homeostasis. Proteomic data corroborated these findings, revealing differential expression of proteins related to immune response, energy metabolism, and cardiac structure, thereby illustrating that the 2-MCPD-induced perturbation of heart tissue went beyond the transcriptome. The targeted lipidomic analysis further elucidated the proinflammatory conditions within the heart tissue by identifying decreased levels of anti-inflammatory DHA derived oxylipins (Bento et al., 2011; Croset et al., 1988; González-Périz et al., 2006; Weylandt et al., 2011). Additionally, the absence of significant alterations in OxPCs and limited upregulation of oxidative stress response genes indicate oxidative stress did not play a predominant role in 2-MCPD-induced cardiotoxicity. Overall, the molecular alterations implicate both inflammation and energy deprivation as mechanisms central to the cardiotoxicity of 2-MCPD in rats.

The data presented here are well-supported by the histopathological changes reported in (Raju et al., 2019), which included lesion development of characterized by inflammatory cell infiltrate, fibrosis, necrosis, and vacuolation in myocardial tissue. We characterize the immune response through a series of activated processes, pathways, and individual molecules. For instance, the identification of coronin-1A (gene and protein) upregulation further enhances the understanding of the detrimental inflammation. Coronin-1A is an actin binding protein that is involved in leukocyte adhesion, phagocytosis, and persistence (Moriceau et al., 2009; Pick et al., 2017; Siegmund et al., 2015; Yan et al., 2005). Upregulation of coronin-1A may have inhibited inflammation resolution and should be a target for future study. The activation of fibroblast-related processes comports with the observed cardiac fibrosis. Furthermore, fibrotic cardiac tissue decreases contractility, corresponding to the molecular results (Frangogiannis, 2021). The suppression of DHA-derived oxylipins, which are known for their inflammation resolving properties (Gabbs et al., 2015), suggests that 2-MCPD exposure may compromise the heart's protective mechanisms against inflammation, contributing to the observed cardiotoxicity. We can also postulate that decreased energy metabolism could contribute to necrotic cell death, which in turn promotes inflammation (Festjens et al., 2006; Koo et al., 2015). Further work is needed to

determine this causal chain. Overall, the results suggest that 2-MCPD exposure disrupts cardiac homeostasis by triggering a persistent inflammatory state and decreasing energy metabolism, leading to cardiac lesion development and decreased heart contractility. Although specific data on heart rate changes in 2-MCPD-treated rats are lacking, it is noteworthy that the heart weights in these animals were significantly higher compared to controls (Raju et al., 2019), which suggests an adaptive compensation to maintain cardiac output.

The suppression of DHA-derived oxylipins was congruent with the overall downregulation of the PLA2 genes measured because the altered genes (*Pla2g2a*, *Pla2g2d*, and *Pla2g5*) are sPLA2 isoforms, which have selective preference for DHA and regulate the majority of downstream DHA oxylipin production (Hernandez-Anzaldo et al., 2015; Manson et al., 2023). *Pla2g5*, the most differentially expressed of the PLA2 genes, is implicated in regulating cardiac inflammation via oxylipin manipulation (Berry et al., 2015). In addition to the anti-inflammatory functions of the DHA oxylipins measured (Bento et al., 2011; Croset et al., 1988; González-Périz et al., 2006; Weylandt et al., 2011), the reduced levels of 14-HDoHE and 17-HDoHE suggest a reduction in the synthesis of the potent anti-inflammatory, pro-resolving, and anti-fibrotic maresins, protectins, and Rvs, because they are derived from common hydroperoxyl-DHA precursors (Figure 6) (Deng et al., 2014; Gabbs et al., 2015; Lagarde et al., 2020; Serhan, 2014). Thus, the suppression of DHA oxylipins and their biosynthetic pathways explicate the effects of 2-MCPD on cardiac inflammation via lipid mediators. Additionally, the property of oxylipins to be modifiable by dietary PUFA suggests n-3 PUFAs supplementation to increase cardiac DHA oxylipins could mitigate the adverse effects of 2-MCPD (Ferdouse et al., 2019).

The oxylipin analysis also further emphasized the importance of a multi-omics approach in revealing the complex molecular effects of 2-MCPD exposure. The lack of alterations to oxylipins from PUFA precursors excluding DHA, despite the differential expression of oxylipin synthesis genes, such as *Ptgs2*, exemplified the issues with predicting biological effects based solely on genetic analyses. Namely, that metabolite expression does not necessarily reflect changes at the genetic level.

Previously, oxidative stress had been postulated as a molecular contributor to 2-MCPD-induced toxicity (Buhrke et al., 2018). Here we identified a sparse set of oxidative stress response related genes in the heart upregulated with 2-MCPD exposure, while OxPCs, lipid markers of oxidative stress, were not altered. Furthermore, the GSEA did not identify oxidative

stress response activation, and instead revealed decreased metabolic processes, such as oxidative phosphorylation, which would theoretically produce less oxidative stress (Kowalczyk et al., 2021). Additionally, oxidative stress analyses conducted on the rodents used in this study demonstrated an absence of alterations in the systemic oxidative stress markers: 4-HNE, 8-OHdG, nitrotyrosine, reported in (Raju et al., 2019); and in kidney, muscle, and serum level oxidative stress markers: isoprostanes and OxPCs, reported in (Cayer, 2019). Similarly, mice given a 28-day exposure of 2-MCPD showed limited evidence of oxidative stress in the kidney and testes only (Schultrich et al., 2020). Taking all this into account, oxidative stress response was not likely to be a primary driver of the cardiotoxic effects observed.

The implications of our findings for public health remain to be determined, but considering the widespread presence of 2-MCPD in processed foods and that the highest per BW consumers are young children (European Food Safety Authority, 2016), determining the impact to humans should remain a priority. While our study provides crucial insights into the cardiotoxic mode-of-action of 2-MCPD, the translation of these findings from animals to humans requires careful consideration. The 40 mg/kg BW/day dose used in this study is over four orders of magnitude greater than the estimated high human intake of 1 µg/kg BW/day (European Food Safety Authority, 2016). Furthermore, virtually no effects were observed in the next lowest dose group of 10 mg/kg BW/d reported in (Raju et al., 2019). Therefore, it is unlikely that dietary exposure to 2-MCPD alone would have comparable impacts for human heart health. It should, however, be noted that the duration of human exposure is much longer, and chronic sub-toxic exposure levels should be taken into consideration. Moreover, there are almost no data available regarding the absorption, distribution, metabolism, and excretion of 2-MCPD in the human body. These bioavailability data, however, are required to characterize the toxic potential of this substance. Finally, there is also the potential of a toxic mixture effect with isomeric substances 3-MCPD and glycidol, as 2-MCPD occurs concomitantly with these other contaminants in processed food oils (Nguyen and Fromberg, 2020; Wöhrlin et al., 2015). A robust understanding of the impacts of 2-MCPD, as contributed to by this study, is however a prerequisite of that work. Nonetheless, our study supports the importance of monitoring 2-MCPD levels in food products and the need for further research into its health impacts.

3.6. Conclusions

Our study examined the multifaceted impact of 2-MCPD on cardiac tissue at the molecular level, implicating inflammatory responses, suppressed energy metabolism, and impaired cardiac function. These findings highlight the complexity of 2-MCPD's cardiotoxic mode-of-action and build upon our understanding of the biological processes underpinning it, in a manner consistent with the histopathological findings. Ultimately, this study supports the necessity for comprehensive risk assessments of 2-MCPD as a food contaminant.

3.7. Chapter Transition

The findings from Study A prompted further study into the potential role inadequate levels of dietary ALA, provided in the corn oil-based experimental diets, may have impacted the baseline oxylipins levels and the subsequent oxylipin response to 2-MCPD exposure.

Study B expanded upon the initial focus on the heart from Study A by including analyses of secondary target organs: the liver and kidney, as well as serum. This expansion not only enabled the evaluation of oxylipin alterations to multiple tissues, but it also afforded us the opportunity to integrate these data layers using MSM to identify a common indicator of 2-MCPD exposure across tissues.

This broader scope allowed us to assess the systemic effects of ALA and 2-MCPD across tissues, providing a comprehensive view of their interactions and building on the foundational data regarding the impacts of 2-MCPD exposure. Moreover, Study B explored the protective potential of dietary ALA, the essential n-3 PUFA, against the toxicity of 2-MCPD. This approach not only sought to mitigate the identified gaps in dietary influences on oxylipin profiles but also enhanced the applicability of the findings to nutritional strategies that could reduce the health risks associated with 2-MCPD exposure.

An important objective of Study B, which was not explicitly stated in the manuscript, was to establish a systematic approach for data analysis and the presentation of results. This strategy was aimed at ensuring consistency across the analyses of each tissue. By developing a standardized methodology, we sought to enhance the clarity and transparency of the research.

Chapter 4: Study B: Increased cardiac oxylipins in response to 2-monochloropropane-1,3-diol exposure are partially ameliorated by dietary adequacy of the essential n-3 fatty acid, α-linolenic acid

Authors: Lucien GJ Cayer[1,2], Tobias Karakach[1,3], Jennifer Roberts[4], Stephen PJ Brooks[4], Jayadev Raju[1,4], Harold M Aukema[1,2]

[1]Food and Human Nutritional Sciences, University of Manitoba, Winnipeg, MB, Canada;
[2]Canadian Centre for Agri-Food Research in Health and Medicine, St Boniface Hospital Albrechtsen Research Centre, Winnipeg, MB, Canada;
[3]Pharmacology, Dalhousie University, Halifax, NS, Canada;
[4]Food Directorate, Health Products and Food Branch, Health Canada, Ottawa, Canada.

Manuscript submitted to *Food and Chemical Toxicology*, May 2024 (see Appendix 1).

4.1. Abstract

2-MCPD is a food contaminant with demonstrated cardiotoxicity. PUFA-derived oxylipins are bioactive metabolites that mediate an array of physiological effects, including toxicity-induced inflammation. Oral-toxicity studies may employ n-3 PUFA-deficient diets; crucially, these alter the normal oxylipin profile which may influence toxic effects. We therefore tested whether deficient or adequate dietary ALA, the dietary essential n-3 PUFA, would alter the oxylipin profiles in heart, liver, kidney, and serum of rats exposed to 0 or 50 mg 2-MCPD/kg BW/day for ≤ 14 days in a two-way study design. Adequate ALA increased most n-3 oxylipins in all tissues examined, reflecting greater n-3 PUFA substrate availability. 2-MCPD increased pro-inflammatory arachidonic acid-derived oxylipins formed via cyclooxygenase in heart and to a lesser extent in the liver. The adequate ALA diet revealed 2-MCPD-induced reductions of cardiac DHA-derived oxylipins; these were not apparent in the ALA-deficient diet as these n-3 PUFA oxylipins were already reduced. 2-MCPD also increased cardiac 13-hydroxy-octadecatrienoic acid-γ (13-HOTrE-γ) with deficient, but not adequate ALA diets. Multi-tissue analysis identified 13-HOTrE-γ as a marker of 2-MCPD exposure. This study demonstrates oxylipins are potential markers of early changes in 2-MCPD toxicity and confirms that studies of chemical hazards should use n-3 PUFA adequate diets.

Keywords: 2-MCPD, oxylipins, α-linolenic acid, dietary fatty acid deficiency, heart.

4.2. Introduction

2-MCPD is a chlorinated propanol isomer that has emerged as a toxicological concern due to its occurrence as a food contaminant. It can be found in various processed food products, including those containing hydrolyzed vegetable protein, refined edible oils, and water-resistant paper products (Becalski et al., 2016; Fu et al., 2007; Kuhlmann, 2016; Wöhrlin et al., 2015). Previous animal models have identified cardiotoxicity as the primary outcome of oral 2-MCPD-exposure; it is characterized by heart lesions including inflammation, vacuolation, fibrosis, and necrosis with immune cell infiltration. Secondary target organs, such as the liver and kidney, have inconsistent effects (Raju et al., 2019; Schilter et al., 2011).

Oxylipins are a class of lipid that encompass the oxidized metabolites of 18-22 carbon PUFA, produced by COX, CYP, LOX, or autooxidation (Gabbs et al., 2015). These molecules mediate various physiological processes, including inflammation, apoptosis, and fibrosis (Gabbs et al., 2015; Li et al., 2021). Furthermore, oxylipins are increasingly reported to be perturbed in response to various chemical hazards, with elevated AA-COX-derived PGs and elevated DiHETrE:EpETrE ratios, both indicative of pro-inflammatory states (Dai et al., 2023; Huang et al., 2020; Wu et al., 2023, 2016). However, it is not clear whether these alterations are due to direct effects of the toxin or to secondary effects of pathological changes in the tissues. Hence, the early response of oxylipins to 2-MCPD exposure is of interest.

Consistent with its primary effect on the heart, we have previously shown sub-chronic 90-days dietary 2-MCPD exposure to altered F344 rat cardiac oxylipin profiles, with less effect on the kidney and serum oxylipins (Cayer, 2019). Specifically, 2-MCPD exposure decreased levels of anti-inflammatory DHA derived oxylipins (Cayer, 2019). However, it also was noted that the overall levels of DHA oxylipins (DHA_{Ox}) in the hearts of these F344 rats from this study were well below that of hearts from Sprague-Dawley rats that were provided adequate levels of the essential n-3 PUFA ALA (Cayer, 2019; Ferdouse et al., 2019). This could be a strain-related difference, but the previous study used corn oil-based diets to comport with prior toxicological literature and the low DHA oxylipin levels were more likely due to deficient dietary n-3 PUFA (Raju et al., 2019). Corn oil contains low levels of ALA, at around 1% of total fatty acids (Dunlap et al., 1995; Kim et al., 2020). Using a typical 7 g oil/100 g diet therefore provides approximately 0.07 g ALA/100 g diet; levels well below the recommended 0.5 g ALA/100 g diet considered to be adequate and widely used in the AIN-93 diets (Reeves et al., 1993). This has

implications for toxicological investigation because dietary ALA adequacy may ameliorate toxic outcomes (Bourre et al., 1989). Since n-3 oxylipins have many beneficial bioactivities, such as mediating inflammation resolution and tissue repair, and dietary n-3 PUFA can increase tissue n-3 oxylipins and decrease n-6 oxylipins (Du et al., 2020; Ferdouse et al., 2019; Gabbs et al., 2015; Leng et al., 2018b), we hypothesized that providing adequate dietary ALA would mitigate the 2-MCPD-induced decrease in cardiac DHA_{Ox}.

In this study, we acquired samples from a project that was halted early for humane reasons due to signs of distress in the 2-MCPD exposure groups. This provided an opportunity to evaluate the early tissue oxylipin responses to 2-MCPD exposure in combination with dietary ALA adequacy. Specifically, we conducted targeted oxylipin analyses on the heart, liver, kidney, and serum of rats provided ALA deficient and adequate diets with and without 2-MCPD. These findings indicate that there are early oxylipin alterations in response to 2-MCPD exposure that are influenced by dietary ALA adequacy.

4.3. Materials and Methods

4.3.1. Animals and experimental design

Male Sprague-Dawley rats, 5-weeks old and weighing 100-125 g, were procured from Charles River Laboratories (Montreal, Canada). After a three-week acclimatization period, the rats were randomly divided into four groups, each comprising eight rats (n=8/group). The deficient ALA group (D) received an AIN-93G diet (Reeves et al., 1993) that was modified to replace soybean oil with 7 g corn oil/100 g diet, which provided approximately 0.07 g ALA/100 g. The deficient ALA diet with 2-MCPD (D2M) received the D diet with 972.2 ppm 2-MCPD (Toronto Research Chemicals Inc., Toronto, Canada) to provide an estimated dose of 50 mg/kg BW/day. The adequate ALA group (A) received an AIN-93G diet modified isocalorically to contain corn oil and purified ALA (Larodan, MI) to provide adequate n-3 PUFA intake of 0.5 g ALA/100 g diet. The adequate ALA with 2-MCPD group (A2M) received the A diet with 972.2 ppm 2-MCPD, to investigate the combined effects of 2-MCPD exposure and adequate n-3 PUFA intake. On day 6 following the initiation of 2-MCPD exposure, rats in the 2-MCPD-treated groups exhibited signs of respiratory distress and notable weight loss. As a result, two rats from A2M were euthanized for humane reasons. Similarly, on Day 9, two additional rats in A2M

displaying respiratory distress were sacrificed. The D2M and remaining A2M were euthanized on Day 10 and the D and A groups were euthanized on day 14. The study design has been summarized in Figure 1. The number of samples analyzed per tissue ranged from 5-8 and is detailed in Supplemental Tables 1-4. Heart, liver, kidney, and serum samples were immediately collected and frozen at -80°C until analysis.

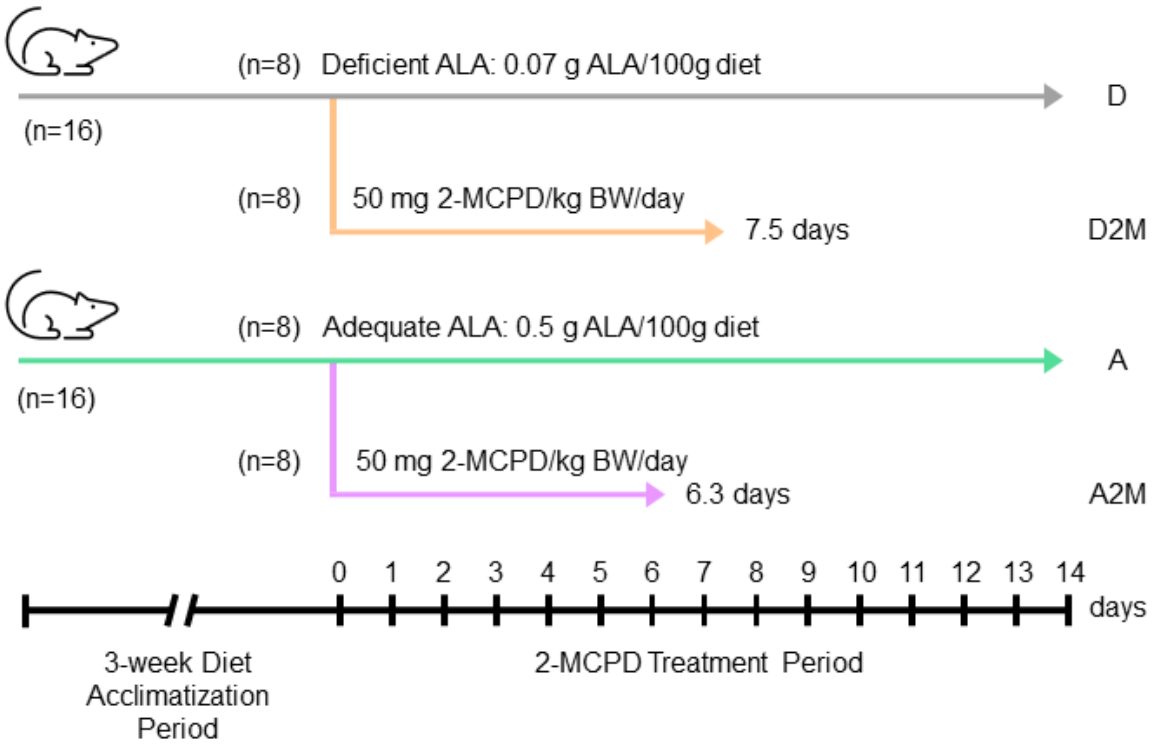

Figure 4.1 Experimental design.

5-week-old male Sprague Dawley rats were fed either deficient ALA or adequate ALA diets for 3-weeks. After the acclimatization period, 2-MCPD treatment was initiated for a subset of rats. The study was halted, and rats were euthanized when those treated with 2-MCPD began to exhibit distress, the mean duration each group received 2-MCPD treatment is listed.

4.3.2. Oxylipin analyses

Free oxylipins from the heart, kidney, liver, and serum were extracted and quantified as described in (Leng et al., 2017; Monirujjaman et al., 2017), with modifications. Briefly,

homogeneous portions of the pulverized whole hearts, kidneys, and livers were placed in ice-cold Tyrode's salt solution (9.6 g/L) and homogenized using an Omni Bead Ruptor 24 (Omni International, Inc., GA, USA). To prevent sample oxidation, antioxidant cocktail (0.2 g/L BHT, 0.2 g/L EDTA, 2 g/L triphenylphosphine, and 2 g/L indomethacin in methanol/ethanol/water (2:1:1, v/v/v)) was added at 1:20 (v/v), followed by the 4:3 (v/v) addition of methanol/formic acid (100:1, v/v). Deuterated oxylipin internal standards (Cayman Chemical, MI) were added uniformly to all samples. To extract oxylipins, solid phase extraction was employed using polymeric reversed phase extraction columns (33 μm, Phenomenex, CA, USA) that were pre-conditioned with methanol and pH 3 water. The samples were diluted with pH 3 water, applied to the columns, rinsed with pH 3 water and then hexane. Oxylipins were eluted from the column using methanol. Subsequently, samples were evaporated and resuspended in a 70:30:0.02 (v/v/v) mass spectrometry (MS) grade water: acetonitrile: acetic acid solution. High performance liquid chromatography-MS/MS (Shimadzu Nexera XR coupled to a QTRAP 6500; Sciex, ON, Canada) analysis of samples was performed by a procedure modified from (Deems et al., 2007) and described in (Aukema et al., 2016; Leng et al., 2017). Oxylipins were quantified using the stable isotope dilution method (Hall and Murphy, 1998), where oxylipin concentrations are calculated based on comparison of their peak area ratio to that of a deuterated internal standard. The quantification limit was set at five times above the baseline.

4.3.3. Statistical analyses

All statistical analyses were performed using R (version 4.2.2). To systematically analyze the oxylipin profiles of each tissue, PCA models were created using $\log_{10}$ normalized oxylipin values which were then mean-centered and scaled to z-scores. For the PCs that most distinguished the groups, the top loadings values ($|loading| > 0.2$) were used to assess which oxylipins most contributed to the group differences. Two-way ANOVA (ALA x 2-MCPD) followed by Tukey's HSD Test was then used to confirm alterations in individual oxylipins, or in the sums of oxylipins derived from a specific PUFA or PUFA-enzyme pathway (indicated by Σ).When oxylipins were not normally distributed, values were transformed using Tukey's ladder of powers to achieve normality, otherwise the Kruskal-Wallis Test followed by Dunn's Test was used for non-parametric data. *P* value adjustment for multiple comparisons was applied using the FDR procedure; FDR < 0.05 was considered significant. Then, to explore which oxylipins contributed to group differences similarly between tissues, a multivariate integration of the

oxylipins quantified in all four tissues was performed using multivariate integrative method partial least squares discriminant analysis (MINT-PLS-DA), from the mixomics R-package (Rohart et al., 2017).

4.4. Results

4.4.1. Heart

In the rat heart, PCA modeling of all cardiac oxylipins illustrated unique pattern alterations due to both dietary ALA and 2-MCPD treatment. Group separation occurred primarily along PC2, with the D2M positively associated, the A strongly negatively associated, while D and A2M were neutral (Figure 2A). The oxylipins that most strongly contributed to the group separation of A, as shown in the PC2 loadings plot, were DHA oxylipins and ALA oxylipins, specifically HDoHEs and hydroxy-octadecatrienoic acids (HOTrEs), respectively. Oxylipins contributing to the D2M group separation were AA-CYP-epoxygenase (CYPe) derived metabolites (EpETrEs), the AA-COX derived PGD2, and the γ-linoleic acid metabolite 13-HOTrE-γ (Figure 2B).

Two-way ANOVA was then performed and individual or groups of oxylipins highlighted by the PCA are shown in Figures 2C-2N (for detailed ANOVA results on all 48 cardiac oxylipins quantified see Supplemental Table 1). Consistent with the PCA model, DHA oxylipins and the sum of DHA oxylipins (ΣDHA_{Ox}) had significant interaction-effects between ALA status and 2-MCPD (two DHA oxylipins and ΣDHA_{Ox} are shown in Figures 2C-E). These oxylipins were elevated only in the A, showing that 2-MCPD inhibited the normal levels of DHA oxylipins present when rats are provided with an ALA adequate diet. The ALA oxylipin 13-HOTrE also showed this interaction with ALA and 2-MCPD (Figure 2F), while for the other three ALA oxylipins quantified there were main effects of dietary ALA, as reflected by the sum of ALA oxylipins (ΣALA_{Ox}; an ALA oxylipin and ΣALA_{Ox} are shown in Figures 2G-H). PGD2 was identified among the top oxylipins positively associated with PC2. This AA-COX oxylipin did not have a significant 2-MCPD effect when analyzed by ANOVA, likely due to a large variance in the A2M (Figure 2I). There was, however, a 2-MCPD main effect of increased ΣAA-COX (Figure 2H), reflecting a pattern observed in several of these metabolites. Interaction effects were also observed for 13-HOTrE-γ, which was distinctly elevated in the D2M compared to the D

group, but not in the adequate ALA groups (A & A2M), shown in Figure 2K. A similar pattern was observed with the AA-CYPe oxylipins and ΣAA-CYPe, although this was significant only for 14,15-DiHETrE (Figures 2L-N).

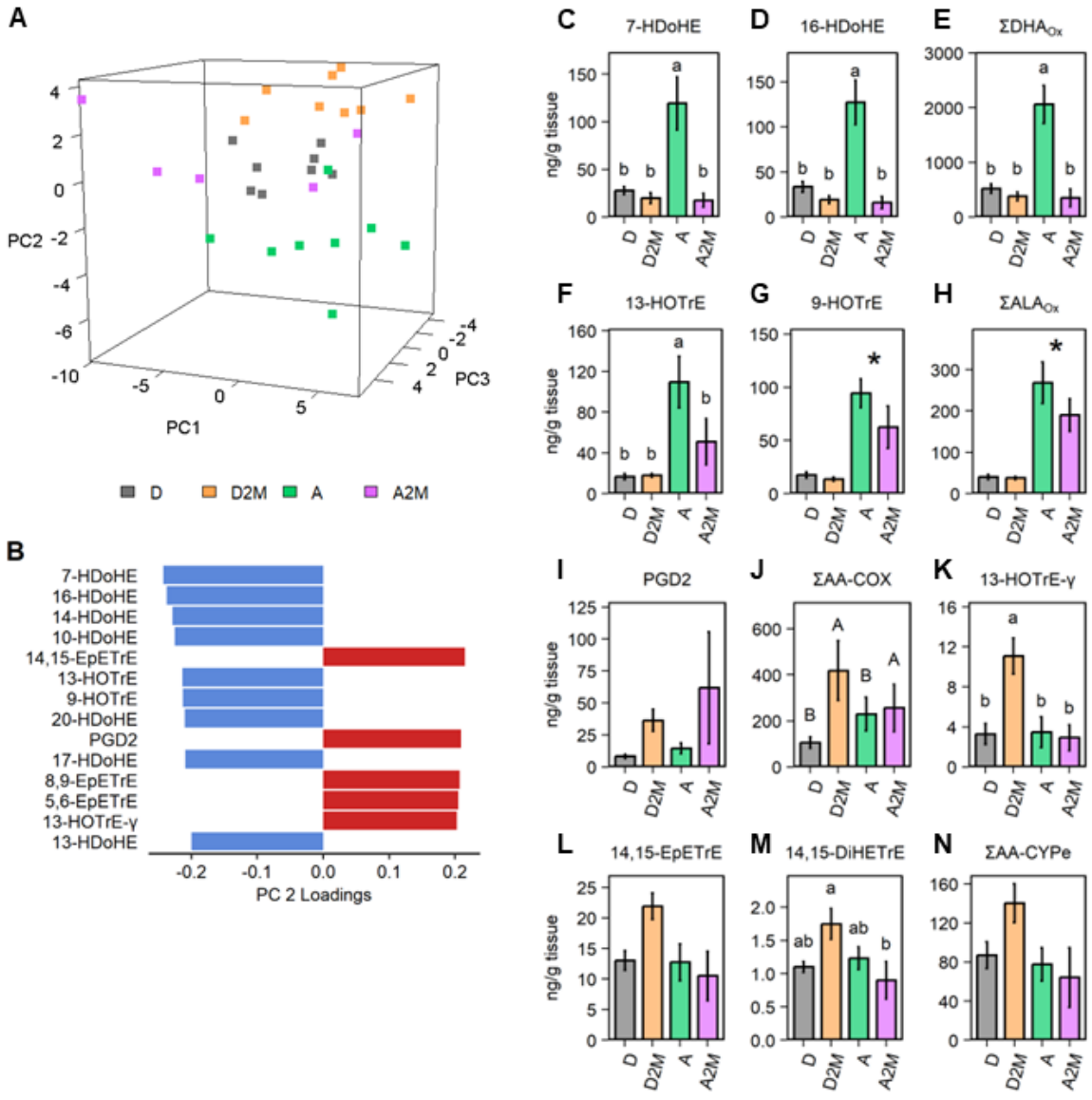

Figure 4.2. Rat heart oxylipin profile and individual oxylipins compared between experimental groups.

A) PCA model of rat heart oxylipins. Individual scores projected onto PC1-3 from PCA model containing all cardiac oxylipins. Colour overlayed by group affiliation. **B)** Top absolute loadings for PC2 of the PCA model. Displays the contribution of variables to the PC. Oxylipins with loadings values > 0.2 displayed. **C-N)** Cardiac oxylipins highlighted by the PCA model.

Significant effects (FDR <0.05) are indicated by: * for a diet-effect, upper-case letters for a 2-MCPD-effect, or lower-case letters for an ALA x 2-MCPD interaction.

4.4.2. Liver

In the liver, PCA, which modelled all the hepatic oxylipins quantified, revealed group distinctions in each of the oxylipin profiles, as displayed in Figure 3A. The group separation along PC2 distinguished groups by ALA status, with the adequate ALA groups associated with n-3 metabolites from DHA (HDoHEs), ALA (13-HOTrE), and EPA [dihydroxy-eicosatetraenoic acids (DiHETEs) and hydroxy-eicosapentaenoic acids (HEPEs)], highlighted in Figure 3B. PC3 separated groups by 2-MCPD status, with the 2-MCPD treated groups (D2M & A2M) most strongly associated with the AA-COX prostanoids, although the separation between A and A2M was less robust (Figure 3C). Thus, hepatic oxylipin alterations between experimental groups were primarily due to dietary ALA, with less pronounced 2-MCPD effects.

Comparison by two-way ANOVA of oxylipins highlighted by the PCA clarify these observations; for detailed statistics on all 64 oxylipins see Supplemental Table 2. n-3 oxylipins predominantly contributed to PC2 and were broadly increased in both adequate ALA diets. This was reflected in the ΣALA_{Ox}, sum of EPA oxylipins (ΣEPA_{Ox}), and ΣDHA_{Ox} which displayed main effects of ALA (Figures 3D-F). The AA-COX metabolites [PGs, TXB2, and 12-HHTrE], which predominantly contributed to the 2-MCPD status related separation along PC3, did not have significant 2-MCPD effects, however. Contrarily, AA-COX oxylipins and the ΣAA-COX either had no significant effects (two AA-COX PGs and ΣAA-COX are shown in Figures 3G-I), or had ALA main effects (Figures 3J-K). Notably, for the AA-COX oxylipins, the D2M consistently had the highest values, and A2M had higher values than A; which, although not significant, was consistent with the PC3 separation by 2-MCPD.

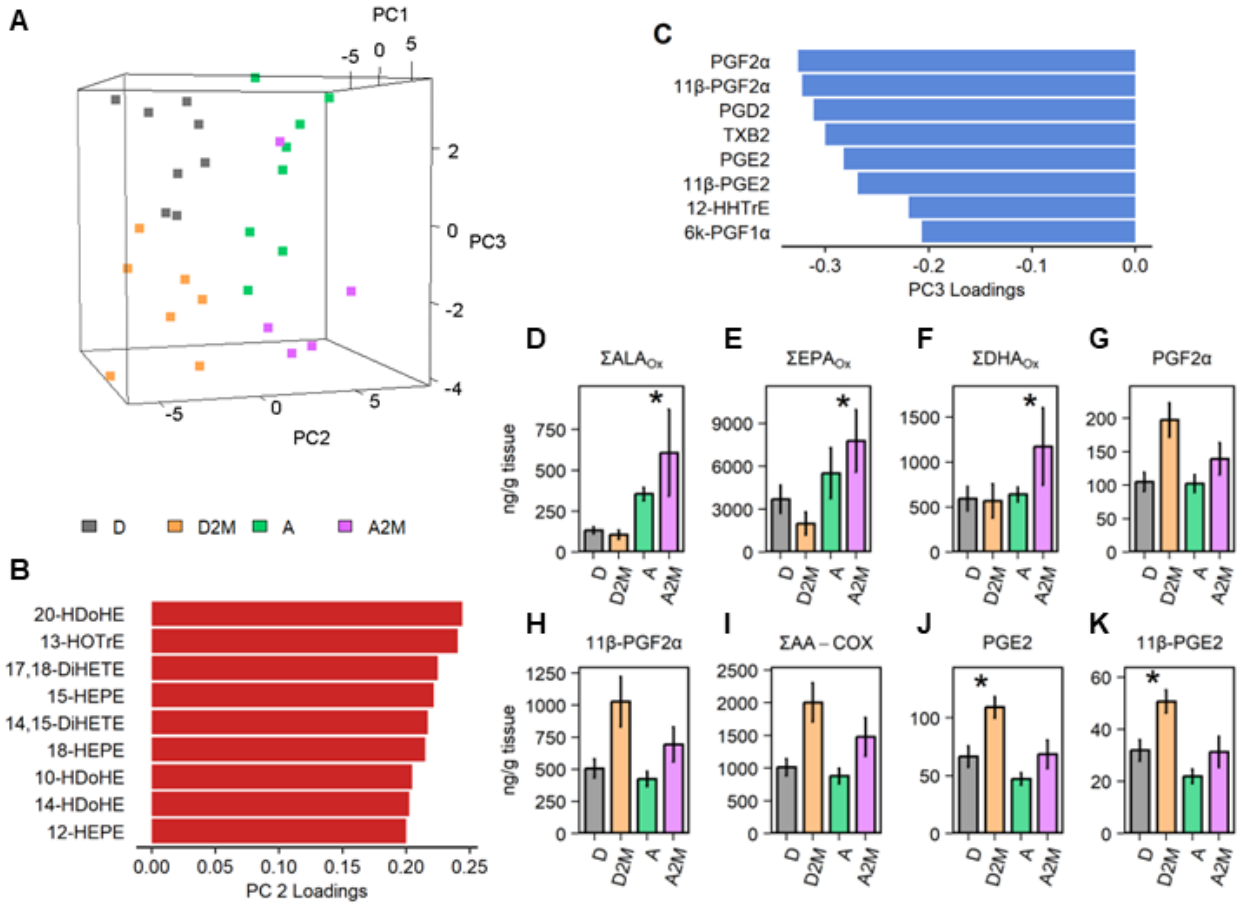

Figure 4.3. Rat liver oxylipin profile and individual oxylipins compared between experimental groups.

A) PCA model of rat liver oxylipins. Individual scores projected onto PC1-3 from PCA model containing all hepatic oxylipins. Colour overlayed by group affiliation. **B)** Top absolute loadings for PC2. **C)** Top absolute loadings for PC3. **D-I)** Hepatic oxylipins highlighted by the PCA model. *, indicates a significant ALA-effect (FDR <0.05).

4.4.3. Kidney

In the kidney, PCA modelling revealed renal oxylipins were differentiated by ALA status, as displayed in Figure 4A. The separation of groups occurred along PC1 and PC2, with the deficient ALA groups associated with AA-LOX oxylipins (HETEs and one LT) and the dihomo-γ-linolenic acid (DGLA) oxylipin 15-hydroxy-eicosatrienoic acid (HETrE) (Figure 4B), while the adequate ALA groups were most associated with n-3 oxylipins from ALA (HOTrEs), EPA (HEPEs), and DHA [19,20-dihydroxy-docosapentaenoic acid (DiHDoPE) and 17-HDoHE]

(Figure 4C). It should be noted that the PC1 loadings values were all below the selected cutoff of +/- 0.2, these lower magnitude loadings values were in part due to a high number of variables similarly contributing to the PC. So, for PC1 only the cutoff for was reduced to +/- 0.18.

Two-way ANOVA was performed and individual or groups of oxylipins highlighted by the PCA are shown in Figures 4D-K (for the detailed statistics on all 66 oxylipins see Supplemental Table 3). For the AA-LOX oxylipins, 8/10 (7 HETEs and 6t-LTB4) were significantly elevated in the deficient ALA groups (D & D2M), and this was reflected in the ΣAA-LOX (two AA-LOX oxylipins and ΣAA-LOX are shown in Figures 4D-F). The ALA effect was specific to the AA-LOX oxylipins, thus ΣAA-COX and ΣAA-CYPe were not altered (Figures 4G-H). 15-HETrE was also a top oxylipin associated with PC1; it and the other two DGLA oxylipins quantified had ALA main effects, reflected in the sum of DGLA oxylipins ($\Sigma DGLA_{Ox}$) shown in Figure 4I. Both ALA oxylipins and EPA oxylipins were broadly increased with adequate ALA, as reflected in the ΣALA_{Ox} and ΣEPA_{Ox} displayed in Figures 4J-K. Neither of the DHA oxylipins most associated with PC2 were significantly altered, nor was the ΣDHA_{Ox} (Figures 4L, M & O). However, 1 DHA oxylipin did have a main effect of ALA, as shown in Figure 4N. Thus, in the kidney there was a clear effect of dietary ALA to reduce specific n-6 oxylipins and elevate ALA oxylipins and EPA oxylipins, but less distinct effects occurred to the DHA oxylipins.

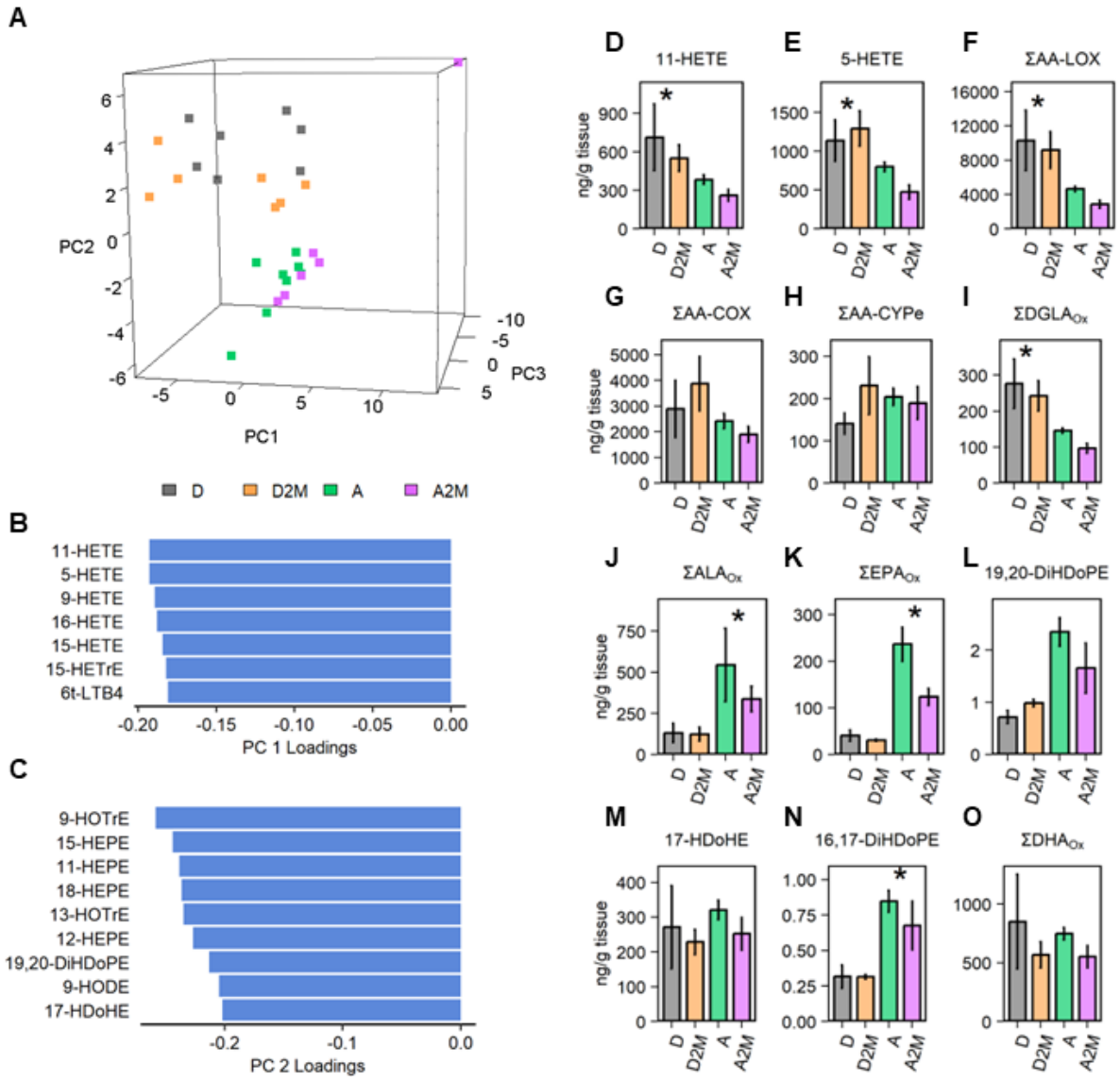

Figure 4.4. Rat kidney oxylipin profile and individual oxylipins compared between experimental groups.

A) PCA model of rat kidney oxylipins Individual scores projected onto PC1-3. Colour overlayed by group affiliation. **B)** Top absolute loadings for PC1. **C)** Top absolute loadings for PC2. **D-O)** Renal oxylipins highlighted by the PCA model. *, indicates a significant ALA-effect (FDR <0.05).

4.4.4. Serum

In the serum, the PCA model of all serum oxylipins quantified revealed distinct separation of experimental groups by ALA status only (Figure 5A). The separation occurred along PC3; the top contributors to which were the n-3 oxylipins from EPA (HEPEs), ALA (HOTrEs and 9-oxoOTrE), and DHA (16,17-DiHDoPE), shown in Figure 5B. Two-way ANOVA revealed 3/3 ALA oxylipins and EPA oxylipins were elevated in adequate ALA groups, as reflected in ΣALA_{Ox} and ΣEPA_{Ox} displayed in Figure 5C-D (for the detailed statistics on all 57 oxylipins see Supplemental Table 4). The DHA oxylipins had a smaller proportion with significant ALA effects (2/8); however, DHA oxylipins were still generally elevated, as reflected in ΣDHA_{Ox} which did have a main effect of ALA, shown in Figure 5E. Thus, serum oxylipins were specifically altered by dietary ALA, such that n-3 oxylipins were elevated, with more pronounced effects to ALA oxylipins and EPA oxylipins.

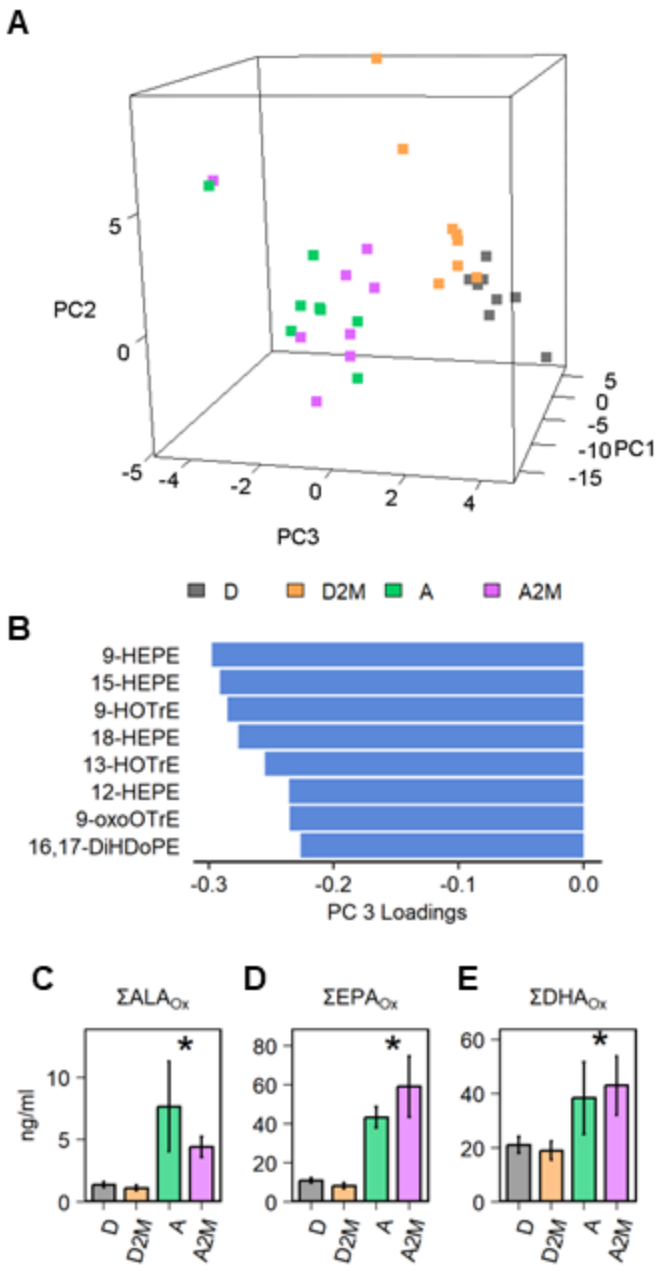

Figure 4.5. Rat serum oxylipin profile and individual oxylipins compared between experimental groups.

A) PCA model of rat serum oxylipins. Individual scores projected onto PC1-3. Colour overlayed by group affiliation. **B)** Top absolute loadings for PC3 of the model. **C-E)** Serum oxylipins highlighted by the PCA model. *, indicates a significant ALA-effect (FDR < 0.05).

4.4.5. Multi-tissue analysis: P-integration

To systematically investigate which oxylipins contributed to group differences consistently across tissues, a multivariate integration of oxylipins from each tissue was performed using MINT-PLS-DA. The model was constructed from the oxylipins values for each sample from the heart, liver, kidney, and serum, using the 44 oxylipins mutually quantified in each tissue. Oxylipins were normalized to %total oxylipins per sample in each tissue. Figure 6A shows each individual tissue sample on the first two components of the model and Figure 6B displays them separately by tissue for clarity.

This analysis separated samples by ALA status along component 1 (Figure 6A), with n-3 oxylipins as the variables contributing to the axis (Figures 6C). Notably, there were no EPA oxylipins included in the model because there were none quantified in the heart, and thus were not among the n-3 oxylipins highlighted. Also, in the heart the A2M group is less positively associated with component 1 than the A (Figure 6B), displaying the interaction effect described in section 4.4.1.

The component 2 separations are less distinct; however, the heart, and to a lesser extent the liver, displayed separation of the deficient ALA groups along this component (Figure 6B). 13-HOTrE-γ was identified as having contributed particularly strongly to this component (Figure 6D). Two-way ANOVA for 13-HOTrE-γ in each tissue showed that it was only significantly altered in the heart but was consistently the highest in the D2M for each tissue (Figure 6E).

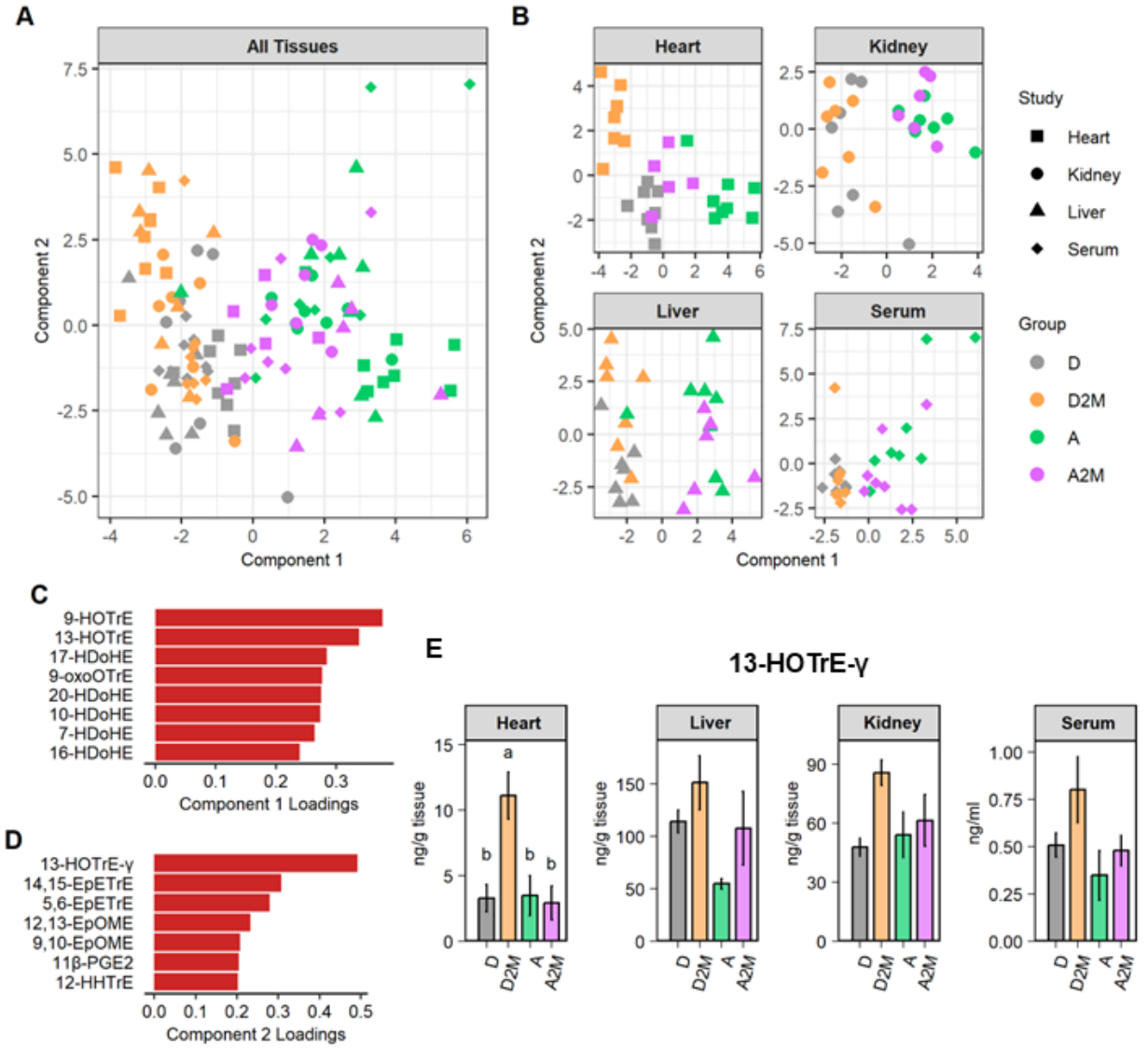

Figure 4.6. Multivariate Integration-Partial Least Squares-Discriminant Analysis of cardiac, hepatic, renal, and serum oxylipins.

A) Combined tissues scores plot displaying all samples on components 1 and 2. **B)** Scores plots of components 1 and 2 of the model divided by tissue. **C & D)** Top absolute loadings of component 1 and component 2 of the model. **E)** 13-HOTrE-γ values by tissue. Lower case letters indicate a significant ALA x 2-MCPD interaction (FDR < 0.05).

4.5. Discussion

In the analyses presented here, oral exposure of 50 mg 2-MCPD/kg BW/day perturbed oxylipins primarily in the heart and to a lesser extent in the liver. Of these alterations, elevated AA-COX oxylipins (prostanoids) are indicative of a pro-inflammatory milieu as they mediate both acute and chronic inflammation (Yao and Narumiya, 2019). Further, these molecules are associated with inflammatory lesions and various pathophysiological responses including fibrosis (Li et al., 2021; Ricciotti and Fitzgerald, 2011), which directly connects to the histopathological characterization of 2-MCPD-induced cardiotoxicity (Raju et al., 2019). Previous studies of 2-MCPD exposure have consistently identified the heart as a major site of injury induced by 2-MCPD exposure (Raju et al., 2019; Schilter et al., 2011). Thus, the data presented here support that conclusion as the most profound 2-MCPD-induced effects were to the cardiac oxylipins and add to the molecular characterization. Our findings of elevated hepatic AA-COX oxylipins are also consistent with previous studies that have identified the liver as a secondary target of 2-MCPD exposure (Raju et al., 2019; Schilter et al., 2011). However, these alterations were not significant in the two-way ANOVA model and should only be considered as possible findings that require further study to confirm.

In each of the tissues analyzed, adequate dietary ALA resulted in higher levels of n-3 PUFA-derived oxylipins than deficient dietary ALA. The higher levels of n-3 oxylipins suggest improved anti-inflammatory and tissue repair properties (Gabbs et al., 2015). There were also lower levels of n-6 oxylipins with adequate ALA (AA-COX in the liver and AA-LOX in the kidney). In addition to the AA-COX prostanoids, there are other pro-inflammatory oxylipins such as the AA-LOX derived HETEs and LTs which mediate immune cell migration and can promote tumor proliferation (Gabbs et al., 2015). Thus, ALA adequacy influenced the baseline of bioactive lipids and the resulting balance of inflammatory mediators, irrespective of 2-MCPD exposure, highlighting the importance of dietary ALA in animal models.

A key finding from this study was the interaction between dietary ALA and 2-MCPD, in which cardiac DHA oxylipins were reduced by 2-MCPD exposure in rats provided ALA sufficient, but not deficient diets. This suppression of DHA oxylipins may be a result of the 2-MCPD-induced downregulation of sPLA2 (see Chapter 3 Section 5). PLA2 is a superfamily of enzymes which includes upstream regulators of oxylipin production via PUFA liberation from the cell membrane. The sPLA2 family, which is particularly prevalent in the heart, has substrate

preference for DHA, and sPLA2 inhibition supresses DHA oxylipins and increases cardiac inflammation (Berry et al., 2015; Hayashi et al., 2021; Hernandez-Anzaldo et al., 2015; Manson et al., 2023). A 2-MCPD induced reduction in DHA oxylipins was not observed in the deficient ALA groups ostensibly due to levels being near baseline values. This further underscores the importance of adequate dietary ALA in animal models, as the 2-MCPD effect was masked by deficient levels of ALA.

There was also an ALA by 2-MCPD interaction for heart 13-HOTrE-γ, which was elevated with 2-MCPD exposure in rats deficient in ALA only; this was ameliorated in ALA sufficient rats. Nevertheless, the multi-tissue analysis highlighted 13-HOTrE-γ as a potential biomarker of 2-MCPD toxicity. There is currently a paucity of information regarding the biological function of 13-HOTrE-γ, so the implications of the elevation cannot be speculated, but further investigation of its effect on cellular processes are warranted. Additionally, the mechanism by which 13-HOTrE-γ is altered by 2-MCPD is not clear, as it is not meaningfully produced by sPLA2 activity (Manson et al., 2023). Thus, further study will be needed to elucidate the specificity of the elevation of 13-HOTrE-γ to 2-MCPD and the nature of the amelioration by adequate dietary ALA.

Oxidative stress has been previously explored as a possible mechanism underlying 2-MCPD toxicity (Buhrke et al., 2018). However, recent investigations into 2-MCPD toxicity in an array of rodent tissues with a lack of alteration to oxidative stress markers from lipids (OxPCs, isoprostanes, and 4-HNE), DNA (8-OHdG), and protein (nitrotyrosine) (Cayer, 2019; Raju et al., 2019), as well as minimal changes to oxidative stress related genes and proteins (Schultrich et al., 2020; see Chapter 4), do not support this hypothesis. Our findings revealed no significant changes in the non-enzymatically produced isoprostanes (quantified in liver and kidney), further supporting the conclusion that oxidative stress is not elevated with 2-MCPD exposure.

Our comprehensive examination of oxylipin profiles, coupled with a robust methodological approach, provided substantial insights into the oxylipins affected by 2-MCPD in conjunction with dietary ALA adequacy. This work also highlighted several avenues for further investigation. The 2-MCPD dosage used well exceeds typical human exposure levels (European Food Safety Authority, 2016), thus there remains a need for studies that explore a wider range of concentrations and durations, particularly those reflecting the human dietary context. Additionally, while 2-MCPD generally induces similar effects to males and females, sex-specific

differences have been reported (Raju et al., 2019), thus future research should address the intersection of sex, diet, and 2-MCPD.

4.6. Conclusion

This study showed tissue-specific alterations in the oxylipin profiles of rats with 2-MCPD-exposure, dietary ALA manipulation, and interactions between 2-MCPD and dietary ALA. In the heart, 2-MCPD exposure elevated pro-inflammatory AA-COX derived oxylipins and lowered cardioprotective anti-inflammatory DHA oxylipins, with the effect on DHA oxylipins only apparent when adequate levels of dietary ALA were provided. 13-HOTrE-γ was highlighted as a potential biomarker of 2-MCPD exposure. These findings elucidate the impacts of 2-MCPD exposure on oxylipin metabolism as well as emphasize the importance of considering dietary factors in toxicological experimental design.

4.7. Chapter Transition

The next study in this thesis, Study C, shifts in focus from the previous studies, which examined oxylipins in combination with other omics data or across different tissues, to a more direct clinical context. This transition is in keeping with the overarching theme of integrating oxylipin data with other data layers and exemplifies another application of this approach by exploring the impact of AVS on oxylipin profiles in AV and plasma samples.

In Study C, we investigated how AVS influenced oxylipin profiles of the human AV and plasma. By analyzing how oxylipins changed in relation to disease severity, we sought to uncover important biomolecular alterations associated with AVS. To achieve this, MSM were utilized to integrate oxylipin data with the abundance of clinical parameters available from the patients in the study, which included various risk factors for AVS. This integration allowed for the construction of robust models that allowed us to identify novel associations between oxylipins and AVS severity, crucial to the future develop of therapies for alleviating the burden of AVS.

Chapter 5: Study C: Valvular prostaglandins are elevated in severe human aortic valve stenosis

Authors: Lucien G.J. Cayer MSc[1,2], Arun Surendran BE, MBA[3,4], Tobias Karakach PhD[1,5], Harold M. Aukema PhD[1,2,4], Amir Ravandi MD, PhD[2,4,6]

[1]Food and Human Nutritional Sciences, University of Manitoba, Winnipeg, MB, Canada;
[2]Canadian Centre for Agri-Food Research in Health and Medicine, Winnipeg, MB, Canada;
[3]Physiology and Pathophysiology, Rady Faculty of Health Sciences, University of Manitoba, Winnipeg, MB, Canada;
[4]Precision Cardiovascular Medicine Group, St. Boniface Hospital Research Centre, Winnipeg, MB, Canada;
[5]Pharmacology, Dalhousie University, Halifax, NS, Canada;
[6]Section of Cardiology, Max Rady College of Medicine, University of Manitoba, Winnipeg, MB, Canada.

This manuscript has been published in *Arteriosclerosis, Thrombosis, and Vascular Biology*, 2024;44:e131–e144. https://doi-org.uml.idm.oclc.org/10.1161/ATVBAHA.123.320001

5.1. Abstract

Background: AVS is the most common valvular disease in the developed world. AVS involves the progressive fibro-calcific remodeling of the aortic valve (AV), which impairs function and can ultimately lead to heart failure. Due to gaps in our understanding of the underlying mechanisms of AVS, there are no pharmacological treatments nor dietary interventions known to slow AVS progression. Recent studies have begun to suggest oxylipins, a class of bioactive lipid, may be dysregulated in the valves of AVS-patients.

Methods: We utilized HPLC-MS/MS to conduct a targeted oxylipin analysis on human AV tissue and plasma from a cohort of 110 patients undergoing AV surgery.

Results: We identified 36 oxylipins in human AV tissue with all showing significant increase in patients with severe AVS. A multivariate model including patient characteristics and valvular oxylipins identified arachidonic acid-cyclooxygenase (COX) pathway derived prostanoids to be the most associated with AVS severity. Plasma oxylipin levels were measured in a subset of aortic valve surgery patients and compared to a control group of healthy participants, showing distinct oxylipin profiles between control and disease.

Conclusion: Our comprehensive analysis of oxylipins in the human AV identified the inflammatory and osteogenic regulating prostanoids to be positively correlated with AVS severity. This elucidation of prostanoid dysregulation warrants further research into COX inhibition to mitigate AVS.

Graphical abstract:

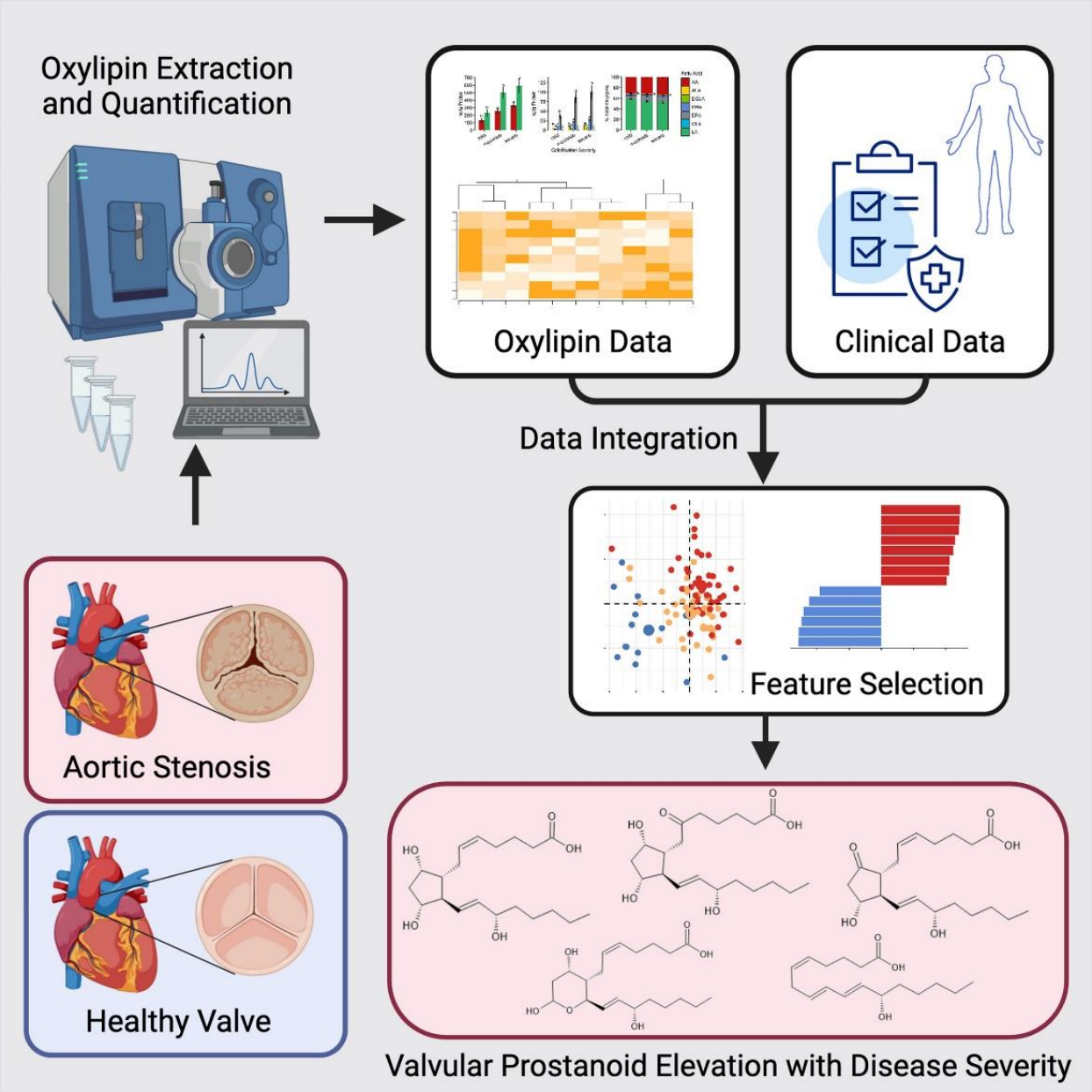

Keywords: aortic valve stenosis, cyclooxygenase, lipidomics, oxylipins, prostaglandins

Highlights:

- Aortic valvular oxylipin concentrations are broadly increased with aortic valve stenosis severity.
- Arachidonic acid-derived prostanoids were found to be particularly correlated with disease severity in a multivariate model.
- Plasma oxylipins were found to be distinct between healthy patients and those with the disease. However, plasma oxylipins could not be used to distinguish disease severity.

5.2. Introduction

AVS is a debilitating cardiovascular condition that affects millions of individuals worldwide and is a major cause of heart failure and cardiovascular mortality. The number of patients suffering from AVS has increased over the last 20 years and is and projected to more than double by 2050 (Coffey et al., 2021; Tsao et al., 2023; Yadgir et al., 2020). The progression of AVS is characterized by fibro-calcific remodelling of the AV leaflets which result in a narrowing of the valve opening and diminished function (Dweck et al., 2012; Hulin et al., 2018). Risk factors of AVS include age, elevated LDL and Lp(a), smoking history, hypertension, diabetes, CKD, bone mineral disorder, and bicuspid aortic valve (Guddeti et al., 2020; Gupta et al., 2022; Messika-Zeitoun et al., 2007; Shen et al., 2020; Stewart et al., 1997). There is currently no effective pharmacological intervention for AVS, and surgical valve replacement or transcatheter AV implantation are the current best treatment methods, but they may not be feasible for patients with significant comorbidities (Baumgartner et al., 2017). There is a growing need to better understand the underlying mechanisms of AVS to develop medical treatments and dietary recommendations, both to reduce the incidence and progression, while minimizing the need for invasive therapies.

AVS was previously thought to be a passive disease associated with aging and wear-and-tear of the valve but has since been shown to be an active inflammatory process. The AV leaflet is comprised primarily of VICs that with AVS develop an osteoblast-like phenotype (Grim et al., 2020). This process is initiated at points of mechanical stress on the AV leaflet, which incur infiltration of immune cells and oxidized lipoproteins (LDL and Lp(a)) that occur in early lesions (Bouchareb et al., 2019; Dweck et al., 2012; Zheng et al., 2020). Oxidized lipoproteins are cytotoxic and propagate further inflammation. The inflammatory cytokines released, stimulate fibrosis via VICs differentiation into myofibroblasts. Calcification occurs with the presence of macrophages in the initial stages of inflammation, but is accelerated due to continued release of cytokines promoting differentiation of myofibroblasts to osteoblast-like cells (Grim et al., 2020; Hulin et al., 2018). This in turn stimulates the production of calcification regulating proteins (osteopontin, osteocalcin, osteonectin and bone morphogenetic protein-2 & -4), such that mineral deposition in the extracellular matrix occurs, resulting in bone-like tissue within the leaflet that is supported by angiogenesis (Dweck et al., 2012; Hulin et al., 2018; Mohler et al., 2001). It has been hypothesized that statin-therapy would reduce the risk of AVS, similarly to atherosclerosis,

by reducing lipoproteins. Unfortunately, large-scale prospective randomized control clinical trials have failed to show beneficial results from multiple intensive statin-therapies (Chan et al., 2010; Cowell et al., 2005; Rossebø et al., 2008; Van Der Linde et al., 2011). However, a post hoc analysis of the simvastatin and ezetimibe in aortic stenosis (SEAS) trial did find a benefit to statin therapy specifically in patients with mild AVS and high LDL (Greve et al., 2019). Given the lack of standardized pharmacological treatment for AVS, further elucidation of the mechanism of AVS is required.

Oxylipins are a class of lipid mediators that have essential roles in homeostatic functions and are produced by enzymatic oxidation of PUFA. It has now been shown that enzymes involved in oxylipin synthesis, namely PLA2, COX-1, COX-2, and 5-LOX, are elevated in calcified areas of AV leaflet tissue (Nagy et al., 2011; Sakaue et al., 2020; Suzuki et al., 2014; Wirrig et al., 2015). Further, a recent study has identified two specialized pro-resolving mediators, the EPA derived resolvin RvE1 and DHA derived RvD3 to be lower, while LTB4 was elevated, in the calcified regions of the AVS leaflet (Artiach et al., 2020). However, like the endothelial cells or whole heart, the lipidomic profile of AV leaflets is complex and we anticipate that there is a larger panel of bioactive oxylipins that more accurately characterize calcification of AV leaflets. (Du et al., 2020; Ferdouse et al., 2019).

The progression of AVS is, in part, driven by inflammatory mechanisms that resemble those of maladapted tissue repair. The COX derived PGs and TXs (collectively termed prostanoids) mediate inflammation, with those derived from arachidonic acid generally responsible for proinflammatory cellular processes, while the n-3 PUFA derived oxylipins, which include the specialized pro-resolving mediators, mediate anti-inflammatory and tissue repair processes (Du et al., 2020; Gabbs et al., 2015). The dysregulation of inflammation-regulating oxylipins should consequently be expected in AVS. Further, oxylipins mediate cellular functions other than inflammation. Of particular relevance to AVS are PGE2 and PGF2α due to their involvement in the process of osteogenesis, which plays a critical role in the development of the disease (Koshihara and Kawamura, 1989; Kruger et al., 2010; Quarles et al., 1993; Sato et al., 2003). Thus, there is a need to compare the oxylipins in calcified and non-calcified human aortic valves to further our understanding of the underlying pathophysiology of AVS. Here we quantify for the first time whole profiles of oxylipins in the human AV and plasma of patients receiving aortic valve surgery and identify the alterations in oxylipin profiles

with AVS severity.

5.3. Methods

All study data has been made available at Figshare and can be accessed at https://doi.org/10.6084/m9.figshare.24962391.v1.

5.3.1. Human aortic valve tissue

The full details of the participant recruitment and tissue collection have been previously reported (Surendran et al., 2020). Research ethics boards at the University of Manitoba and St. Boniface Hospital approved collection of these tissues for biomolecular study. Briefly, male and female aortic valve surgery patients (n=110) at St. Boniface Hospital (Winnipeg, Canada) were recruited and provided written informed consent. AV mean transvalvular gradient (MPG) and calcification severity were based on transthoracic echocardiography measurements (Baumgartner et al., 2009). Pre-surgical plasma samples were also collected from a subset of patients (n=17). The AV leaflets were surgically removed and immediately placed in an ice-cold ethylenediaminetetraacetic acid/phosphate buffered saline solution, and then flash frozen for storage at -80°C.

Plasma was obtained from an additional group of patients with moderate to severe AVS based on echocardiographic assessment (n=55) and a group of healthy control patients with no history of AVS (n=44). A complete table of characteristics for the control patients can be found in Supplemental Table 1.

5.3.2. Oxylipin extraction and quantification

For this study, free oxylipins were extracted and quantified from AV leaflets as described in (Leng et al., 2017; Monirujjaman et al., 2017), with modifications. Briefly, whole leaflets were weighed and homogenized in Tyrode's salt solution (9.6 g/L, pH 7.6) at a ratio of 7 mg to 40 µL, using an Omni Bead Ruptor 24 (Omni International, Inc., GA, USA). Antioxidant cocktail (0.2 g/L butylated hydroxytoluene, 0.2 g/L ethylenediaminetetraacetic acid, 2 g/L triphenylphosphine, and 2 g/L indomethacin in methanol/ethanol/water (2:1:1, v/v/v)) was added (1:20, v/v) to 400 µL of homogenate, followed by the addition (4:3, v/v) of methanol/formic acid (100:1, v/v). A mixture of deuterated oxylipin internal standards (Cayman Chemical, MI) was

added to the AV homogenates or to 250 µL of plasma. Samples were diluted in acidified water (1:5, v/v) to adjust to pH 3 and applied to 33 µm polymeric reverse phase extraction columns (Phenomenex, CA, USA) pre-conditioned with methanol and pH 3 water. The columns were rinsed with pH 3 water followed by hexane. Oxylipins were eluted from the column with methanol, collected, evaporated, and resuspended in MS grade water: acetonitrile: acetic acid (70:30:0.02; v/v/v) for high performance liquid chromatography tandem mass spectrometry (Shimadzu Nexera XR coupled to a QTRAP 6500 triple quadruple; Sciex, ON) analysis, by a procedure modified from (Deems et al., 2007) and described in (Aukema et al., 2016; Leng et al., 2017). The complete list of internal standards, oxylipins scanned for, and instrument limits of detection can be found in Supplemental Table 2. Oxylipins were quantified using the stable isotope dilution method described in (Hall and Murphy, 1998). Oxylipins detected, at the established t_R and mass-to-charge ratio, were selected for quantification when peaks exceeded 5-times baseline (Supplemental Figure 1). The concentration was calculated from the ratio of the peak area to that of a known amount of deuterated internal standard, with patient AVS status blinded to the researcher. Oxylipin concentrations were reported in relation to total valvular protein determined by extraction with RIPA lysis buffer followed by bicinchoninic acid protein assay.

5.3.3. Data analyses

All statistical analyses were performed using R (version 4.2.2) implemented through RStudio (version 2023.03.1+446) for graphical visualization. Patients were grouped into AVS severity groups using MPG (mild <20 mmHg, moderate ≥20 to <40 mmHg, and severe ≥40 mmHg, and severe ≥40 mmHg, based on the 2014 AHA/ACC guidelines (Nishimura et al., 2014)), or by calcification score (mild: 1-2, moderate: 3, and severe 4-5). The categorical clinical parameters were compared using the chi-square test. The continuous clinical parameters, oxylipins and oxylipin category totals (as concentrations and percentages of total oxylipins) were compared by ANOVA, using AVS severity groups. Data was transformed using Tukey's ladder of powers, to achieve normality and homogeneity of variance, followed by ANOVA and Tukey's HSD test. When the ANOVA assumptions were not achieved after transformation, the Kruskal-Wallis test was used with Dunn's post hoc test. The Bonferroni correction for multiple comparisons was then applied. Linear correlations between oxylipins and clinical parameters were determined using Pearson's correlation test. PCA was performed on per sample unit sum

normalized clinical data and $\log_{10}$ oxylipins. For the PCA models, clinical variables with >20% missing values were excluded from the analysis. The remaining missing values were imputed using a regularized iterative PCA algorithm (missMDA package). Stepwise linear regression was also performed to identify which oxylipins and clinical parameters independently were predictive of AVS. This was conducted specifically with MPG as the outcome variable and modeled initially with all the clinical variables (excluding the other hemodynamic parameters due to multicollinearity) as predictor variables. The non-significant variables were discarded, then oxylipins were individually added (due to multicollinearity) as predictor variables to improve the global p-value of the model.

5.4. Results

5.4.1. Patient characteristics

The baseline characteristics of the patients grouped by MPG severity from which valve samples were are displayed in Table 1. Age, sex, height, body surface area, blood pressure, blood lipids, blood glucose, creatinine, hypertension history, medications, and bicuspid aortic valve did not differ significantly between severity groups. Only weight and body mass index differed between groups, with a significant increase with AVS severity. Smoking history was highest among the moderate group. Calcification and echocardiograph parameters predictably worsened with MPG severity. Further details have been previously reported in (Surendran et al., 2020).

Table 5.1. Patient characteristics for AV oxylipin analysis

	Total (n=99)	MPG-Mild (n=15)	MPG-Moderate (n=39)	MPG-Severe (n=45)	*P* value
Age (y)	68.9 (11.2)	69.9 (9.59)	70.5 (11.6)	67.2 (11.3)	0.321
Sex (Male)	68 (68.7%)	12 (80.0%)	23 (59.0%)	33 (73.3%)	0.217
Height (cm)	170 (8.40)	171 (9.87)	169 (8.55)	171 (7.85)	0.584
Weight (kg)	87.3 (23.1)	76.6 (17.7)	86.4 (27.1)	91.4 (19.9)	0.021
BSA (m^2)	1.97 (0.214)	1.89 (0.260)	1.95 (0.225)	2.02 (0.179)	0.089
BMI	29.4 (5.50)	26.0 (4.27)	29.0 (5.01)	30.8 (5.82)	0.009
Systolic Blood Pressure (mmHg)	134 (20.1)	132 (18.5)	137 (26.5)	132 (13.2)	0.529
Diastolic Blood Pressure (mmHg)	71.3 (13.8)	63.1 (15.9)	73.1 (12.6)	72.4 (14.0)	0.077
LDL (mM)	2.88 (0.991)	2.90 (0.520)	3.09 (1.22)	2.65 (0.849)	0.654
HDL (mM)	1.24 (0.321)	1.20 (0.100)	1.34 (0.373)	1.16 (0.300)	0.452
Triglycerides (mM)	1.64 (0.672)	1.73 (0.757)	1.33 (0.387)	1.88 (0.836)	0.350
Random glucose (mM)	7.28 (2.81)	6.49 (1.56)	7.56 (2.97)	7.29 (2.97)	0.821
Creatinine (μM)	88.2 (35.1)	97.5 (70.7)	82.8 (18.7)	90.1 (29.5)	0.786
History of Hypertension	68 (73.1%)	7 (53.8%)	31 (79.5%)	30 (73.2%)	0.196
History of Smoking	52 (55.3%)	6 (46.2%)	27 (72.9%)	19 (43.2%)	0.021
Current	10 (10.6%)	0 (0%)	5 (13.5%)	5 (11.4%)	0.052
Previous	42 (44.7%)	6 (46.2%)	22 (59.5%)	14 (31.8%)	
Never	42 (44.7%)	7 (53.8%)	10 (27.0%)	25 (56.8%)	
Medications					
ASA	25 (26.9%)	2 (15.4%)	8 (21.6%)	15 (34.9%)	0.247
Antihypertensive	62 (65.3%)	9 (64.3%)	26 (68.4%)	27 (62.8%)	0.865

ACE inhibitors	31 (32.6%)	6 (75.0%)	13 (34.2%)	12 (27.9%)	0.564
ARBs	10 (10.6%)	3 (21.4%)	3 (8.11%)	4 (9.30%)	0.360
Statin	54 (56.8%)	4 (28.6%)	22 (57.9%)	28 (65.1%)	0.056
Bicuspid Aortic Valve	29 (31.2%)	5 (35.7%)	10 (26.3%)	14 (34.1%)	0.697
Calcification					<0.001
1	9 (9.09%)	8 (53.3%)	0 (0%)	1 (2.22%)	
2	27 (27.3%)	3 (20.0%)	16 (41.0%)	8 (17.8%)	
3	38 (38.4%)	3 (20.0%)	16 (41.0%)	19 (42.2%)	
4	18 (18.2%)	0 (0%)	6 (15.4%)	12 (26.7%)	
5	7 (7.07%)	1 (6.67%)	1 (2.56%)	5 (11.1%)	
Peak aortic jet velocity (m/s)	3.99 (0.989)	2.27 (0.631)	3.72 (0.284)	4.71 (0.631)	<0.001
Peak aortic jet pressure (mmHg)	66.7 (30.6)	21.7 (9.30)	55.6 (8.65)	91.4 (3.55)	<0.001
Mean aortic jet pressure (mmHg)	40.5 (19.1)	11.5 (4.02)	33.1 (4.93)	56.5 (13.8)	<0.001
Aortic valve area (cm^2)	1.01 (0.494)	1.86 (0.651)	0.924 (0.264)	0.810 (0.240)	<0.001
Indexed aortic valve area (cm^2/m^2)	0.496 (0.221)	0.915 (0.333)	0.477 (0.135)	0.409 (0.115)	<0.001
Left ventricular mass index (g/m^2)	127 (37.9)	153 (36.3)	115 (35.1)	129 (37.1)	0.007

Continuous variables are given as mean (SD), with P values calculated by 1-way ANOVA. Categorical variables are given as count (proportion), with *P* values calculated by the $\chi 2$ test. ACE indicates angiotensin-converting enzyme; ARB, angiotensin II receptor blocker; ASA, aspirin; AV, aortic valve; BMI, body mass index; HDL, high-density lipoprotein; LDL, low-density lipoprotein; and MPG, mean transvalvular pressure gradient.

Table 2 displays the baseline patient characteristics for the plasma oxylipins analysis. There were notable differences between the healthy control and AVS groups. The control group was younger, with lower rates of current and past smoking, and had lesser use of ACE inhibitors or ARBs and statins.

Table 5.2. Shared Patient Characteristics for Plasma Analysis

	Total (n=104)	Control (n=31)	MPG-Mild (n=5)	MPG-Moderate (n=27)	MPG-Severe (n=41)	*P* value
Age	73.6 (13.1)	60.2 (11.1)	77.2 (7.40)*	80.7 (6.53)*	78.7 (10.8)*	<0.001
Sex (Male)	57 (54.8%)	18 (58.1%)	4 (80.0%)	16 (59.3%)	19 (46.3%)	0.421
Height (cm)	167 (9.27)	168 (9.92)	166 (6.12)	167 (9.97)	165 (8.43)	0.214
Weight (kg)	81.3 (21.0)	84.9 (22.7)	81.3 (11.1)	83.9 (20.1)	77.5 (21.4)	0.406
BSA (m^2)	1.90 (0.265)	1.98 (0.309)	1.89 (0.150)	1.94 (0.254)	1.83 (0.242)	0.147
BMI		29.8 (6.86)	29.6 (2.53)	29.2 (5.08)	28.5 (7.93)	0.636
Type 2 Diabetes	37 (35.6%)	5 (16.1%)	2 (40.0%)	13 (48.1%)	17 (41.5%)	0.054
History of Hypertension	69 (69.0%)	15 (50.0%)	5 (100%)	24 (88.9%)	25 (65.8%)	0.006
History of Smoking	35 (34.7%)	4 (12.9%)	1 (25.0%)	12 (46.2%)	18 (45.0%)	0.018
Current	7 (7.00%)	2 (6.45%)	0 (0%)	1 (4.00%)	4 (10.0%)	0.068
Previous	27 (27.0%)	2 (6.45%)	1 (25.0%)	10 (40.0%)	14 (35.0%)	
Never	66 (66.0%)	27 (87.1%)	3 (75.0%)	14 (56.0%)	22 (55.0%)	
Medications						
ACE inhibitor or ARBs	10 (9.62%)	5 (16.1%)	0 (0%)	3 (11.1%)	2 (4.88%)	0.366
Statin	44 (43.6%)	5 (16.1%)	1 (20.0%)	19 (73.1%)	19 (48.7%)	<0.001

Continuous variables are given as mean (SD), with P values calculated by 1-way ANOVA. Categorical variables are given as count (proportion), with *P* values calculated by the $\chi 2$ test.

ACE indicates angiotensin-converting enzyme; ARB, angiotensin II receptor blocker; BMI, body mass index; and MPG, mean transvalvular pressure gradient. * Compared to control.

5.4.2. Valvular oxylipins

We quantified 36 unique oxylipins in valvular tissue. The complete list of the oxylipins quantified and comparisons by MPG severity can be found in Supplemental Table 3. Total oxylipin levels were found to increase with disease severity, and this was reflected in the total oxylipin mass by MPG (Fig. 1A). When patients were grouped by MPG severity, total oxylipins was elevated when comparing MPG mild to moderate and mild to severe (Fig. 1B). Similarly, the total oxylipins increased when patients were grouped by calcification score (Fig. 1C). Each oxylipin quantified increased with AVS severity and 35/36 oxylipins were significantly different ($\alpha=0.05$) (Fig. 2). Considering Bonferroni correction for multiple comparisons, 32/36 oxylipins remained significantly altered ($\alpha=0.0014$).

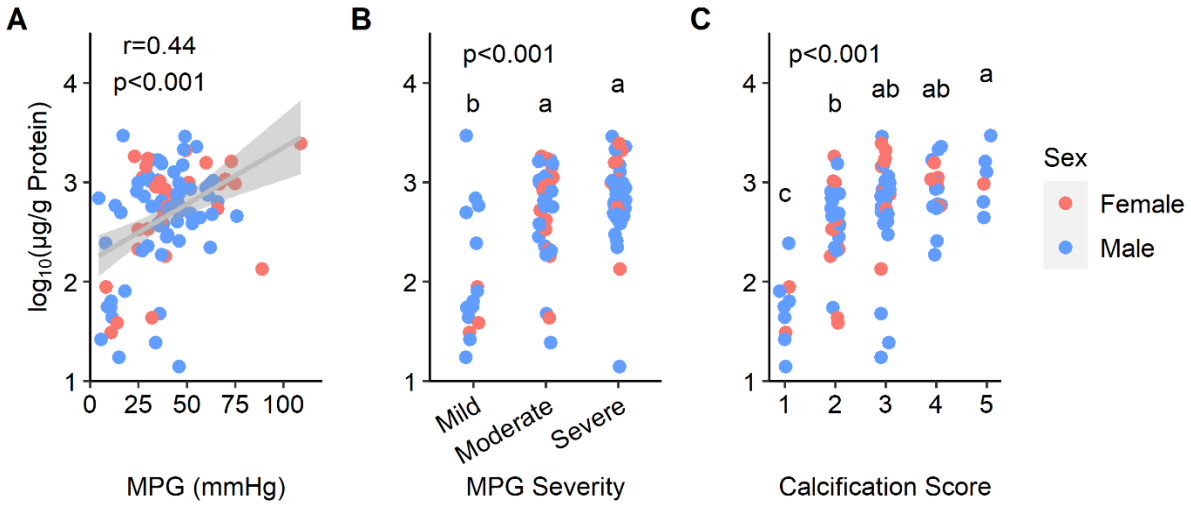

Figure 5.1. Correlation of oxylipins with severity of aortic valve stenosis.
A) Total aortic valve oxylipins by mean transvalvular pressure gradient (MPG). Trend line has a 95% CI. **B)** Total aortic valve oxylipins by MPG severity. **C)** Total aortic valve oxylipins by calcification score. The compact letter display indicates significant differences in which a > b > c by the Tukey honestly significant difference test.

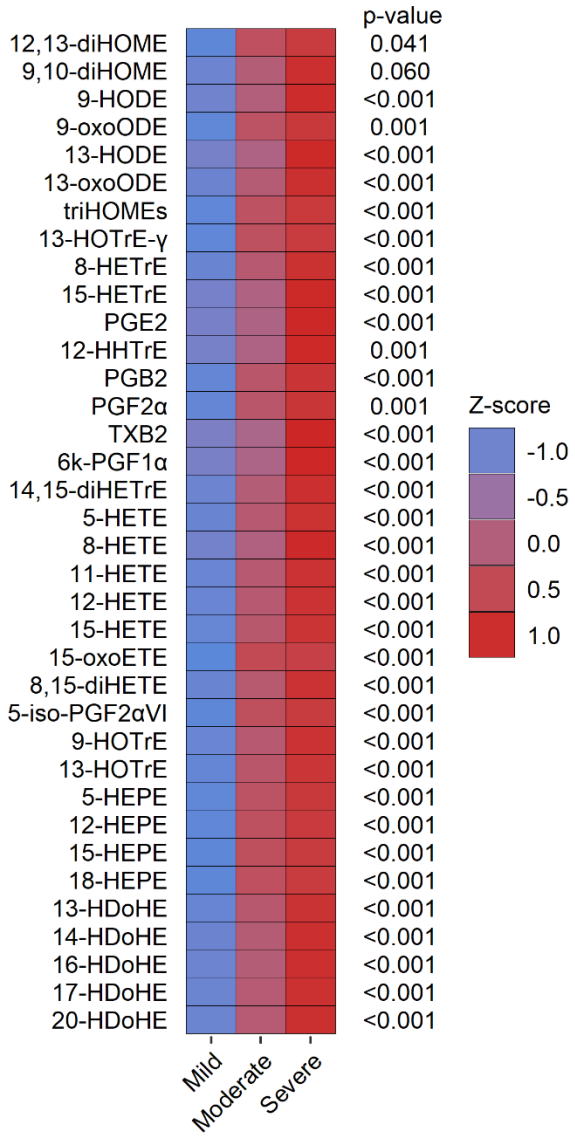

Figure 5.2. Heatmap of aortic valve oxylipins by mean transvalvular pressure gradient (MPG) severity.

Values are normalized for each oxylipin with mean centering and root-mean-square scaling. diHETE indicates dihydroxy-eicosatetraenoic acid; diHETrE, dihydroxy-eicosatrienoic acid; diHOME, dihydroxy-octadecaenoic acid; HDoHE, hydroxy-docosahexaenoic acid; HEPE, hydroxy-eicosapentaenoic acid; HETE, hydroxy-eicosatetraenoic acid; HETrE, hydroxy-eicosatrienoic acid; HHTrE, hydroxyheptadecatrienoic acid; HODE, hydroxy-octadecadienoic acid; HOTrE, hydroxy-octadecatrienoic acid; oxoETE, oxo-eicosatetraenoic acid; oxoODE, oxo-octadecadienoic acid; PG, prostaglandin; triHOME, trihydroxy-octadecenoic acid (9,10,13-triHOME and 9,12,13-triHOME peaks could not be separated); and TX, thromboxane.

When oxylipins levels were categorized based on the fatty acid precursor from which they are derived, each of the fatty acid precursors was elevated with AVS severity whether dividing patients by MPG or calcification severity. Specifically, the moderate and severe groups were significantly elevated from mild, but not distinct from each other (Fig. 3A,B,D,E). When the fatty acid totals were considered as proportions of the total oxylipins, we see that the relative amount of linoleic acid oxylipins decreased with between MPG mild and severe, while AA, α-linolenic acid, DGLA, and EPA oxylipins increased (Fig. 3C). For calcification severity, only the increased proportion of ALA reached significance (Fig. 3F). When oxylipins were totalled by the major enzymatic pathways from which they were derived, each pathway was increased with AVS severity (MPG and calcification), such that moderate and severe groups were significantly elevated from mild, but not distinct from each other (Fig. 4A,B,D,E). For enzyme pathways, the proportions of the total oxylipins did not change with AVS severity (Fig. 4C,F).

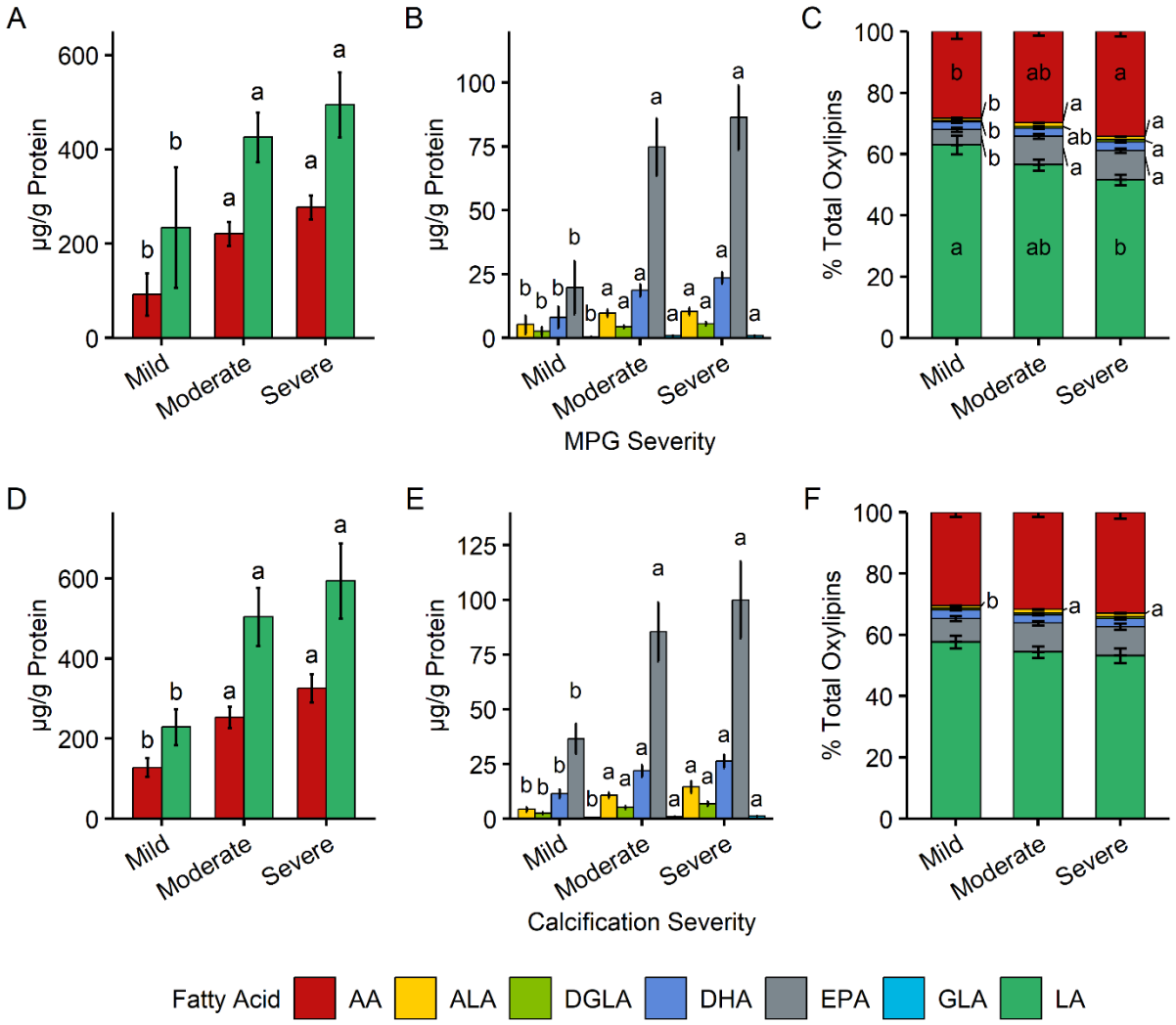

Figure 5.3. Aortic valve oxylipins totaled by fatty acid precursor.

A & B) Absolute totals by mean transvalvular pressure gradient (MPG) severity. *P* values: arachidonic acid (AA), $P < 0.001$; linoleic acid (LA), $P < 0.001$; α-linolenic acid (ALA), $P < 0.001$; dihomo-γ-linolenic acid (DGLA), $P < 0.001$; docosahexaenoic acid (DHA), $P < 0.001$; eicosapentaenoic acid (EPA), $P < 0.001$; γ-linolenic acid (GLA), $P < 0.001$. **C)** %Total oxylipins by MPG severity. *P* values: AA, $P = 0.033$; ALA, $P = 0.008$; DGLA, $P = 0.012$; EPA, $P < 0.001$; LA, $P = 0.003$. **D & E)** Absolute totals by calcification severity. *P* values: AA, $P < 0.001$; LA, $P < 0.001$; ALA, $P < 0.001$; DGLA, $P < 0.001$; DHA, $P < 0.001$; EPA, $P < 0.001$; GLA, $P < 0.001$. **F)** %Total oxylipins by calcification severity. *P* value: ALA, $P = 0.011$. Comparisons are between severity groups for each fatty acid precursor. The compact letter display indicates significant differences in which a > b by Tukey honestly significant difference test

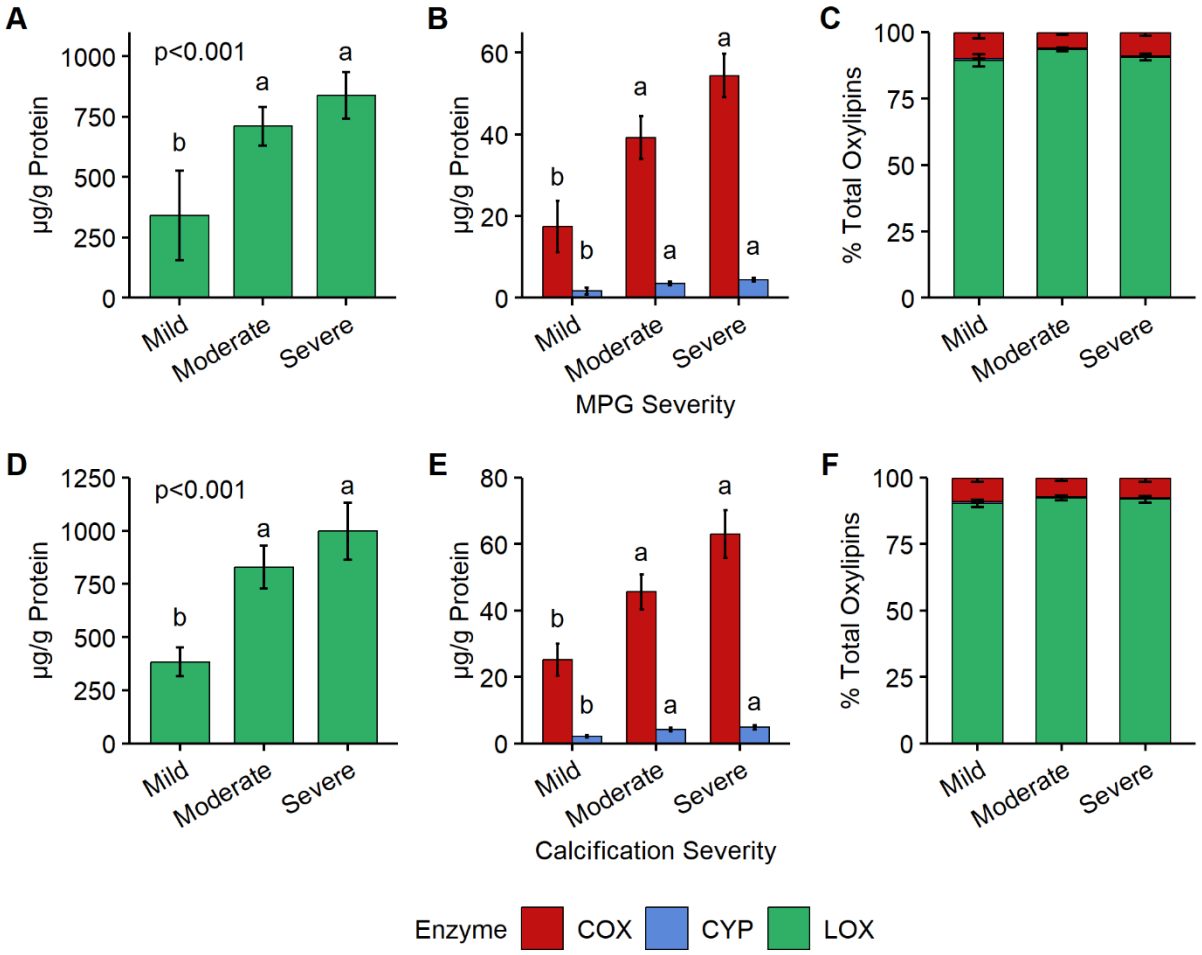

Figure 5.4. Aortic valve oxylipins totaled by enzymatic pathway.

A & B) Absolute totals by mean transvalvular pressure gradient (MPG) severity. *P* values: COX (cyclooxygenase), $P < 0.001$; CYP (cytochrome P450), $P < 0.001$. **C)** %Total oxylipins by MPG severity. **D & E)** Absolute totals by calcification severity. *P* values: COX, $P < 0.001$; CYP, $P < 0.001$. **F)** %Total oxylipins by calcification severity. Comparisons are between severity groups for each enzymatic pathway. The compact letter display indicates significant differences in which a > b by Tukey honestly significant difference test. LOX indicates lipoxygenase.

5.4.3. Valvular oxylipins and clinical parameters

Given the function of ASA as a COX-inhibitor, we compared each oxylipin by patient ASA use status to determine the impact of ASA on valvular oxylipins (Supplemental Table 4). It was found that 4 DHA oxylipins were altered ($\alpha=0.05$) but were not significant considering the Bonferroni adjustment for multiple comparisons ($\alpha=0.0014$).

Figure 5 depicts the Pearson correlations between each of the valvular oxylipins and clinical parameters. There are distinct groupings of highly correlated variables, such as the AVS severity parameters. Also, the majority of oxylipins are highly correlated with each other; notable exceptions were PGE2, 12-hydroxy-heptadecatrienoic acid, PGF2α, TXB2, and 6-keto-PGF1α, which are best correlated with each other and are all derived from the AA-COX pathway.

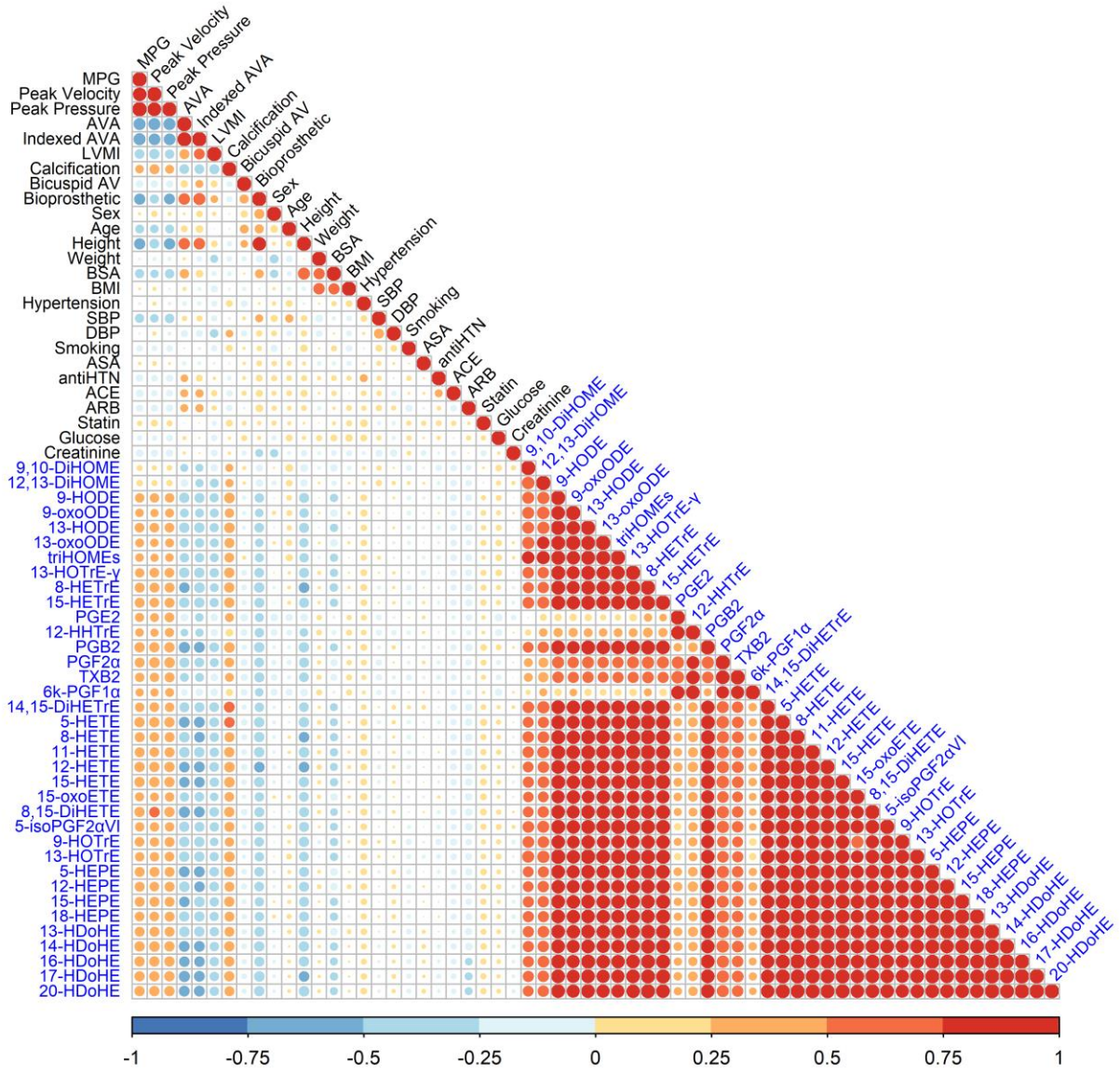

Figure 5.5. Pearson correlations of valvular oxylipins and clinical parameters.

Variables in black text are clinical parameters, and variables in blue text are oxylipins. ACE indicates angiotensin-converting enzyme; antiHTN, antihypertensive; ARB, angiotensin II receptor blocker; ASA, aspirin; AV, aortic valve; AVA, aortic valve area; BMI, body mass index; DBP, diastolic blood pressure; DiHETE, dihydroxy-eicosatetraenoic acid; DiHETrE, dihydroxy-eicosatrienoic acid; DiHOME, dihydroxy-octadecaenoic acid; HDoHE, hydroxy-docosahexaenoic acid; HEPE, hydroxy-eicosapentaenoic acid; HETE, hydroxy-eicosatetraenoic acid; HETrE, hydroxy-eicosatrienoic acid; HHTrE, hydroxyheptadecatrienoic acid; HODE,

hydroxy-octadecadienoic acid; HOTrE, hydroxy-octadecatrienoic acid; LVMI, left ventricular mass index; MPG, mean transvalvular pressure gradient; oxoETE, oxo-eicosatetraenoic acid; oxoODE, oxo-octadecadienoic acid; PG, prostaglandin; SBP, systolic blood pressure; triHOME, trihydroxy-octadecenoic acid; and TX, thromboxane.

Next, a multivariate model, that included all oxylipins and clinical parameters was constructed. From PCA, figure 6A depicts the scores plot, in which each patient is projected on to components 1 and 2. The AVS severity status has been overlayed onto each patient and AVS severity can be seen to be positively associated with each component. Figures 6B and C display the top absolute loadings values for variables on components 1 and 2, respectively. These show that component 1 primarily accounts for the variance in the model attributed to the majority of oxylipins, while the variables contributing to component 2 include AVS severity markers and AA COX-derived prostanoids. Specifically, MPG, peak aortic jet velocity, peak aortic jet pressure, PGE2, PGF2α, 6k-PGF1α, 12-hydroxy-heptadecatrienoic acid, and TXB2 were positively associated, and AV area, indexed AV area, and left ventricle mass index – which are inversely related to increased AVS severity – were negatively associated. Thus, this multivariate model shows that prostanoids in the aortic valve are highly correlated with AVS severity. These findings are validated by a multiple linear regression model with MPG as the dependant variable that was optimized by stepwise selection and resulted in the inclusion of the clinical parameters (age, weight, systolic blood pressure, and creatinine) and PGF2α as independent variables (Table 3).

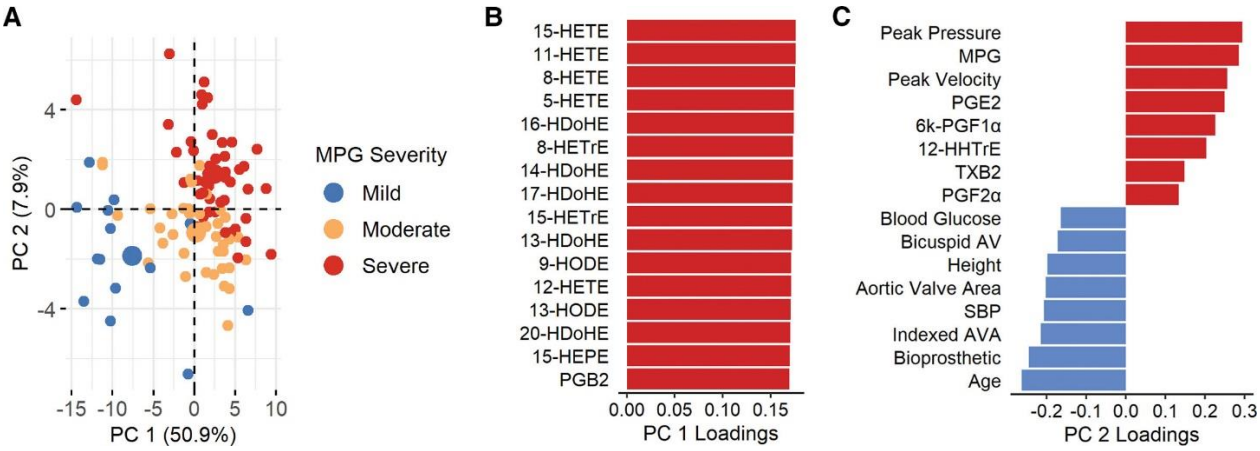

Figure 5.6. Patient characteristics and valvular oxylipins modeled by principal component (PC) analysis.

A) Score plots of individuals on PCs 1 and 2. Color overlayed by mean transvalvular pressure gradient (MPG) severity group. **B)** Loading values of the top variables by absolute value for component 1. **C)** Loading values of the top variables by absolute value for component 2. 6k-PGF1α indicates 6-keto-prostaglandin F1alpha; AV, aortic valve; AVA, aortic valve area; DiHOME, dihydroxy-octadecaenoic acid; HDoHE, hydroxy-docosahexaenoic acid; HEPE, hydroxy-eicosapentaenoic acid; HETE, hydroxy-eicosatetraenoic acid; HETrE, hydroxy-eicosatrienoic acid; HHTrE, hydroxyheptadecatrienoic acid; HODE, hydroxy-octadecadienoic acid; PG, prostaglandin; SBP, systolic blood pressure; and TX, thromboxane.

Table 5.3. Effect of Clinical Parameters and Oxylipins on Aortic Valve Mean Transvalvular Gradient

	Estimate	SE	t value	Pr(>|t|)
Intercept	0.153	0.0157	9.74	<0.001
Age	-0.400	0.108	-3.71	<0.001
Weight	-0.181	0.0663	-2.73	0.008
SBP	-0.319	0.0692	-4.61	<0.001
Creatinine	-0.197	0.0438	-4.50	<0.001
PGF2α	6.95	2.27	3.06	0.003

PGF2α indicates prostaglandin F2alpha; and SBP, systolic blood pressure.

5.4.4. Plasma oxylipins

Plasma oxylipins from patients with AVS were compared to control healthy participants without AVS (Supplemental Table 5). Total oxylipins were found to be higher in the severe AVS patients compared to controls (Fig. 7A). Unlike the valvular oxylipins, dysregulation of plasma oxylipins occurred in both directions, with both up and down-regulation with disease severity (Fig. 7B). The oxylipin totals by fatty acid precursors were compared: AA, DHA, γ-linolenic acid oxylipins were decreased and α-linolenic acid, dihomo-γ-linolenic acid, DPA, EPA, and linoleic acid oxylipins increased in AVS patients (Fig. 7C). When compared as proportions of the total oxylipin mass all oxylipin classes except EPA were significantly different between control and severe AVS patients (Fig. 7D).

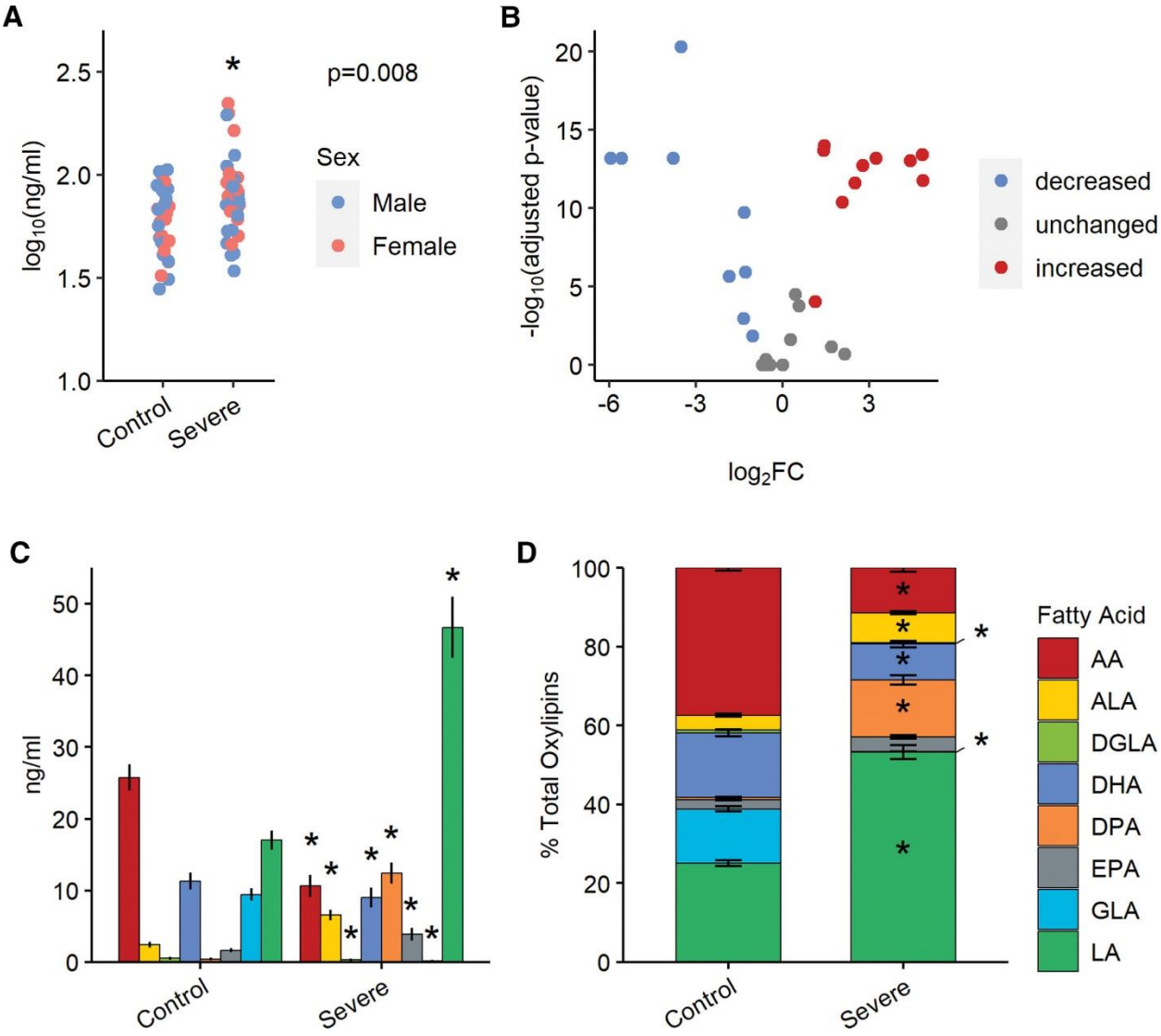

Figure 5.7. Plasma oxylipins of control and mean transvalvular pressure gradient (MPG)-severe patients.

A) Total oxylipins. **B)** Volcano plot of plasma oxylipins, control vs severe. Oxylipins were considered altered if |LFC| > 1 and adjusted $P < 0.05$. **C)** Absolute oxylipin totals by fatty acid precursor. *P* values: arachidonic acid (AA), $P < 0.001$; α-linolenic acid (ALA), $P < 0.001$; dihomo-γ-linolenic acid (DGLA), $P < 0.001$; docosahexaenoic acid (DHA), $P = 0.019$; docosapentaenoic acid (DPA), $P < 0.001$; eicosapentaenoic acid (EPA), $P = 0.045$; γ-linolenic acid (GLA), $P < 0.001$; linoleic acid (LA), $P < 0.001$. **D)** %Total oxylipins by fatty acid precursor. *P* values: AA, $P < 0.001$; ALA, $P < 0.001$; DGLA, $P < 0.001$; DHA, $P < 0.001$; DPA, $P < 0.001$; GLA, $P < 0.001$; LA, $P < 0.001$. Comparisons are between severity groups for each fatty acid precursor. *Significantly different from control by ANOVA ($P < 0.05$).

A PCA model that included the plasma oxylipins and clinical parameters of the control participants and patients from each AVS severity group shows clear separation between control and AVS patients along PC1 (Fig. 8A). The top absolute loadings values for variables on component 1 of this model are displayed in figure 8B. When we removed the controls from the model the is no separation based on AVS severity (Fig. 8C).

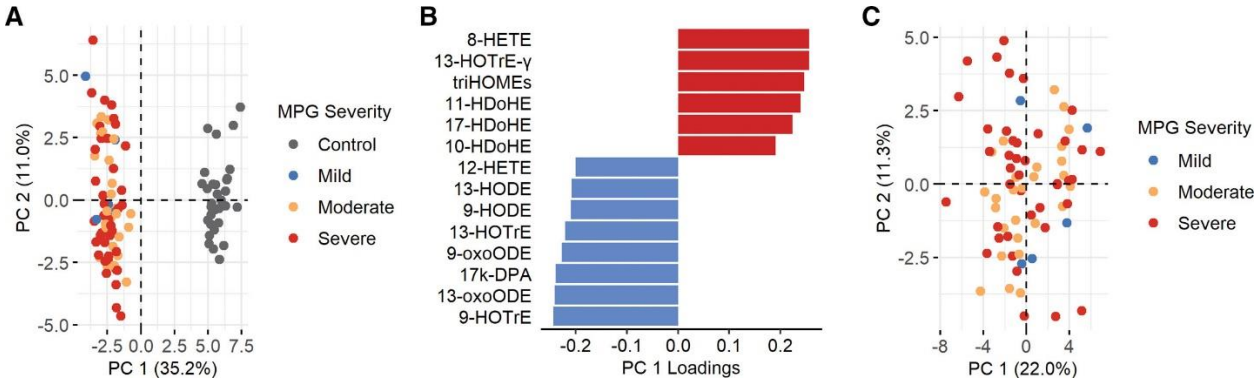

Figure 5.8. Patient characteristics and plasma oxylipins modeled by principal component analysis.

A) Score plots, all plasma sample patients on components 1 and 2 with color overlayed by mean transvalvular pressure gradient (MPG) severity group. **B)** Loading values of the top variables on principal component 1. **C)** Score plots from model excluding control patients. DPA indicates docosapentaenoic acid; HDoHE, hydroxy-docosahexaenoic acid; HETE, hydroxy-eicosatetraenoic acid; HODE, hydroxy-octadecadienoic acid; HOTrE, hydroxy-octadecatrienoic acid; oxoODE, oxo-octadecadienoic acid; and triHOME, trihydroxy-octadecenoic acid (9,10,13-triHOME and 9,12,13-triHOME peaks could not be separated).

5.5. Discussion

This study provides the first comprehensive targeted analysis of the oxylipin profile in calcified human AV tissue. Our results indicate a broad increase in oxylipins with increasing AVS severity, suggesting a significant disruption of physiological homeostasis occurs. The dysregulation of oxylipins may contribute to the progression of AVS, as these lipid mediators play crucial roles in inflammation and osteogenesis.

The alterations in the valvular oxylipin profile, particularly the increase in the proportion of valvular AA oxylipins (Fig. 3C) and the identification of the AA-COX prostanoids as variables of importance by the multivariate modelling (Fig. 6C, Table 3), are informative to the mechanistic understanding of the chronic inflammation characteristic of AVS. The prostanoids are inflammatory mediators which play key roles in the initiation of inflammatory response (Ricciotti and Fitzgerald, 2011; Serhan, 2014). There is also evidence that prostanoids are involved in chronic inflammatory states by promoting persistent cellular infiltration by immune cells (Yao and Narumiya, 2019). For instance, the elevated systemic inflammation exhibited in RA is known to be mediated by prostanoids (Fattahi and Mirshafiey, 2012; Korotkova and Jakobsson, 2014). Intriguingly, patients with RA have now been shown to be at increased risk of AVS progression (Johnson et al., 2023).

Lp(a) has been identified as a risk factor for developing AVS. One proposed mechanism for Lp(a) as a proinflammatory molecule is its propensity to oxidation compared to other lipoproteins. Because of this, Lp(a) has the highest concentration of oxidized phospholipids in plasma (Bergmark et al., 2008). To date there has not been any investigation of the oxylipin profile differences among Lp(a) and other lipoproteins. We have previously shown that as LDL is oxidized, 8 PGs, namely PGE1, PGE2, dhk-PGE2, dhk-PGD2, PGF2α, PGJ2, 15k-PGE2, and 11β-PGE2, showed substantial elevation (Surendran et al., 2019). This would suggest that the increased Lp(a) oxidation, associated with AVS, may also contribute to the rise in prostaglandins. Thus, our study supports the current mechanism and builds upon it by quantifying the elevation of specific prostanoids with AVS severity.

In addition to the contribution of inflammatory processes to AVS development, prostanoids are likely to contribute to AV calcification. Of the five prostanoids highlighted in this analysis, two have direct functionality connections to osteogenesis. Both PGE2 and PGF2α are mediators of calcium resorption and bone remodelling. PGE2 modulates the differentiation of myofibroblasts, osteoblasts, and osteoclasts (Choudhary et al., 2013; Kobayashi et al., 2005; Take et al., 2005; Wettlaufer et al., 2016); while, PGF2α regulates proliferation and differentiation of osteoblasts and their mineralization of Ca^{2+} and inorganic phosphate (Quarles et al., 1993; Sato et al., 2003). 6k-PGF1α was also identified in this analysis, and it is a stable hydrolysis product of the short-lived prostacyclin (PGI2). There is emerging evidence that PGI2 may have osteogenic properties. A PGI2 synthase knockout mouse model had increased bone

formation, resorption, and bone mass (Nakalekha et al., 2010). Also, the stable PGI2 analog Iloprost improved bone regeneration in a mouse osteotomy trial (Wendler et al., 2019). Similarly, TXB2 is a stable hydrolysis product of TXA2, which may induce the formation of osteoclasts (Gruber et al., 2003). The effect of these PGs specifically in VICs has not yet been demonstrated, but these molecules are likely candidates for mediating the connection between COX up-regulation and the development of the osteoblast-like phenotype and mineral deposition that is characteristic of AVS progression. Thus, these data support and enhance the current understanding of the mechanisms of AVS development with the chronic inflammatory environment promoting calcification mediated through valvular prostanoids.

Currently, there is conflicting data on the role of COX in AVS. Firstly, COX-1 and COX-2 mRNA and protein expression have been found to be elevated in *ex-vivo* calcified AV tissues and *in vitro* calcification models (Sakaue et al., 2020; Suzuki et al., 2014; Wirrig et al., 2015); while, one study conflictingly found decreased COX-2 expression *ex-vivo* (Sega et al., 2020). Our study's findings of increased COX derived oxylipins supports the former. If we accept that COX expression increases with AVS, whether increased COX promotes valvular calcification or is a product of it is not known. On the other hand, it should be noted that COX expression and activity level are not always positively correlated (Warford-Woolgar et al., 2006).

In our cohort 27% of patients were on ASA therapy. Given that ASA is a non-selective COX-inhibitor that irreversibly inhibits COX, we would have predicted that this would underestimate the COX metabolites. However, ASA therapy had little impact on valvular oxylipin levels (Figure 5, Supplemental Table 5). This may be explained by the distribution of ASA, primarily binding to plasma proteins, and a relatively short half-life compared to other NSAIDs, such that impact on valvular COX activity would likely be limited (Lanas, 2016). While ASA is the most widely consumed NSAID, future research into oxylipins in AVS would be well-served to collect data on other NSAIDs.

Previous studies of COX inhibition with AVS models have been conducted but provide ambiguous data. In a *Klotho*-deficient mouse model for AVS and in cultured porcine aortic VICs in osteogenic conditions, the use of celecoxib (selective COX-2 inhibitor) was shown to slow calcification (Wirrig et al., 2015). Also, this mouse model demonstrated that increased valvular COX-2 expression preceded calcification. Contradictorily, in *ex vivo* human and *in vitro* porcine VICs, calcification induced with treatment of transforming growth factor β1 or osteogenic media

was enhanced with celecoxib (Bowler et al., 2019; Sega et al., 2020; Vaidya et al., 2020). However, Vaidya et al. (2020) found that celecoxib reduced calcification *in* vitro when glucocorticoids present in osteogenic media were removed, concluding that the increased calcification observed was due to an interaction between glucocorticoids and not COX-2 inhibition (Vaidya et al., 2020).

Two retrospective analyses of observational studies have looked at AVS and COX inhibitors with one finding an association between selective COX-2 inhibitors and increased AVS risk and the other finding no association (Bowler et al., 2019; Delaney et al., 2013). Both studies also found non-selective COX inhibitors did not influence AVS risk (Bowler et al., 2019; Delaney et al., 2013). It is also worth noting that selective COX-2 inhibitors have been associated with an increased risk of cardiovascular adverse events (Solomon et al., 2005).

There have been fewer studies that focussed on the COX-1 isozyme. Recently, Sakaue et al. (2020) found the elevation of COX-1 in calcified valvular tissue to be greater than that of COX-2 and identified COX-1 activity as being essential to the differentiation of VICs to the osteoblast-like phenotype *in vitro* (Sakaue et al., 2020). Yet, in an observational study no association between AVS risk and ASA was found, and a potential increased risk was shown in one cohort, but did not replicate (Delaney et al., 2013).

Thus, there is increasing evidence of the role of COX in AVS, while the evidence for the efficacy of COX-inhibition is confounded by the contradictory findings and inconsistent associations. This study's findings that ASA therapy has limited impact on valvular COX metabolites sheds an important light on this controversy. Further research is needed to elucidate the specific roles of AA-COX products in AVS pathogenesis and to explore the shortcomings of COX inhibition.

Future study of dietary modulation to slow AVS progression is also warranted. In many tissues, it has been found that oxylipins can be modified by dietary PUFA (Cayer et al., 2019; Leng et al., 2018b, 2017; Mendonça et al., 2018). It is not yet known whether this is possible specifically in the AV. Our group has, however, previously shown high dietary n-3 PUFA (particularly DHA) to lower prostanoids in the rodent heart (Ferdouse et al., 2019). Whether this can be replicated in the human AV could have potential for future AVS dietary intervention.

A recent study by Artiach et al. (2020) quantified three oxylipins in the AV leaflets of AVS patients and found RvE1 and RvD3 lowered and LTB4 elevated in calcified compared to

non-calcified portions of the tissue (Artiach et al., 2020). While we did scan for Rvs and LTs, they were not above our limits of quantification, thus we cannot comment on them directly. However, we did quantify molecules which are the direct precursors (18-hydroxy-eicosapentaenoic acid and RvE1) or share common precursors (17-HDoHE and RvD3; 5-HETE and LTB4) and can be considered activation markers. Our finding that 18-hydroxy-eicosapentaenoic acid, 17-HDoHE, and 5-HETE each increased with AVS conforms with the previous study's result for LTtB4, but not RvE1 and RvD3. The discrepancy may be due to down-regulation of enzymes downstream of the oxylipins we quantified or due to sampling; they compared calcified to non-calcified portions from the same valve, while we homogenized whole leaflets.

In addition to analyzing the oxylipin profile in AV tissue, we also measured plasma oxylipins. We found that the plasma oxylipin profiles were distinct between a healthy control population and patients with AVS. There was not a clear pattern to the plasma oxylipin alterations. Despite some trends in the oxylipin totals by PUFA precursor, at the individual oxylipin level biphasic alterations were exhibited by metabolites from the same PUFA precursors and the same enzyme pathways (i.e. 5-LOX, 12-LOX, or 15-LOX). Thus, multiple factors may have collectively influenced these molecules, such as fatty acid conversion, enzymatic and non-enzymatic oxidation, and oxylipin turnover. Further study will be needed to elucidate the influences of plasma oxylipins in AVS.

Despite the distinct differences in plasma oxylipins from control patients, AVS severity could not be discerned from plasma oxylipins. This suggests that the differences in plasma oxylipin profiles between the control and severe AVS groups were more reflective of systemic differences in the two populations than in the AV tissue. We also acknowledge the limitations in the plasma oxylipin analysis. The control population was considerably younger and had lower rates of smoking and medication use. Also, there was a lack of mild AVS patients (n=5), so it is possible that modest group differences could have occurred with a greater number of patients. The lack of change in plasma oxylipins with AVS progression is also in stark contrast to the alterations observed in the AV oxylipins. These findings indicate that AV oxylipins alterations are not simply a result of systemic inflammation but are specific to the localized pathophysiology of AVS. This underscores the importance of studying oxylipins directly in AV tissue to understand the underlying mechanisms of AVS.

Sexual dimorphism of oxylipin levels has been observed in various animal tissues and human plasma (Ferdouse et al., 2019; Leng et al., 2017; Pauls et al., 2021). Similarly, established sex-related differences exist in AVS outcomes (Kararigas et al., 2014; Toyofuku et al., 2017). Despite prior studies examining AV leaflet oxylipins and their synthesizing enzymes, none have reported sex-specific effects, and it is unclear if they considered testing for sex-effects (Artiach et al., 2020; Nagy et al., 2011; Sakaue et al., 2020; Suzuki et al., 2014; Wirrig et al., 2015). In this study cohort, the number of female patients with mild AVS was insufficient for a robust evaluation of sex-effects using two-way ANOVA (MPG severity by sex) on the AV or plasma oxylipin data (Supplemental Table 6&7). Notably, when patients were stratified by MPG severity and sex, trends in AV oxylipin values arose, with female-mild consistently lower than male-mild, and female-severe consistently higher than male-severe. These trends highlight the need for further investigation into the influence of sex on oxylipins and AVS.

The present study provides evidence for the presence of elevated prostanoid levels with AVS severity. These findings suggest that prostanoids play a role in the pathophysiology of AVS and may represent a potential target for novel interventions. Further studies are needed to confirm the causative relationship between elevated prostanoids and AVS, and to explore the specific mechanisms underlying this association. Additionally, future research could also evaluate the potential therapeutic benefit of targeting prostanoid signalling in individuals with AVS. Our findings provide novel insights into the role of oxylipins in the pathophysiology of AVS and suggest that targeting oxylipin pathways may be a promising avenue for developing new therapies for this debilitating cardiac condition.

5.6. Article Information

5.6.1. Acknowledgements

We would like to thank Tanja Winter for support with the oxylipin analysis and Negar Atefi for performing the protein assay. Also, we are grateful to all the patients whose participation made this study possible.

5.6.2. Sources of Funding

A Ravandi was supported by a grant from St. Boniface Hospital Foundation and the Heart and Stroke Foundation of Canada. LGJ Cayer was supported by the University of Manitoba Graduate Fellowship. HM Aukema was supported by a Discovery Grant from the Natural Sciences and Engineering Council of Canada.

Chapter 6: Discussion

6.1. Overall Discussion

The studies presented in this thesis demonstrate robust data interpretation through the integration of oxylipin data, from human calcified aortic valves and rodent models of 2-MCPD exposure, with other biological datasets. This integration was predominantly achieved through the application of MSM. The synthesis of oxylipin data with other omics layers, clinical data, and additional tissue analyses facilitated deeper insights into the mechanisms underlying disease and toxicity at the molecular level. The application of MSM enabled comprehensive evaluation of all variables within the dataset, moving beyond the limitations of analyzing individual variables and ensuring a more nuanced interpretation of biological data. This approach ultimately facilitated the identification of novel therapeutic targets and biomarkers.

In Study A, the individual analyses of each biological layer—mRNA, protein, and oxylipins—provided distinct insights, with comparison of individual molecules expression and MSM, including PCA and GSEA. The integration of these data layers then augmented our understanding of the mechanisms of action of 2-MCPD cardiotoxicity. A major revelation from this approach was the elucidation of the specific reduction to DHA-derived oxylipins. The integration of mRNA data filtered for oxylipin metabolism genes, identified dysregulation of the sPLA2 isoforms which have substrate preference for DHA. Additionally, the integration of transcriptomic and proteomic data layers aided the identification and provided a robust rationale for coronin-1A as a significant regulator of 2-MCPD cardiotoxicity. The overlapping findings regarding the biological processes affected by 2-MCPD exposure further enriched the characterization of the overall disturbance to homeostasis that occurred and illustrated the value of a multi-omics approach which incorporates oxylipins in analyzing biological responses.

In Study B, oxylipin data was analyzed by first applying PCA and then individually comparing oxylipins between groups by ANOVA. This systematic methodology was developed to efficiently and unbiasedly present oxylipin data from multiple tissues in one study. The integration of oxylipin data across the four tissues then successfully highlighted 13-HOTrE-γ as a potential biomarker of acute 2-MCPD exposure, as well as identified differences in the response to 2-MCPD exposure of oxylipin profiles by tissue. The integration of oxylipin data across the four tissues then successfully identified differences in the response to 2-MCPD

exposure of oxylipin profiles by tissue and highlighted 13-HOTrE-γ as a potential biomarker of acute 2-MCPD exposure. This particular oxylipin may often be overlooked due to the lack of data existing regarding biological functions and because it is derived for a minor oxylipin producing PUFA. However, 13-HOTrE-γ was identified as a molecule of importance in group categorization regarding 2-MCPD-exposure through the application of *p*-integration using MINT-PLS-DA. The prominence of 13-HOTrE-γ in these findings marks it as a promising candidate for further investigation, both in terms of understanding the mechanisms underlying 2-MCPD toxicity and as a biomarker for detecting exposure.

In Study C, the integration of the clinical data with the valvular oxylipin data was critical to the major finding that AA prostanoids were uniquely correlated with AVS severity. Initial analyses focusing solely on valvular oxylipins provided limited differentiation among oxylipin subclasses, as nearly all were elevated with increased AVS severity. Furthermore, basic Pearson correlation analysis between oxylipins and clinical data was also inadequate. It was the addition of clinical data to the PCA model that allowed for the detection of the relationship between AA prostanoids and AVS severity markers. By including clinical risk factors in the PCA model, the analysis controlled for these variables, enhancing the robustness and reliability of the findings. This approach not only highlighted the significant role of AA-derived prostanoids in AVS progression but also demonstrated the value of integrating clinical data to achieve a more nuanced understanding interpretation of results.

In addition to the demonstrating the overall approach to oxylipins research, each study made important contributions to their respective fields. 2-MCPD has been understudied and the toxic mechanisms of action are poorly understood. Studies A and B provide critical data regarding the underlying mechanisms of 2-MCPD toxicity needed for future hazard assessment, as well as identified targets for future research. As knowledge on 2-MCPD expands, hazard characterization of 2-MCPD will be enabled. Thus, these studies' contributions to the weight of the evidence for 2-MCPD toxicity are ultimately relevant to food manufacturing practices, especially those involving products intended for young children, such as infant formula. Young children are among the highest consumers of chloropropanol (CP) compounds, highlighting the urgency and relevance of this research. Given the toxicity concerns associated with 2-MCPD, advocating for the substitution of high CP content oils with lower ones in processed foods could be justified. Future research should consider employing animal models that replicate the CP

exposure levels in exclusively infant formula-fed children to assess potential risks to this vulnerable group more accurately.

Study B focussed on 2-MCPD toxicity in the context of dietary ALA adequacy. By providing additional ALA to a corn oil based diet, we addressed a limitation of a previous study that identified n-3 PUFA derived oxylipins in the heart to be lowered with 2-MCPD exposure (Cayer, 2019). This study provided valuable findings for future toxicological studies, emphasizing the importance of adequate dietary ALA in experimental rodent diets. The study demonstrated that the levels of the generally anti-inflammatory n-3 oxylipins were suppressed with an ALA-deficient diet, even over a study duration as short as 6 days, suggesting that oxylipin profiles are less protective against toxic insults without adequate ALA. Furthermore, the specific reduction of cardiac DHA oxylipins from normal levels under conditions of deficient ALA and 2-MCPD exposure was demonstrative of the importance of adequate dietary ALA, as the 2-MCPD-induced effect was not evident with deficient dietary ALA. This discovery holds significant implications for toxicological animal models, by showing that not only can dietary ALA alter baseline levels of oxylipins, but the alterations to these bioactive lipids induced by toxicant exposure can also be dependent on dietary ALA levels. The are also implications to the human food system, particularly in the formulation of infant formulas. The necessity for n-3 PUFA fortification in infant nutrition could be further justified if ALA is shown to offer protection against 2-MCPD toxicity. Additionally, for adults, demonstrating a potential protective effect of ALA against a food-borne toxicant could strengthen the argument for improving the n-3/n-6 PUFA ratio in Western diets, promoting better health outcomes.

There is also a pressing need to further the pathophysiological understanding of AVS, because it is a major cardiovascular disease with no preventative treatment options. Study C identified oxylipins to be broadly elevated and a particular correlation between AA-derived prostanoids and AVS severity. This finding is well-aligned with the existing literature on PGs roles in mediating inflammation, bone calcium dynamics, and fibrosis. An important finding from Study C was that ASA therapy, despite its role as a non-selective COX inhibitor, had limited impact on valvular AA-COX oxylipin levels. This result contributes significantly to the ambiguous data surrounding COX inhibitors effectiveness in AVS, as discussed in Section 5.5. Future research should explore the effects of different COX inhibitors on valvular oxylipins to potentially identify more effective therapeutic options. Additionally, while dietary PUFA can

influence the oxylipins of the whole rodent heart as shown in Study B and previous work (Ferdouse et al., 2019), it is not known whether dietary PUFA can alter oxylipins in the AV leaflet or even in the human heart. Investigating this could provide critical insights into how diet might impact AVS progression, potentially leading to dietary recommendations for AVS patients. Finally, as the first comprehensive profiling of oxylipins in the AVS leaflet, this study has produced foundational data for further study of valvular heart disease.

The field of oxylipin research is still relatively young, and many oxylipins remain poorly characterized in terms of their biological roles. A notable example from this thesis is the identification of 13-HOTrE-γ as a marker of 2-MCPD exposure in Study B, a finding for which there currently exists no literature elucidating its functional implications. Additionally, the functions that are known for various oxylipins are often restricted to a limited number of tissues, highlighting the need for broader studies across different biological contexts to elucidate the diverse roles of this class of molecules. Given these challenges, there is a clear impetus to explore oxylipins more extensively. This could significantly enhance our understanding of their involvement in biological processes and disease mechanisms.

The methodologies and approaches applied in this thesis to study oxylipins can also serve as a model for other targeted omics research. While different biomolecular subclasses will undoubtedly present unique challenges, the principles of integrating data layers and applying robust statistical methods to uncover relationships within complex datasets are broadly applicable. This not only paves the way for advancements in oxylipin research but also sets a foundation for exploring other molecular classes with emerging importance for understanding of physiology and pathophysiology.

6.2. Strengths & Limitations

A major strength of the studies presented in this thesis lies in the overall approach of integrating oxylipin profiles with multiple types of data, to enhance interpretation. For Studies A and B, the inclusion of multiple layers of biological data enabled the identification of biological processes, molecular pathways, and specific molecules that were deregulated by 2-MCPD exposure. Similarly, in Study C, the incorporation of clinical data with oxylipin profiles allowed for more robust associations between oxylipins and AVS to be achieved. The utilization of MSM in the data analysis was particularly advantageous for reducing the complexity of multivariate data, enhancing the explanatory power of the analyses. MSM were instrumental in addressing the

challenges of visualizing large datasets, as they facilitated dimensionality reduction that enabled effective graphical representations of multivariate datasets. This capability not only helped in elucidating intricate biological phenomena but also in communicating complex results in a more comprehensible manner.

For Study A, a major strength was the comprehensive, multi-omics approach that included multiple data layers—genomics, proteomics, and lipidomics. This broad scope allowed for a well-rounded investigation into the effects of 2-MCPD exposure, and the high-quality measurement of each data layer ensured that the findings were robust and well-aligned with the study's hypotheses. The integration of these various layers provided a richer, more detailed understanding of the molecular disruptions caused by 2-MCPD, showcasing the benefits of such an integrative approach in toxicological studies.

However, the study faced some limitations, notably the use of a corn oil-based diets, which are inherently deficient in n-3 PUFAs. The use of corn oil offered some benefits from a toxicological perspective including standardization with previous toxicological literature. However, as we showed in Study B, inadequate dietary ALA impacts bioactive oxylipins. Fortunately, in this model the effect of 2-MCPD to reduce DHA oxylipins was able to be identified, though there may have been a greater decrease if adequate dietary ALA was used. Another limitation in Study A was related to the proteomic analysis, which only identified the top deregulated proteins. This selective identification raised concerns about whether some proteins were not detected due to them being unaltered or simply below the detection limits of the employed techniques. Consequently, this limitation restricted the ability to conduct a comprehensive GSEA on the protein data, which ideally requires a broader dataset including proteins that may not exhibit significant changes.

A strength of both studies A and B was their alignment with the NAMs framework. By employing a multi-omics and a multi-tissue approach, these studies captured a comprehensive array of molecular alterations induced by 2-MCPD. These studies not only enhanced the understanding of the toxicological pathways affected by 2-MCPD, such as inflammation and energy metabolism dysregulation, but also reduced the necessity for multiple separate studies that would otherwise require a larger number of animals. Additionally, the identification of biomarkers and the elucidation of mechanisms underlying 2-MCPD toxicity provide a foundation for future non-animal studies that employ NAMs. By maximizing the data obtained

from each animal, this approach aligns with the principles of NAMs, emphasizing the reduction, refinement, and eventual replacement of animal testing while maintaining the robustness and reliability of the toxicological assessment.

For both Studies A and B, the use of free 2-MCPD was strategically chosen to establish foundational data crucial for hazard assessment. This approach provided a clear, controlled view of 2-MCPD's effects, essential for initial toxicological studies. However, this treatment does not fully mimic the typical human dietary exposure, which for levels of 2-MCPD is approximately 4 orders of magnitude less than what was used in our studies (European Food Safety Authority, 2016), and typically involves a mixture of CP and glycidyl esters (Becalski et al., 2016; Kuhlmann, 2016; Wöhrlin et al., 2015). Future studies could enhance the representativeness by using these substances in the form found in human diets, thus providing a more accurate assessment of their health impacts under typical consumption patterns. Regarding potential differences in toxicity between free and esterified 2-MCPD, it is important to note that 2-MCPD is primarily absorbed by the gut in its free form. Moreover, the stereospecific positions of esterification on the 2-MCPD molecule allow esterified fatty acids to be located in the sn-1 and sn-3 positions, which are readily cleaved by gastrointestinal lipases (Buhrke et al., 2015; Kaze et al., 2016). This process suggests that differences in bioavailability between the free and esterified forms may be limited due to the efficient breakdown of ester bonds by lipases, but *in vivo* testing of the differences in the maximal plasma concentration of free and esterified 2-MCPD, with various esterified fatty acids, would ultimately be beneficial for hazard characterization.

Another limitation of Studies A and B was the exclusive use of male rats, dictated by the expansive nature of the multi-omics analyses conducted, which necessitated the selection of fewer groups to manage the scope and resources effectively. This choice, while practical, omitted potential mechanistic sex differences in 2-MCPD toxicity. While males and females have been found to have similar histopathological outcomes from 2-MCPD exposure, differences have been found in the 2-MCPD-induced alterations to serum immunophenotype profiles, serum biochemistry and hematology (Raju et al., 2019). Therefore, future work should include the characterization of female rats to ensure that the data encompass the full spectrum of potential impacts and provide a more comprehensive understanding of 2-MCPD toxicity across sexes. Ultimately enhancing the applicability of the hazard assessment to the broader population.

For Study B, the study design enabled the elucidation of the effects of dietary ALA adequacy on oxylipin profiles in the context of 2-MCPD exposure and significant insights were gained about the importance dietary ALA in toxicological animal models. The use of corn oil with added purified ALA, instead of the typically used soybean oil, was crucial to the elimination of confounding factors such as differences in the fatty acid profile other than PUFA, polyphenols, and antioxidant capacity (Siger et al., 2008). However, it would have been ideal to be able to provide a dose-response with a range of dietary ALA levels to provide a more comprehensive assessment of the impact of ALA on oxylipins with 2-MCPD exposure.

The study also had limitations that included the small sample sizes used in some groups of the study, due to animals needing to be euthanatized early for humane reasons. This likely affected the sensitivity of the statistical models to detect differences between treatment groups, particularly increasing the risk of Type II errors. Additionally, the study was constrained by incomplete histopathological data, as only some groups underwent histopathological evaluation. This gap in data limited the ability to assess whether dietary ALA mitigated the histopathological impacts of 2-MCPD exposure. Without a full set of histopathological results across all experimental groups, the extent to which the observed oxylipin changes impacted tissue damage. These limitations highlight the need for further research, ideally with larger sample sizes and more extensive histopathological analysis, to validate and expand upon the findings of this study.

An important strength of Studies B and C was the identification of potential roles for specific oxylipins. As oxylipins are an emerging area of research, there remains a paucity of data regarding the functions of many oxylipins. In Study B, the association of 13-HOTrE-γ with 2-MCPD toxicity, and in Study C, the association of AA prostanoids with AVS severity, were novel connections for these oxylipins. The findings suggest promising avenues for future research, particularly for cell culture studies to elucidate novel roles for these oxylipins.

In Study C, an important strength was the acquisition of over 100 human AV leaflet samples. Access to such tissues is particularly valuable given the challenges and ethical considerations involved in obtaining human samples. This provided a unique opportunity to study AVS in human subjects directly, enhancing the relevance and applicability of the findings to clinical practice. Additionally, unlike many other AVS studies which typically have access only to severely diseased AV leaflets and compare calcified with non-calcified regions, Study C included a mild AVS group. Although these patients were not healthy controls—being

asymptomatic for AVS but still requiring aortic root surgery—they represented a less diseased cohort than those usually studied, offering a broader perspective on the disease's progression.

However, the study did have limitations. One issue was the restricted collection of plasma from many patients, which limited the ability to perform statistical analyses that directly connected valve and plasma oxylipin profiles. This gap in the data collection reduced the potential to fully explore systemic biomarkers alongside local tissue changes. Although we were able to add a healthy control group to the plasma data. Another limitation was the lack of comprehensive data on the usage of COX inhibitors other than ASA. While we were able to show that ASA had little impact on valvular oxylipins, the absence of detailed data on other NSAIDs, known to affect bone healing and potentially influence prostanoid synthesis, inhibited further contribution to the controversy surrounding COX-inhibition and AVS.

There were some common methodological limitations across each of the studies presented in this thesis. For instance, the oxylipin analyses utilized in each study specifically measured free oxylipins and did not extend to esterified oxylipins. Despite the relative abundance of esterified oxylipins in various tissues, such as the heart, liver, and kidney, this form of oxylipin is less frequently measured in studies throughout the literature, and as a result there is a data gap regarding their function (Annevelink et al., 2022). Additionally, each of the studies also only collected data at a single time point. This constraint limited our ability to establish causation from the molecular alterations observed. While identifying altered molecules provided valuable insights, without longitudinal data, it is challenging to ascertain whether these changes are causative or resultant from the conditions being studied. This limitation is largely due to practical and ethical constraints associated with the tissues involved. For example, safely conducting multiple biopsies of the heart for longitudinal data is not feasible, considering the invasive nature of such procedures. Additionally, while more accessible samples such as plasma could technically be collected at multiple time points, financial realities present significant challenges. The operational costs of running repeated analyses, particularly with the sample sizes required for statistical validity, can quickly become prohibitive. As analytical technology progresses these costs will improve; but in the meantime, this highlights the importance of extracting as much information out of cross-sectional data as possible. This is particularly true in the field of oxylipin research, where the complexity of the biological processes involved demands a robust analytical approach.

Therefore, it is imperative to integrate oxylipin data within the broader omics framework, as demonstrated in this thesis. By doing so, we can leverage the interconnected insights provided by genomics, proteomics, lipidomics, and clinical data, among others. This integration enables a more holistic understanding of the larger biological system, allowing for deeper insights into the pathophysiological mechanisms of diseases and the identification of potential therapeutic targets. The approach taken in this thesis not only underscores the value of oxylipin data but also sets a precedent for future research, emphasizing the necessity of sophisticated MSM to augment interpretational capabilities in biological research.

Chapter 7: References

Abraham, K., Appel, K.E., Berger-Preiss, E., Apel, E., Gerling, S., Mielke, H., Creutzenberg, O., Lampen, A., 2013. Relative oral bioavailability of 3-MCPD from 3-MCPD fatty acid esters in rats. Arch. Toxicol. 87, 649–659. https://doi.org/10.1007/s00204-012-0970-8

Ait-Said, F., Elalamy, I., Werts, C., Gomard, M.T., Jacquemin, C., Couetil, J.P., Hatmi, M., 2003. Inhibition by eicosapentaenoic acid of IL-1β-induced PGHS-2 expression in human microvascular endothelial cells: Involvement of lipoxygenase-derived metabolites and p38 MAPK pathway. Biochim. Biophys. Acta - Mol. Cell Biol. Lipids 1631, 77–84. https://doi.org/10.1016/S1388-1981(02)00358-X

Allen, D., Hasanally, D., Ravandi, A., 2013. Role of oxidized phospholipids in cardiovascular pathology. Clin. Lipidol. 8, 205–215. https://doi.org/10.2217/clp.13.13

Andres, S., Appel, K.E., Lampen, A., 2013. Toxicology, occurrence and risk characterisation of the chloropropanols in food: 2-Monochloro-1,3-propanediol, 1,3-dichloro-2-propanol and 2,3-dichloro-1-propanol. Food Chem. Toxicol. 58, 467–478. https://doi.org/10.1016/j.fct.2013.05.024

Annevelink, C.E., Walker, R.E., Shearer, G.C., 2022. Esterified Oxylipins: Do They Matter? Metabolites 12. https://doi.org/10.3390/METABO12111007

Anwar-Mohamed, A., El-Sherbeni, A., Hee Kim, S., Elshenawy, O.H., Althurwi, H.N., M Zordoky, B.N., S El-Kadi, A.O., 2013. Acute arsenic treatment alters cytochrome P450 expression and arachidonic acid metabolism in lung, liver and kidney of C57Bl/6 mice. Xenobiotica 43, 1366–5928. https://doi.org/10.3109/00498254.2012.754113

Anwar-Mohamed, A., El-Sherbeni, A.A., Kim, S.H., Althurwi, H.N., Zordoky, B.N.M., El-Kadi, A.O.S., 2012. Acute arsenic toxicity alters cytochrome P450 and soluble epoxide hydrolase and their associated arachidonic acid metabolism in C57Bl/6 mouse heart. Xenobiotica 42, 1235–1247. https://doi.org/10.3109/00498254.2012.693971

Anwar-Mohamed, A., Elshenawy, O.H., El-Sherbeni, A.A., Abdelrady, M., El-Kadi, A.O.S., 2014. Acute arsenic treatment alters arachidonic acid and its associated metabolite levels in the brain of C57Bl/6 mice. Can. J. Physiol. Pharmacol. 92, 693–702. https://doi.org/10.1139/cjpp-2014-0136

Aragno, M., Mastrocola, R., Alloatti, G., Vercellinatto, I., Bardini, P., Geuna, S., Catalano, M.G., Danni, O., Boccuzzi, G., 2008. Oxidative Stress Triggers Cardiac Fibrosis in the

Heart of Diabetic Rats. Endocrinology 149, 380–388. https://doi.org/10.1210/EN.2007-0877

Artiach, G., Carracedo, M., Plunde, O., Wheelock, C.E., Thul, S., Sjövall, P., Franco-Cereceda, A., Laguna-Fernandez, A., Arnardottir, H., Bäck, M., 2020. Omega-3 Polyunsaturated Fatty Acids Decrease Aortic Valve Disease Through the Resolvin E1 and ChemR23 Axis. Circulation 142, 776–789. https://doi.org/10.1161/CIRCULATIONAHA.119.041868

Aukema, H.M., Ravandi, A., 2023. Factors affecting variability in free oxylipins in mammalian tissues. Curr. Opin. Clin. Nutr. Metab. Care 26, 91–98. https://doi.org/10.1097/MCO.0000000000000892

Aukema, H.M., Winter, T., Ravandi, A., Dalvi, S., Miller, D.W., Hatch, G.M., 2016. Generation of Bioactive Oxylipins from Exogenously Added Arachidonic, Eicosapentaenoic and Docosahexaenoic Acid in Primary Human Brain Microvessel Endothelial Cells. Lipids 51, 591–9. https://doi.org/10.1007/s11745-015-4074-0

Baer, I., de la Calle, B., Taylor, P., 2010. 3-MCPD in food other than soy sauce or hydrolysed vegetable protein (HVP). Anal. Bioanal. Chem. 396, 443–456. https://doi.org/10.1007/s00216-009-3177-y

Bal-Price, A., Crofton, K.M., Leist, M., Allen, S., Arand, M., Buetler, T., Delrue, N., FitzGerald, R.E., Hartung, T., Heinonen, T., Hogberg, H., Bennekou, S.H., Lichtensteiger, W., Oggier, D., Paparella, M., Axelstad, M., Piersma, A., Rached, E., Schilter, B., Schmuck, G., Stoppini, L., Tongiorgi, E., Tiramani, M., Monnet-Tschudi, F., Wilks, M.F., Ylikomi, T., Fritsche, E., 2015. International STakeholder NETwork (ISTNET): creating a developmental neurotoxicity (DNT) testing road map for regulatory purposes. Arch. Toxicol. 89, 269–287. https://doi.org/10.1007/S00204-015-1464-2/TABLES/2

Baumgartner, H., Falk, V., Bax, J.J., De Bonis, M., Hamm, C., Holm, P.J., Iung, B., Lancellotti, P., Lansac, E., Muñoz, D.R., Rosenhek, R., Sjögren, J., Tornos Mas, P., Vahanian, A., Walther, T., Wendler, O., Windecker, S., Zamorano, J.L., Roffi, M., Alfieri, O., Agewall, S., Ahlsson, A., Barbato, E., Bueno, H., Collet, J.P., Coman, I.M., Czerny, M., Delgado, V., Fitzsimons, D., Folliguet, T., Gaemperli, O., Habib, G., Harringer, W., Haude, M., Hindricks, G., Katus, H.A., Knuuti, J., Kolh, P., Leclercq, C., McDonagh, T.A., Piepoli, M.F., Pierard, L.A., Ponikowski, P., Rosano, G.M.C., Ruschitzka, F., Shlyakhto, E., Simpson, I.A., Sousa-Uva, M., Stepinska, J., Tarantini, G., Tche, D., Aboyans, V.,

Kzhdryan, H.K., Mascherbauer, J., Samadov, F., Shumavets, V., Van Camp, G., Loncar, D., Lovric, D., Georgiou, G.M., Linhartova, K., Ihlemann, N., Abdelhamid, M., Pern, T., Turpeinen, A., Srbinovska-Kostovska, E., Cohen, A., Bakhutashvili, Z., Ince, H., Vavuranakis, M., Temesvari, A., Gudnason, T., Mylotte, D., Kuperstein, R., Indolfi, C., Pya, Y., Bajraktari, G., Kerimkulova, A., Rudzitis, A., Mizariene, V., Lebrun, F., Demarco, D.C., Oukerraj, L., Bouma, B.J., Steigen, T.K., Komar, M., De Moura Branco, L.M., Popescu, B.A., Uspenskiy, V., Foscoli, M., Jovovic, L., Simkova, I., Bunc, M., de Prada, J.A.V., Stagmo, M., Kaufmann, B.A., Mahdhaoui, A., Bozkurt, E., Nesukay, E., Brecker, S.J.D., 2017. 2017 ESC/EACTS Guidelines for the management of valvular heart disease. Eur. Heart J. 38, 2739–2786. https://doi.org/10.1093/eurheartj/ehx391

Baumgartner, H., Hung, J., Bermejo, J., Chambers, J.B., Evangelista, A., Griffin, B.P., Iung, B., Otto, C.M., Pellikka, P.A., Quiñones, M., 2009. Echocardiographic Assessment of Valve Stenosis: EAE/ASE Recommendations for Clinical Practice. J. Am. Soc. Echocardiogr. 22, 1–23. https://doi.org/10.1016/j.echo.2008.11.029

Baumgartner, H., Walther, T., Camm, A.J., Lüscher, T.F., Maurer, G., Serruys, P.W., 2018. ESC CardioMed, 3rd ed, ESC CardioMed. https://doi.org/10.1093/med/9780198784906.001.0001

Becalski, A., Zhao, T., Breton, F., Kuhlmann, J., 2016. 2- and 3-Monochloropropanediols in paper products and their transfer to foods. Food Addit. Contam. Part A 33, 1499–1508. https://doi.org/10.1080/19440049.2016.1223353

Bento, A.F., Claudino, R.F., Dutra, R.C., Marcon, R., Calixto, J.B., Dutra, C., Marcon, R., Calixto, J.B., 2011. Omega-3 Fatty Acid-Derived Mediators 17(R)-Hydroxy Docosahexaenoic Acid, Aspirin-Triggered Resolvin D1 and Resolvin D2 Prevent Experimental Colitis in Mice. J. Immunol. 1957–1969. https://doi.org/10.4049/jimmunol.1101305

Bergmark, C., Dewan, A., Orsoni, A., Merki, E., Miller, E.R., Shin, M.-J., Binder, C.J., Hörkkö, S., Krauss, R.M., Chapman, M.J., Witztum, J.L., Tsimikas, S., 2008. A novel function of lipoprotein [a] as a preferential carrier of oxidized phospholipids in human plasma. J. Lipid Res. 49, 2230–2239. https://doi.org/10.1194/jlr.M800174-JLR200

Berry, E., Hernandez-Anzaldo, S., Ghomashchi, F., Lehner, R., Murakami, M., Gelb, M.H., Kassiri, Z., Wang, X., Fernandez-Patron, C., 2015. Matrix metalloproteinase-2 negatively

regulates cardiac secreted phospholipase A2 to modulate inflammation and fever. J. Am. Heart Assoc. 4. https://doi.org/10.1161/JAHA.115.001868

Blum, M., Dogan, I., Karber, M., Rothe, M., Schunck, W.H., 2019. Chiral lipidomics of monoepoxy and monohydroxy metabolites derived from long-chain polyunsaturated fatty acids. J. Lipid Res. 60, 135–148. https://doi.org/10.1194/JLR.M089755

Bouchareb, R., Boulanger, M.C., Tastet, L., Mkannez, G., Nsaibia, M.J., Hadji, F., Dahou, A., Messadeq, Y., Arsenault, B.J., Pibarot, P., Bossé, Y., Marette, A., Mathieu, P., 2019. Activated platelets promote an osteogenic programme and the progression of calcific aortic valve stenosis. Eur. Heart J. 40, 1362–1373. https://doi.org/10.1093/EURHEARTJ/EHY696

Bourre, J.M., Francois, M., Youyou, A., Dumont, O., Piciotti, M., Pascal, G., Durand, G., 1989. The effects of dietary α-linolenic acid on the composition of nerve membranes, enzymatic activity, amplitude of electrophysiological parameters, resistance to poisons and performance of learning tasks in rats. J. Nutr. 119, 1880–1892. https://doi.org/10.1093/jn/119.12.1880

Bowler, M.A., Raddatz, M.A., Johnson, C.L., Lindman, B.R., Merryman, W.D., 2019. Celecoxib Is Associated With Dystrophic Calcification and Aortic Valve Stenosis. JACC Basic to Transl. Sci. 4, 135–143. https://doi.org/10.1016/J.JACBTS.2018.12.003

Buczynski, M.W., Dumlao, D.S., Dennis, E.A., 2009. Thematic Review Series: Proteomics. An integrated omics analysis of eicosanoid biology1[S]. J. Lipid Res. 50, 1015–1038. https://doi.org/10.1194/JLR.R900004-JLR200

Buhrke, T., Frenzel, F., Kuhlmann, J., Lampen, A., 2015. 2-Chloro-1,3-propanediol (2-MCPD) and its fatty acid esters: cytotoxicity, metabolism, and transport by human intestinal Caco-2 cells. Arch. Toxicol. 89, 2243–2251. https://doi.org/10.1007/s00204-014-1395-3

Buhrke, T., Schultrich, K., Braeuning, A., Lampen, A., 2017. Comparative analysis of transcriptomic responses to repeated-dose exposure to 2-MCPD and 3-MCPD in rat kidney, liver and testis. Food Chem. Toxicol. 106, 36–46. https://doi.org/10.1016/j.fct.2017.05.028

Buhrke, T., Voss, L., Briese, A., Stephanowitz, H., Krause, E., Braeuning, A., Lampen, A., 2018. Oxidative inactivation of the endogenous antioxidant protein DJ-1 by the food contaminants 3-MCPD and 2-MCPD. Arch. Toxicol. 92, 289–299. https://doi.org/10.1007/s00204-017-2027-5

Caligiuri, S.P.B., Parikh, M., Stamenkovic, A., Pierce, G.N., Aukema, H.M., 2017. Dietary

modulation of oxylipins in cardiovascular disease and aging. Am. J. Physiol. - Hear. Circ. Physiol. 313, H903–H918. https://doi.org/10.1152/ajpheart.00201.2017

Cattan, N., Mary, D., Peleraux, A., Mari, B., Aussel, C., Rossi, B., 2000. Prostaglandin B2 delivers a co-stimulatory signal leading to T cell activation. Eur. Cytokine Netw. 11, 293–300.

Cattaneo, I., Astuto, M.C., Binaglia, M., Devos, Y., Dorne, J.L.C.M., Fernandez Agudo, A., Fernandez Dumont, A., Garcia-Vello, P., Kass, G.E.N., Lanzoni, A., Liem, A.K.D., Panzarea, M., Paraskevopulos, K., Parra Morte, J.M., Tarazona, J. V., Terron, A., 2023. Implementing New Approach Methodologies (NAMs) in food safety assessments: Strategic objectives and actions taken by the European Food Safety Authority. Trends Food Sci. Technol. 133, 277–290. https://doi.org/10.1016/J.TIFS.2023.02.006

Cayer, L.G.J., 2019. Effects of sub-chronic dietary 2-monochloro-1,3-propanediol on oxidized lipids in rat heart, kidney, serum, and skeletal muscle. University of Manitoba.

Cayer, L.G.J., Mendonça, A.M., Pauls, S.D., Winter, T., Leng, S., Taylor, C.G., Zahradka, P., Aukema, H.M., 2019. Adipose tissue oxylipin profiles vary by anatomical site and are altered by dietary linoleic acid in rats. Prostaglandins Leukot. Essent. Fat. Acids 141, 24–32. https://doi.org/10.1016/j.plefa.2018.12.004

Cebo, M., Fu, X., Gawaz, M., Chatterjee, M., Lämmerhofer, M., 2020. Enantioselective ultra-high performance liquid chromatography-tandem mass spectrometry method based on sub-2μm particle polysaccharide column for chiral separation of oxylipins and its application for the analysis of autoxidized fatty acids and platelet releasates. J. Chromatogr. A 1624, 461206. https://doi.org/10.1016/J.CHROMA.2020.461206

Chan, K.L., Teo, K., Dumesnil, J.G., Ni, A., Tam, J., 2010. Effect of lipid lowering with rosuvastatin on progression of aortic stenosis: Results of the aortic stenosis progression observation: Measuring effects of rosuvastatin (Astronomer) trial. Circulation 121, 306–314. https://doi.org/10.1161/CIRCULATIONAHA.109.900027

Choudhary, S., Blackwell, K., Voznesensky, O., Roy, D., Pilbeam, C., Deb Roy, A., Pilbeam, C., 2013. Prostaglandin E2 acts via bone marrow macrophages to block PTH-stimulated osteoblast differentiation in vitro. Bone 56, 31–41. https://doi.org/10.1016/j.bone.2013.04.017

Coecke, S., Pelkonen, O., Leite, S.B., Bernauer, U., Bessems, J.G.M., Bois, F.Y., Gundert-

Remy, U., Loizou, G., Testai, E., Zaldívar, J.M., 2013. Toxicokinetics as a key to the integrated toxicity risk assessment based primarily on non-animal approaches. Toxicol. In Vitro 27, 1570–1577. https://doi.org/10.1016/J.TIV.2012.06.012

Coffey, S., Roberts-Thomson, R., Brown, A., Carapetis, J., Chen, M., Enriquez-Sarano, M., Zühlke, L., Prendergast, B.D., 2021. Global epidemiology of valvular heart disease. Nat. Rev. Cardiol. https://doi.org/10.1038/s41569-021-00570-z

Cowell, S.J., Newby, D.E., Prescott, R.J., Bloomfield, P., Reid, J., Northridge, D.B., Boon, N.A., 2005. A Randomized Trial of Intensive Lipid-Lowering Therapy in Calcific Aortic Stenosis. N. Engl. J. Med. 352, 2389–2397. https://doi.org/10.1056/nejmoa043876

Croset, M., Sala, A., Folco, G., Lagarde, M., 1988. Inhibition by lipoxygenase products of TXA2-like responses of platelets and vascular smooth muscle. Biochem. Pharmacol. 37, 1275–1280. https://doi.org/10.1016/0006-2952(88)90782-4

Cui, X., Zhang, L., Yang, D., Li, J., Liu, Q., Sui, H., Liu, Z., Zhou, P., 2021. Occurrence of 3- and 2-monochloropropanediol esters in infant formulas in China and exposure assessment 38, 1470–1480. https://doi.org/10.1080/19440049.2021.1925164

Dai, Y., Cheng, Z., Zeng, Z., Hylkema, M.N., Faas, M.M., Huo, X., 2023. A Targeted Lipidomic Reveals CYP450-Derived Oxylipin Linked to the Inflammatory Response by Polycyclic Aromatic Hydrocarbon Exposure in Children. Expo. Heal. 15, 455–466. https://doi.org/10.1007/S12403-022-00503-2/FIGURES/4

Deems, R., Buczynski, M.W., Bowers-Gentry, R., Harkewicz, R., Dennis, E.A., 2007. Detection and Quantitation of Eicosanoids via High Performance Liquid Chromatography-Electrospray Ionization-Mass Spectrometry. Methods Enzymol. 432, 59–82. https://doi.org/10.1016/S0076-6879(07)32003-X

Delaney, J.A., Lehmann, N., Jöckel, K.H., Elmariah, S., Psaty, B.M., Mahabadi, A.A., Budoff, M., Kronmal, R.A., Nasir, K., O'Brien, K.D., Möhlenkamp, S., Moebus, S., Dragano, N., Winterstein, A.G., Erbel, R., Kälsch, H., 2013. Associations between aspirin and other non-steroidal anti-inflammatory drugs and aortic valve or coronary artery calcification: The multi-ethnic study of atherosclerosis and the heinz nixdorf recall study. Atherosclerosis 229, 310–316. https://doi.org/10.1016/j.atherosclerosis.2013.05.002

Deng, B., Wang, C.W., Arnardottir, H.H., Li, Y., Cheng, C.Y.C., Dalli, J., Serhan, C.N., 2014. Maresin Biosynthesis and Identification of Maresin 2, a New Anti-Inflammatory and Pro-

Resolving Mediator from Human Macrophages. PLoS One 9, e102362. https://doi.org/10.1371/JOURNAL.PONE.0102362

Dennis, E.A., Cao, J., Hsu, Y.H., Magrioti, V., Kokotos, G., 2011. Phospholipase A2 Enzymes: Physical Structure, Biological Function, Disease Implication, Chemical Inhibition, and Therapeutic Intervention. Chem. Rev. 111, 6130. https://doi.org/10.1021/CR200085W

Dobin, A., Gingeras, T.R., 2015. Mapping RNA-seq Reads with STAR. Curr. Protoc. Bioinforma. 51, 11.14.1-11.14.19. https://doi.org/10.1002/0471250953.BI1114S51

Dorris, S.L., Stokes Peebles Jr, R., 2012. PGI 2 as a Regulator of Inflammatory Diseases. Mediators Inflamm. 2012. https://doi.org/10.1155/2012/926968

Du, Y., Taylor, C.G., Aukema, H.M., Zahradka, P., 2020. Role of oxylipins generated from dietary PUFAs in the modulation of endothelial cell function. Prostaglandins Leukot. Essent. Fat. Acids. https://doi.org/10.1016/j.plefa.2020.102160

Dunlap, F.G., White, P.J., Pollak, L.M., Brumm, T.J., 1995. Fatty acid composition of oil from adapted, elite corn breeding materials. J. Am. Oil Chem. Soc. 72, 981–987. https://doi.org/10.1007/BF02660709/METRICS

Dweck, M.R., Boon, N.A., Newby, D.E., 2012. Calcific aortic stenosis: A disease of the valve and the myocardium. J. Am. Coll. Cardiol. 60, 1854–1863. https://doi.org/10.1016/j.jacc.2012.02.093

EPA, 2024. EPA Releases Updated New Approach Methodologies (NAMs) Work Plan [WWW Document]. URL https://www.epa.gov/sciencematters/epa-releases-updated-new-approach-methodologies-nams-work-plan

European Food Safety Authority, 2018. Update of the risk assessment on 3-monochloropropane diol and its fatty acid esters. EFSA J. https://doi.org/10.2903/j.efsa.2018.5083

European Food Safety Authority, 2016. Risks for human health related to the presence of 3- and 2-monochloropropanediol (MCPD), and their fatty acid esters, and glycidyl fatty acid esters in food. EFSA J. 14, e04426. https://doi.org/10.2903/j.efsa.2016.4426

Farrés, M., Platikanov, S., Tsakovski, S., Tauler, R., 2015. Comparison of the variable importance in projection (VIP) and of the selectivity ratio (SR) methods for variable selection and interpretation. J. Chemom. 29, 528–536. https://doi.org/10.1002/cem.2736

Fattahi, M.J., Mirshafiey, A., 2012. Prostaglandins and Rheumatoid Arthritis. Arthritis 2012, 1–7. https://doi.org/10.1155/2012/239310

Ferdouse, A., Leng, S., Winter, T., Aukema, H.M., 2019. Dietary n-6 and n-3 PUFA alter the free oxylipin profile differently in male and female rat hearts. Br. J. Nutr. 122, 252–261. https://doi.org/10.1017/S0007114519001211

Festjens, N., Vanden Berghe, T., Vandenabeele, P., 2006. Necrosis, a well-orchestrated form of cell demise: Signalling cascades, important mediators and concomitant immune response. Biochim. Biophys. Acta - Bioenerg. 1757, 1371–1387. https://doi.org/10.1016/J.BBABIO.2006.06.014

Frangogiannis, N.G., 2021. Cardiac fibrosis. Cardiovasc. Res. 117, 1450–1488. https://doi.org/10.1093/CVR/CVAA324

Frei, H., Würgler, F.E., 1997. The vicinal chloroalcohols 1,3-dichloro-2-propanol (DC2P), 3-chloro-1,2-propanediol (3CPD) and 2-chloro-1,3-propanediol (2CPD) are not genotoxic in vivo in the wing spot test of Drosophila melanogaster. Mutat. Res. Toxicol. Environ. Mutagen. 394, 59–68. https://doi.org/10.1016/S1383-5718(97)00125-3

Fu, W.S., Zhao, Y., Zhang, G., Zhang, L., Li, J.G., Tang, C.D., Miao, H., Bo, J., Zhang, Q., Wu, Y.N., 2007. Occurrence of chloropropanols in soy sauce and other foods in China between 2002 and 2004. Food Addit. Contam. 24, 812–819. https://doi.org/10.1080/02652030701246039

Funk CD, 2001. Prostaglandins and leukotrienes: advances in eicosanoid biology. Science (80-.). 294, 1871–1875.

Gabbs, M., Leng, S., Devassy, J.G., Monirujjaman, M.M., Aukema, H.M., Leng, S., Gabbs, M., 2015. Advances in Our Understanding of Oxylipins Derived from Dietary PUFAs. Adv. Nutr. An Int. Rev. J. 6, 513–540. https://doi.org/10.3945/an.114.007732

Gladine, C., Ostermann, A.I., Newman, J.W., Schebb, N.H., 2019. MS-based targeted metabolomics of eicosanoids and other oxylipins: Analytical and inter-individual variabilities. Free Radic. Biol. Med. 144, 72–89. https://doi.org/10.1016/J.FREERADBIOMED.2019.05.012

González-Périz, A., Planagumà, A., Gronert, K., Miquel, R., López-Parra, M., Titos, E., Horrillo, R., Ferré, N., Deulofeu, R., Arroyo, V., Rodés, J., Clària, J., González-Périz, A., Planagumà, A., Gronert, K., Miquel, R., López-Parra, M., Titos, E., Horrillo, R., Ferré, N., Deulofeu, R., Arroyo, V., Rodés, J., Clària, J., 2006. Docosahexaenoic acid (DHA) blunts liver injury by conversion to protective lipid mediators: protectin D1 and 17S-hydroxy-

DHA. FASEB J. 20, 2537–2539. https://doi.org/10.1096/fj.06-6250fje

Grear, T., Avery, C., Patterson, J., Jacobs, D.J., 2021. Molecular function recognition by supervised projection pursuit machine learning. Sci. Rep. 11, 4247. https://doi.org/10.1038/s41598-021-83269-y

Greve, A.M., Bang, C.N., Boman, K., Egstrup, K., Kesäniemi, Y.A., Ray, S., Pedersen, T.R., Wachtell, K., 2019. Relation of Lipid-Lowering Therapy to Need for Aortic Valve Replacement in Patients With Asymptomatic Mild to Moderate Aortic Stenosis. Am. J. Cardiol. 124, 1736–1740. https://doi.org/10.1016/J.AMJCARD.2019.08.037

Grim, J.C., Aguado, B.A., Vogt, B.J., Batan, D., Andrichik, C.L., Schroeder, M.E., Gonzalez-Rodriguez, A., Yavitt, F.M., Weiss, R.M., Anseth, K.S., 2020. Secreted Factors From Proinflammatory Macrophages Promote an Osteoblast-Like Phenotype in Valvular Interstitial Cells. Arterioscler. Thromb. Vasc. Biol. 40, E296–E308. https://doi.org/10.1161/ATVBAHA.120.315261

Gruber, R., Schöfnagl, M., Karreth, F., Fischer, M.B., Watzek, G., 2003. The stable analog carbocyclic TXA2 but not platelet-released TXA2 induces osteoclast-like cell formation. Prostaglandins, Leukot. Essent. Fat. Acids 68, 267–272. https://doi.org/10.1016/S0952-3278(03)00005-X

Guddeti, R.R., Patil, S., Ahmed, A., Sharma, A., Aboeata, A., Lavie, C.J., Alla, V.M., 2020. Lipoprotein(a) and calcific aortic valve stenosis: A systematic review. Prog. Cardiovasc. Dis. 63, 496–502. https://doi.org/10.1016/J.PCAD.2020.06.002

Gupta, J.I., Gualano, S.K., Bhave, N., 2022. Aortic stenosis in chronic kidney disease: challenges in diagnosis and treatment. Heart 108, 1260–1266. https://doi.org/10.1136/HEARTJNL-2021-319604

Hall, L.M., Murphy, R.C., 1998. Electrospray mass spectrometric analysis of 5-hydroperoxy and 5-hydroxyeicosatetraenoic acids generated by lipid peroxidation of red blood cell ghost phospholipids. J. Am. Soc. Mass Spectrom. 9, 527–532. https://doi.org/10.1016/S1044-0305(98)00013-0

Hamlet, C.G., Sadd, P.A., Crews, C., Velíšek, J., Baxter, D.E., 2002. Occurrence of 3-chloro-propane-1,2-diol (3-MCPD) and related compounds in foods: A review. Food Addit. Contam. 19, 619–631. https://doi.org/10.1080/02652030210132391

Hartung, T., 2009. Toxicology for the twenty-first century. Nat. 2009 4607252 460, 208–212.

https://doi.org/10.1038/460208A

Hasin, Y., Seldin, M., Lusis, A., 2017. Multi-omics approaches to disease. Genome Biol. https://doi.org/10.1186/s13059-017-1215-1

Hayashi, D., Mouchlis, V.D., Dennis, E.A., 2021. Omega-3 versus Omega-6 fatty acid availability is controlled by hydrophobic site geometries of phospholipase A2s. J. Lipid Res. 63. https://doi.org/10.1016/J.JLR.2021.100113

Health Canada, 2023. Use of new approach methods (NAMs) in risk assessment [WWW Document]. URL https://www.canada.ca/en/health-canada/services/chemical-substances/fact-sheets/use-new-approach-methods-risk-assessment.html

Hernandez-Anzaldo, S., Berry, E., Brglez, V., Leung, D., Yun, T.J., Lee, J.S., Filep, J.G., Kassiri, Z., Cheong, C., Lambeau, G., Lehner, R., Fernandez-Patron, C., 2015. Identification of a novel heart-liver axis: Matrix metalloproteinase-2 negatively regulates cardiac secreted phospholipase A2 to modulate lipid metabolism and inflammation in the liver. J. Am. Heart Assoc. 4. https://doi.org/10.1161/JAHA.115.002553

Hodgson, E., 2004. A Textbook of Modern Toxicology, Third. ed. John Wiley & Sons, Inc., Hoboken, New Jersey. https://doi.org/DOI:10.1002/0471646776

Honn, K. V., Nelson, K.K., Renaud, C., Bazaz, R., Diglio, C.A., Timar, J., 1992. Fatty acid modulation of tumor cell adhesion to microvessel endothelium and experimental metastasis. Prostaglandins 44, 413–429. https://doi.org/10.1016/0090-6980(92)90137-I

Huang, Y., Rajput, I.R., Sanganyado, E., Yajing, S., Yu, F., Liang, B., Liu, W., 2020. Immune stimulation effect of PBDEs via prostaglandin pathway in pantropical spotted dolphin: An in vitro study. Chemosphere 254, 126717. https://doi.org/10.1016/j.chemosphere.2020.126717

Hulin, A., Hego, A., Lancellotti, P., Oury, C., 2018. Advances in Pathophysiology of Calcific Aortic Valve Disease Propose Novel Molecular Therapeutic Targets. Front. Cardiovasc. Med. https://doi.org/10.3389/fcvm.2018.00021

Imig, J.D., Walsh, K.A., Khan, M.A.H., Nagasawa, T., Cherian-Shaw, M., Shaw, S.M., Hammock, B.D., 2012. Soluble epoxide hydrolase inhibition and peroxisome proliferator activated receptor γ agonist improve vascular function and decrease renal injury in hypertensive obese rats. https://doi.org/10.1258/ebm.2012.012225 237, 1402–1412. https://doi.org/10.1258/EBM.2012.012225

International Agency for Research on Cancer, 2013. Some chemicals present in industrial and consumer products, food and drinking-water. IARC Monogr. Eval. Carcinog. Risks Hum.

Iung, B., Baron, G., Butchart, E.G., Delahaye, F., Gohlke-Bärwolf, C., Levang, O.W., Tornos, P., Vanoverschelde, J.L., Vermeer, F., Boersma, E., Ravaud, P., Vahanian, A., 2003. A prospective survey of patients with valvular heart disease in Europe: The Euro Heart Survey on valvular heart disease. Eur. Heart J. 24, 1231–1243. https://doi.org/10.1016/S0195-668X(03)00201-X

Johnson, T.M., Mahabir, C.A., Yang, Y., Roul, P., Goldsweig, A.M., Binstadt, B.A., Baker, J.F., Sauer, B.C., Cannon, G.W., Mikuls, T.R., England, B.R., 2023. Aortic Stenosis Risk in Rheumatoid Arthritis. JAMA Intern. Med. 183. https://doi.org/10.1001/JAMAINTERNMED.2023.3087

Joint FAO/WHO Expert Committee on Food Additives, 2017. Evaluation of certain contaminants in food, WHO Technical Report Series.

Kararigas, G., Dworatzek, E., Petrov, G., Summer, H., Schulze, T.M., Baczko, I., Knosalla, C., Golz, S., Hetzer, R., Regitz-Zagrosek, V., 2014. Sex-dependent regulation of fibrosis and inflammation in human left ventricular remodelling under pressure overload. Eur. J. Heart Fail. 16, 1160–1167. https://doi.org/10.1002/EJHF.171

Kaze, N., Watanabe, Y., Sato, H., Murota, K., Kotaniguchi, M., Yamamoto, H., Inui, H., Kitamura, S., 2016. Estimation of the Intestinal Absorption and Metabolism Behaviors of 2- and 3-Monochloropropanediol Esters. Lipids 51, 913–922. https://doi.org/10.1007/s11745-016-4143-z

Kenkel, N.C., 2006. On selecting an appropriate multivariate analysis. Can. J. Plant Sci. 86, 663–676. https://doi.org/10.4141/P05-164

Kim, N.H., Jung, S.Y., Park, Y.A., Lee, Y.J., Jo, J.Y., Lee, S.M., Oh, Y.H., 2020. Fatty acid composition and characterisation of commercial vegetable oils with chemometric approaches. Int. food Res. J. 270–279.

Knoll, M., Lodish, H.F., Sun, L., 2015. Long non-coding RNAs as regulators of the endocrine system. Nat. Rev. Endocrinol. https://doi.org/10.1038/nrendo.2014.229

Kobayashi, Y., Mizoguchi, T., Take, I., Kurihara, S., Udagawa, N., Takahashi, N., 2005. Prostaglandin E2 enhances osteoclastic differentiation of precursor cells through protein kinase A-dependent phosphorylation of TAK1. J. Biol. Chem. 280, 11395–11403.

https://doi.org/10.1074/jbc.M411189200

Koo, M.J., Rooney, K.T., Choi, M.E., Ryter, S.W., Choi, A.M.K., Moon, J.S., 2015. Impaired oxidative phosphorylation regulates necroptosis in human lung epithelial cells. Biochem. Biophys. Res. Commun. 464, 875. https://doi.org/10.1016/J.BBRC.2015.07.054

Korotkova, M., Jakobsson, P.J., 2014. Persisting eicosanoid pathways in rheumatic diseases. Nat. Rev. Rheumatol. 10, 229–242. https://doi.org/10.1038/NRRHEUM.2014.1

Koshihara, Y., Kawamura, M., 1989. Prostaglandin D2 stimulates calcification of human osteoblastic cells. Biochem. Biophys. Res. Commun. 159, 1206–1212. https://doi.org/10.1016/0006-291X(89)92238-9

Kowalczyk, P., Sulejczak, D., Kleczkowska, P., Bukowska-Ośko, I., Kucia, M., Popiel, M., Wietrak, E., Kramkowski, K., Wrzosek, K., Kaczyńska, K., 2021. Mitochondrial Oxidative Stress—A Causative Factor and Therapeutic Target in Many Diseases. Int. J. Mol. Sci. 22, 22. https://doi.org/10.3390/IJMS222413384

Kruger, M.C., Coetzee, M., Haag, M., Weiler, H., 2010. Long-chain polyunsaturated fatty acids: Selected mechanisms of action on bone. Prog. Lipid Res. 49, 438–449. https://doi.org/10.1016/j.plipres.2010.06.002

Kuhlmann, J., 2016. Analysis and occurrence of dichloropropanol fatty acid esters and related process-induced contaminants in edible oils and fats. Eur. J. Lipid Sci. Technol. 118, 382–395. https://doi.org/10.1002/ejlt.201400518

Kuhn, H., Banthiya, S., Van Leyen, K., 2015. Mammalian lipoxygenases and their biological relevance. Biochim. Biophys. Acta - Mol. Cell Biol. Lipids 1851, 308–330. https://doi.org/10.1016/J.BBALIP.2014.10.002

Lagarde, M., Guichardant, M., Bernoud-Hubac, N., 2020. Anti-inflammatory and anti-virus potential of poxytrins, especially protectin DX. Biochimie 179, 281–284. https://doi.org/10.1016/J.BIOCHI.2020.09.008

Lanas, A., 2016. NSAIDs and aspirin: Recent advances and implications for clinical management, NSAIDs and Aspirin: Recent Advances and Implications for Clinical Management. Springer International Publishing. https://doi.org/10.1007/978-3-319-33889-7

Law, C.W., Chen, Y., Shi, W., Smyth, G.K., 2014. voom: Precision weights unlock linear model analysis tools for RNA-seq read counts. Genome Biol. 15. https://doi.org/10.1186/GB-2014-15-2-R29

Leitch, A.G., Lee, T.H., Ringel, E.W., Prickett, J.D., Robinson, D.R., Pyne, S.G., Corey, E.J., Drazen, J.M., Austen, K.F., Lewis, R.A., 1984. Immunologically induced generation of tetraene and pentaene leukotrienes in the peritoneal cavities of menhaden-fed rats. J. Immunol. 132.

Leng, S., Winter, T., Aukema, H.M., 2018a. Dietary ALA, EPA and DHA have distinct effects on oxylipin profiles in female and male rat kidney, liver and serum. J. Nutr. Biochem. 57, 228–237. https://doi.org/10.1016/J.JNUTBIO.2018.04.002

Leng, S., Winter, T., Aukema, H.M., 2018b. Dietary ALA, EPA and DHA have distinct effects on oxylipin profiles in female and male rat kidney, liver and serum. J. Nutr. Biochem. 57, 228–237. https://doi.org/S0955286317309087

Leng, S., Winter, T., Aukema, H.M., 2017. Dietary LA and sex effects on oxylipin profiles in rat kidney, liver, and serum differ from their effects on PUFAs. J. Lipid Res. 58, 1702–1712. https://doi.org/10.1194/jlr.M078097

Li, K., Zhao, J., Wang, M., Niu, L., Wang, Y., Li, Y., Zheng, Y., 2021. The roles of various prostaglandins in fibrosis: A review. Biomolecules. https://doi.org/10.3390/biom11060789

Li, Y., Zhang, Z., Jiang, S., Xu, F., Tulum, L., Li, K., Liu, S., Li, S., Chang, L., Liddell, M., Tu, F., Gu, X., Carmichael, P.L., White, A., Peng, S., Zhang, Q., Li, J., Zuo, T., Kukic, P., Xu, P., 2023. Using transcriptomics, proteomics and phosphoproteomics as new approach methodology (NAM) to define biological responses for chemical safety assessment. Chemosphere 313, 137359. https://doi.org/10.1016/J.CHEMOSPHERE.2022.137359

Lien, E.L., Boyle, F.G., Wrenn, J.M., Perry, R.W., Thompson, C.A., Borzelleca, J.F., 2001. Comparison of AIN-76A and AIN-93G diets: A 13-week study in rats. Food Chem. Toxicol. 39, 385–392. https://doi.org/10.1016/S0278-6915(00)00142-3

Loidl, A., Sevcsik, E., Riesenhuber, G., Deigner, H.-P., Hermetter, A., 2003. Oxidized phospholipids in minimally modified low density lipoprotein induce apoptotic signaling via activation of acid sphingomyelinase in arterial smooth muscle cells. J. Biol. Chem. 278, 32921–8. https://doi.org/10.1074/jbc.M306088200

Mackie, A., Mulet-Cabero, A.I., Torcello-Gomez, A., 2020. Simulating human digestion: developing our knowledge to create healthier and more sustainable foods. Food Funct. 11, 9397–9431. https://doi.org/10.1039/D0FO01981J

Manson, A., Winter, T., Aukema, H.M., 2023. Phospholipase A2 enzymes differently impact

PUFA release and oxylipin formation ex vivo in rat hearts. Prostaglandins Leukot. Essent. Fat. Acids 191, 102555. https://doi.org/10.1016/j.plefa.2023.102555

Massart, D.L., Vandeginste, B.G.M., Buydens, L.M.C., DeJong, S., Lewi, P.J., Smeyers-Verbeke, J., 1997. Handbook of Chemometrics and Qualimetrics: Part A, 1st ed. Elsevier, Amsterdam.

Maulik, S.K., Kumar, S., 2012. Oxidative stress and cardiac hypertrophy: a review. Toxicol. Mech. Methods 22, 359–366. https://doi.org/10.3109/15376516.2012.666650

Mazaleuskaya, L.L., Salamatipour, A., Sarantopoulou, D., Weng, L., FitzGerald, G.A., Blair, I.A., Mesaros, C., 2018. Analysis of HETEs in human whole blood by chiral UHPLC-ECAPCI/HRMS. J. Lipid Res. 59, 564–575. https://doi.org/10.1194/jlr.D081414

Mendonça, A.M., Cayer, L.G.J., Pauls, S.D., Winter, T., Leng, S., Taylor, C.G., Zahradka, P., Aukema, H.M., 2018. Distinct effects of dietary ALA, EPA and DHA on rat adipose oxylipins vary by depot location and sex. Prostaglandins, Leukot. Essent. Fat. Acids 129, 13–24. https://doi.org/10.1016/J.PLEFA.2017.12.004

Messika-Zeitoun, D., Bielak, L.F., Peyser, P.A., Sheedy, P.F., Turner, S.T., Nkomo, V.T., Breen, J.F., Maalouf, J., Scott, C., Tajik, A.J., Enriquez-Sarano, M., 2007. Aortic valve calcification: Determinants and progression in the population. Arterioscler. Thromb. Vasc. Biol. 27, 642–648. https://doi.org/10.1161/01.ATV.0000255952.47980.c2

Mohler, E.R., Gannon, F., Reynolds, C., Zimmerman, R., Keane, M.G., Kaplan, F.S., 2001. Bone formation and inflammation in cardiac valves. Circulation 103, 1522–1528. https://doi.org/10.1161/01.CIR.103.11.1522

Monirujjaman, M., Devassy, J.G., Yamaguchi, T., Sidhu, N., Kugita, M., Gabbs, M., Nagao, S., Zhou, J., Ravandi, A., Aukema, H.M., 2017. Distinct oxylipin alterations in diverse models of cystic kidney diseases. Biochim. Biophys. Acta - Mol. Cell Biol. Lipids 1862, 1562–1574. https://doi.org/10.1016/j.bbalip.2017.08.005

Moriceau, S., Kantari, C., Mocek, J., Davezac, N., Gabillet, J., Guerrera, I.C., Brouillard, F., Tondelier, D., Sermet-Gaudelus, I., Danel, C., Lenoir, G., Daniel, S., Edelman, A., Witko-Sarsat, V., 2009. Coronin-1 Is Associated with Neutrophil Survival and Is Cleaved during Apoptosis: Potential Implication in Neutrophils from Cystic Fibrosis Patients. J. Immunol. 182, 7254–7263. https://doi.org/10.4049/JIMMUNOL.0803312

Nagy, E., Andersson, D.C., Caidahl, K., Eriksson, M.J., Eriksson, P., Franco-Cereceda, A.,

Hansson, G.K., Bäck, M., 2011. Upregulation of the 5-lipoxygenase pathway in human aortic valves correlates with severity of stenosis and leads to leukotriene-induced effects on valvular myofibroblasts. Circulation 123, 1316–1325. https://doi.org/10.1161/CIRCULATIONAHA.110.966846

Nakalekha, C., Yokoyama, C., Miura, H., Alles, N., Aoki, K., Ohya, K., Morita, I., 2010. Increased bone mass in adult prostacyclin-deficient mice. J. Endocrinol. 204, 125–133. https://doi.org/10.1677/JOE-09-0376

Nathaniel, D.J., Evans, J.F., Leblanc, Y., Léveillé, C., Fitzsimmons, B.J., Ford-Hutchinson, A.W., 1985. Leukotriene A5 is a substrate and an inhibitor of rat and human neutrophil LTA4 hydrolase. Biochem. Biophys. Res. Commun. 131, 827–835. https://doi.org/10.1016/0006-291X(85)91314-2

Nathaniel, S., Saligram, S., Innasimthu, A.L., 2010. Aortic stenosis: An update. World J. Cardiol. 2, 135–139. https://doi.org/10.4330/wjc.v2.i6.135

Nguyen, K.H., Fromberg, A., 2020. Occurrence of MCPD and glycidyl fatty acid esters in standard and specialised infant formula in Denmark. Food Addit. Contam. - Part A Chem. Anal. Control. Expo. Risk Assess. 37, 1847–1853. https://doi.org/10.1080/19440049.2020.1817572/SUPPL_FILE/TFAC_A_1817572_SM3013.DOCX

Nishimura, R.A., Otto, C.M., Bonow, R.O., Carabello, B.A., Erwin, J.P., Guyton, R.A., O'Gara, P.T., Ruiz, C.E., Skubas, N.J., Sorajja, P., Sundt, T.M., Thomas, J.D., 2014. 2014 AHA/ACC Guideline for the Management of Patients With Valvular Heart Disease: Executive Summary. Circulation 129, 2440–2492. https://doi.org/10.1161/CIR.0000000000000029

Nkomo, V.T., Gardin, J.M., Skelton, T.N., Gottdiener, J.S., Scott, C.G., Enriquez-Sarano, M., 2006. Burden of valvular heart diseases: a population-based study. Lancet 368, 1005–1011. https://doi.org/10.1016/S0140-6736(06)69208-8

OECD, 2023. OECD Releases new Test Guidelines for NAMs in 2023 [WWW Document]. URL https://www.icapo.org/news/oecd-releases-new-test-guidelines-nams-2023

OECD, 2017. Guidance Document for the Use of Adverse Outcome Pathways in Developing Integrated Approaches to Testing and Assessment (IATA), OECD Series on Testing and Assessment. OECD Publishing, Paris. https://doi.org/10.1787/44bb06c1-en

Oliveira, R. V, Valéria, A., Simionato, C., Cass, Q.B., Tiritan, E., Pinto, M., Sofia, C., Fernandes, G., 2021. Enantioselectivity Effects in Clinical Metabolomics and Lipidomics. Mol. 2021, Vol. 26, Page 5231 26, 5231. https://doi.org/10.3390/MOLECULES26175231

Ostermann, A.I., Willenberg, I., Schebb, N.H., 2015. Comparison of sample preparation methods for the quantitative analysis of eicosanoids and other oxylipins in plasma by means of LC-MS/MS. Anal. Bioanal. Chem. 407, 1403–1414. https://doi.org/10.1007/S00216-014-8377-4/FIGURES/3

Pauls, S.D., Du, Y., Clair, L., Winter, T., Aukema, H.M., Taylor, C.G., Zahradka, P., 2021. Impact of Age, Menopause, and Obesity on Oxylipins Linked to Vascular Health. Arterioscler. Thromb. Vasc. Biol. 41, 883–897. https://doi.org/10.1161/atvbaha.120.315133

Perkins, D.N., Pappin, D.J.C., Creasy, D.M., Cottrell, J.S., 1999. Probability-based protein identification by searching sequence databases using mass spectrometry data. Electrophoresis 20, 3551–3567. https://doi.org/10.1002/(SICI)1522-2683(19991201)20:18<3551::AID-ELPS3551>3.0.CO;2-2

Pick, R., Begandt, D., Stocker, T.J., Salvermoser, M., Thome, S., Böttcher, R.T., Montanez, E., Harrison, U., Forné, I., Khandoga, A.G., Coletti, R., Weckbach, L.T., Brechtefeld, D., Haas, R., Imhof, A., Massberg, S., Sperandio, M., Walzog, B., 2017. Coronin 1A, a novel player in integrin biology, controls neutrophil trafficking in innate immunity. Blood 130, 847–858. https://doi.org/10.1182/BLOOD-2016-11-749622

Pozzi, A., Macias-Perez, I., Abair, T., Wei, S., Su, Y., Zent, R., Falck, J.R., Capdevila, J.H., 2005. Characterization of 5,6- and 8,9-epoxyeicosatrienoic acids (5,6- and 8,9-EET) as potent in vivo angiogenic lipids. J. Biol. Chem. 280, 27138–27146. https://doi.org/10.1074/jbc.M501730200

Qi, Y., 2012. Random Forest for Bioinformatics, in: Ensemble Machine Learning. Springer US, pp. 307–323. https://doi.org/10.1007/978-1-4419-9326-7_11

Quarles, L.D., Haupt, D.M., Davidai, G., Middleton, J.P., 1993. Prostaglandin F2 alpha-induced mitogenesis in MC3T3-E1 osteoblasts: role of protein kinase-C-mediated tyrosine phosphorylation. Endocrinology 132, 1505–1513. https://doi.org/10.1210/ENDO.132.4.8462449

Rajamannan, N.M., Subramaniam, M., Caira, F., Stock, S.R., Spelsberg, T.C., 2005. Atorvastatin inhibits hypercholesterolemia-induced calcification in the aortic valves via the Lrp5

receptor pathway. Circulation 112. https://doi.org/10.1161/01.CIRCULATIONAHA.104.524306

Raju, J., Cayer, L.G., Roberts, J., Caldwell, D., Nunnikhoven, A., Reinhold, A., Schultrich, K., Oberemm, A., Curran, I., Aukema, H.M., Braeuning, A., Buhrke, T., 2022. SOC-V-07 Cardiotoxicity effects of dietary 2-MCPD, a food processing-induced chemical, in male and female F344 rats. Toxicol. Lett. 368, S66. https://doi.org/10.1016/j.toxlet.2022.07.196

Raju, J., Roberts, J., Kocmarek, A.L., Fine, J., 2016. Toxicology of 2-monochloro-1,3-propanediol (2-MCPD) in F344 rats: 28-days dietary study.

Raju, J., Roberts, J., Patry, D., Caldwell, D., Curran, I., Mehta, R., 2019. Toxicology of 2-monochloro-1-3, propanediol (2-MCPD) in F344 rats: 90-days sub-chronic exposure study.

Reeves, P.G., Nielsen, F.H., Fahey, G.C., 1993. AIN-93 Purified Diets for Laboratory Rodents: Final Report of the American Institute of Nutrition Ad Hoc Writing Committee on the Reformulation of the AIN-76A Rodent Diet. J. Nutr. 123, 1939–1951. https://doi.org/10.1093/jn/123.11.1939

Ricciotti, E., Fitzgerald, G.A., 2011. Prostaglandins and Inflammation. Arterioscler. Thromb. Vasc. Biol. 31, 986–1000. https://doi.org/10.1161/ATVBAHA.110.207449

Robinson, M.D., McCarthy, D.J., Smyth, G.K., 2010. edgeR: a Bioconductor package for differential expression analysis of digital gene expression data. Bioinformatics 26, 139–140. https://doi.org/10.1093/BIOINFORMATICS/BTP616

Robinson, M.D., Oshlack, A., 2010. A scaling normalization method for differential expression analysis of RNA-seq data. Genome Biol. 11, 1–9. https://doi.org/10.1186/GB-2010-11-3-R25/FIGURES/3

Rohart, F., Eslami, A., Matigian, N., Bougeard, S., Lê Cao, K.A., 2017. MINT: A multivariate integrative method to identify reproducible molecular signatures across independent experiments and platforms. BMC Bioinformatics 18, 1–13. https://doi.org/10.1186/S12859-017-1553-8/FIGURES/3

Rosenhek, R., Baumgartner, H., 2008. Aortic sclerosis, aortic stenosis and lipid-lowering therapy. Expert Rev. Cardiovasc. Ther. https://doi.org/10.1586/14779072.6.3.385

Rossebø, A.B., Pedersen, T.R., Boman, K., Brudi, P., Chambers, J.B., Egstrup, K., Gerdts, E., Gohlke-Bärwolf, C., Holme, I., Kesäniemi, Y.A., Malbecq, W., Nienaber, C.A., Ray, S., Skjærpe, T., Wachtell, K., Willenheimer, R., 2008. Intensive Lipid Lowering with

Simvastatin and Ezetimibe in Aortic Stenosis. N. Engl. J. Med. 359, 1343–1356. https://doi.org/10.1056/NEJMoa0804602

Ruiz-Perez, D., Narasimhan, G., 2017. So you think you can PLS-DA? bioRxiv. https://doi.org/https://doi.org/10.1101/207225

Sakaue, T., Hamaguchi, M., Aono, J., Nakashiro, K.-I. ichi, Shikata, F., Kawakami, N., Oshima, Y., Kurata, M., Nanba, D., Masumoto, J., Yamaguchi, O., Higashiyama, S., Izutani, H., 2020. Valve Interstitial Cell-Specific Cyclooxygenase-1 Associated With Calcification of Aortic Valves. Ann. Thorac. Surg. 110, 40–49. https://doi.org/10.1016/j.athoracsur.2019.09.085

Sato, I., Suzuki, A., Kakita, A., Ono, Y., Miura, Y., Itoh, M., Oiso, Y., 2003. Stimulatory effect of prostaglandin F2α on Na-dependent phosphate transport in osteoblast-like cells. Prostaglandins, Leukot. Essent. Fat. Acids 68, 311–315. https://doi.org/10.1016/S0952-3278(03)00021-8

Sawada, S., Oberemm, A., Buhrke, T., Meckert, C., Rozycki, C., Braeuning, A., Lampen, A., 2015. Proteomic analysis of 3-MCPD and 3-MCPD dipalmitate toxicity in rat testis. Food Chem. Toxicol. 83, 84–92. https://doi.org/10.1016/j.fct.2015.06.002

Sawada, S., Oberemm, A., Buhrke, T., Merschenz, J., Braeuning, A., Lampen, A., 2016. Proteomic analysis of 3-MCPD and 3-MCPD dipalmitate-induced toxicity in rat kidney. Arch. Toxicol. 90, 1437–1448. https://doi.org/10.1007/s00204-015-1576-8

Schilter, B., Scholz, G., Seefelder, W., 2011. Fatty acid esters of chloropropanols and related compounds in food: Toxicological aspects. Eur. J. Lipid Sci. Technol. 113, 309–313. https://doi.org/10.1002/ejlt.201000311

Schmittgen, T.D., Livak, K.J., 2008. Analyzing real-time PCR data by the comparative CT method. Nat. Protoc. 3, 1101–1109. https://doi.org/10.1038/NPROT.2008.73

Schneider, J.F., Becalski, A., Zhao, T., Chen, F., Liao, Y., Rawn, D.F.K., 2022. Occurrence of 2- and 3-monochloropropanediol esters (MCPDE) in infant formula products on the Canadian market between 2015 and 2019. Food Addit. Contam. - Part A 39, 1663–1673. https://doi.org/10.1080/19440049.2022.2104934

Schultrich, K., Frenzel, F., Oberemm, A., Buhrke, T., Braeuning, A., Lampen, A., 2017. Comparative proteomic analysis of 2-MCPD- and 3-MCPD-induced heart toxicity in the rat. Arch. Toxicol. 91, 3145–3155. https://doi.org/10.1007/s00204-016-1927-0

Schultrich, K., Henderson, C.J., Buhrke, T., Braeuning, A., 2020. Effects of 2-MCPD on oxidative stress in different organs of male mice. Food Chem. Toxicol. 142, 111459. https://doi.org/10.1016/J.FCT.2020.111459

Sega, F.V.D., Fortini, F., Cimaglia, P., Marracino, L., Tonet, E., Antonucci, A., Moscarelli, M., Campo, G., Rizzo, P., Ferrari, R., 2020. COX-2 Is Downregulated in Human Stenotic Aortic Valves and Its Inhibition Promotes Dystrophic Calcification. Int. J. Mol. Sci. 2020, Vol. 21, Page 8917 21, 8917. https://doi.org/10.3390/IJMS21238917

Serhan, C.N., 2014. Pro-resolving lipid mediators are leads for resolution physiology. Nature 510, 92–101. https://doi.org/10.1038/nature13479

Serhan, C.N., Chiang, N., Dalli, J., Levy, B.D., 2015. Lipid mediators in the resolution of inflammation. Cold Spring Harb. Perspect. Biol. 7, a016311. https://doi.org/10.1101/cshperspect.a016311

Shen, M., Tastet, L., Capoulade, R., Arsenault, M., Bedard, E., Clavel, M.A., Pibarot, P., 2020. Effect of bicuspid aortic valve phenotype on progression of aortic stenosis. Eur. Hear. J. - Cardiovasc. Imaging 21, 727–734. https://doi.org/10.1093/EHJCI/JEAA068

Siegmund, K., Thuille, N., Posch, N., Fresser, F., Baier, G., 2015. Novel Protein kinase C θ: Coronin 1A complex in T lymphocytes. Cell Commun. Signal. 13, 1–8. https://doi.org/10.1186/S12964-015-0100-3/FIGURES/4

Siger, A., Nogala-Kalucka, M., Lampart-Szczapa, E., 2008. The content and antioxidant activity of phenolic compounds in cold-pressed plant oils. J. Food Lipids 15, 137–149. https://doi.org/10.1111/j.1745-4522.2007.00107.x

Šmidrkal, J., Tesařová, M., Hrádková, I., Berčíková, M., Adamčíková, A., Filip, V., 2016. Mechanism of formation of 3-chloropropan-1,2-diol (3-MCPD) esters under conditions of the vegetable oil refining. Food Chem. 211, 124–129. https://doi.org/10.1016/j.foodchem.2016.05.039

Solomon, S.D., McMurray, J.J. V, Pfeffer, M.A., Wittes, J., Fowler, R., Finn, P., Anderson, W.F., Zauber, A., Hawk, E., Bertagnolli, M., Adenoma Prevention with Celecoxib (APC) Study Investigators, 2005. Cardiovascular risk associated with celecoxib in a clinical trial for colorectal adenoma prevention. N. Engl. J. Med. 352, 1071–80. https://doi.org/10.1056/NEJMoa050405

Stewart, B.F., Siscovick, D., Lind, B.K., Gardin, J.M., Gottdiener, J.S., Smith, V.E., Kitzman,

D.W., Otto, C.M., 1997. Clinical factors associated with calcific aortic valve disease. J. Am. Coll. Cardiol. 29, 630–634. https://doi.org/10.1016/S0735-1097(96)00563-3

Subramanian, A., Tamayo, P., Mootha, V.K., Mukherjee, S., Ebert, B.L., Gillette, M.A., Paulovich, A., Pomeroy, S.L., Golub, T.R., Lander, E.S., Mesirov, J.P., 2005. Gene set enrichment analysis: A knowledge-based approach for interpreting genome-wide expression profiles. Proc. Natl. Acad. Sci. U. S. A. 102, 15545–15550. https://doi.org/10.1073/pnas.0506580102

Surendran, A., Edel, A., Chandran, M., Bogaert, P., Hassan-Tash, P., Kumar Asokan, A., Hiebert, B., Solati, Z., Sandhawalia, S., Raabe, M., Kass, M., Shah, A., Jassal, D.S., Jaleel, A., Ravandi, A., 2020. Metabolomic Signature of Human Aortic Valve Stenosis. JACC Basic to Transl. Sci. 5, 1163–1177. https://doi.org/10.1016/j.jacbts.2020.10.001

Surendran, A., Zhang, H., Winter, T., Edel, A., Aukema, H., Ravandi, A., 2019. Oxylipin profile of human low-density lipoprotein is dependent on its extent of oxidation. Atherosclerosis 288, 101–111. https://doi.org/10.1016/J.ATHEROSCLEROSIS.2019.07.018

Suzuki, K., Takahashi, S., Watanabe, K., Fujioka, D., Nakamura, T., Obata, J.-E.E., Kawabata, K.-I.I., Katoh, R., Matsumoto, M., Kugiyama, K., 2014. The expression of groups IIE and V phospholipase A2 is associated with an increased expression of osteogenic molecules in human calcified aortic valves. J. Atheroscler. Thromb. 21, 1308–1325. https://doi.org/10.5551/jat.24273

Taguchi, Y. -h., Oono, Y., 2005. Relational patterns of gene expression via non-metric multidimensional scaling analysis. Bioinformatics 21, 730–740. https://doi.org/10.1093/bioinformatics/bti067

Take, I., Kobayashi, Y., Yamamoto, Y., Tsuboi, H., Ochi, T., Uematsu, S., Okafuji, N., Kurihara, S., Udagawa, N., Takahashi, N., 2005. Prostaglandin E2 Strongly Inhibits Human Osteoclast Formation. Endocrinology 146, 5204–5214. https://doi.org/10.1210/EN.2005-0451

Tanaka, M., Sakai, A., Uchida, S., Tanaka, S., Nagashima, M., Katayama, T., Yamaguchi, K., Nakamura, T., 2004. Prostaglandin E2 receptor (EP4) selective agonist (ONO-4819.CD) accelerates bone repair of femoral cortex after drill-hole injury associated with local upregulation of bone turnover in mature rats. Bone 34, 940–948. https://doi.org/10.1016/J.BONE.2004.01.002

Terano, T., Salmon, J.A., Moncada, S., 1984. Biosynthesis and biological activity of leukotriene B5. Prostaglandins 27, 217–232. https://doi.org/10.1016/0090-6980(84)90075-3

Theken, K.N., Schuck, R.N., Edin, M.L., Tran, B., Ellis, K., Bass, A., Lih, F.B., Tomer, K.B., Poloyac, S.M., Wu, M.C., Hinderliter, A.L., Zeldin, D.C., Stouffer, G.A., Lee, C.R., 2012. Evaluation of cytochrome P450-derived eicosanoids in humans with stable atherosclerotic cardiovascular disease. Atherosclerosis 222, 530–536. https://doi.org/10.1016/j.atherosclerosis.2012.03.022

Toyofuku, M., Taniguchi, T., Morimoto, T., Yamaji, K., Furukawa, Y., Takahashi, K., Tamura, T., Shiomi, H., Ando, K., Kanamori, N., Murata, K., Kitai, T., Kawase, Y., Izumi, C., Miyake, M., Mitsuoka, H., Kato, M., Hirano, Y., Matsuda, S., Inada, T., Murakami, T., Takeuchi, Y., Yamane, K., Ishii, M., Minamino-Muta, E., Kato, T., Inoko, M., Ikeda, T., Komasa, A., Ishii, K., Hotta, K., Higashitani, N., Kato, Y., Inuzuka, Y., Maeda, C., Jinnai, T., Morikami, Y., Saito, N., Minatoya, K., Kimura, T., 2017. Sex differences in severe aortic stenosis: Clinical presentation and mortality. Circ. J. 81, 1213–1221. https://doi.org/10.1253/circj.CJ-16-1244

Tsao, C.W., Aday, A.W., Almarzooq, Z.I., Anderson, C.A.M., Arora, P., Avery, C.L., Baker-Smith, C.M., Beaton, A.Z., Boehme, A.K., Buxton, A.E., Commodore-Mensah, Y., Elkind, M.S.V., Evenson, K.R., Eze-Nliam, C., Fugar, S., Generoso, G., Heard, D.G., Hiremath, S., Ho, J.E., Kalani, R., Kazi, D.S., Ko, D., Levine, D.A., Liu, J., Ma, J., Magnani, J.W., Michos, E.D., Mussolino, M.E., Navaneethan, S.D., Parikh, N.I., Poudel, R., Rezk-Hanna, M., Roth, G.A., Shah, N.S., St-Onge, M.-P., Thacker, E.L., Virani, S.S., Voeks, J.H., Wang, N.-Y., Wong, N.D., Wong, S.S., Yaffe, K., Martin, S.S., 2023. Heart Disease and Stroke Statistics—2023 Update: A Report From the American Heart Association. Circulation 147. https://doi.org/10.1161/CIR.0000000000001123

Vaidya, K.A., Donnelly, M.P., Gee, T.W., Ibrahim Aibo, M.A., Byers, S., Butcher, J.T., 2020. Induction of aortic valve calcification by celecoxib and its COX-2 independent derivatives is glucocorticoid-dependent. Cardiovasc. Pathol. 46, 107194. https://doi.org/10.1016/j.carpath.2019.107194

van Bergen, C.A., Collier, P.D., Lucas, R.A., Preston, H.D., Sissons, D.J., 1992. Determination of chloropropanols in protein hydrolysates. J. Chromatogr. A 589, 109–119. https://doi.org/10.1016/0021-9673(92)80011-I

Van Der Linde, D., Yap, S.C., Van Dijk, A.P.J., Budts, W., Pieper, P.G., Van Der Burgh, P.H., Mulder, B.J.M., Witsenburg, M., Cuypers, J.A.A.E., Lindemans, J., Takkenberg, J.J.M., Roos-Hesselink, J.W., 2011. Effects of rosuvastatin on progression of stenosis in adult patients with congenital aortic stenosis (PROCAS Trial). Am. J. Cardiol. 108, 265–271. https://doi.org/10.1016/j.amjcard.2011.03.032

Waclawiková, B., Codutti, A., Alim, K., El Aidy, S., 2022. Gut microbiota-motility interregulation: insights from in vivo, ex vivo and in silico studies. Gut Microbes 14. https://doi.org/10.1080/19490976.2021.1997296

Warford-Woolgar, L., Peng, C.Y.C., Shuhyta, J., Wakefield, A., Sankaran, D., Ogborn, M., Aukema, H.M., 2006. Selectivity of cyclooxygenase isoform activity and prostanoid production in normal and diseased Han:SPRD-cy rat kidneys. Am. J. Physiol. - Ren. Physiol. 290, 897–904. https://doi.org/10.1152/AJPRENAL.00332.2005/ASSET/IMAGES/LARGE/ZH20040642600007.JPEG

Wendler, S., Schlundt, C., Bucher, C.H., Birkigt, J., Schipp, C.J., Volk, H.D., Duda, G.N., Schmidt-Bleek, K., 2019. Immune modulation to enhance bone healing-a new concept to induce bone using prostacyclin to locally modulate immunity. Front. Immunol. 10, 713. https://doi.org/10.3389/FIMMU.2019.00713/BIBTEX

Wettlaufer, S.H., Scott, J.P., McEachin, R.C., Peters-Golden, M., Huang, S.K., 2016. Reversal of the transcriptome by prostaglandin E2 during Myofibroblast dedifferentiation. Am. J. Respir. Cell Mol. Biol. 54, 114–127. https://doi.org/10.1165/rcmb.2014-0468OC

Weylandt, K.H., Krause, L.F., Gomolka, B., Chiu, C.Y., Bilal, S., Nadolny, A., Waechter, S.F., Fischer, A., Rothe, M., Kang, J.X., 2011. Suppressed liver tumorigenesis in fat-1 mice with elevated omega-3 fatty acids is associated with increased omega-3 derived lipid mediators and reduced TNF-α. Carcinogenesis 32, 897–903. https://doi.org/10.1093/carcin/bgr049

Wirrig, E.E., Gomez, M.V., Hinton, R.B., Yutzey, K.E., 2015. COX2 inhibition reduces aortic valve calcification in vivo. Arterioscler. Thromb. Vasc. Biol. 35, 938–947. https://doi.org/10.1161/ATVBAHA.114.305159

Wöhrlin, F., Fry, H., Lahrssen-Wiederholt, M., Preiß-Weigert, A., 2015. Occurrence of fatty acid esters of 3-MCPD, 2-MCPD and glycidol in infant formula. Food Addit. Contam. Part A 32, 1810–1822. https://doi.org/10.1080/19440049.2015.1071497

Worley, B., Powers, R., 2013. Multivariate Analysis in Metabolomics. Curr. Metabolomics 1, 92–107. https://doi.org/10.2174/2213235x11301010092

Wu, S., Zhou, X., Qin, W., An, X., Wang, F., Lv, L., Tang, T., Liu, X., He, Y., 2023. Prostaglandin Metabolome Profiles in Zebrafish (Danio rerio) Exposed to Acetochlor and Butachlor. Int. J. Mol. Sci. 24, 3488. https://doi.org/10.3390/IJMS24043488/S1

Wu, X., Yang, J., Morisseau, C., Robertson, L.W., Hammock, B., Lehmler, H.J., 2016. 3,3',4,4',5-pentachlorobiphenyl (PCB 126) decreases hepatic and systemic ratios of epoxide to diol metabolites of unsaturated fatty acids in male rats. Toxicol. Sci. 152, 309–322. https://doi.org/10.1093/toxsci/kfw084

Xie, C., Jauhari, S., Mora, A., 2021. Popularity and performance of bioinformatics software: the case of gene set analysis. BMC Bioinformatics 22, 1–16. https://doi.org/10.1186/S12859-021-04124-5/FIGURES/2

Yadgir, S., Johnson, C.O., Aboyans, V., Adebayo, O.M., Adedoyin, R.A., Afarideh, M., Alahdab, F., Alashi, A., Alipour, V., Arabloo, J., Azari, S., Barthelemy, C.M., Benziger, C.P., Berman, A.E., Bijani, A., Carrero, J.J., Carvalho, F., Daryani, A., Durães, A.R., Esteghamati, A., Farid, T.A., Farzadfar, F., Fernandes, E., Filip, I., Gad, M.M., Hamidi, S., Hay, S.I., Ilesanmi, O.S., Naghibi Irvani, S.S., Jürisson, M., Kasaeian, A., Kengne, A.P., Khan, A.R., Kisa, A., Kisa, S., Kolte, D., Manafi, N., Manafi, A., Mensah, G.A., Mirrakhimov, E.M., Mohammad, Y., Mokdad, A.H., Negoi, R.I., Thi Nguyen, H.L., Nguyen, T.H., Nixon, M.R., Otto, C.M., Patel, S., Pilgrim, T., Radfar, A., Rawaf, D.L., Rawaf, S., Rawasia, W.F., Rezapour, A., Roever, L., Saad, A.M., Saadatagah, S., Senthilkumaran, S., Sliwa, K., Tesfay, B.E., Tran, B.X., Ullah, I., Vaduganathan, M., Vasankari, T.J., Wolfe, C.D.A., Yonemoto, N., Roth, G.A., 2020. Global, Regional, and National Burden of Calcific Aortic Valve and Degenerative Mitral Valve Diseases, 1990–2017. Circulation 141, 1670–1680. https://doi.org/10.1161/CIRCULATIONAHA.119.043391

Yamazato, R., Yamamoto, H., Tadehara, F., Teragawa, H., Kurisu, S., Dohi, Y., Ishibashi, K., Kunita, E., Utsunomiya, H., Oka, T., Kihara, Y., 2012. Association between aortic valve calcification and myocardial ischemia, especially in asymptomatic patients. J. Nucl. Med. 53, 1216–1221. https://doi.org/10.2967/jnumed.111.099275

Yan, M., Collins, R.F., Grinstein, S., Trimble, W.S., 2005. Coronin-1 Function Is Required for

Phagosome Formation. Mol. Biol. Cell 16, 3077. https://doi.org/10.1091/MBC.E04-11-0989

Yang, Y., Wu, W., Wu, A., 2019. Toxicity Evaluation Using Animal and Cell Models, in: Food Safety & Mycotoxins. Springer Singapore, Singapore, pp. 33–64. https://doi.org/10.1007/978-981-32-9038-9_3

Yao, C., Narumiya, S., 2019. Prostaglandin-cytokine crosstalk in chronic inflammation. Br. J. Pharmacol. 176, 337–354. https://doi.org/10.1111/BPH.14530

Yost, R.A., Enke, C.G., 1979. Triple quadrupole mass spectrometry for direct mixture analysis and structure elucidation. Anal. Chem. 51, 1251–1264. https://doi.org/10.1021/ac50048a002

Yu, H., Samuels, D.C., Zhao, Y. yong, Guo, Y., 2019. Architectures and accuracy of artificial neural network for disease classification from omics data. BMC Genomics 20, 1–12. https://doi.org/10.1186/s12864-019-5546-z

Zelinková, Z., Svejkovská, B., Velíšek, J., Doležal, M., Zelinkov, Z., Svejkovsk, B., Vel, J., Ek, Š., Dolež Al, M., 2006. Fatty acid esters of 3-chloropropane-1,2-diol in edible oils. Food Addit. Contam. 2312, 1290–1298. https://doi.org/10.1080/02652030600887628

Zhang, G., Panigrahy, D., Mahakian, L.M., Yang, J., Liu, J.Y., Lee, K.S.S., Wettersten, H.I., Ulu, A., Hu, X., Tam, S., Hwang, S.H., Ingham, E.S., Kieran, M.W., Weiss, R.H., Ferrara, K.W., Hammock, B.D., 2013. Epoxy metabolites of docosahexaenoic acid (DHA) inhibit angiogenesis, tumor growth, and metastasis. Proc. Natl. Acad. Sci. U. S. A. 110, 6530–6535. https://doi.org/10.1073/pnas.1304321110

Zheng, K.H., Tzolos, E., Dweck, M.R., 2020. Pathophysiology of Aortic Stenosis and Future Perspectives for Medical Therapy. Cardiol. Clin. 38, 1–12. https://doi.org/10.1016/j.ccl.2019.09.010

Žuvela, P., Skoczylas, M., Jay Liu, J., Bączek, T., Kaliszan, R., Wong, M.W., Buszewski, B., 2019. Column Characterization and Selection Systems in Reversed-Phase High-Performance Liquid Chromatography. Chem. Rev. 119, 3674–3729. https://doi.org/10.1021/acs.chemrev.8b00246

Appendices

1. Linkage to Health Canada's Projects on 2-Monochloro-1-3, propanediol (2-MCPD)

Health Canada Santé Canada

Linkage to Health Canada's Projects on 2-Monochloro-1-3, propanediol (2-MCPD)

This is to state and confirm that this PhD thesis for evaluation submitted by Lucien GJ Cayer contains original laboratory research conducted at the *University of Manitoba* and is directly linked to *Health Canada*'s Hazard Identification of 2-MCPD, a process-induced food contaminant.

Health Canada conducted three independent rodent bioassays for the Hazard Identification of 2-MCPD (Principle & Responsible Investigator: Dr Jayadev Raju). To address mode-of-action and mechanistic details of 2-MCPD that are ancillary to Hazard Identification, facilitate biomarker discovery pertinent to cardiotoxicity, and support knowledge transfer activities, Lucien GJ Cayer was designated as the Graduate Student in these three projects. Two of the studies were regulatory test guideline-compliant addressing sub-acute and sub-chronic dietary exposure of 2-MCPD. The third was a topical study that included groups to test Lucien GJ Cayer's original hypothesis that *nutritional manipulation of the diet matrix providing supplemental versus adequate levels of α-Linolenic acid (ALA) will alter the hazard outcomes of 2-MCPD*. Tissues and supplementary mechanistic data (including data generated by collaborators at BfR – the Federal Risk Assessment Institute, Berlin, Germany) derived from these three studies were given to Lucien GJ Cayer for graduate studies: (a) research published in the MSc Thesis (2019), and (b) to this PhD thesis submitted for evaluation. The Health Canada Study Reports (listed below) were shared and the contents, data and its interpretation of apical toxicological endpoints provided evidence of the cardiotoxicity of 2-MCPD.

1. Raju J: Technical Report / Toxicology of 2-Monochloro-1-3, propanediol (2-MCPD) in F344 rats: 28-days Sub-Acute Dietary Study, 2016.
2. Raju J: Technical Report / Toxicology of 2-Monochloro-1-3, propanediol (2-MCPD) in F344 rats: 90-days Sub-Chronic Dietary Study, 2019.
3. Raju J: Technical Report / Influence of Nutritional Manipulation of the Diet Matrix (with Fermentable Fibre Material or α-Linolenic acid) on the Toxicity of 2-Monochloro-1-3, propanediol (2-MCPD) in Sprague-Dawley Rats, 2023.

Manuscripts

The mechanistic research conducted by Lucien GJ Cayer have been developed into three manuscripts (listed below), that have all gone through Health Canada's Review for Scientific Publications. The manuscript provides new discovery interlinking the role of cellular and molecular markers and nutritional influence in the diet matrix to cardiotoxicity and Hazard Identification of 2-MCPD, a priority food contaminant.

Canada

Health Canada / Santé Canada

MSc Thesis

Submitted to *Food and Chemical Toxicology*, May 2024

- Bioactive lipids are altered in the heart, kidney, and serum of male and female F344 rats sub-chronically exposed to dietary 2-MCPD.
  Authors: Lucien G.J. Cayer, Jennifer Roberts, Don Caldwell, Jayadev Raju, Harold M. Aukema.

PhD Thesis submitted for Evaluation

Study A submission to *Archives of Toxicology*, June 2024

- An integrated multi-omics analysis of the effects of the food processing-induced contaminant 2-monochloropropane-1,3-diol (2-MCPD) in rat heart.
  Authors: Lucien GJ Cayer, Thorsten Buhrke, Katharina Sommerkorn, Anna Reinhold, Jennifer Roberts, Albert Braeuning, Jayadev Raju, Harold M Aukema, Tobias Karakach.

Study B submitted to *Food and Chemical Toxicology*, May 2024

- Increased cardiac oxylipins in response to 2-monochloropropane-1,3-diol exposure are partially ameliorated by dietary adequacy of the essential n-3 fatty acid, α-linolenic acid
  Authors: Lucien GJ Cayer, Tobias Karakach, Jennifer Roberts, Stephen PJ Brooks, Jayadev Raju, Harold M Aukema.

Truly,

Jayadev Raju

Jayadev Raju, PhD
Research Scientist

Food Directorate
Health Canada/ Government of Canada

C238 Frederick G. Banting Research Centre/ Postal Locator 2202C
251 Sir Frederick Banting Driveway, Ottawa, K1A 0K9, Ontario, Canada
(343) 575-0151 / (613) 796-3521 (Cellular)
(613) 941-6959 (FAX)
jayadev.raju@hc-sc.gc.ca

Canada

2. Oxylipin Synthesis Pathway Diagrams

Images of WikiPathways entries. The online versions contain annotations for the oxylipins linking them to external databases including PubChem (https://pubchem.ncbi.nlm.nih.gov) and ChEBI (https://www.ebi.ac.uk/chebi/init.do).

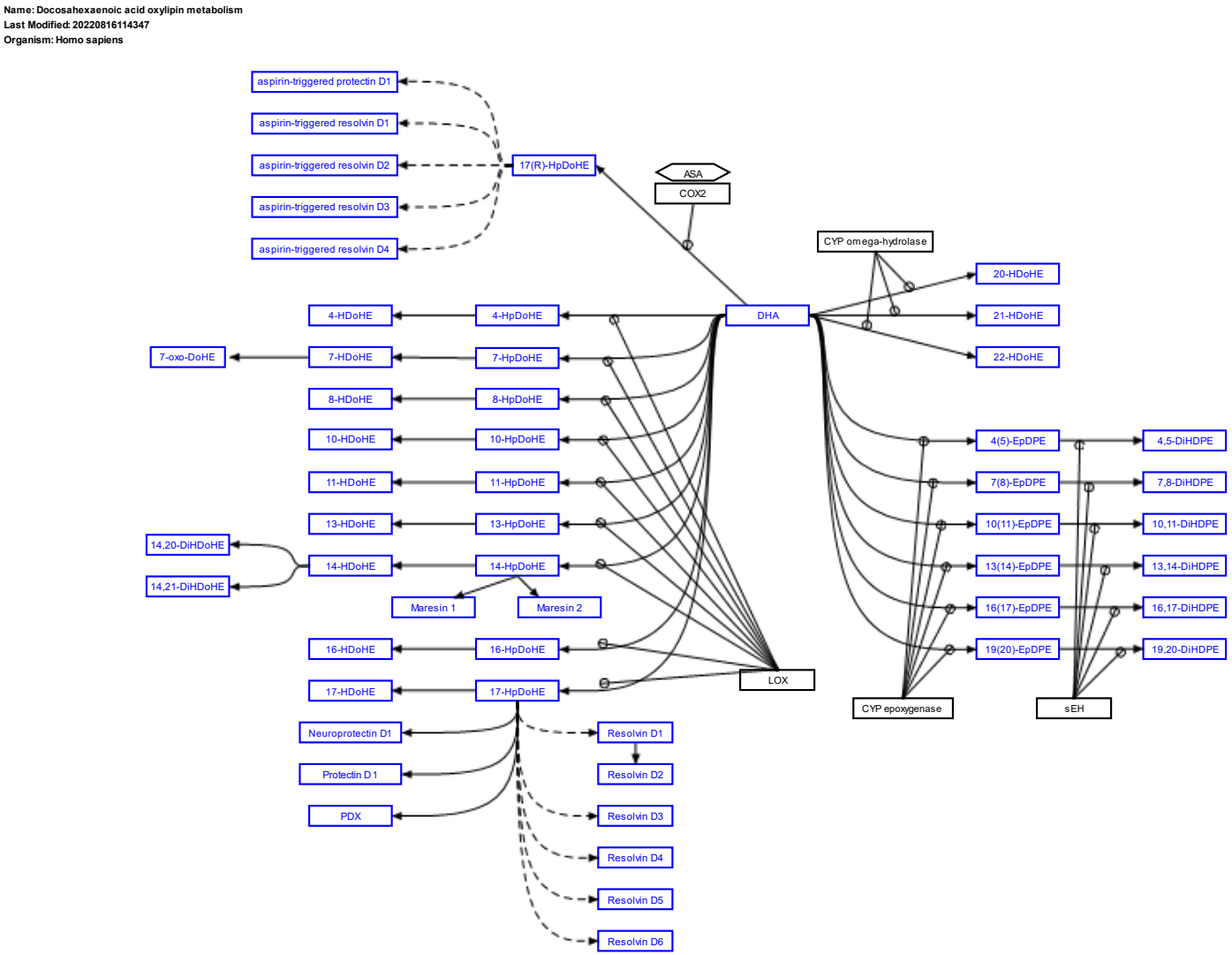

Appendix Figure 2.1. Docosahexaenoic acid oxylipin metabolism (WP5154)

https://www.wikipathways.org/pathways/WP5154.html

Name: ALA oxylipin metabolism
Last Modified 20230531180130
Organism: Homo sapiens

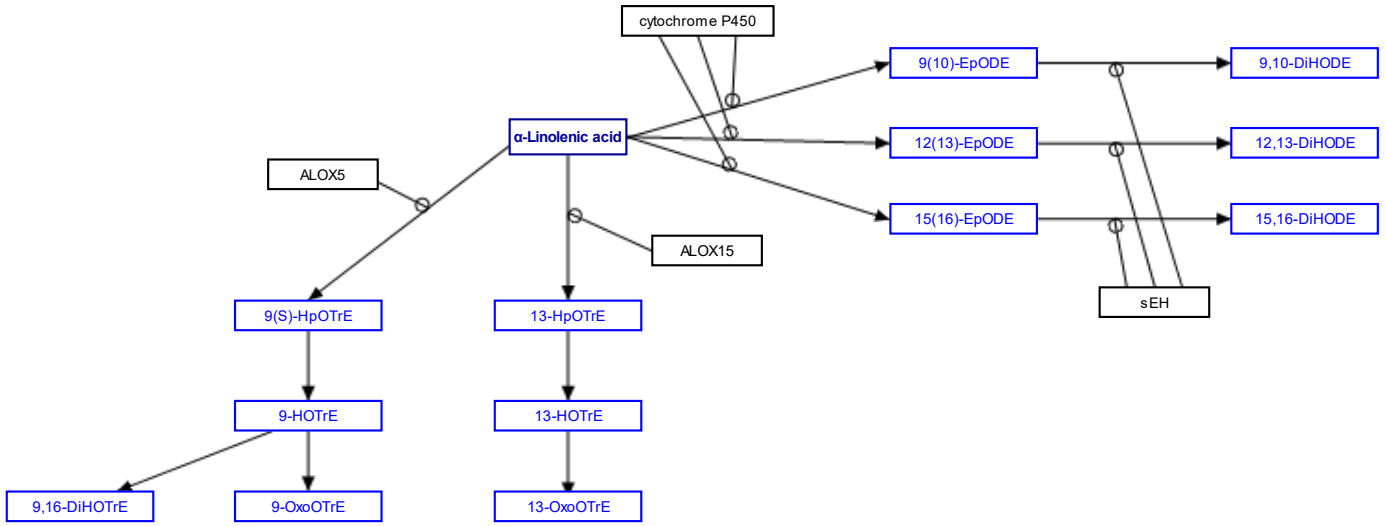

Appendix Figure 2.2. ALA oxylipin metabolism (WP5136)

https://www.wikipathways.org/pathways/WP5136.html

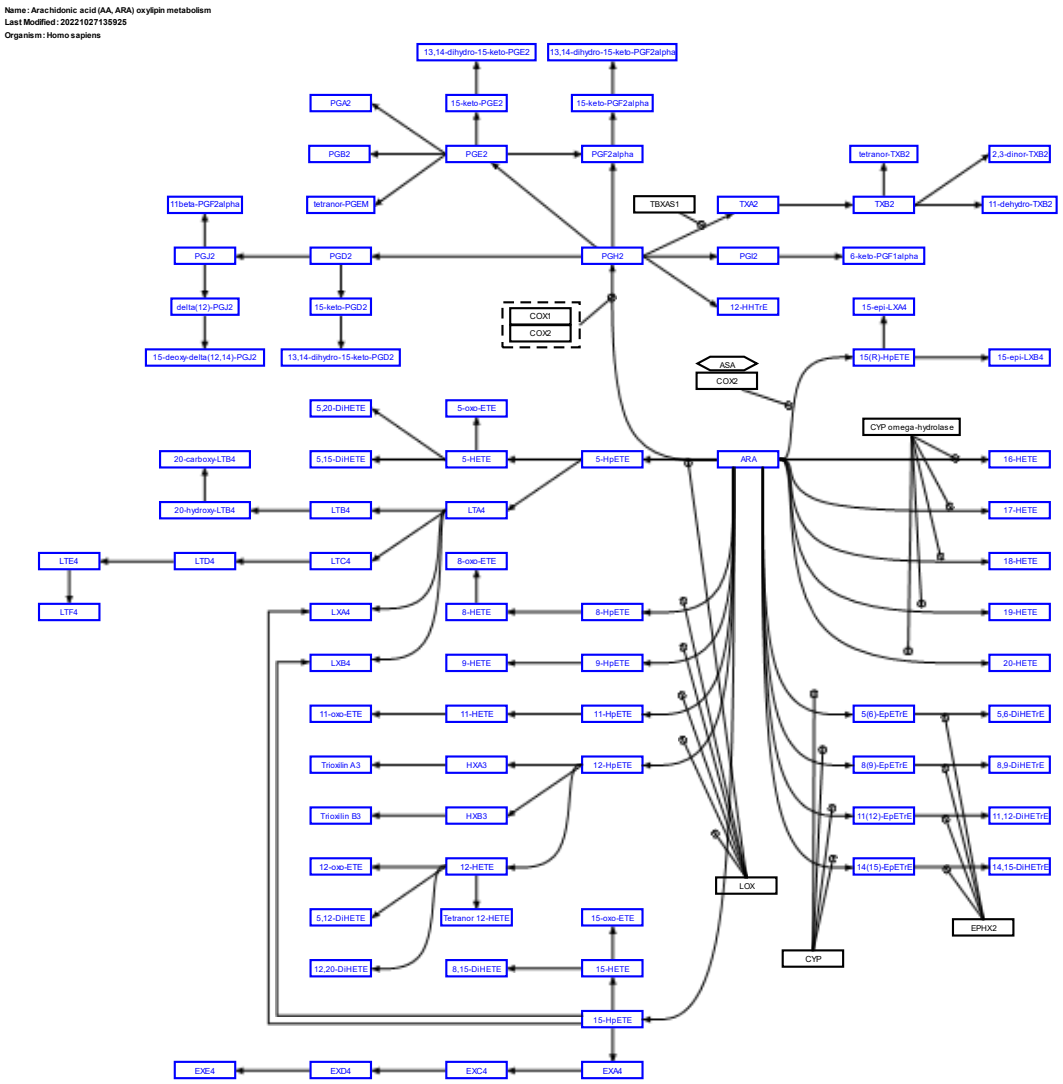

Appendix Figure 2.3. Arachidonic acid (AA, ARA) oxylipin metabolism (WP5155)

https://www.wikipathways.org/pathways/WP5155.html

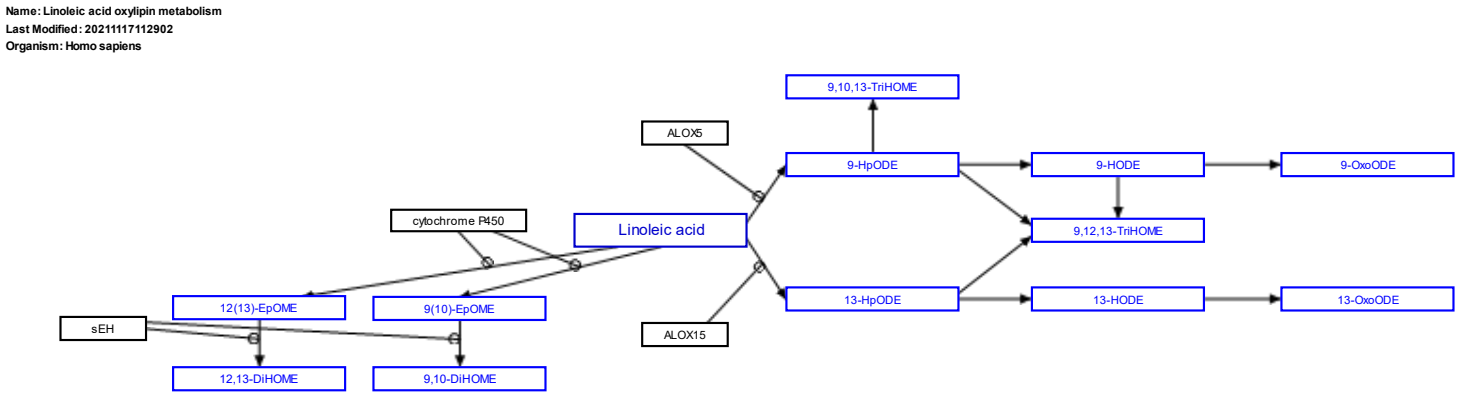

Appendix Figure 2.4. Linoleic acid oxylipin metabolism (WP5137)

https://www.wikipathways.org/pathways/WP5137.html

3. Study A: Supplemental Tables

Study A: Supplemental Table 1. RNA-seq rat heart DEGs with 40 mg/kg BW/d 2-MCPD exposure.

ENSEMBL	Gene	LFC	*P* value	FDR
ENSRNOG00000000047	Cd82	1.09	<0.001	0.011
ENSRNOG00000000239	Ccl7	3.23	<0.001	<0.001
ENSRNOG00000000451	RT1-Ba	1.04	<0.001	0.002
ENSRNOG00000000528	Fgd2	1.52	<0.001	0.005
ENSRNOG00000000569	Vsir	1.43	<0.001	0.002
ENSRNOG00000000640	Egr2	3.03	<0.001	0.003
ENSRNOG00000000827	Ier3	1.14	<0.001	0.004
ENSRNOG00000000853	Aif1	1.02	<0.001	0.007
ENSRNOG00000000855	Lst1	1.72	0.001	0.024
ENSRNOG00000000907	Alox5ap	1.10	<0.001	<0.001
ENSRNOG00000000994	Stxbp2	1.37	0.002	0.028
ENSRNOG00000001005	Fcer2	-1.15	<0.001	0.004
ENSRNOG00000001224	Itgb2	1.92	0.002	0.033
ENSRNOG00000001304	Bcr	1.41	0.003	0.038
ENSRNOG00000001414	Serpine1	2.35	<0.001	<0.001
ENSRNOG00000001427	Orai2	1.15	0.001	0.027
ENSRNOG00000001704	Runx1	2.10	<0.001	0.001
ENSRNOG00000002052	Ccdc80	1.25	<0.001	<0.001
ENSRNOG00000002385	Prg4	1.67	<0.001	<0.001
ENSRNOG00000002418	Tgfb2	1.57	<0.001	<0.001
ENSRNOG00000002434	Tmem100	1.90	<0.001	<0.001
ENSRNOG00000002524	Gpr37	2.79	0.002	0.035
ENSRNOG00000002643	Ugdh	1.40	0.002	0.034
ENSRNOG00000002653	Kcnk2	-1.13	<0.001	0.002
ENSRNOG00000002746	Fstl1	1.14	<0.001	0.005

ENSRNOG00000002810	Gfpt2	1.41	<0.001	0.014
ENSRNOG00000002926	Uap1	1.48	<0.001	0.007
ENSRNOG00000003120	Prelp	1.01	<0.001	0.018
ENSRNOG00000003357	Col3a1	1.61	<0.001	<0.001
ENSRNOG00000003486	Mnda	1.39	<0.001	0.008
ENSRNOG00000003533	Clcn4	-1.60	0.002	0.034
ENSRNOG00000003546	Tnfrsf12a	1.65	0.002	0.028
ENSRNOG00000003622	Cybb	1.21	<0.001	0.004
ENSRNOG00000003703	Mcm6	1.03	<0.001	0.007
ENSRNOG00000003715	Srpx2	1.81	<0.001	0.019
ENSRNOG00000003745	Atf3	2.22	<0.001	0.008
ENSRNOG00000003778	Opn3	2.31	0.001	0.023
ENSRNOG00000003802	Pttg1	1.16	0.003	0.045
ENSRNOG00000003897	Col1a1	1.55	<0.001	<0.001
ENSRNOG00000003984	Apln	-1.10	<0.001	0.002
ENSRNOG00000004078	Eno3	-1.16	<0.001	0.002
ENSRNOG00000004147	Abca8a	-1.01	<0.001	0.010
ENSRNOG00000004229	Tac3	4.90	<0.001	<0.001
ENSRNOG00000004273	Ifitm1	1.86	<0.001	<0.001
ENSRNOG00000004578	Cthrc1	4.15	<0.001	0.004
ENSRNOG00000004589	Galnt16	1.12	<0.001	0.008
ENSRNOG00000004624	Rnd3	1.09	<0.001	0.004
ENSRNOG00000004649	Il1b	1.70	0.002	0.032
ENSRNOG00000004699	Fibin	1.19	<0.001	0.002
ENSRNOG00000005214	Plek	1.53	<0.001	0.003
ENSRNOG00000005243	Pop1	1.28	0.003	0.046
ENSRNOG00000005248	Slc1a4	1.36	<0.001	0.012
ENSRNOG00000005378	Gna15	1.54	0.003	0.045
ENSRNOG00000005387	Rbm3	1.01	<0.001	0.001
ENSRNOG00000005695	Mgp	1.12	<0.001	0.005
ENSRNOG00000005825	Lyz2	1.94	<0.001	<0.001

ENSRNOG00000005854	Angpt1	-1.46	<0.001	0.003
ENSRNOG00000005871	Il1rn	2.60	<0.001	0.002
ENSRNOG00000005935	A3galt2	1.81	<0.001	0.004
ENSRNOG00000005965	Irak4	1.10	0.002	0.034
ENSRNOG00000006094	Cd44	1.12	0.003	0.041
ENSRNOG00000006151	Reg3b	5.07	<0.001	<0.001
ENSRNOG00000006231	Ptpro	1.20	<0.001	0.003
ENSRNOG00000006460	Amdhd2	1.30	0.003	0.040
ENSRNOG00000006553	Bnc2	2.05	<0.001	<0.001
ENSRNOG00000007159	Ccl2	3.01	<0.001	0.020
ENSRNOG00000007290	Atp1a2	-1.08	<0.001	0.002
ENSRNOG00000007302	Fbn1	1.53	<0.001	<0.001
ENSRNOG00000007319	Trib3	2.93	<0.001	<0.001
ENSRNOG00000007437	Irf5	1.50	<0.001	0.007
ENSRNOG00000007546	Asns	2.92	0.002	0.028
ENSRNOG00000007613	C1qtnf5	1.11	0.003	0.038
ENSRNOG00000007679	Cyth4	1.23	<0.001	0.003
ENSRNOG00000008015	Fos	2.75	<0.001	<0.001
ENSRNOG00000008045	Slamf9	1.80	<0.001	0.003
ENSRNOG00000008115	Arhgap11a	1.16	0.002	0.037
ENSRNOG00000008141	Nppb	1.35	<0.001	0.005
ENSRNOG00000008187	Ubash3b	1.46	0.003	0.041
ENSRNOG00000008336	Tnfrsf11b	3.27	0.001	0.026
ENSRNOG00000008409	Myo1f	1.16	<0.001	0.004
ENSRNOG00000008439	Gprc5d	1.86	0.001	0.022
ENSRNOG00000008680	Loxl1	1.69	<0.001	<0.001
ENSRNOG00000008736	Slamf8	1.17	<0.001	0.010
ENSRNOG00000008816	Gpnmb	2.56	<0.001	<0.001
ENSRNOG00000008837	Ass1	2.04	0.001	0.022
ENSRNOG00000009197	Asb4	-1.26	0.002	0.031
ENSRNOG00000009211	C3ar1	2.76	0.003	0.038

ENSRNOG00000009331	Hck	1.60	<0.001	0.004
ENSRNOG00000009334	Knstrn	1.54	0.004	0.047
ENSRNOG00000009341	Hivep3	1.41	<0.001	0.004
ENSRNOG00000009594	Snai1	1.20	0.002	0.033
ENSRNOG00000009724	Tstd2	-1.20	0.002	0.033
ENSRNOG00000009730	Cyp7b1	2.69	<0.001	0.020
ENSRNOG00000009848	Il18	1.33	<0.001	0.015
ENSRNOG00000009946	Ldlr	1.33	<0.001	0.008
ENSRNOG00000010047	Ddit4l	-1.36	<0.001	0.008
ENSRNOG00000010092	Magix	-1.06	<0.001	0.019
ENSRNOG00000010208	Timp1	3.68	<0.001	<0.001
ENSRNOG00000010319	Lcp1	1.22	<0.001	0.005
ENSRNOG00000010362	Anxa2	1.03	<0.001	<0.001
ENSRNOG00000010466	Chpf2	1.24	0.001	0.022
ENSRNOG00000010626	Sphk1	2.26	<0.001	0.012
ENSRNOG00000010645	Lgals3	1.88	<0.001	<0.001
ENSRNOG00000010833	Mthfd2	1.88	<0.001	<0.001
ENSRNOG00000010986	-	1.02	<0.001	0.008
ENSRNOG00000010994	Has1	2.99	<0.001	0.004
ENSRNOG00000011296	Cenpn	1.26	0.003	0.044
ENSRNOG00000011406	Ccl4	1.13	0.002	0.032
ENSRNOG00000011631	Fst	2.66	<0.001	0.004
ENSRNOG00000011644	Slc1a7	2.40	<0.001	0.010
ENSRNOG00000011647	S100a6	1.02	<0.001	<0.001
ENSRNOG00000011821	S100a4	1.39	<0.001	<0.001
ENSRNOG00000012094	Ltbp2	3.03	<0.001	<0.001
ENSRNOG00000012098	Adcyap1r1	1.58	<0.001	<0.001
ENSRNOG00000012160	Syk	1.24	0.001	0.023
ENSRNOG00000012172	Spi1	1.55	<0.001	0.005
ENSRNOG00000012208	Itgb7	2.21	<0.001	0.019
ENSRNOG00000012390	Npw	3.56	<0.001	0.007

ENSRNOG00000012458	Cyp2e1	-1.77	<0.001	0.002
ENSRNOG00000012471	Thbs4	3.84	<0.001	<0.001
ENSRNOG00000012494	Kctd14	1.30	0.003	0.046
ENSRNOG00000012616	Ppt1	1.06	<0.001	0.002
ENSRNOG00000012660	Postn	3.45	<0.001	<0.001
ENSRNOG00000012749	C1qb	1.03	<0.001	0.006
ENSRNOG00000012807	C1qa	1.23	<0.001	0.014
ENSRNOG00000012881	Fgl2	1.60	<0.001	0.002
ENSRNOG00000013014	Cyba	1.10	<0.001	0.015
ENSRNOG00000013024	Csgalnact1	1.03	<0.001	0.008
ENSRNOG00000013231	Ptafr	1.14	<0.001	0.016
ENSRNOG00000013306	Pcdh20	-2.13	<0.001	0.017
ENSRNOG00000013330	Cdhr1	2.64	0.003	0.038
ENSRNOG00000013564	Dok3	1.76	0.002	0.037
ENSRNOG00000013653	Pdlim7	1.06	0.002	0.029
ENSRNOG00000013744	Akip1	1.22	<0.001	<0.001
ENSRNOG00000013747	Sh3bp2	1.76	<0.001	0.006
ENSRNOG00000013794	Rbp1	1.29	<0.001	0.003
ENSRNOG00000013862	Dusp2	1.67	<0.001	0.008
ENSRNOG00000013914	Gpr132	3.03	<0.001	0.014
ENSRNOG00000013917	Igsf10	1.43	<0.001	0.002
ENSRNOG00000013981	Ptpn5	-2.51	0.002	0.029
ENSRNOG00000013987	Sbno2	1.58	0.001	0.022
ENSRNOG00000014117	Hmox1	2.16	<0.001	<0.001
ENSRNOG00000014202	Snx20	1.71	0.001	0.025
ENSRNOG00000014258	Rab32	1.15	<0.001	0.011
ENSRNOG00000014288	Fn1	1.39	<0.001	<0.001
ENSRNOG00000014320	Inhba	1.67	0.002	0.035
ENSRNOG00000014333	Vcam1	1.43	<0.001	0.003
ENSRNOG00000014387	Chac1	5.43	<0.001	<0.001
ENSRNOG00000014426	Lox	1.71	<0.001	<0.001

ENSRNOG00000014504	Il1r1	2.75	0.002	0.030
ENSRNOG00000014532	Lbp	1.55	<0.001	0.001
ENSRNOG00000014653	Arl11	1.33	<0.001	0.019
ENSRNOG00000014816	Slc1a1	1.08	<0.001	0.007
ENSRNOG00000014956	Slc11a1	1.36	0.003	0.042
ENSRNOG00000015159	Slc9a3	2.95	<0.001	0.008
ENSRNOG00000015505	Mfap5	1.75	<0.001	<0.001
ENSRNOG00000015514	Bcat1	2.93	<0.001	<0.001
ENSRNOG00000015904	Wfdc1	-1.14	<0.001	<0.001
ENSRNOG00000015906	Tgif1	1.98	<0.001	0.005
ENSRNOG00000015941	Fkbp10	1.00	0.002	0.032
ENSRNOG00000015992	Ccl20	3.53	<0.001	0.017
ENSRNOG00000016085	Mpzl2	2.18	0.002	0.034
ENSRNOG00000016151	Ankrd23	1.52	<0.001	0.002
ENSRNOG00000016257	Cotl1	1.60	<0.001	<0.001
ENSRNOG00000016483	Myo16	-1.76	<0.001	0.020
ENSRNOG00000016581	Serpinb1a	1.68	<0.001	0.001
ENSRNOG00000016643	Lpcat2	1.29	<0.001	0.015
ENSRNOG00000016756	Ptgir	1.28	0.004	0.047
ENSRNOG00000016758	Loxl2	1.29	<0.001	0.002
ENSRNOG00000016825	Polr1g	1.06	<0.001	0.011
ENSRNOG00000016980	Qprt	2.54	<0.001	0.014
ENSRNOG00000017020	Inpp5d	1.13	<0.001	0.004
ENSRNOG00000017120	Abhd2	1.73	0.003	0.038
ENSRNOG00000017259	Tacc3	1.22	0.002	0.032
ENSRNOG00000017445	Tubb2b	1.18	<0.001	0.016
ENSRNOG00000017477	Mmp23	1.07	<0.001	0.018
ENSRNOG00000017786	Acta1	1.05	<0.001	0.006
ENSRNOG00000017869	Irf8	1.23	<0.001	0.004
ENSRNOG00000017874	Cd53	1.09	0.001	0.025
ENSRNOG00000018092	Cd83	1.13	0.001	0.024

ENSRNOG00000018251	Mrc1	1.35	<0.001	0.001
ENSRNOG00000018285	Kcna2	-1.13	0.002	0.028
ENSRNOG00000018371	Tubb6	1.89	<0.001	<0.001
ENSRNOG00000018414	Csf1r	1.19	<0.001	0.018
ENSRNOG00000018484	Plk3	1.38	0.001	0.022
ENSRNOG00000018646	Hbegf	1.12	0.003	0.042
ENSRNOG00000018669	Jak3	1.01	<0.001	0.011
ENSRNOG00000018681	Nes	1.02	0.002	0.036
ENSRNOG00000018690	Rgs17	-1.64	0.002	0.037
ENSRNOG00000018715	Clec10a	1.35	<0.001	<0.001
ENSRNOG00000018778	Cadm1	1.15	0.003	0.042
ENSRNOG00000019161	Cpeb1	1.66	<0.001	0.016
ENSRNOG00000019211	Olfml3	1.31	<0.001	<0.001
ENSRNOG00000019270	P2ry6	1.12	0.002	0.036
ENSRNOG00000019365	Ablim3	-1.17	<0.001	0.019
ENSRNOG00000019387	Ifi30	1.07	<0.001	0.001
ENSRNOG00000019422	Egr1	2.12	<0.001	<0.001
ENSRNOG00000019430	Coro1a	1.22	<0.001	<0.001
ENSRNOG00000019440	Kcnn4	1.65	<0.001	0.004
ENSRNOG00000019587	Ptprn	2.40	<0.001	0.008
ENSRNOG00000019648	Col6a3	1.35	<0.001	0.004
ENSRNOG00000019680	Mst1	-1.67	<0.001	0.008
ENSRNOG00000019780	Sypl2	1.82	<0.001	0.018
ENSRNOG00000019854	Napsa	1.55	<0.001	0.011
ENSRNOG00000019890	Folr2	1.14	<0.001	0.004
ENSRNOG00000020030	Crlf1	1.73	<0.001	<0.001
ENSRNOG00000020251	Art1	-1.29	<0.001	0.004
ENSRNOG00000020300	Lsp1	1.73	<0.001	<0.001
ENSRNOG00000020465	Ripk3	1.27	0.002	0.030
ENSRNOG00000020587	Efemp2	1.01	<0.001	0.005
ENSRNOG00000020679	Icam1	1.56	<0.001	0.002

ENSRNOG00000020848	Coq8b	1.10	<0.001	0.005
ENSRNOG00000020867	Numbl	1.07	<0.001	0.006
ENSRNOG00000020991	Ms4a6a	1.36	0.002	0.029
ENSRNOG00000021027	Dbp	1.64	<0.001	0.004
ENSRNOG00000021062	Fxyd5	1.19	<0.001	0.004
ENSRNOG00000021084	-	2.06	0.001	0.026
ENSRNOG00000021104	Emp3	1.13	<0.001	0.005
ENSRNOG00000021155	Ctsk	1.20	<0.001	0.002
ENSRNOG00000021199	Fcgr1a	1.76	<0.001	0.004
ENSRNOG00000021243	Siglec1	1.41	0.001	0.024
ENSRNOG00000021445	Tas2r120	-1.77	0.002	0.028
ENSRNOG00000021560	Cass4	1.18	0.003	0.042
ENSRNOG00000021663	Vxn	1.67	<0.001	0.020
ENSRNOG00000022012	Tnfrsf18	3.13	<0.001	0.016
ENSRNOG00000022256	Cxcl10	1.63	<0.001	0.012
ENSRNOG00000022268	Pnpla3	-1.19	<0.001	0.007
ENSRNOG00000022657	-	1.13	<0.001	0.013
ENSRNOG00000022975	Nfam1	1.29	0.001	0.022
ENSRNOG00000023209	Slamf7	1.17	0.001	0.025
ENSRNOG00000023628	Tmem106a	1.29	<0.001	0.016
ENSRNOG00000023799	Pak1ip1	1.25	<0.001	0.007
ENSRNOG00000024899	Cxcl13	1.31	0.003	0.046
ENSRNOG00000025001	Pcolce	1.14	<0.001	0.003
ENSRNOG00000025130	Ltk	2.62	0.003	0.044
ENSRNOG00000026306	Clec5a	3.16	<0.001	<0.001
ENSRNOG00000026548	Dhrs7c	-1.18	<0.001	0.005
ENSRNOG00000026604	Cercam	1.06	0.004	0.047
ENSRNOG00000026647	Cxcl16	1.04	<0.001	0.001
ENSRNOG00000027024	Rgs16	1.31	0.002	0.029
ENSRNOG00000027096	Ctsw	1.82	0.002	0.032
ENSRNOG00000027811	Lilrb4	2.00	<0.001	0.019

ENSRNOG00000027888	Cmss1	1.35	0.003	0.042
ENSRNOG00000028930	Dab2	1.02	<0.001	<0.001
ENSRNOG00000029145	-	-1.24	<0.001	<0.001
ENSRNOG00000029212	Vcan	1.63	<0.001	0.004
ENSRNOG00000029662	Wdfy4	1.05	0.002	0.029
ENSRNOG00000029682	Clic1	1.55	<0.001	0.008
ENSRNOG00000029784	Pak1	1.59	<0.001	0.006
ENSRNOG00000029911	Cilp	2.39	<0.001	0.003
ENSRNOG00000029980	Zbtb16	-1.87	<0.001	0.005
ENSRNOG00000030012	Clec4a2	2.79	0.003	0.041
ENSRNOG00000030330	-	-1.49	0.002	0.030
ENSRNOG00000030355	Mroh1	-1.04	<0.001	0.010
ENSRNOG00000030530	Gzmm	1.30	<0.001	0.019
ENSRNOG00000031163	Nfkbiz	1.23	0.002	0.036
ENSRNOG00000031312	Tnfrsf1a	1.01	<0.001	0.009
ENSRNOG00000031506	LOC120102993	1.05	<0.001	0.002
ENSRNOG00000031930	Cela1	1.39	<0.001	0.003
ENSRNOG00000031930	Bin2	1.39	<0.001	0.003
ENSRNOG00000032659	Plcl1	-1.73	0.001	0.025
ENSRNOG00000032708	RT1-Bb	1.23	<0.001	<0.001
ENSRNOG00000032844	RT1-Da	1.08	<0.001	0.012
ENSRNOG00000033215	RT1-Db1	1.03	<0.001	0.007
ENSRNOG00000033256	LOC691141	2.82	<0.001	0.019
ENSRNOG00000033433	Csrnp1	1.13	0.003	0.043
ENSRNOG00000033693	Naip6	1.25	0.004	0.050
ENSRNOG00000033932	-	-1.14	<0.001	0.021
ENSRNOG00000036711	Spn	1.08	<0.001	<0.001
ENSRNOG00000037298	C1h19orf81	-1.05	0.003	0.045
ENSRNOG00000037563	Cd68	1.69	<0.001	0.004
ENSRNOG00000038047	-	1.23	<0.001	0.003
ENSRNOG00000038881	Hcls1	1.20	<0.001	0.001

ENSRNOG00000039390	Slc37a2	1.15	<0.001	0.003
ENSRNOG00000039668	Col8a1	1.30	0.002	0.031
ENSRNOG00000039754	Rab7b	1.83	0.001	0.025
ENSRNOG00000040198	-	-1.13	0.003	0.042
ENSRNOG00000040287	Cyp1b1	1.95	<0.001	<0.001
ENSRNOG00000042018	RGD1306750	-1.21	0.002	0.031
ENSRNOG00000042139	Clec4a1	1.34	<0.001	0.004
ENSRNOG00000042455	Tlr12	3.00	<0.001	0.004
ENSRNOG00000042717	Ciart	3.17	<0.001	0.016
ENSRNOG00000042785	Sesn2	1.84	<0.001	0.001
ENSRNOG00000042838	-	1.77	<0.001	0.002
ENSRNOG00000042897	Nmrk2	1.27	<0.001	0.005
ENSRNOG00000043098	Mt2A	2.79	<0.001	0.005
ENSRNOG00000043416	Bcl3	1.48	<0.001	0.019
ENSRNOG00000043451	Spp1	2.72	0.002	0.032
ENSRNOG00000045829	Thbs1	3.17	<0.001	0.005
ENSRNOG00000046254	Adgre1	1.05	<0.001	0.006
ENSRNOG00000046313	-	1.30	<0.001	0.002
ENSRNOG00000046452	Fcgr2b	2.18	0.001	0.027
ENSRNOG00000046699	Slpi	2.39	<0.001	<0.001
ENSRNOG00000047143	Fkbp1b	3.08	0.002	0.036
ENSRNOG00000047606	Bcl2a1	1.57	<0.001	0.003
ENSRNOG00000047800	-	1.06	0.001	0.021
ENSRNOG00000048053	Slfn1	1.55	0.002	0.034
ENSRNOG00000048114	Echdc3	-1.11	0.003	0.038
ENSRNOG00000048831	-	1.34	0.002	0.033
ENSRNOG00000048924	Islr	1.27	<0.001	0.019
ENSRNOG00000049828	Crlf2	1.12	<0.001	0.013
ENSRNOG00000050251	-	2.20	<0.001	<0.001
ENSRNOG00000050624	Lysmd4	-1.32	0.004	0.048
ENSRNOG00000050647	Hspa1a	1.49	0.003	0.044

ENSRNOG00000050697	Ctsz	1.44	<0.001	0.002
ENSRNOG00000050792	Tnfaip6	3.48	<0.001	0.002
ENSRNOG00000050819	Birc5	1.49	0.003	0.04
ENSRNOG00000050869	Cebpd	1.27	<0.001	0.006
ENSRNOG00000051470	Card9	-1.49	<0.001	0.002
ENSRNOG00000051690	Clec9a	1.26	<0.001	0.014
ENSRNOG00000052017	Dio3	4.43	<0.001	0.003
ENSRNOG00000052064	Parvg	2.70	0.002	0.029
ENSRNOG00000052070	Aldh1a3	1.82	<0.001	0.007
ENSRNOG00000052150	-	3.94	<0.001	0.002
ENSRNOG00000052219	Gm2a	1.08	<0.001	0.002
ENSRNOG00000052389	-	-1.14	<0.001	0.010
ENSRNOG00000053272	Chi3l1	2.04	<0.001	<0.001
ENSRNOG00000054212	Pde1a	1.10	<0.001	0.006
ENSRNOG00000054251	Clec7a	1.78	<0.001	0.008
ENSRNOG00000054461	-	1.18	0.003	0.044
ENSRNOG00000054622	-	1.53	0.004	0.050
ENSRNOG00000054957	Sfrp4	3.21	<0.001	0.011
ENSRNOG00000055411	-	1.05	0.002	0.034
ENSRNOG00000055650	Pou2f2	1.13	<0.001	0.016
ENSRNOG00000055962	Bgn	1.62	<0.001	0.002
ENSRNOG00000056219	Olr1	3.78	0.001	0.024
ENSRNOG00000056756	Actn1	1.09	<0.001	0.003
ENSRNOG00000057092	-	1.33	<0.001	0.003
ENSRNOG00000057501	Fam81a	-2.03	<0.001	0.002
ENSRNOG00000057855	F5	2.14	0.002	0.033
ENSRNOG00000058003	Spon1	1.41	<0.001	0.007
ENSRNOG00000058186	Errfi1	1.38	0.001	0.026
ENSRNOG00000058388	Zfp36	1.19	<0.001	0.017
ENSRNOG00000058545	Arhgap4	1.31	<0.001	0.021
ENSRNOG00000058645	Tnc	4.64	0.001	0.022

ENSRNOG00000059857	Rnd1	2.23	<0.001	0.005
ENSRNOG00000059947	Sdc1	2.64	<0.001	0.003
ENSRNOG00000060057	-	-1.46	<0.001	0.001
ENSRNOG00000061379	-	1.50	0.001	0.021
ENSRNOG00000061850	-	-1.09	<0.001	0.013
ENSRNOG00000062252	-	1.30	<0.001	<0.001

Study A: Supplemental Table 2. Gene set enrichment analysis: Gene Ontology top activated and suppressed biological processes in rat heart with 40 mg/kg BW/d 2-MCPD exposure.

A) Top Activated Processes			
ID	Description	Enrichment Score	FDR
GO:0006954	inflammatory response	0.545	3.63E-29
GO:0001819	positive regulation of cytokine production	0.562	5.71E-22
GO:0002252	immune effector process	0.529	6.53E-21
GO:0046649	lymphocyte activation	0.481	2.29E-19
GO:0050900	leukocyte migration	0.578	9.00E-19
GO:0040017	positive regulation of locomotion	0.488	2.75E-17
GO:0050865	regulation of cell activation	0.493	2.77E-17
GO:2000147	positive regulation of cell motility	0.488	4.19E-17
GO:0009617	response to bacterium	0.476	4.34E-17
GO:0050778	positive regulation of immune response	0.488	5.13E-17
GO:0002443	leukocyte mediated immunity	0.559	1.65E-16
GO:0030335	positive regulation of cell migration	0.485	2.11E-16
GO:0002253	activation of immune response	0.519	3.09E-16
GO:0002694	regulation of leukocyte activation	0.492	6.05E-16
GO:0060326	cell chemotaxis	0.581	7.90E-16
GO:0042330	taxis	0.538	2.11E-15
GO:0002250	adaptive immune response	0.543	4.76E-15
GO:0006935	chemotaxis	0.537	4.79E-15
GO:0042110	T cell activation	0.496	5.14E-15
GO:0002683	negative regulation of immune system process	0.506	6.76E-15
GO:0002263	cell activation involved in immune response	0.578	1.10E-14
GO:0002757	immune response-activating signaling pathway	0.521	1.29E-14
GO:0045785	positive regulation of cell adhesion	0.498	1.53E-14
GO:0002521	leukocyte differentiation	0.474	1.81E-14
GO:0002764	immune response-regulating signaling pathway	0.518	1.81E-14

B) Top Suppressed Processes			
ID	Description	Enrichment Score	FDR
GO:0006091	generation of precursor metabolites and energy	-0.554	1.43E-29
GO:0015980	energy derivation by oxidation of organic compounds	-0.598	9.80E-28
GO:0045333	cellular respiration	-0.632	4.66E-25
GO:0009060	aerobic respiration	-0.665	8.32E-24
GO:0006119	oxidative phosphorylation	-0.701	1.64E-20
GO:0022904	respiratory electron transport chain	-0.728	2.29E-19
GO:0022900	electron transport chain	-0.675	4.19E-17
GO:0042773	ATP synthesis coupled electron transport	-0.749	4.34E-17
GO:0042775	mitochondrial ATP synthesis coupled electron transport	-0.746	3.93E-16
GO:0033108	mitochondrial respiratory chain complex assembly	-0.701	1.35E-15
GO:0019646	aerobic electron transport chain	-0.762	3.87E-15
GO:0010257	NADH dehydrogenase complex assembly	-0.738	3.86E-12
GO:0032981	mitochondrial respiratory chain complex I assembly	-0.738	3.86E-12
GO:0060047	heart contraction	-0.524	3.86E-12
GO:0008016	regulation of heart contraction	-0.552	2.08E-11
GO:0060048	cardiac muscle contraction	-0.576	1.74E-10
GO:0016054	organic acid catabolic process	-0.511	1.84E-10
GO:0046395	carboxylic acid catabolic process	-0.511	1.84E-10
GO:0006941	striated muscle contraction	-0.536	1.95E-10
GO:0044282	small molecule catabolic process	-0.458	3.74E-10
GO:0003015	heart process	-0.485	1.20E-09
GO:1902600	proton transmembrane transport	-0.607	1.53E-09
GO:0007005	mitochondrion organization	-0.364	7.83E-09
GO:0032787	monocarboxylic acid metabolic process	-0.358	2.01E-08
GO:0061337	cardiac conduction	-0.673	2.46E-08

Study A: Supplemental Table 3. Gene set enrichment analysis: Gene Ontology fibroblast related biological processes in rat heart with 40 mg/kg BW/d 2-MCPD exposure.

ID	Description	Enrichment score	FDR
GO:0010762	regulation of fibroblast migration	0.571	0.004
GO:0010761	fibroblast migration	0.484	0.014
GO:0048146	positive regulation of fibroblast proliferation	0.483	0.021
GO:0044344	cellular response to fibroblast growth factor stimulus	0.435	0.022
GO:0071774	response to fibroblast growth factor	0.430	0.024
GO:0010764	negative regulation of fibroblast migration	0.762	0.028
GO:0048144	fibroblast proliferation	0.396	0.029

Study A: Supplemental Table 4. Rat heart oxidative stress qPCR panel.

Gene	LFC	*P* value	FDR
18S	0.042	0.723	0.812
Aass	0.795	0.137	0.268
Actb	1.22	<0.001	0.002
Als2	-0.096	0.721	0.812
Apc	0.049	0.472	0.600
Apoe	1.03	<0.001	0.007
Aqr	0.322	0.010	0.044
Atr	0.625	0.002	0.014
B2m	0.357	0.036	0.118
Cat	-0.040	0.985	0.985
Ccs	0.216	0.090	0.217
Ctsb	0.670	0.001	0.011
Cygb	0.735	<0.001	0.004
Dhcr24	0.054	0.547	0.673
Dnm2	0.175	0.160	0.277
Duox1	0.066	0.475	0.600
Duox2	0.699	0.037	0.118
Ehd2	0.007	0.280	0.417
Ercc2	0.186	0.093	0.217
Ercc6	0.289	0.038	0.118
Fancc	0.296	0.016	0.065
Fmo2	-0.423	0.128	0.264
Gab1	0.103	0.072	0.198
Gapdh	-0.093	0.697	0.809
Gpx1	0.115	0.313	0.439
Gpx2	1.26	0.049	0.149
Gpx3	0.628	0.124	0.262
Gpx4	0.097	0.148	0.275

Gpx7	0.831	<0.001	0.005
Gpx8	0.814	<0.001	0.009
Gsr	0.452	0.004	0.022
Gstk1	-0.262	0.086	0.217
Gusb	0.768	0.004	0.023
Hbb;Hba1	-0.382	0.146	0.275
Hmbs	-0.012	0.823	0.881
Hprt1	0.047	0.372	0.498
Idh1	0.438	0.003	0.020
Ift172	0.061	0.341	0.463
Kif9	0.487	0.083	0.217
Mb	-0.297	0.138	0.268
Mpo	-0.716	0.643	0.76
Mpp4	-0.051	0.979	0.985
Mss51	0.319	0.151	0.275
Ncf1	-0.247	0.154	0.275
Ncf2	2.07	0.002	0.014
Ngb	1.06	0.139	0.268
Nos2	0.951	0.029	0.101
Nox4	0.574	<0.001	0.009
Noxo1	1.26	0.112	0.254
Nqo1	0.304	0.023	0.083
Nudt1	0.244	0.117	0.260
Nudt15	0.808	0.053	0.156
Nxn	0.136	0.302	0.436
Park7	-0.071	0.752	0.835
Pgk1	-0.048	0.967	0.985
Ppp1r15b	0.524	0.002	0.014
Prdx1	0.143	0.426	0.562
Prdx2	0.082	0.199	0.318
Prdx3	-0.157	0.319	0.440

Prdx4	0.764	<0.001	0.004
Prdx5	-0.085	0.784	0.859
Prdx6	0.027	0.508	0.634
Prnp	0.274	0.021	0.083
Psmb5	-0.121	0.445	0.578
Ptgs1	0.581	0.005	0.024
Ptgs2	3.24	0.002	0.014
Rplp0	0.502	0.009	0.044
Rplp2	0.008	0.796	0.862
Scd1	-1.509	0.274	0.415
Slc38a1	0.023	0.585	0.701
Slc38a4	-0.296	0.314	0.439
Slc38a5	0.016	0.864	0.900
Slc41a3	-0.287	0.175	0.289
Sod1	-0.068	0.870	0.900
Sod2	-0.011	0.702	0.809
Sod3	-0.243	0.289	0.424
Srxn1	1.88	<0.001	0.002
Tbp	0.204	0.180	0.292
Tfrc	0.314	0.084	0.217
Tmod1	-0.174	0.217	0.341
Txnip	-0.395	0.164	0.277
Txnrd1	1.02	0.002	0.014
Txnrd2	-0.165	0.577	0.700
Ubc	0.209	0.023	0.083
Ucp3	-0.412	0.057	0.161
Vim	0.662	0.011	0.049
Xpa	-0.006	0.834	0.883

Study A: Supplemental Table 5. Identified rat heart proteins expression.

Protein	Symbol	LFC	*P* value	FDR
14-3-3 protein epsilon	1433E	0.759	<0.001	0.008
2,4-dienoyl-CoA reductase, mitochondrial	DECR	-0.496	0.036	0.179
26 s protease regulatory subunit 4	PRS4	-0.838	<0.001	0.011
26S protease regulatory subunit 7	PRS7	-0.351	0.160	0.380
2-oxoisovalerate dehydrogenase subunit alpha, mitochondrial	ODBA	-0.621	0.005	0.061
3-hydroxyisobutyrate dehydrogenase, mitochondrial	3HIDH	-0.361	0.022	0.142
3-ketoacyl-CoA thiolase, mitochondrial	THIM	1.31	<0.001	0.022
78 kDa glucose-regulated protein	GRP78	-0.554	0.040	0.184
		-0.469	0.002	0.036
		-0.228	0.379	0.604
Acetyl-CoA acetyltransferase, mitochondrial	THIL	-1.09	<0.001	<0.001
		-0.253	0.230	0.454
		1.66	<0.001	0.008
		1.69	0.001	0.028
Actin aortic smooth muscle	ACTA	-0.706	0.017	0.119
		-0.576	0.008	0.073
		-0.517	0.005	0.061
		-0.500	0.082	0.265
		-0.459	0.055	0.217
		-0.175	0.372	0.599
Actin, alpha cardiac muscle 1	ACTC	0.34	0.572	0.748
Acyl-CoA synthetase family member 2, mitochondrial	ACSF2	0.731	<0.001	0.023
Aldehyde dehydrogenase, mitochondrial	ALDH2	-0.427	0.077	0.259
		-0.427	0.077	0.259
		-0.308	0.295	0.528

		-0.308	0.295	0.528
Alpha-2-HS-glycoprotein	FETUA	-0.403	0.016	0.116
		-0.382	0.027	0.154
		-0.338	0.072	0.250
Alpha-actinin-1	ACTN1	-1.07	0.005	0.060
Alpha-enolase	ENOA	1.18	<0.001	<0.001
Annexin A1	ANXA1	-0.645	0.015	0.113
Annexin A4	ANXA4	-0.423	0.006	0.062
Annexin A5	ANXA5	-0.339	0.055	0.217
Aspartate aminotransferase, cytoplasmic	AATC	-0.619	0.016	0.115
ATP synthase subunit alpha, mitochondrial	ATPA	-0.692	0.043	0.190
		-0.647	0.025	0.151
		0.089	0.837	0.914
		0.539	0.003	0.043
		1.06	<0.001	0.020
ATP synthase subunit beta, mitochondrial	ATPB	0.797	0.001	0.025
ATP synthase subunit gamma, mitochondrial	ATPG	-0.448	0.21	0.431
		-0.448	0.21	0.431
		-0.249	0.117	0.318
		-0.249	0.117	0.318
Beta-enolase	ENOB	0.968	<0.001	<0.001
cAMP-dependent protein kinase type I-alpha regulatory subunit	KAP0	-0.253	0.141	0.350
Catalase	CATA	0.846	<0.001	0.020
Ceruloplasmin	CERU	-0.488	0.133	0.342
Coiled-coil domain-containing protein 22	CCD22	-0.632	0.009	0.080
Complement C3	CO3	-0.300	0.413	0.635
		-0.282	0.137	0.345
Coronin-1A	COR1A	-1.01	<0.001	<0.001
Cytoglobin	CYGB	-0.507	0.039	0.183
Cytoplasmic aconitate hydratase	ACOC	-0.705	0.023	0.144

Cytosol aminopeptidase	AMPL	-0.388	0.040	0.184
Cytosolic non-specific dipeptidase	CNDP2	-0.329	0.046	0.196
Delta(3,5)-Delta(2,4)-dienoyl-CoA isomerase, mitochondrial	ECH1	-0.969	0.005	0.059
Desmin	DESM	-0.361	0.331	0.561
Dihydrolipoyl dehydrogenase, mitochondrial	DLDH	-1.40	<0.001	<0.001
Dihydrolipoyllysine-residue acetyltransferase component of pyruvate dehydrogenase complex, mitochondrial	ODP2	-1.02	<0.001	0.009
		-0.360	0.015	0.113
		-0.290	0.244	0.474
		1.24	<0.001	<0.001
EH domain-containing protein 1	EHD1	-0.298	0.069	0.243
Electron transfer flavoprotein subunit beta	ETFB	0.122	0.624	0.780
		0.635	<0.001	0.021
Endoplasmic reticulum resident protein 29	ERP29	-0.447	0.007	0.073
Endoplasmin	ENPL	-0.51	0.007	0.073
Enoyl-CoA delta isomerase 1, mitochondrial	ECI1	-0.667	0.010	0.087
Ethanolamine-phosphate cytidylyltransferase	PCY2	0.653	<0.001	0.014
Eukaryotic initiation factor 4A-II	IF4A2	-0.881	0.019	0.130
Eukaryotic translation initiation factor 2 subunit 1	IF2A	-0.344	0.075	0.257
Eukaryotic translation initiation factor 3 subunit I	EIF3I	-0.371	0.152	0.370
Evolutionarily conserved signaling intermediate in Toll pathway, mitochondrial	ECSIT	0.677	<0.001	0.012
F-actin-capping protein subunit beta	CAPZB	-0.425	0.012	0.095
Ferritin light chain 1	FRIL1	-0.572	<0.001	0.019
		-0.572	<0.001	0.019
Four and a half LIM domains protein 2	FHL2	0.883	<0.001	0.003
Fructose-bisphosphate aldolase A	ALDOA	-0.589	0.162	0.381
Fumarate hydratase, mitochondrial	FUMH	0.495	0.004	0.047
Gelsolin	GELS	-0.694	0.009	0.079
		-0.525	0.015	0.113
		-0.383	0.067	0.239

Glutamate receptor 3	GRIA3	-0.927	<0.001	0.020
Glutathione peroxidase 1	GPX1	0.486	0.212	0.432
Glycerin-3-phosphate dehydrogenase [NAD+], cytoplasmic	GPDA	0.665	0.141	0.350
Glycogen phosphorylase, muscle form	PYGM	-0.219	0.231	0.456
GrpE protein homolog 1, mitochondrial	GRPE1	-0.398	0.041	0.184
Guanine deaminase	GUAD	-0.832	<0.001	0.002
		-0.638	0.047	0.197
Guanine nucleotide-binding protein subunit beta-2-like 1	GBLP	-0.609	0.003	0.041
Haptoglobin	HPT	-0.509	0.067	0.239
		-0.377	0.175	0.396
Heat shock 70 kDa protein 4	HSP74	-0.459	0.011	0.093
		-0.293	0.150	0.368
Heat shock protein beta-1	HSPB1	-0.424	<0.001	0.020
Heat shock protein HSP 90-beta	HS90B	-0.543	0.025	0.150
		-0.459	0.033	0.169
		-0.239	0.122	0.324
Hemopexin	HEMO	-0.521	0.010	0.085
		-0.442	0.029	0.161
Heterogeneous nuclear ribonucleoprotein F	HNRPF	-0.581	0.004	0.053
Hydroxyacyl-coenzyme A dehydrogenase, mitochondrial	HCDH	0.498	0.003	0.043
Kinesin heavy chain isoform 5A	KIF5A	0.507	0.008	0.073
Lamin-B1	LMNB1	-0.508	0.015	0.113
		-0.467	0.008	0.079
L-lactate dehydrogenase B chain	LDHB	-0.628	0.057	0.220
		-0.427	0.130	0.337
Macrophage-capping protein	CAPG	-0.759	<0.001	0.006
Malate dehydrogenase, mitochondrial	MDHM	0.156	0.437	0.650
		0.533	0.041	0.186

Methylmalonate-semialdehyde dehydrogenase [acylating], mitochondrial	MMSA	-0.453	0.015	0.113
		0.501	0.005	0.061
		0.931	<0.001	0.022
Mitochondrial inner membrane protein (Fragment)	MIC60	-0.387	0.099	0.290
Mu-crystallin homolog	CRYM	-0.732	<0.001	0.003
Murinoglobulin-1	MUG1	-0.416	0.076	0.258
Myosin light chain 3	MYL3	-0.162	0.379	0.604
		0.404	0.058	0.221
Myosin regulatory light chain 2, ventricular/cardiac muscle isoform	MLRV	1.10	0.016	0.115
Myosin-6	MYH6	-0.793	0.025	0.150
		-0.714	0.029	0.161
		-0.686	0.003	0.044
		-0.649	0.095	0.282
		-0.634	0.073	0.252
		-0.591	0.031	0.165
		-0.520	0.036	0.177
		0.366	0.268	0.502
Myosin-7	MYH7	-0.789	0.013	0.103
Myosin-binding protein C, cardiac-type	MYPC	-2.09	<0.001	<0.001
		-0.690	0.008	0.074
		-0.651	0.036	0.178
		-0.432	0.038	0.181
N(G),N(G)-dimethylarginine dimethylaminohydrolase 2	DDAH2	-0.358	0.029	0.161
Nck-associated protein 1	NCKP1	-1.35	<0.001	<0.001
Plasminogen	PLMN	-0.555	0.011	0.093
		-0.410	0.044	0.193
		-0.369	0.093	0.279
Pre-mRNA-processing factor 19	PRP19	-0.122	0.299	0.533

Protein disulfide-isomerase A3	PDIA3	-0.613	0.009	0.079
		-0.563	0.001	0.026
		-0.449	0.001	0.024
		-0.241	0.449	0.659
Protein DJ-1	PARK7	1.27	<0.001	<0.001
Purine nucleoside phosphorylase	PNPH	-0.502	0.001	0.028
Pyruvate carboxylase, mitochondrial	PYC	0.521	0.057	0.221
Pyruvate dehydrogenase E1 component subunit alpha, somatic form, mitochondrial	ODPA	0.447	0.206	0.430
		0.718	0.046	0.196
		0.757	0.004	0.050
Pyruvate kinase isozymes M1/M2	PKM1/M2	-0.266	0.229	0.454
Sarcolemmal membrane-associated protein	SLMAP	-0.390	0.024	0.150
Sarcosine dehydrogenase, mitochondrial	SARDH	-0.312	0.032	0.166
Septin-8	SEPT8	-0.445	0.076	0.258
Serine protease inhibitor A3N	SPA3N	-0.484	0.002	0.034
		-0.456	0.002	0.030
Serine/threonine-protein phosphatase 2A 55 kDa regulatory subunit B alpha isoform	2ABA	-0.438	0.065	0.235
Serine--pyruvate aminotransferase, mitochondrial	SPYA	0.136	0.575	0.748
Transferrin	TRFE	-0.714	0.005	0.058
		-0.454	0.014	0.109
		-0.349	0.389	0.613
		0.364	0.165	0.381
Serum albumin	ALBU	-1.51	<0.001	0.002
		-1.21	<0.001	0.022
		-0.851	<0.001	0.008
		-0.828	<0.001	0.010
		-0.819	0.002	0.035
		-0.695	<0.001	0.022
		-0.636	0.011	0.093
		-0.627	0.001	0.026

		-0.565	<0.001	0.020
		-0.525	0.190	0.411
		-0.446	0.040	0.184
		-0.421	0.163	0.381
		0.024	0.902	0.949
		0.296	0.289	0.523
		0.900	<0.001	0.007
Succinyl-CoA:3-ketoacid coenzyme A transferase 1, mitochondrial	SCOT1	-0.717	0.044	0.192
		-0.585	<0.001	0.011
		-0.353	0.046	0.197
		-0.321	0.047	0.198
Thioredoxin reductase 2, mitochondrial	TRXR2	-0.767	0.003	0.037
		-0.751	0.007	0.071
Trifunctional enzyme subunit alpha, mitochondrial	ECHA	0.400	0.243	0.474
		0.631	0.014	0.108
		0.657	<0.001	0.014
Tripartite motif-containing protein 72	TRI72	-0.516	0.003	0.044
Tubulin alpha-1A chain	TBA1A	-0.963	<0.001	0.016
		-0.963	<0.001	0.016
Ubiquitin-like modifier-activating enzyme 1	UBA1	-1.24	0.001	0.028
Vimentin	VIME	-1.00	<0.001	0.020
		-0.809	0.002	0.031
		-0.807	0.025	0.150
Vinculin	VINC	-0.992	<0.001	0.008
		0.73	0.021	0.138
Vitamin D-binding protein	VTDB	-0.458	0.033	0.168
Voltage-dependent anion-selective channel protein 1	VDAC1	-0.038	0.877	0.934
Voltage-dependent anion-selective channel protein 2	VDAC2	-1.15	<0.001	0.003
		0.431	0.031	0.165

Study A: Supplemental Table 6. Oxylipin metabolism related genes.

ENSEMBL	Gene	LFC	*P* value	FDR
ENSRNOG00000027037	Alox12	0.186	0.853	0.944
ENSRNOG00000019183	Alox15	0.210	0.636	0.848
ENSRNOG00000012972	Alox5	-0.193	0.526	0.785
ENSRNOG00000049911	Cbr1	-0.062	0.815	0.928
ENSRNOG00000049911	Cbr1l2	-0.062	0.815	0.928
ENSRNOG00000001701	Cbr3	0.466	0.053	0.240
ENSRNOG00000040287	Cyp1b1	1.95	<0.001	<0.001
ENSRNOG00000012458	Cyp2e1	-1.77	<0.001	0.002
ENSRNOG00000031004	Cyp2j3	0.183	0.725	0.890
ENSRNOG00000011053	Cyp2u1	-0.147	0.545	0.795
ENSRNOG00000055078	Cyp4b1	-0.918	<0.001	0.010
ENSRNOG00000004786	Cyp4f1	-0.131	0.795	0.919
ENSRNOG00000043233	Cyp4f6	-0.154	0.431	0.724
ENSRNOG00000018239	Dhrs4	-0.419	0.005	0.057
ENSRNOG00000003515	Ephx1	0.044	0.857	0.946
ENSRNOG00000017286	Ephx2	-0.528	0.012	0.104
ENSRNOG00000062276	Ggt5	0.506	0.043	0.217
ENSRNOG00000048812	Gpx1	0.092	0.573	0.812
ENSRNOG00000052564	Gpx3	0.346	0.290	0.607
ENSRNOG00000009751	Gpx7	0.393	0.068	0.279
ENSRNOG00000010461	Gpx8	0.928	<0.001	<0.001
ENSRNOG00000019221	Gstm4	-0.117	0.636	0.848
ENSRNOG00000004494	Lta4h	0.006	0.983	0.992
ENSRNOG00000003244	Ltc4s	-0.961	0.014	0.111
ENSRNOG00000061857	Mgst2	-0.471	0.050	0.233
ENSRNOG00000004245	Mgst3	-0.561	0.085	0.317
ENSRNOG00000057470	Pla2g12a	-0.261	0.479	0.757
ENSRNOG00000016945	Pla2g2a	-0.759	0.019	0.135

ENSRNOG00000016826	Pla2g2d	0.760	0.006	0.068
ENSRNOG00000007447	Pla2g4b	-0.213	0.564	0.807
ENSRNOG00000016838	Pla2g5	-0.959	0.002	0.037
ENSRNOG00000012295	Pla2g6	-0.200	0.526	0.785
ENSRNOG00000015550	Ptgds	-0.213	0.460	0.745
ENSRNOG00000014050	Ptges2	-0.04	0.855	0.945
ENSRNOG00000002642	Ptges3	0.107	0.606	0.832
ENSRNOG00000060486	Ptges3l1	0.436	0.043	0.215
ENSRNOG00000008245	Ptgis	0.737	0.014	0.112
ENSRNOG00000007415	Ptgs1	0.496	0.043	0.217
ENSRNOG00000002525	Ptgs2	2.37	0.007	0.071
ENSRNOG00000007918	Tbxas1	0.761	0.040	0.208

Study A: Supplemental Table 7. Rat heart oxylipin expression with 40 mg/kg BW/d 2-MCPD exposure.

Oxylipins	Enz	LFC	*P* value	FDR
LA oxylipins				
9,10-EpOME	CYPe	-0.112	0.805	0.979
9,10-DiHOME	CYPe	-0.030	0.762	0.979
12,13-EpOME	CYPe	-0.176	0.755	0.979
12,13-DiHOME	CYPe	0.070	0.519	0.979
LA-CYPe total		-0.108	0.965	0.965
9-HODE	LOX	-0.368	0.952	0.979
13-HODE	LOX	-0.353	0.979	0.979
13-oxoODE	LOX	-0.290	0.589	0.979
(9,10,13- & 9,12,13-) triHOME	LOX	-0.402	0.421	0.979
LA-LOX total		-0.355	0.934	0.965
LA total		-0.353	0.935	0.935
GLA oxylipins				
13-HOTrE-γ	LOX	-0.036	0.891	0.979
DGLA oxylipins				
TXB1	COX	-0.216	0.669	0.979
15k-PGE1	COX	0.359	0.240	0.757
DGLA-COX total		-0.066	0.880	0.979
15-HETrE	LOX	-0.059	0.884	0.979

DGLA total		-0.059	0.884	0.979
AA oxylipins				
PGD2	COX	-0.189	0.965	0.979
15d-PGD2	COX	-0.341	0.958	0.979
PGE2	COX	-0.009	0.837	0.979
11b-PGE2	COX	0.198	0.730	0.979
15k-PGE2	COX	-0.036	0.939	0.979
6k-PGF1a	COX	0.624	0.748	0.979
12-HHTrE	COX	-0.266	0.023	0.203
TXB2	COX	-0.022	0.909	0.979
AA-COX total		0.115	0.611	0.965
16-HETE	CYPh	-0.219	0.172	0.757
20-COOH-AA	CYPh	0.780	0.568	0.979
AA-CYPh total		0.494	0.900	0.965
5,6-EpETrE	CYPe	-0.700	0.623	0.979
5,6-DiHETrE	CYPe	0.277	0.463	0.979
8,9-EpETrE	CYPe	0.330	0.009	0.181
8,9-DiHETrE	CYPe	0.268	0.245	0.757
11,12-EpETrE	CYPe	0.199	0.471	0.979
11,12-DiHETrE	CYPe	0.033	0.791	0.979
14,15-EpETrE	CYPe	-0.201	0.415	0.979
14,15-DiHETrE	CYPe	0.180	0.557	0.979
AA-CYPe		0.121	0.275	0.824
5-HETE	LOX	-0.539	0.158	0.757
5-oxoETE	LOX	-1.00	0.187	0.757
8-HETE	LOX	-0.420	0.302	0.800
9-HETE	LOX	-0.361	0.222	0.757

11-HETE	LOX	-0.759	0.257	0.757
12-HETE	LOX	-0.503	0.275	0.766
12-oxoETE	LOX	-0.142	0.693	0.979
15-HETE	LOX	-0.704	0.212	0.757
15-oxoETE	LOX	-0.591	0.237	0.757
LTB4	LOX	0.094	0.847	0.979
12-epi-LTB4	LOX	0.164	0.752	0.979
AA-LOX total		-0.510	0.227	0.824
AA total		-0.251	0.394	0.880
ALA oxylipins				
9,10-EpODE	CYPe	-0.378	0.171	0.757
9,10-DiHODE	CYPe	-0.367	0.933	0.979
12,13-EpODE	CYPe	-0.039	0.903	0.979
9-HOTrE	LOX	-0.499	0.698	0.979
9-oxoOTrE	LOX	-0.706	0.078	0.520
ALA-LOX total		-0.524	0.533	0.965
ALA total		-0.514	0.528	0.880
DHA oxylipins				
20-HDoHE	CYPh	-1.20	0.019	0.203
4-HDoHE	LOX	-2.19	<0.001	0.011
10-HDoHE	LOX	0.092	0.716	0.979
14-HDoHE	LOX	-0.909	0.014	0.181
16-HDoHE	LOX	-1.60	0.028	0.210
17-HDoHE	LOX	-0.806	0.013	0.181
DHA-LOX total		-0.581	0.006	0.054

DHA total	-0.715	0.002	0.009
n-6 total	-0.351	0.915	0.915
n-3 total	-0.627	0.012	0.023
COX total	0.109	0.620	0.909
CYPh total	-0.183	0.561	0.909
CYPe total	-0.065	0.875	0.909
LOX total	-0.358	0.909	0.909
Total	-0.352	0.910	-

Study A: Supplemental Table 8. Rat heart oxidized phosphatidylcholine expression with 40 mg/kg BW/d 2-MCPD exposure.

OxPC	LFC	*P* value	FDR
PGPC	-0.135	0.661	0.661
PONPC	-0.275	0.337	0.421
POVPC	-0.48	0.122	0.203

4. Study A: Supplemental Figures

Gene set enrichment analysis of 2-MCPD-exposed F344 rat heart mRNA using Kyoto Encyclopedia if Genes and Genomes (KEGG) pathways. Significantly enriched KEGG pathways. DEGs ($|LFC| > 0.5$ & $P < 0.05$) coloured green when downregulated and red when upregulated.

Immune Response

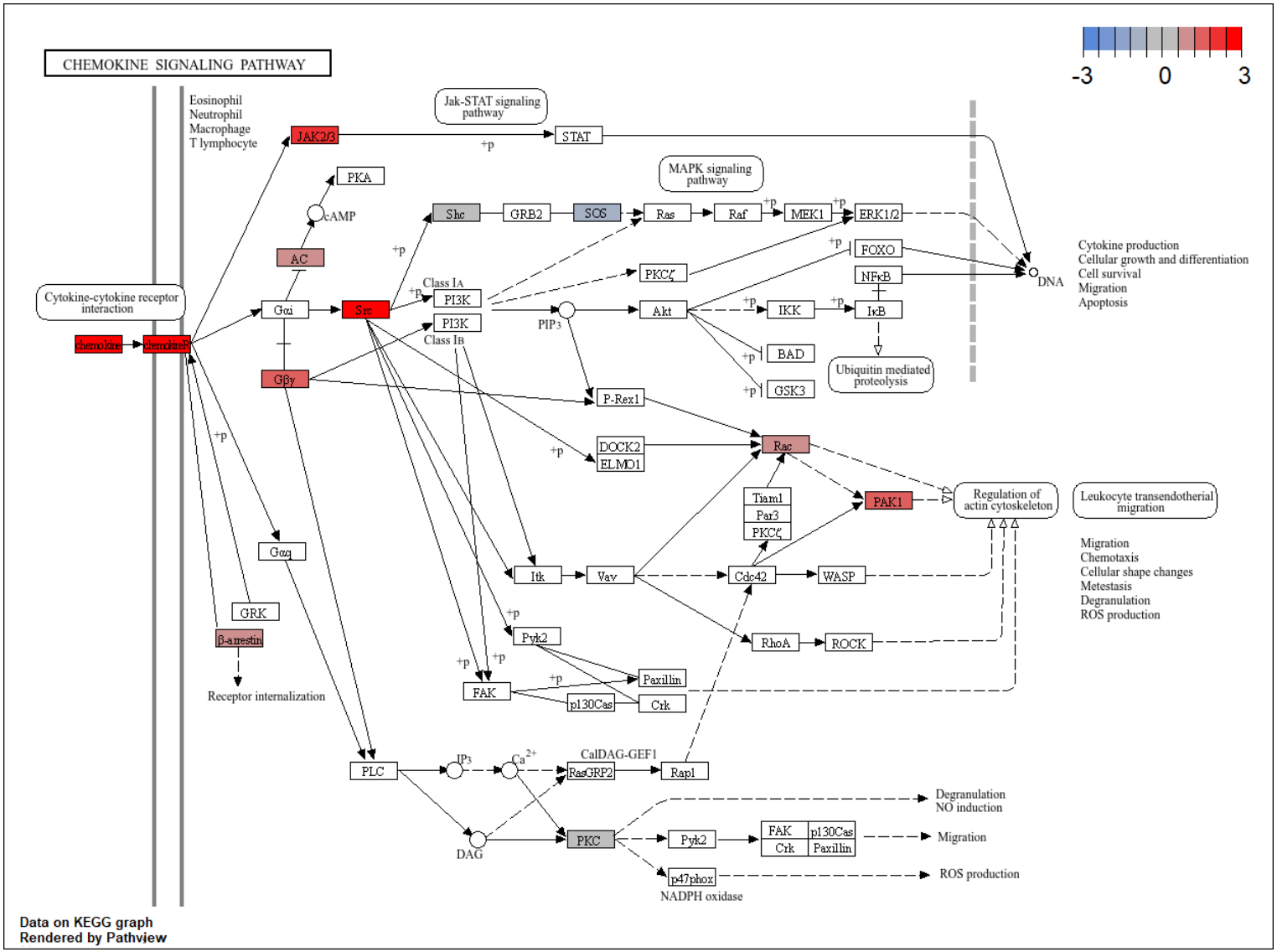

Study A: Supplemental Figure 1. rno04062 "Chemokine signalling pathway"

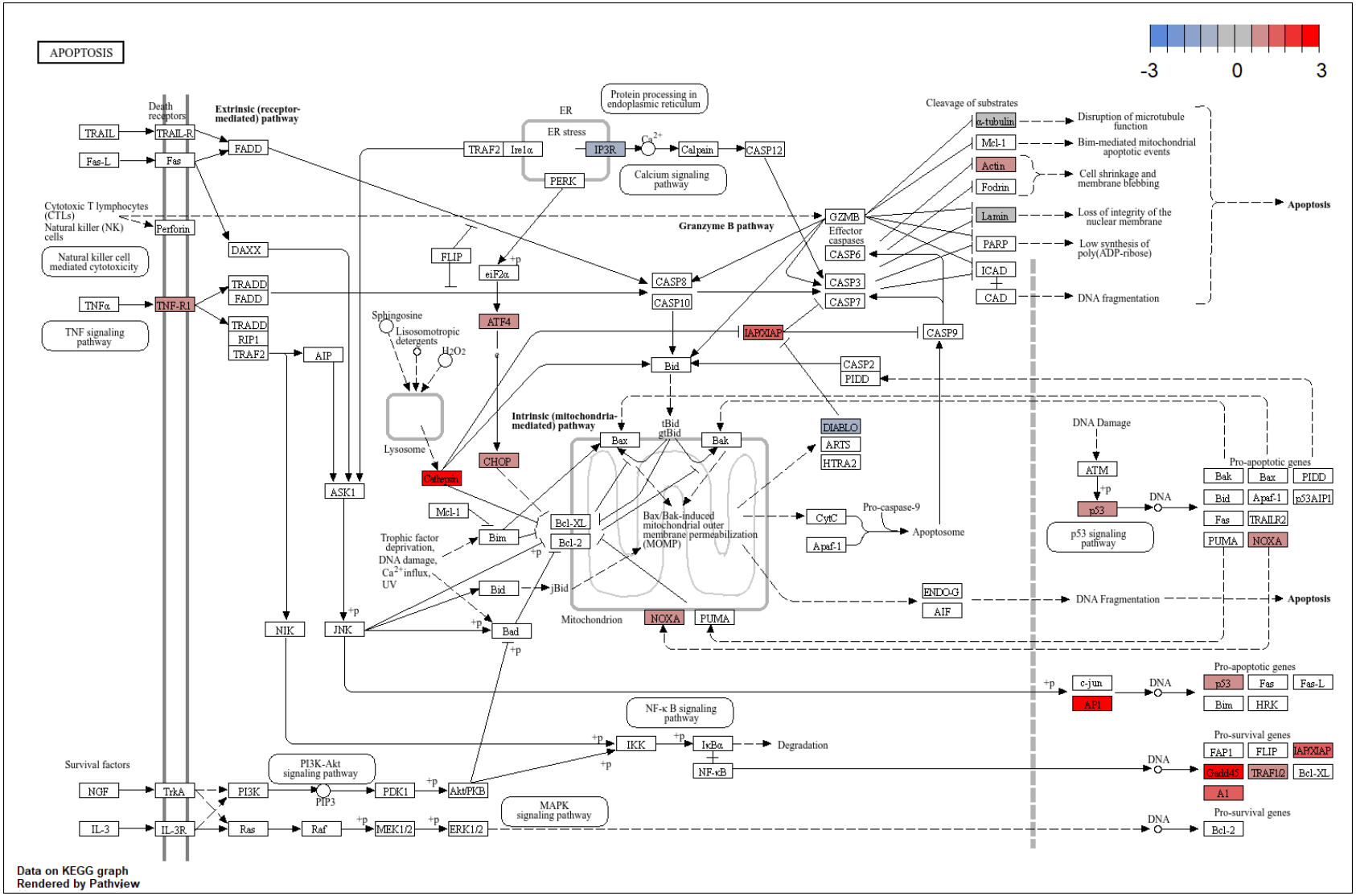

Study A: Supplemental Figure 2. rno04210 "Apoptosis"

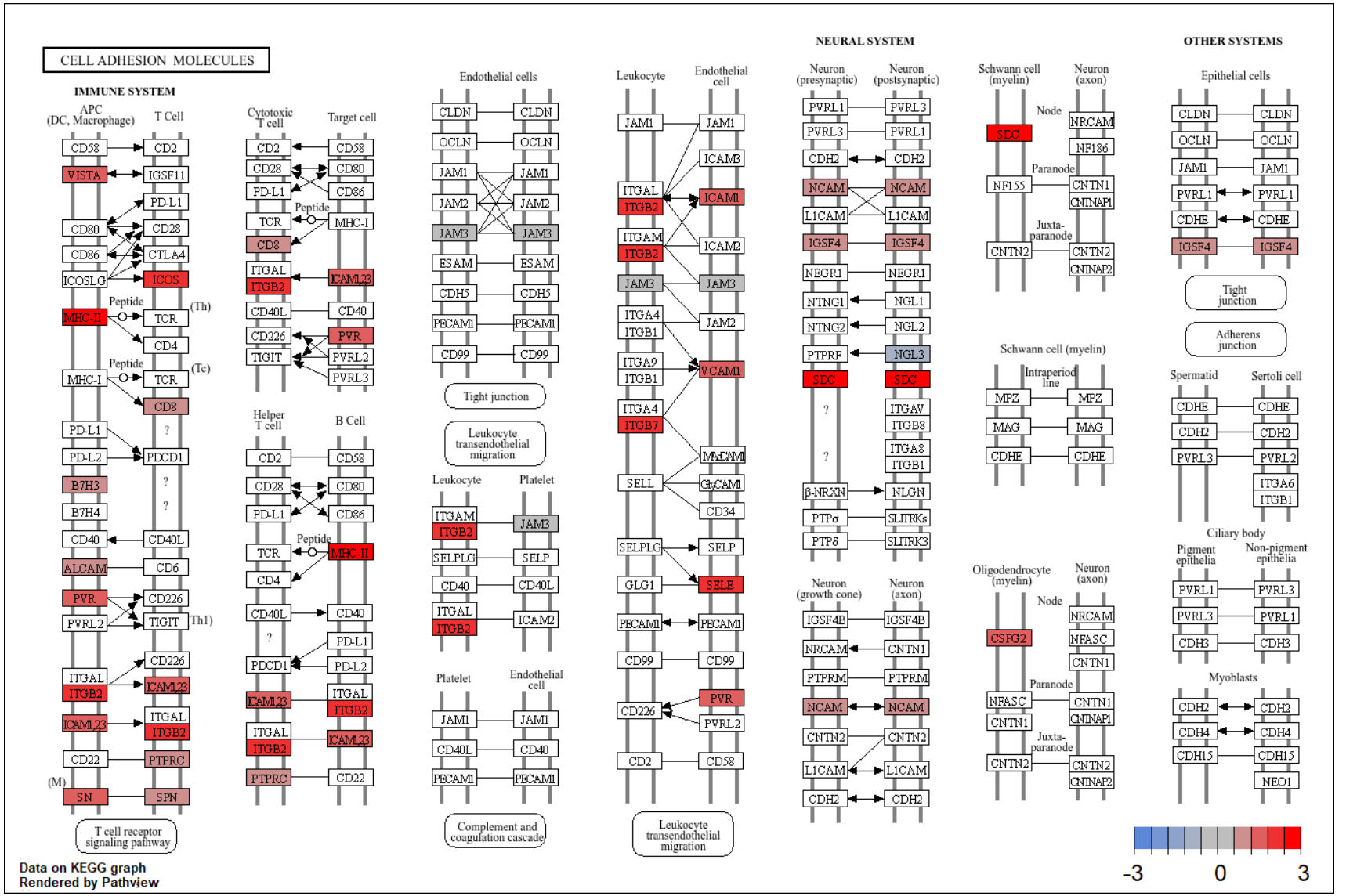

Study A: Supplemental Figure 3. rno04514 “Cell adhesion molecules”

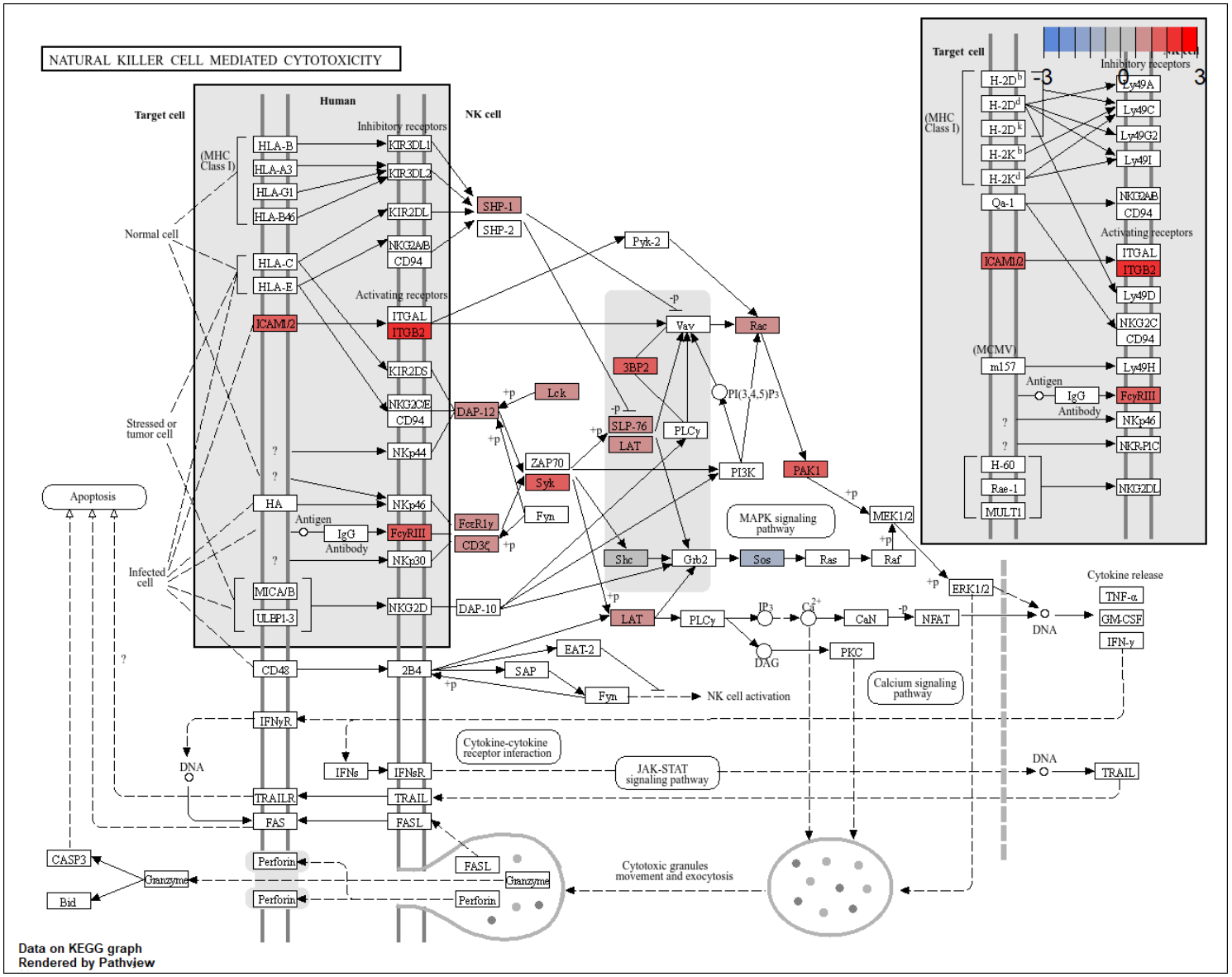

Study A: Supplemental Figure 4. rno04650 "Natural killer cell mediated cytotoxicity"

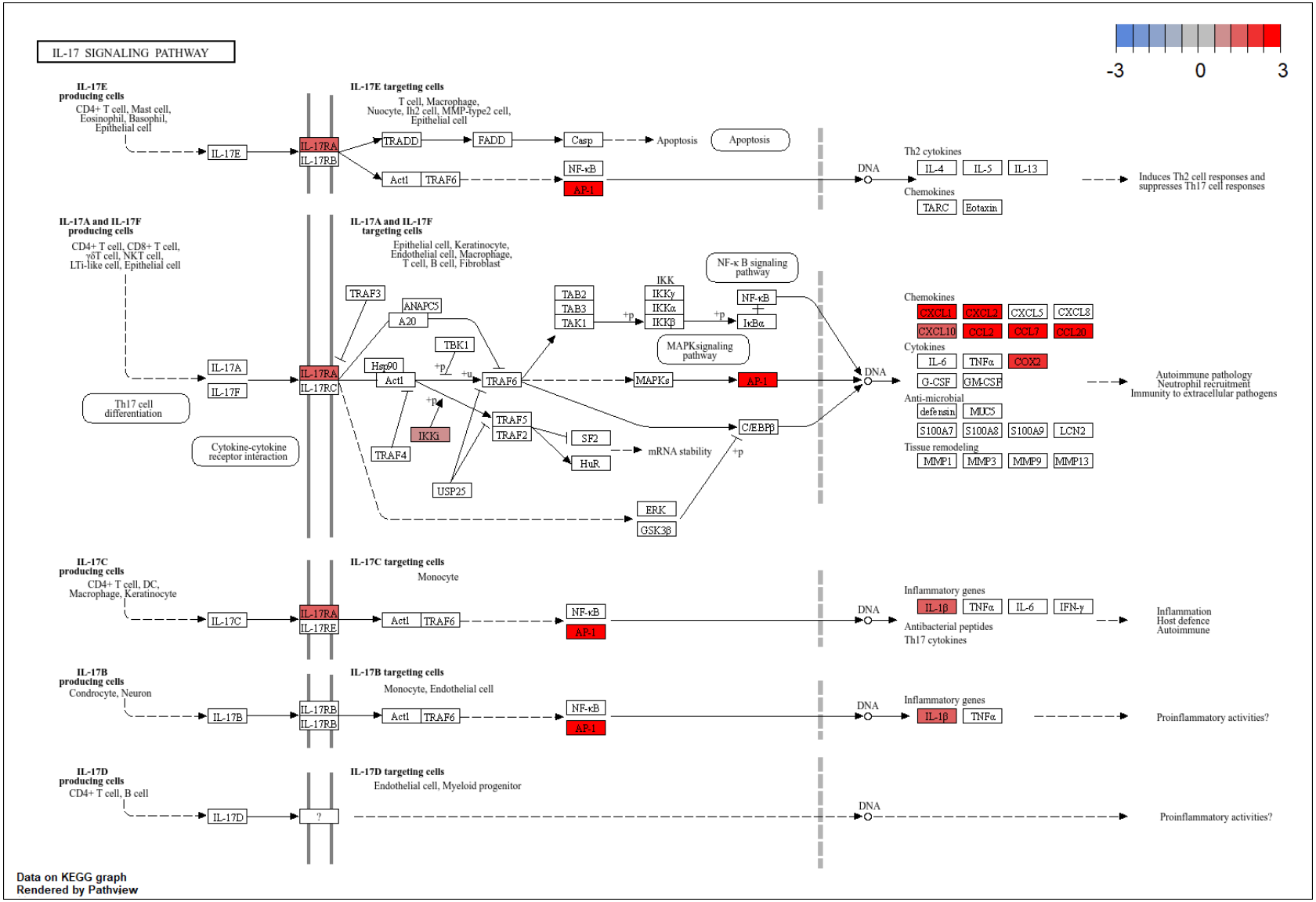

Study A: Supplemental Figure 5. rno04657 "IL-17 signalling pathway"

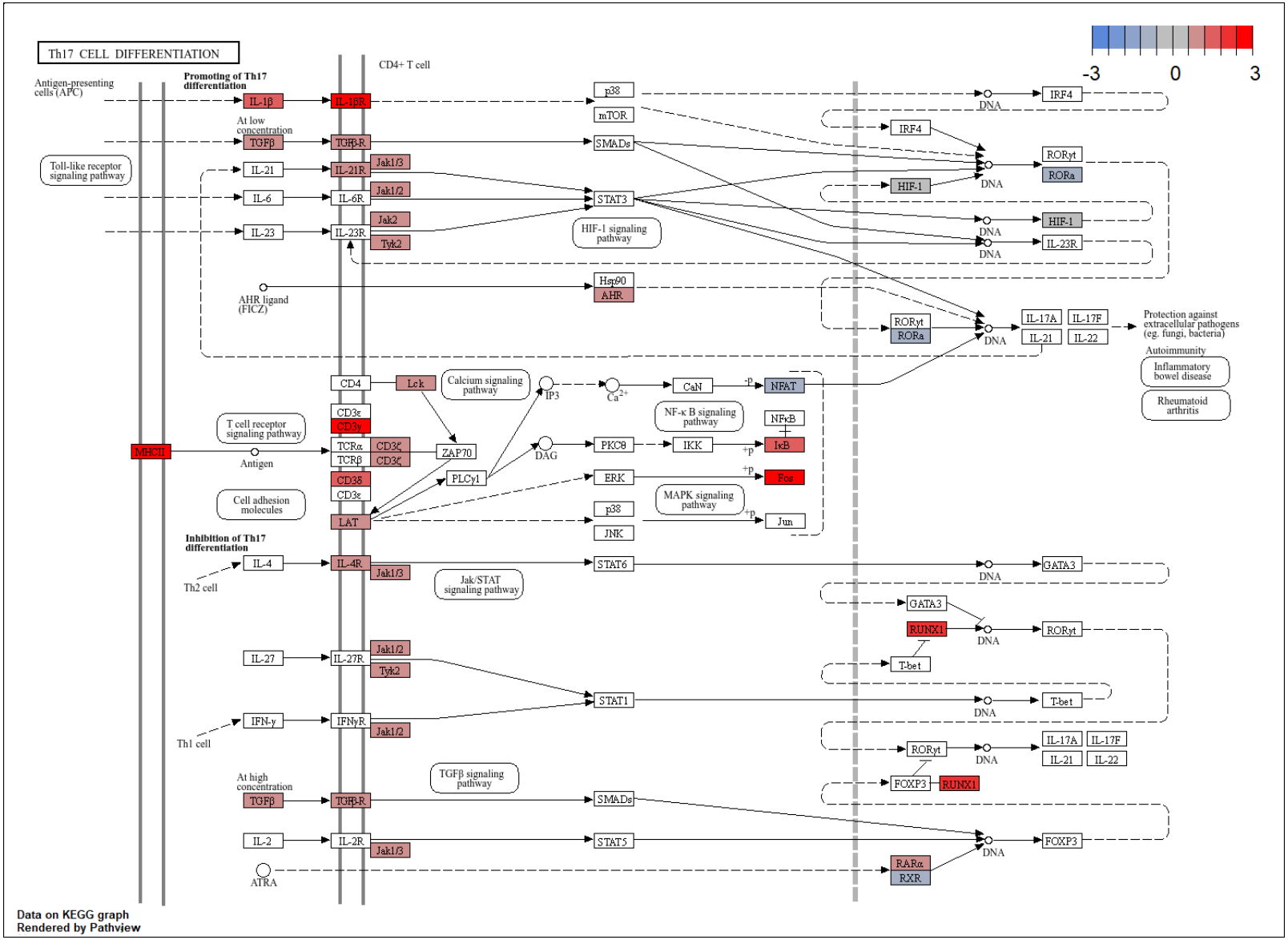

Study A: Supplemental Figure 6. rno04659 "Th17 cell differentiation"

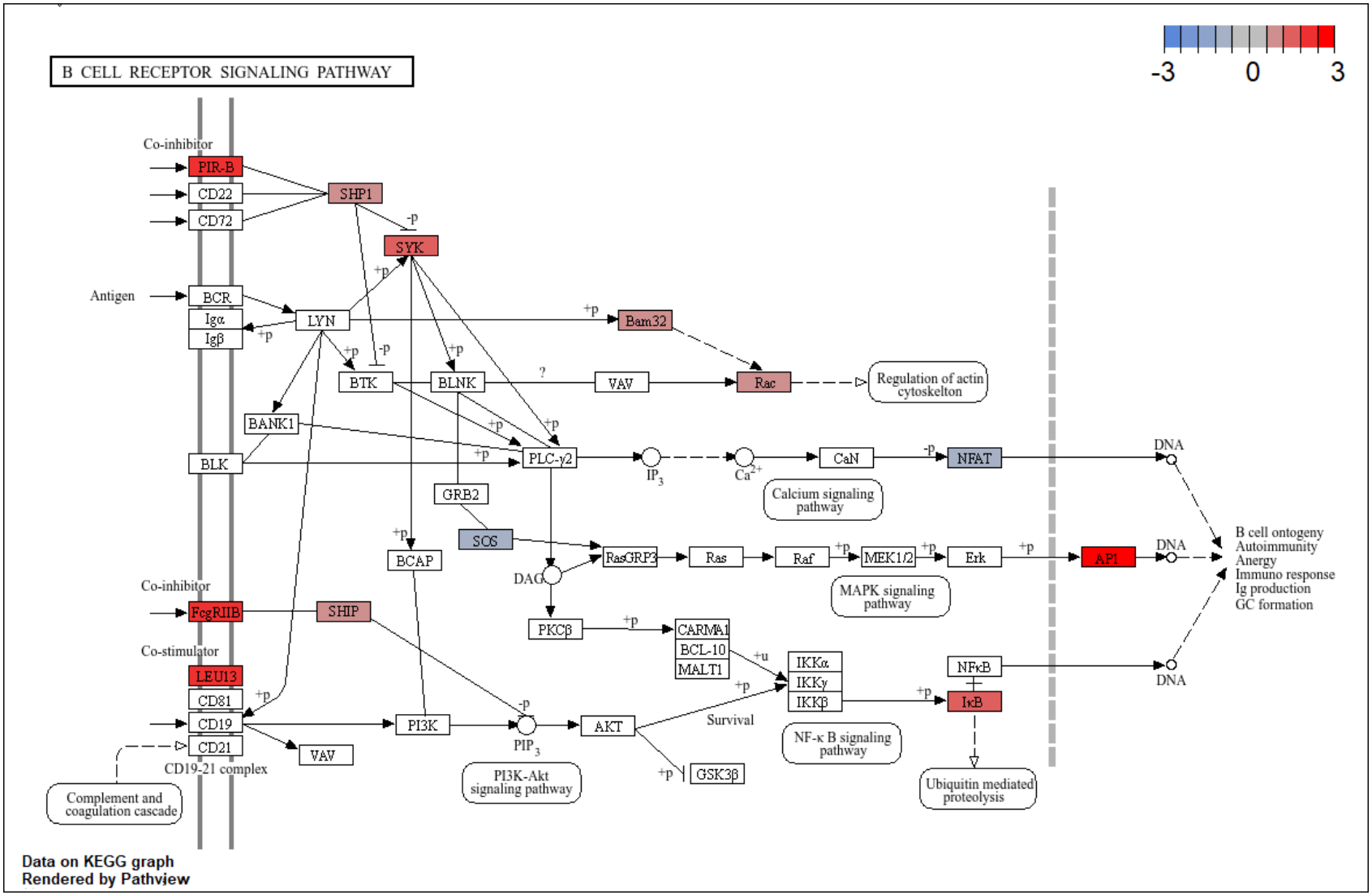

Study A: Supplemental Figure 7. rno04662 “B cell receptor signalling pathway”

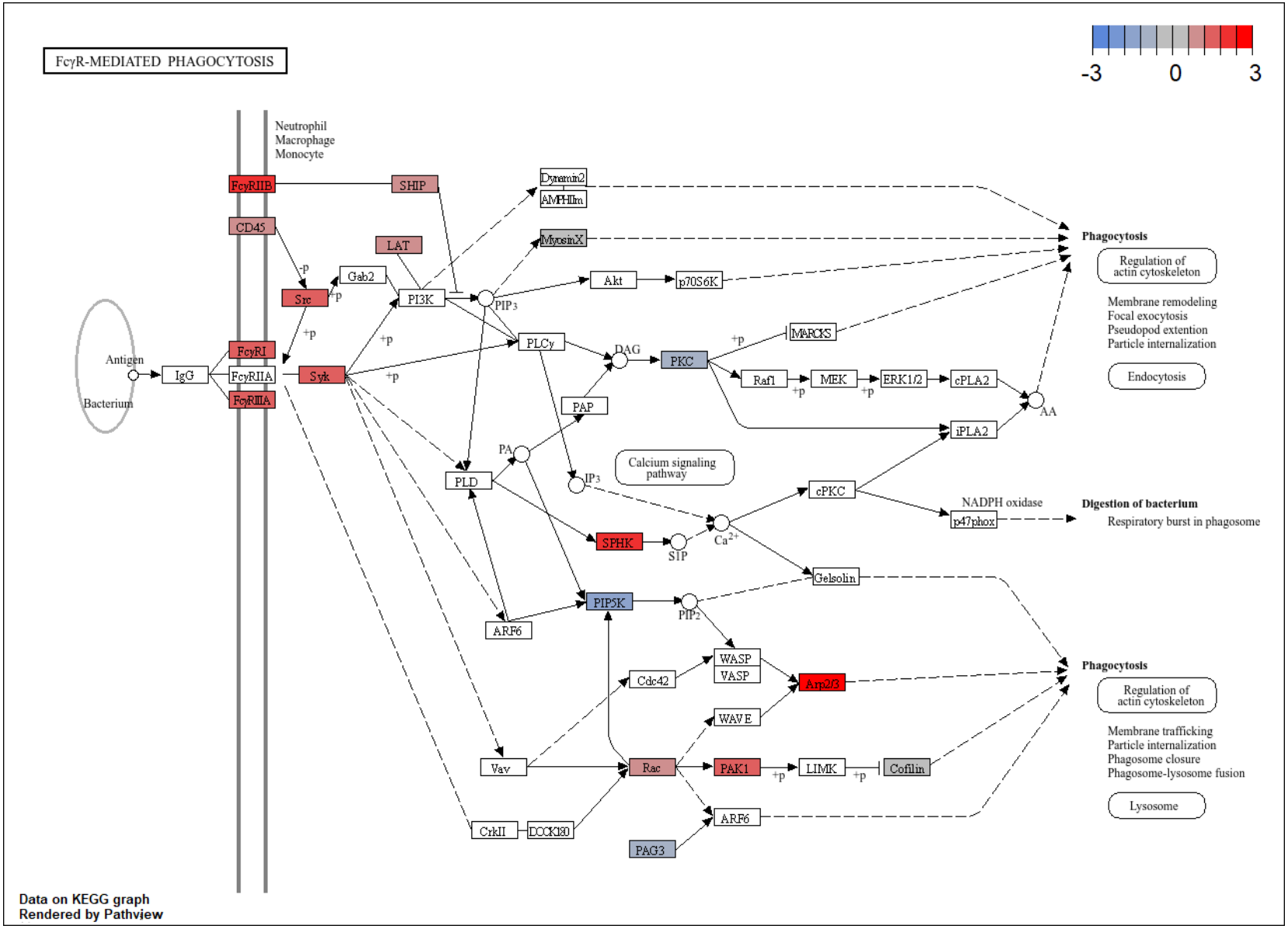

Study A: Supplemental Figure 8. rno04666 "FcγR-mediated phagocytosis"

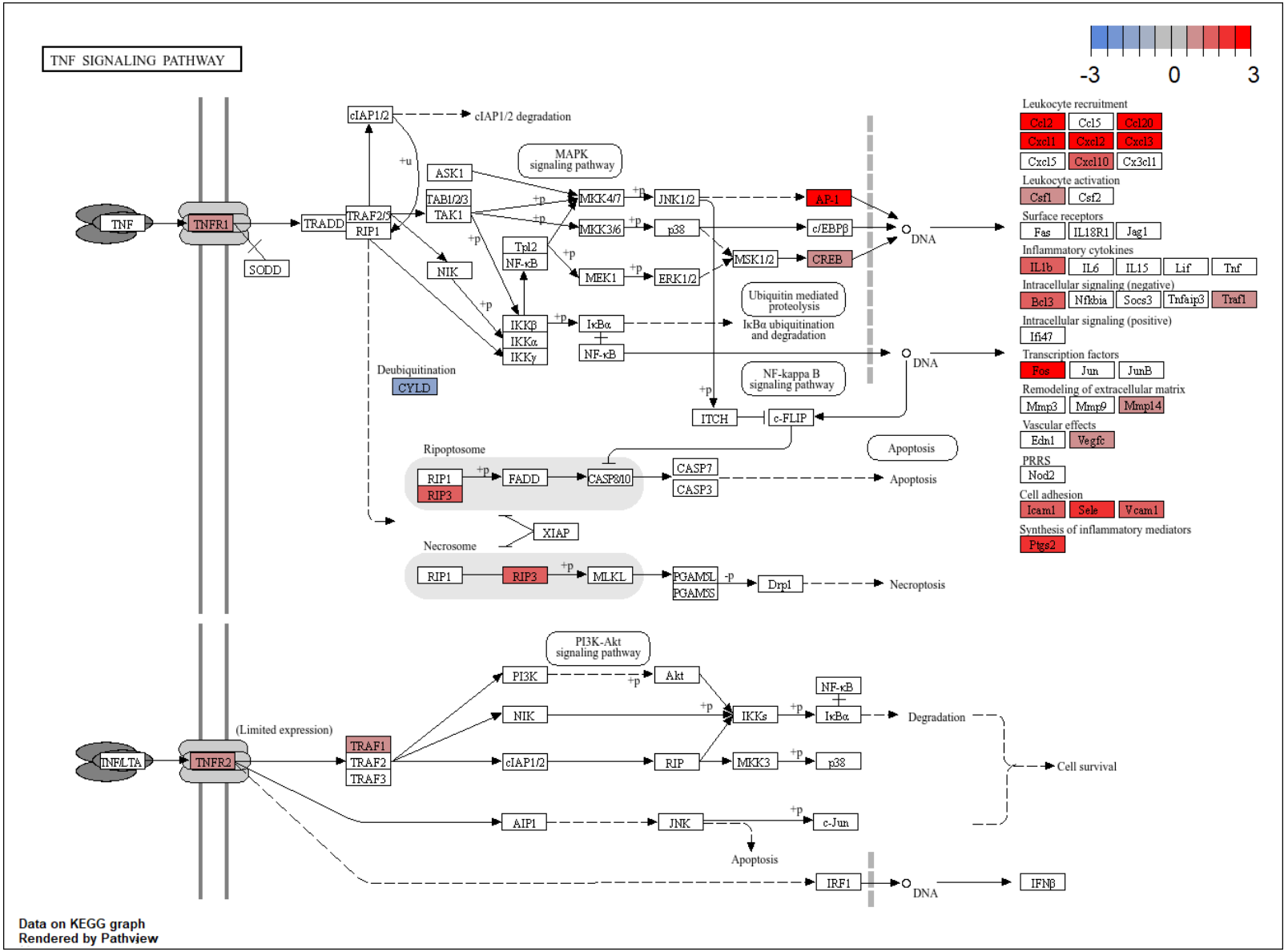

Study A: Supplemental Figure 9. rno04668 "TNF signalling pathway"

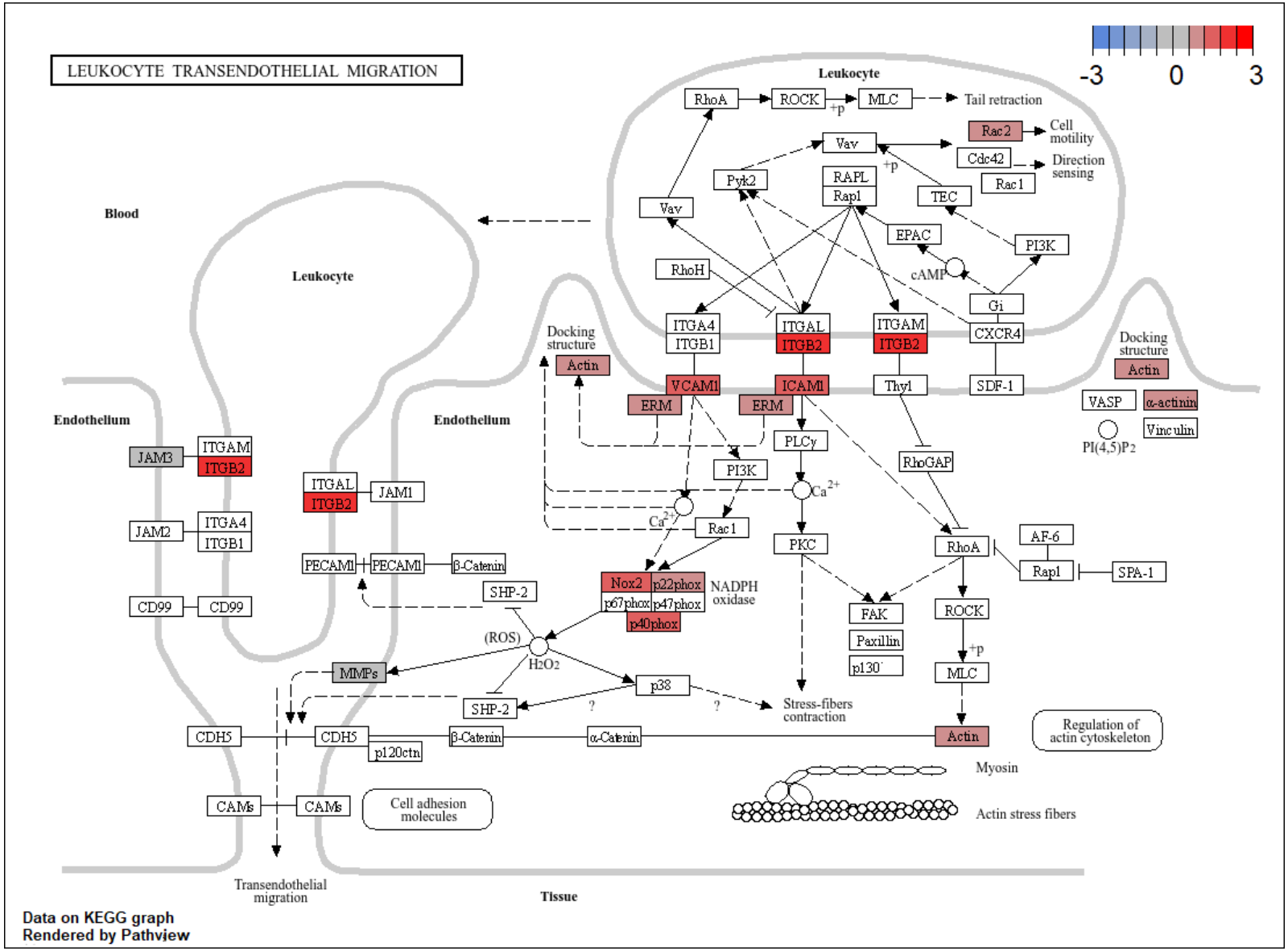

Study A: Supplemental Figure 10. rno04670 "Leukocyte transendothelial migration"

Energy Metabolism

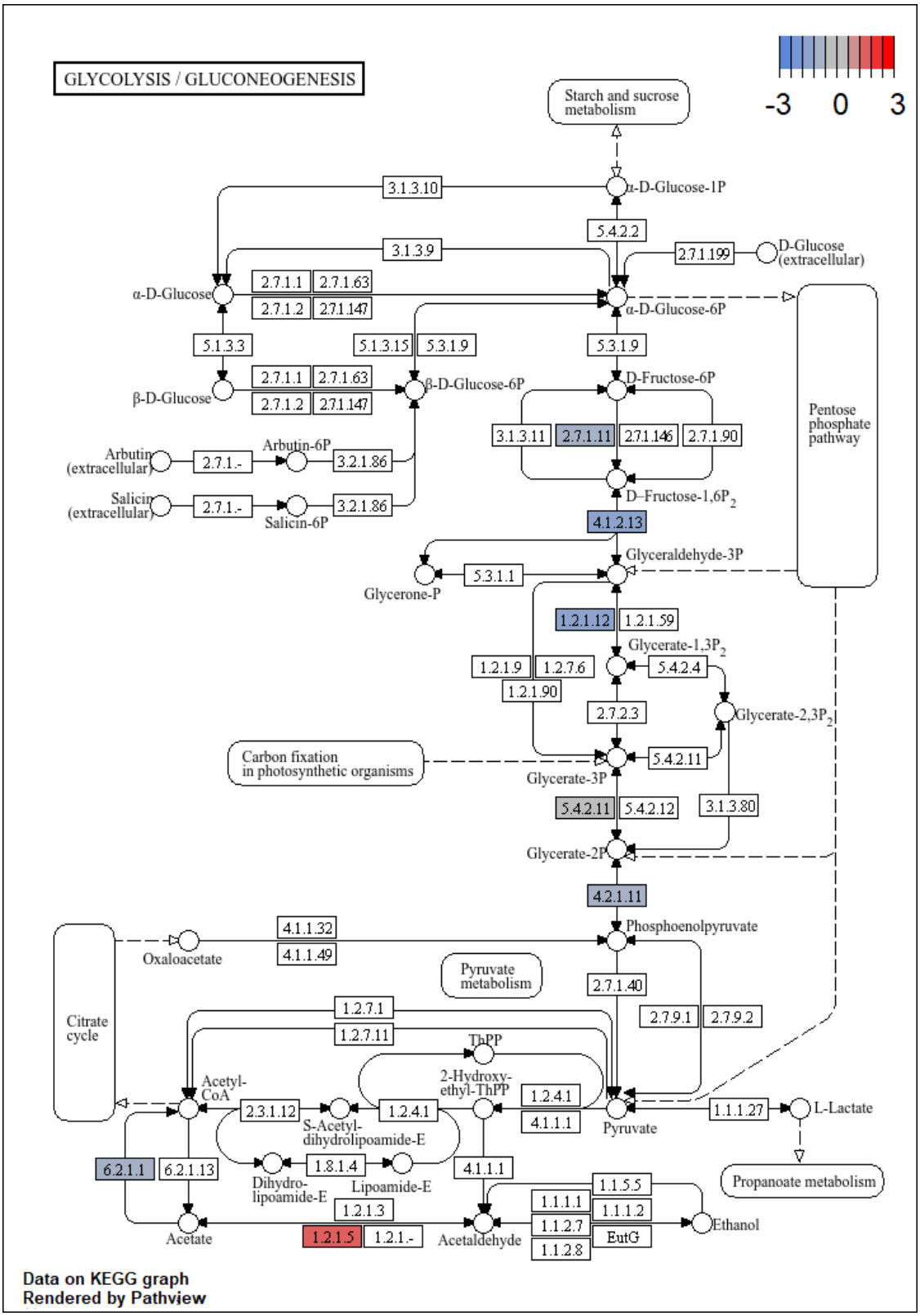

Study A: Supplemental Figure 11. rno00010 "Glycolysis / gluconeogenesis"

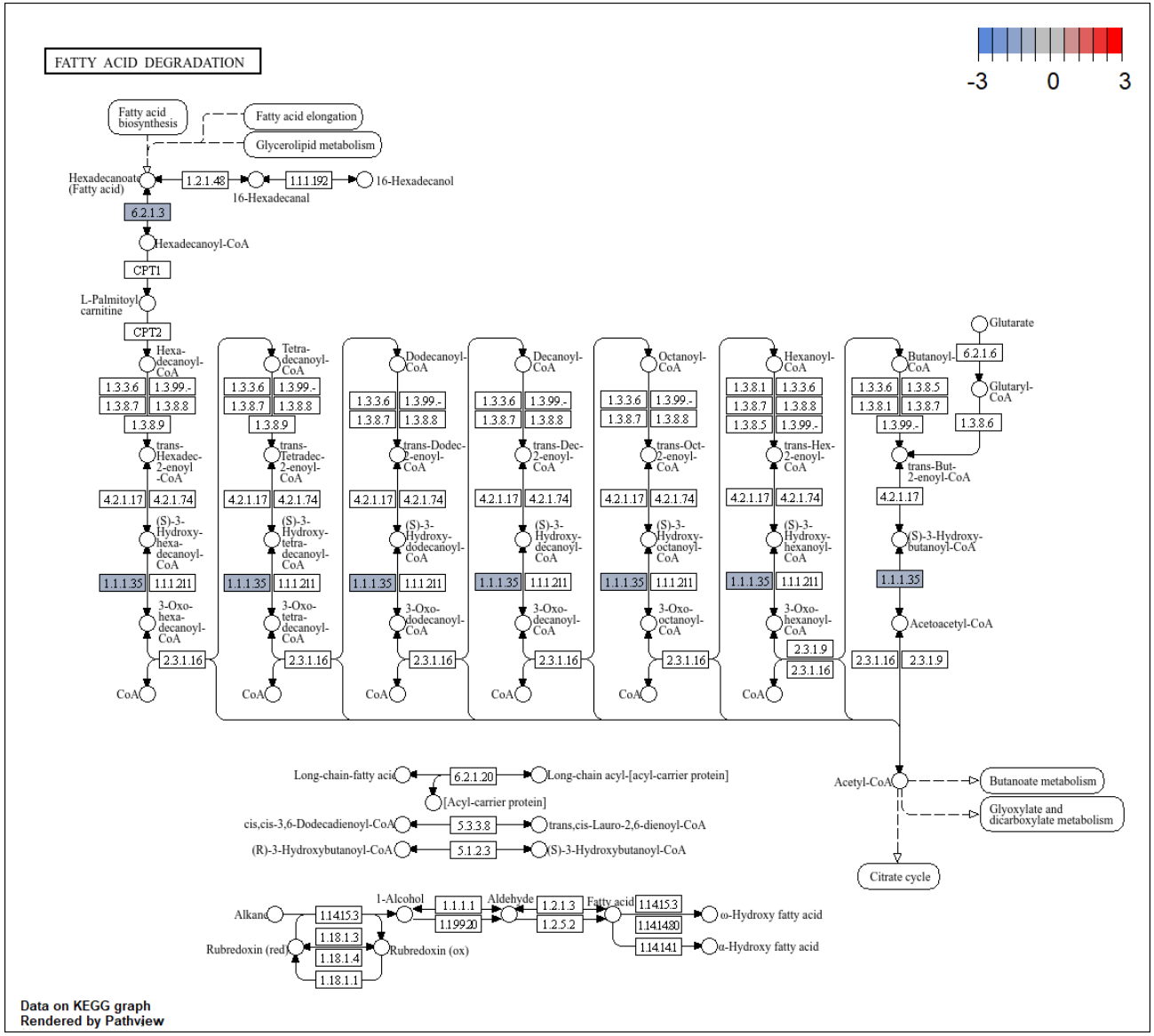

Study A: Supplemental Figure 12. rno00071 “Fatty acid degradation”

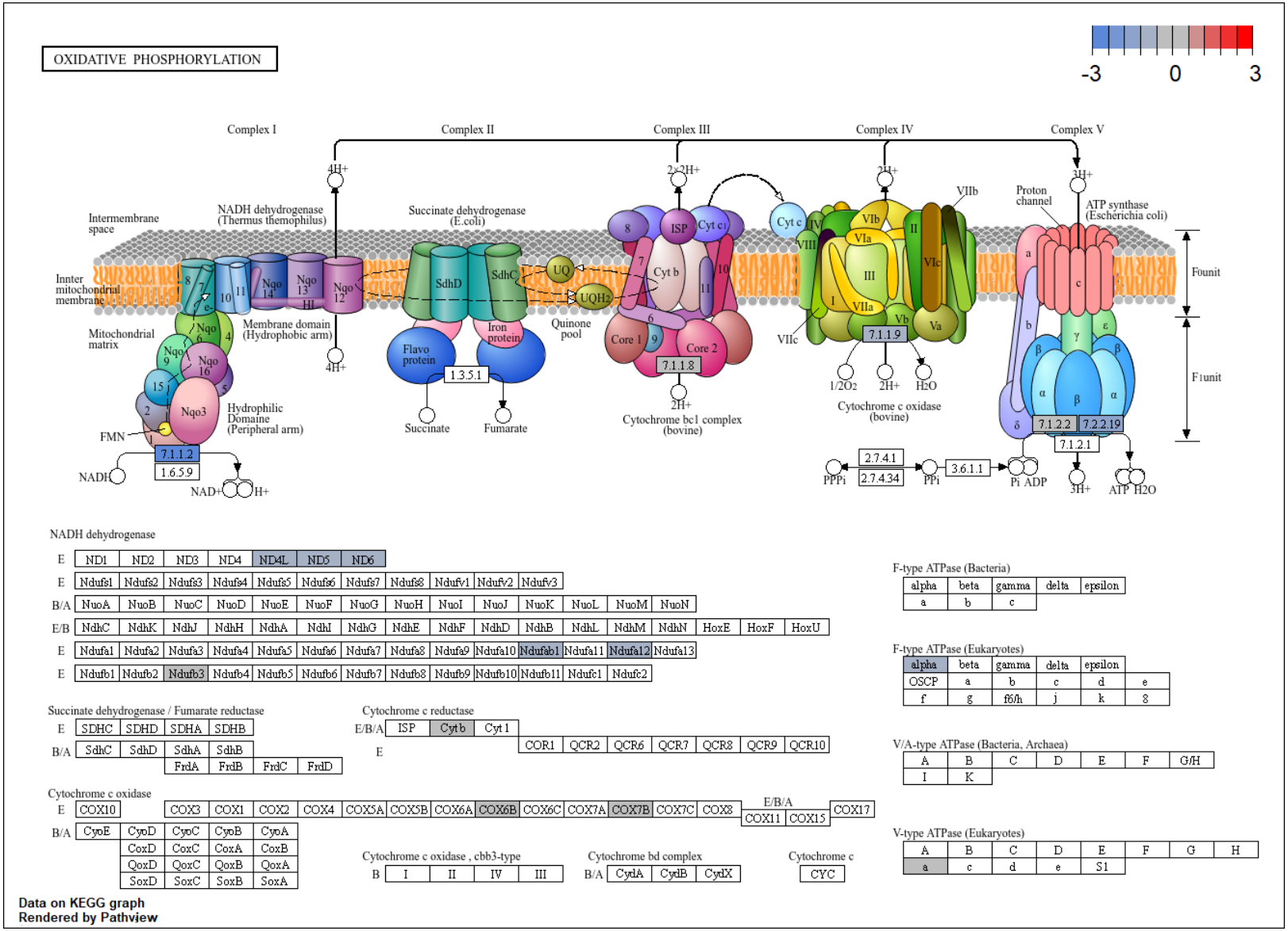

Study A: Supplemental Figure 13. rno00190 “Oxidative phosphorylation”

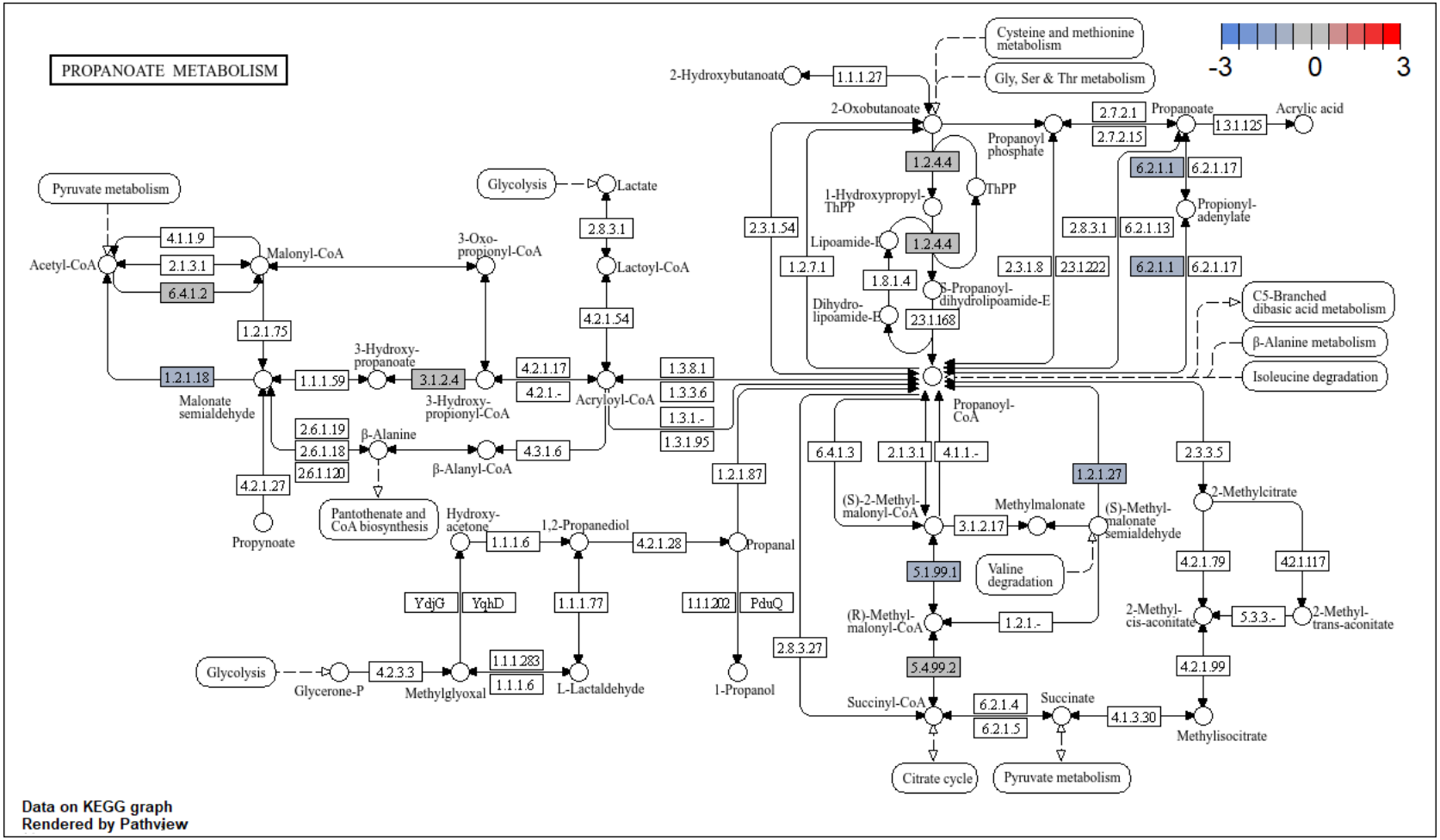

Study A: Supplemental Figure 14. rno00640 “Propanoate metabolism”

Cardiac Function

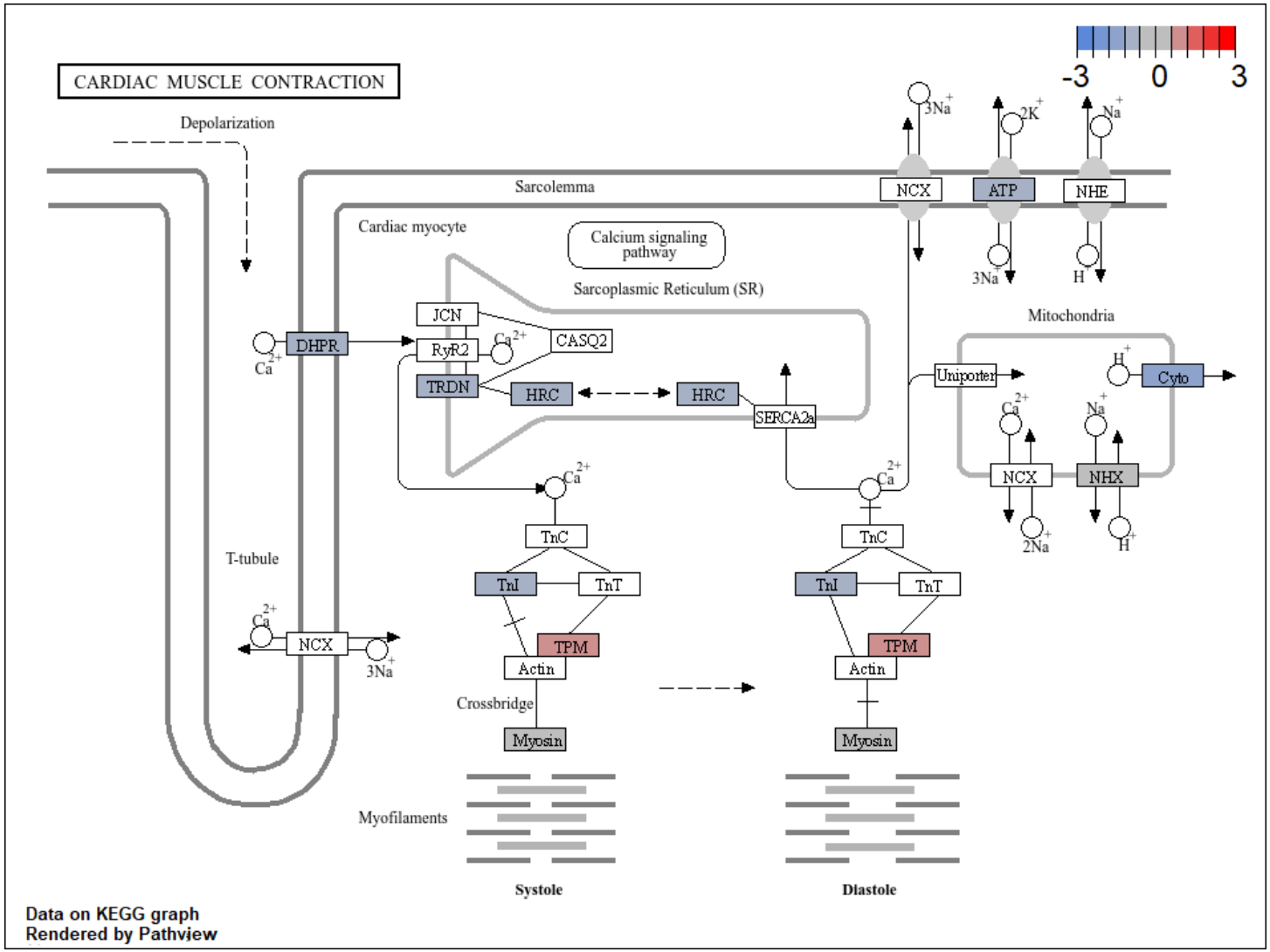

Study A: Supplemental Figure 15. rno04260 "Cardiac muscle contraction"

5. Study B: Supplemental Tables

Study B: Supplemental Table 1. Rat heart oxylipins by diet group.

	Enzyme	Rat Heart Oxylipins (ng/g) D (n=8)	D2M (n=8)	A (n=8)	A2M (n=5)	FDR
LA oxylipins						
9,10-EpOME	CYPe	202±26.3	219±22.3	149±30.2	147±65.7	
9,10-DiHOME	CYPe	17.5±1.69	21.0±5.33	23.6±2.80	16.0±6.17	
12,13-EpOME	CYPe	193±24.3	213±26.0	148±28.5	170±71.6	
12,13-DiHOME	CYPe	7.87±0.990	8.79±2.05	9.88±1.45	3.99±2.02	
LA CYPe		421±51.8	463±48.1	330±57.4	337±144	
9-HODE	LOX	1670±199	1336±200	1438±171	1296±468	
13-HODE	LOX	961±127	784±107	873±109	668±214	
13-oxoODE	LOX	1015±256	700±105	1139±114	1069±288	
(9,10,13- & 9,12,13-) triHOME	LOX	86.2±12.8	88.0±9.77	114±18.3	65.8±20.6	
LA LOX		3732±551	2908±356	3565±312	3099±915	
LA total		4153±584	3371±357	3894±307	3436±1056	

GLA oxylipins						
13-HOTrE-γ	LOX	3.30±1.04[b]	11.1±1.79[a]	3.49±1.52[b]	2.93±1.29[b]	0.025[KW]
DGLA oxylipins						
8-HETrE	LOX	7.22±0.509	13.2±2.75	10.4±1.39	7.93±2.03	
15-HETrE	LOX	11.4±1.32	21.9±3.32	16.4±2.68	12.0±1.85	0.030[INT]
DGLA total		18.7±1.78	35.1±5.88	26.8±3.81	20.0±3.83	0.021[INT]
AA oxylipins						
PGD2	COX	8.37±1.56	36.5±8.62	14.6±4.05	61.8±43.6	
11β-PGF2α	COX	26.3±9.55	78.5±18.6	44.3±17.3	70.5±43.0	
PGE2	COX	2.50±0.514	6.17±1.29	3.93±0.72	4.76±2.56	
11β-PGE2	COX	1.36±0.290	3.17±0.600	2.02±0.328	2.54±1.12	
15k PGE2	COX	9.12±2.08	12.3±1.79	9.71±2.40	9.97±3.61	
6k-PGF1α	COX	23.7±7.94	179±91.7	76.4±30.9	33.4±18.1	0.030[INT]
PGF2α	COX	5.07±0.869	14.3±3.11	8.13±2.39	10.9±7.16	
TXB2	COX	5.06±1.02[B]	15.4±2.70[A]	11.9±4.49[B]	10.7±1.97[A]	0.043[2M]
12-HHTrE	COX	24.4±3.69[b]	73.7±17.2[a]	59.4±18.2[ab]	52.0±24.0[ab]	0.032[INT]
AA COX		106±24.2[B]	419±129[A]	230±72.0[B]	257±103[A]	0.023[2M]
5,6-EpETrE	CYPe	52.4±9.2	86.6±14.8	45.3±11.1	36.3±19.6	
8,9-EpETrE	CYPe	20.0±3.03	29.2±3.72	17.6±3.63	15.9±6.97	

11,12-DiHETrE	CYPe	0.643±0.0557	1.01±0.145	0.736±0.0989	0.632±0.186	
14,15-EpETrE	CYPe	13.1±1.60	21.9±2.14	12.8±2.99	10.5±4.02	
14,15-DiHETrE	CYPe	1.10±0.0821^{ab}	1.75±0.230^{a}	1.23±0.169^{ab}	0.902±0.281^{b}	0.030^{INT}
AA CYPe		87.1±13.7	141±19.8	77.6±16.9	64.3±30.4	
16-HETE	CYPh	9.43±2.00^{ab}	11.3±1.99^{ab}	15.5±2.67^{a}	3.83±2.20^{b}	0.025^{INT}
5-HETE	LOX	100±12.3	131±14.5	149±24.4	81.9±23.9	0.030^{INT}
5-oxoETE	LOX	159±33.0	224±42.7	223±29.7	159±45.1	
8-HETE	LOX	108±10.1^{ab}	156±25.3^{a}	138±28.8^{ab}	65.6±17.1^{b}	0.025^{INT}
9-HETE	LOX	93.9±8.21^{ab}	129±20.5^{ab}	133±24.2^{a}	63.2±16.2^{b}	0.025^{INT}
11-HETE	LOX	91.5±8.47^{ab}	136±29.8^{a}	121±24.3^{ab}	59.2±17.5^{b}	0.030^{INT}
12-HETE	LOX	65.4±5.48	148±32.9	139±45.4	71.3±20.9	0.030^{INT}
12-oxoETE	LOX	215±38.5	321±80.4	355±141	192±54.2	
15-HETE	LOX	170±21.2^{ab}	203±27.2^{ab}	217±34.6^{a}	99.6±23.8^{b}	0.030^{INT}
15-oxoETE	LOX	54.5±13.2	57.5±12.5	76.5±16.4	49.8±14.2	
AA LOX		1058±135	1506±240	1551±299	841±186	0.030^{INT}
AA total		1260±165	2077±378	1874±354	1166±309	0.021^{INT}
ALA oxylipins						
12,13-EpODE	CYPe	0.673±0.183^{B}	0.752±0.142^{B}	3.17±0.587^{A}	3.82±1.74^{A}	0.011^{ALA}

9-HOTrE	LOX	17.7±2.65^{B}	13.6±1.80^{B}	94.5±13.5^{A}	62.5±19.9^{A}	<0.001^{ALA}
9-oxoOTrE	LOX	5.50±1.14^{B}	5.85±1.49^{B}	61.3±13.2^{A}	72.9±19.2^{A}	<0.001^{ALA}
13-HOTrE	LOX	16.8±2.76^{b}	18.1±1.59^{b}	110±25.2^{a}	51.3±22.7^{b}	0.025^{INT}
ALA LOX		40.0±6.24^{B}	37.6±3.51^{B}	265±50.0^{A}	187±37.4^{A}	<0.001^{ALA}
ALA total		40.7±6.39^{B}	38.4±3.54^{B}	269±50.2^{A}	191±39.1^{A}	<0.001^{ALA}
DHA oxylipins						
16,17 EpDoPE	CYPe	73.2±15.8	59.5±13.0	197±49.0	56.4±26.4	
19,20-EpDoPE	CYPe	12.2±2.54^{ab}	10.4±2.67^{ab}	33.6±7.35^{a}	10.4±4.19^{b}	0.046^{ALA}
DHA CYPe		85.4±18.3	69.8±15.6	231±56.2	66.8±30.5	
20-HDoHE	CYPh	46.4±9.94^{b}	31.1±8.44^{b}	172±29.2^{a}	29.5±13.9^{b}	0.013^{INT}
7-HDoHE	LOX	28.0±4.00^{b}	20.1±5.62^{b}	119±27.8^{a}	17.8±7.22^{b}	0.025^{INT}
10-HDoHE	LOX	15.0±2.28^{b}	11.6±2.94^{b}	74.9±17.7^{a}	11.6±5.48^{b}	0.007^{INT}
13-HDoHE	LOX	40.0±7.41^{b}	28.8±7.13^{b}	202±54.7^{a}	32.8±16.5^{b}	0.014^{INT}
14-HDoHE	LOX	33.9±4.94^{b}	29±5.07^{b}	199±50.9^{a}	27.0±11.7^{b}	0.007^{INT}
16-HDoHE	LOX	33.8±5.82^{b}	19.4±4.34^{bc}	127±24.6^{a}	16.1±6.68^{c}	0.007^{INT}
17-HDoHE	LOX	243±39.1^{b}	171±32.8^{b}	939±145^{a}	153±71.9^{b}	0.006^{INT}
DHA LOX		393±60.5^{b}	280±55.1^{b}	1661±298^{a}	258±119^{b}	0.001^{INT}

DHA total	525±85.5[b]	381±78.1[b]	2064±345[a]	355±163[b]	<0.001[INT]
COX total	106±24.2[B]	419±129[A]	230±72.0[B]	257±103[A]	0.012[2M]
CYPe total	594±78.1	674±74.5	641±120	472±203	
CYPh total	55.9±11.4[b]	42.4±9.87[b]	188±31.1[a]	33.4±16.0[b]	0.001[INT]
LOX total	5245±726	4778±516	7073±881	4408±1236	
n-3	566±88.9[b]	419±78.7[b]	2333±376[a]	545±199[b]	0.009[INT]
n-6	5435±735	5494±583	5799±622	4625±1357	
total	6001±804	5914±635	8132±968	5170±1545	

Values mean ± standard error. Superscript uppercase letters indicate a main-effect group difference of diet or treatment. Superscript lowercase letters indicate interaction-effect group differences by Tukey's post-hoc test or pairwise comparison of groups using Dunn's test. FDR < 0.05 are listed, with [ALA] indicating a main-effect of dietary ALA, [2M] indicating a main-effect of 2-MCPD treatment, [INT] indicating an ALA x 2-MCPD interaction-effect, and [KW] indicating pairwise comparison using the Kruskal-Wallis test was used. P-values were adjusted by the Benjamini-Hochberg procedure. P-values of the oxylipin totals were adjusted separately by category such that the comparisons were independent.

Study B: Supplemental Table 2. Rat liver oxylipins by diet group.

		Rat Liver Oxylipins (ng/g)				
	Enzyme	CO (n=8)	C2M (n=7)	CA (n=8)	CA2M (n=5)	FDR
LA oxylipins						
9,10-EpOME	CYPe	137±62.1	176±56.4	178±36.0	110±55.3	
9,10-DiHOME	CYPe	493±25.5	297±36.2	337±33.0	285±49.4	
12,13-EpOME	CYPe	93.7±35.4	184±61.2	217±57.1	95.7±44.7	
12,13-DiHOME	CYPe	350±19.4	212±28.1	249±27.4	180±29.6	
LA CYPe		1072±93.8	870±80.9	980±131	671±149	
9-HODE	LOX	2529±244	2225±332	1418±204	2358±690	
9-oxoODE	LOX	2834±744	1558±641	834±262	1572±673	
13-HODE	LOX	2748±365	2222±479	1404±192	2499±974	
13-oxoODE	LOX	2600±302[a]	1564±274[ab]	959±192[b]	1694±360[ab]	0.016[INT]
(9,10,13- & 9,12,13-) triHOME	LOX	331±58.2	213±45.8	252±14.7	258±49.4	
LA LOX		11043±1503	7782±1369	4867±581	8381±2556	
LA total		12115±1472	8651±1394	5847±530	9053±2540	
GLA oxylipins						
13-HOTrE-γ	LOX	114±10.7	151±25.6	54.8±4.67	108±34.9	

DGLA oxylipins						
8-HETrE	LOX	44.5±13.1	32.9±10.7	14.6±1.83	25.9±6.03	
15-HETrE	LOX	133±44.4	84±17.2	62.4±6.25	84.8±30.8	
DGLA total		177±57.4	117±25.1	77±7.72	111±35.8	
AA oxylipins						
PGD2	COX	124±13.9	260±31.8	108±30.7	167±24.5	
11β-PGF2α	COX	508±72.3	1028±194	426±57.6	694±134	
PGE2	COX	66.6±9.02^{A}	109±9.13^{A}	47.4±5.24^{B}	68.5±12.1^{B}	0.033^{ALA}
11β-PGE2	COX	32.0±4.00^{A}	50.7±4.34^{A}	22.0±2.68^{B}	31.4±5.87^{B}	0.026^{ALA}
15k-PGE2	COX	23.2±7.24	40.5±15.3	23.9±6.83	32.8±9.49	
6k-PGF1α	COX	3.85±0.701	8.72±2.84	9.35±3.71	7.33±2.39	
PGF2α	COX	105±13.8	198±25.3	102±12.9	140±23.6	
TXB2	COX	34.3±3.29	57.5±4.92	25.8±4.81	43.0±8.59	
12-HHTrE	COX	118±19.2	254±102	117±29.0	295±146	
AA COX		1015±128	2007±294	882±116	1479±291	
5,6-EpETrE	CYPe	14.6±7.74	34.6±15.5	19.3±7.65	19.3±14.7	
5,6-DiHETrE	CYPe	10.5±2.14	4.48±1.01	4.33±1.39	4.60±0.988	
8,9-DiHETrE	CYPe	199±16.3^{A}	147±24.6^{A}	98.4±13.9^{B}	69.2±10.6^{B}	0.006^{ALA}
11,12-DiHETrE	CYPe	171±17.1^{A}	125±16.6^{A}	81.0±8.98^{B}	69.2±8.24^{B}	0.013^{ALA}

14,15-EpETrE	CYPe	8.23±3.87	15.8±5.22	8.24±1.32	6.77±2.85	
14,15-DiHETrE	CYPe	165±12.5^{A}	113±9.66^{A}	77.1±5.73^{B}	66.4±5.68^{B}	<0.001^{ALA}
AA CYPe		569±42.9^{A}	439±40.7^{A}	288±28.2^{B}	236±37.4^{B}	0.006^{ALA}
16-HETE	CYPh	227±32.5	134±29.5	88.7±12.4	83.9±25.7	
17-HETE	CYPh	13.0±1.63	8.16±1.19	9.48±1.27	7.51±2.38	
18-HETE	CYPh	15.7±1.73	17.7±3.18	15.1±1.48	11.1±2.84	
20-HETE	CYPh	83.9±17.9	54.5±9.89	55.0±8.63	63.3±9.79	
AA CYPh		340±45.6	214±33.4	168±21.5	166±36.7	
5-HETE	LOX	567±118	457±130	187±44.5	372±98.5	
5-oxoETE	LOX	1269±319	616±201	252±97	616±251	
8-HETE	LOX	256±54.3	241±74.0	91.0±13.0	159±62.5	
9-HETE	LOX	488±163	565±406	82.3±17.7	274±183	
11-HETE	LOX	227±44.7	280±96.2	86.4±9.45	175±59.9	
12-HETE	LOX	198±47.5	209±119	56.1±9.03	133±72.5	
12-oxoETE	LOX	1382±293	756±234	358±126	851±458	
15-HETE	LOX	515±132	406±111	165±25.6	283±74.8	
15-oxoETE	LOX	157±53.1	97.9±24.2	43±12.5	86.9±31.1	
6t-LTB4	LOX	75.8±25.8	30.5±13.7	11.2±3.44	31.3±19.7	
AA LOX		5134±1203	3658±1377	1332±340	2981±1294	

5-isoPGF2αVI		1.61±0.225	2.98±0.721	2.43±0.529	1.28±0.33	
AA total		7058±1275	6322±1529	2673±288	4862±1271	
ALA oxylipins						
9-HOTrE	LOX	29.8±3.23^{B}	30.8±8.44^{B}	159±20.8^{A}	166±26.4^{A}	<0.001^{ALA}
9-oxoOTrE	LOX	19.9±7.03^{B}	19.0±7.98^{B}	71.1±14^{A}	107±32.9^{A}	<0.001^{ALA}
13-HOTrE	LOX	84.9±19.0^{B}	57.7±25.5^{B}	126±17.0^{A}	335±215^{A}	0.006^{ALA}
ALA total		135±20.1^{B}	107±26.3^{B}	356±39.7^{A}	609±264^{A}	<0.001^{ALA}
EPA oxylipins						
PGE3	COX	<LOQ^{b}	3.90±0.603^{b}	13.5±1.76^{a}	22.3±4.35^{a}	<0.001^{KW}
14,15-DiHETE	CYPe	2924±766^{B}	1539±611^{B}	3951±1273^{A}	5761±1698^{A}	0.016^{ALA}
17,18-DiHETE	CYPe	769±196^{B}	436±162^{B}	1421±500^{A}	1752±436^{A}	0.013^{ALA}
EPA CYPe		3693±962^{B}	1975±773^{B}	5371±1763^{A}	7514±2122^{A}	0.012^{ALA}
18-HEPE	CYPh	3.22±0.357^{b}	6.98±2.67^{b}	32.8±3.06^{a}	57.6±18.6^{a}	<0.001^{KW}
8-HEPE	LOX	<LOQ^{b}	2.14±0.538^{b}	9.04±1.37^{a}	13.8±3.00^{a}	0.002^{KW}
11-HEPE	LOX	<LOQ^{b}	8.65±3.82^{b}	45.3±6.74^{a}	78.6±20.1^{a}	<0.001^{KW}
12-HEPE	LOX	0.739±0.0821^{b}	2.45±0.754^{b}	13.6±1.45^{a}	29.4±16.4^{a}	<0.001^{KW}

15-HEPE	LOX	<LOQ[b]	11.2±1.91[b]	44.4±3.69[a]	67.5±18.9[a]	<0.001[KW]
EPA LOX		12.1±0.0821[b]	24.5±6.45[b]	112±8.26[a]	189±55.0[a]	<0.001[KW]
EPA total		3711±961[B]	2010±778[B]	5530±1762[A]	7783±2162[A]	0.005[ALA]
DHA oxylipins						
16,17 EpDoPE	CYPe	27.7±10.2	42.8±12.2	73.7±12.8	66.5±27.8	
19,20-EpDoPE	CYPe	3.53±1.39	9.6±3.05	13.5±1.77	11.4±4.27	
16,17-DiHDoPE	CYPe	5.89±0.893[B]	4.85±0.601[B]	14.5±1.04[A]	8.80±1.56[A]	0.012[ALA]
19,20-DiHDoPE	CYPe	3.96±0.496[B]	3.5±0.296[B]	10.6±0.803[A]	9.26±1.96[A]	<0.001[ALA]
DHA CYPe		41.1±12.5	60.7±15.4	112±13.8	95.9±35.2	
20-HDoHE	CYPh	66.2±10.6[B]	62.3±12.0[B]	107±19.3[A]	182±72.8[A]	0.023[ALA]
7-HDoHE	LOX	17.9±9.17[B]	18.8±4.77[B]	40.6±9.35[A]	73.4±20.9[A]	0.010[ALA]
10-HDoHE	LOX	19.7±4.21	19.5±4.10	23.2±4.99	57.4±22.7	
13-HDoHE	LOX	90.7±27.3	90±53.5	54.8±12.5	175±107	
14-HDoHE	LOX	64.8±17.3	58.6±27.2	64.2±16.6	133±70.3	
16-HDoHE	LOX	49.4±13.8	41.1±13.9	38.4±5.75	70.8±23.9	
17-HDoHE	LOX	246±75.8	219±91.5	201±23.8	387±130	
DHA LOX		488±133	447±187	423±68.9	897±369	

DHA total	596±133^{B}	570±187^{B}	642±79.6^{A}	1175±429^{A}	0.031^{ALA}
COX total	1017±128	2011±294	895±117	1501±293	
CYPe total	5375±935^{ab}	3344±774^{b}	6752±1738^{ab}	8516±1952^{a}	0.007^{ALA}
CYPh total	409±55.3	284±41.7	308±37.8	406±126	
LOX total	17103±2811	12288±2829	7222±922	13275±4559	
n-3	4441±1087^{B}	2688±832^{B}	6528±1818^{A}	9566±2534^{A}	0.003^{ALA}
n-6	19465±2662^{a}	15241±2794^{ab}	8652±714^{b}	14134±3761^{ab}	0.023^{INT}
Total	23905±3669	17929±3357	15181±2310	23700±5758	

Values mean ± standard error. Superscript uppercase letters indicate a main-effect group difference of diet or treatment. Superscript lowercase letters indicate interaction-effect group differences by Tukey's post-hoc test or pairwise comparison of groups using Dunn's test. FDR < 0.05 are listed, with ^{ALA} indicating a main-effect of dietary ALA, ^{2M} indicating a main-effect of 2-MCPD treatment, ^{INT} indicating an ALA x 2-MCPD interaction-effect, and ^{KW} indicating pairwise comparison using the Kruskal-Wallis test was used. P-values were adjusted by the Benjamini-Hochberg procedure. P-values of the oxylipin totals were adjusted separately by category such that the comparisons were independent.

Study B: Supplemental Table 3. Rat kidney oxylipins by diet group.

	Enzyme	Rat Kidney Oxylipins (ng/g) CO (n=7)	C2M (n=7)	CA (n=8)	CA2M (n=6)	FDR
LA oxylipins						
9,10-EpOME	CYPe	40±17.8	99.7±35.6	100±11.7	110±20.2	
9,10-DiHOME	CYPe	54.7±5.6	68±12.5	80.8±24.9	45.8±10.9	
12,13-EpOME	CYPe	43.5±17.3	106±35.2	111±13.9	128±25.0	
12,13-DiHOME	CYPe	22.8±4.71	24.6±6.20	26.0±6.99	13.8±2.75	
LA CYPe		161±34.8	298±60.8	318±36.3	297±47.7	
9-HODE	LOX	1861±246	2783±383	3607±1192	2835±668	
13-HODE	LOX	2824±1116	2602±332	2411±679	2091±512	
13-oxoODE	LOX	812±155	1704±411	1247±217	908±277	
(9,10,13- & 9,12,13-) triHOME	LOX	201±36.5	316±56.5	229±46.8	178±32.8	
LA LOX		5698±1373	7405±849	7494±1994	6012±1399	
LA total		5859±1362	7703±832	7811±2023	6309±1429	
GLA oxylipins						
13-HOTrE-γ		47.9±4.56	85.5±6.42	54.1±11.4	61.4±13.0	

DGLA oxylipins						
TXB1	COX	19.7±4.38^{A}	22.5±5.72^{A}	14.1±1.89^{B}	9.98±2.36^{B}	0.036^{ALA}
8-HETrE	LOX	65.7±19.1^{A}	67.1±9.51^{A}	46.9±2.66^{B}	27.3±4.79^{B}	0.018^{ALA}
15-HETrE	LOX	191±50.5^{A}	153±29.4^{A}	84.9±5.13^{B}	59.6±6.23^{B}	0.021^{ALA}
DGLA LOX		257±68.3^{A}	220±37.6^{A}	132±6.70^{B}	86.8±10.9^{B}	0.008^{ALA}
DGLA total		276±68.7^{A}	242±42.2^{A}	146±6.97^{B}	96.8±13.1^{B}	0.004^{ALA}
AA oxylipins						
PGD2	COX	236±86.6	396±157	155±16.2	133±25.5	
11β-PGF2α	COX	1107±424	1235±347	930±93.1	690±129	
PGE2	COX	150±74.3	177±80.3	81.9±22.6	59.6±12.5	
PGB2	COX	18.1±14.6	14.1±8.53	2.89±0.379	2.49±0.955	
11β-PGE2	COX	67.6±31.9	82.9±36.3	38.4±10.0	28.4±5.78	
15k-PGE2	COX	40.8±15.6	56.3±14.1	30.1±3.26	33.2±9.32	
6k-PGF1α	COX	115±46.6	118±41	85.6±17.5	70.9±15.1	
6,15-dk,dh-PGF1α	COX	59.0±26.8	57.7±22.4	19±3.19	22.1±6.20	
PGF2α	COX	285±108	352±92.5	240±31.2	176±36.5	
15k-PGF2α	COX	78.0±35.0^{A}	145±43.3^{A}	63.1±15.9^{B}	30.5±11.6^{B}	0.023^{ALA}
TXB2	COX	123±38.8	122±33.5	82.2±10.6	65.9±10.9	
12-HHTrE	COX	616±224	1128±248	695±146	594±157	

AA COX		2896±1109	3884±1057	2424±295	1906±310	
5,6-EpETrE	CYPe	39.2±21.4	112±50.6	93.1±16.5	105±27.2	
5,6-DiHETrE	CYPe	9.50±3.50	4.52±1.67	2.65±1.21	0.779±0.140	
8,9-EpETrE	CYPe	17.1±6.24	32.6±10.8	33.3±4.43	27.2±5.88	
8,9-DiHETrE	CYPe	32.6±5.43	27.5±2.72	26.0±4.06	17.0±5.06	
11,12-DiHETrE	CYPe	20.7±3.25	19±1.83	18.8±1.84	12.4±2.77	
14,15-EpETrE	CYPe	9.92±3.43	24.5±10.0	21.6±3.13	20.6±5.05	
14,15-DiHETrE	CYPe	11.9±2.56	10.9±1.19	9.20±1.02	7.15±1.51	
AA CYPe		141±24.5	231±68.3	205±20	190±38.1	
16-HETE	CYPh	132±39.5^{A}	132±20.2^{A}	63.2±5.97^{B}	51.9±10.5^{B}	0.013^{ALA}
18-HETE	CYPh	3.51±1.77	5.36±0.976	3.43±0.586	2.66±0.339	
AA CYPh		135±40.5^{A}	138±20.3^{A}	66.7±6.31^{B}	54.6±10.5^{B}	0.008^{ALA}
5-HETE	LOX	1137±264^{A}	1295±226^{A}	799±57.3^{B}	475±91.6^{B}	0.007^{ALA}
5-oxoETE	LOX	1085±302^{a}	1779±392^{a}	834±92.2^{a}	408±62.8^{b}	0.014^{INT}
8-HETE	LOX	601±173^{A}	458±57.3^{A}	358±43.0^{B}	189±28.7^{B}	0.013^{ALA}
9-HETE	LOX	1532±786^{A}	793±273^{A}	370±43.6^{B}	213±37.5^{B}	0.024^{ALA}
11-HETE	LOX	714±260^{A}	552±102^{A}	384±35.8^{B}	262±46.0^{B}	0.036^{ALA}
12-HETE	LOX	1225±809	365±106	248±35.2	155±32.2	
12-oxoETE	LOX	1468±656^{A}	2188±759^{A}	631±126^{B}	387±77.4^{B}	0.036^{ALA}

15-HETE	LOX	2080±970	1296±189	838±52.5	669±105	
15-oxoETE	LOX	272±79.1^{A}	371±89.8^{A}	169±29.7^{B}	95.1±22.5^{B}	0.013^{ALA}
6t-LTB4	LOX	199±106^{A}	110±46.5^{A}	27.4±4.75^{B}	14.4±2.46^{B}	0.013^{ALA}
AA LOX		10313±3508^{A}	9206±2144^{A}	4659±312^{B}	2868±446^{B}	0.008^{ALA}
5-isoPGF2αVI	-	38.6±9.59	50.0±18.1	36.9±6.16	48.4±16.8	
8-iso-PGF2αIII	-	41.2±9.53	46.8±9.29	32.6±3.65	30.9±6.99	
AA non-enzymatic		79.8±14.1	96.8±23.6	69.5±9.26	79.3±23.4	
AA total		13564±3194	13556±2637	7424±350	5098±799	
ALA oxylipins						
12,13-EpODE	CYPe	3.74±3.68^{B}	0.355±0.142^{B}	1.59±0.241^{A}	2.26±0.459^{A}	0.038^{ALA}
9-HOTrE	LOX	16.3±2.46^{c}	34.5±4.31^{b}	291±133^{a}	169±37.4^{a}	<0.001^{ALA}
9-oxoOTrE	LOX	39.4±20.5	41.4±30.9	58.4±17.8	24.9±7.20	
13-HOTrE	LOX	72.9±34.7^{B}	48.6±11.0^{B}	195±73.2^{A}	142±36.1^{A}	0.039^{ALA}
ALA LOX		129±54.1^{B}	124±40.3^{B}	544±222^{A}	336±75.8^{A}	
ALA total		132±57.6^{B}	125±40.3^{B}	546±222^{A}	338±76.0^{A}	0.042^{ALA}
EPA oxylipins						

14,15-EpETE	CYPe	3.47±3.42	0.060±0.0125	0.447±0.128	0.520±0.133	
17,18-DiHETE	CYPe	23.5±11.9^{bc}	<LOQ^{c}	140±35.0^{a}	44.2±10.0^{ab}	0.003^{KW}
EPA CYPe		26.9±11.7^{bc}	9.77±0.0125^{c}	140±35.0^{a}	44.8±9.99^{ab}	0.001^{KW}
18-HEPE	CYPh	3.64±0.898^{B}	12.3±1.64^{B}	35.1±5.72^{A}	33.3±4.63^{A}	<0.001^{ALA}
11-HEPE	LOX	3.81±0.791^{b}	<LOQ^{b}	26.2±4.50^{a}	15.8±3.14^{a}	0.003^{KW}
12-HEPE	LOX	<LOQ^{b}	2.01±0.251^{b}	12±2.94^{a}	8.96±1.41^{a}	0.003^{KW}
15-HEPE	LOX	<LOQ^{b}	<LOQ^{b}	23.6±3.24^{a}	21.0±3.29^{a}	0.002^{KW}
EPA LOX		10.1±0.791^{b}	8.86±0.251^{b}	61.7±9.76^{a}	45.8±6.92^{a}	<0.001^{KW}
EPA total		40.7±12.1^{B}	31.0±1.79^{B}	237±36.2^{A}	124±17.7^{A}	<0.001^{ALA}
DHA oxylipins						
16,17 EpDoPE	CYPe	12.7±3.82	23.8±8.45	53.0±9.35	42.6±10.3	
16,17-DiHDoPE	CYPe	0.317±0.0811^{B}	0.316±0.0152^{B}	0.848±0.0759^{A}	0.677±0.171^{A}	0.036^{ALA}
19,20-DiHDoPE	CYPe	0.719±0.124	0.989±0.0657	2.35±0.266	1.65±0.482	
DHA CYPe		13.7±3.77	25.1±8.42	56.2±9.35	44.9±10.4	
20-HDoHE	CYPh	81.1±28.2	66.3±11.2	97.9±13.6	72.0±13.3	
7-HDoHE	LOX	25.4±7.47	22.3±4.23	45.6±5.54	22.7±3.72	

10-HDoHE	LOX	24.6±7.46	17.8±5.07	31.1±6.88	16.9±3.15
13-HDoHE	LOX	175±105	91.4±31.8	76.6±7.15	58.7±7.30
14-HDoHE	LOX	194±119	72.0±25.9	71.3±8.02	49.9±9.49
16-HDoHE	LOX	67.2±27.8	44.5±11.3	49.8±5.86	35.7±6.42
17-HDoHE	LOX	271±119	229±35.6	321±27.8	253±46.8
DHA LOX		757±375	477±105	595±46.3	436±74.6
DHA total		852±401	569±110	750±51.6	553±94.2
COX total		2915±1112	3907±1062	2438±297	1916±311
CYPe total		346±54.5	564±136	720±45.8	579±92.0
CYPh total		220±64.0	216±29.5	200±23.0	160±26.5
LOX total		17211±5298	17527±2923	13540±2260	9846±1916
n-3		1025±457	724±150	1532±265	1016±171
n-6		19748±4527	21587±3231	15435±2258	11565±2124
total		20773±4959	22311±3342	16968±2515	12581±2285

Values mean ± standard error. Superscript uppercase letters indicate a main-effect group difference of diet or treatment. Superscript lowercase letters indicate interaction-effect group differences by Tukey's post-hoc test or pairwise comparison of groups using Dunn's test. FDR < 0.05 are listed, with ^{ALA} indicating a main-effect of dietary ALA, ^{2M} indicating a main-effect of 2-MCPD treatment, ^{INT} indicating an ALA x 2-MCPD interaction-effect, and ^{KW} indicating pairwise comparison using the Kruskal-Wallis test

was used. P-values were adjusted by the Benjamini-Hochberg procedure. P-values of the oxylipin totals were adjusted separately by category such that the comparisons were independent.

Study B: Supplemental Table 4. Rat serum oxylipins by diet group.

Rat Serum Oxylipins (ng/ml)

	Enzyme	CO (n=8)	C2M (n=8)	CA (n=8)	CA2M (n=8)	FDR
LA oxylipins						
9,10-EpOME	CYPe	2.53±0.455	1.86±0.509	5.57±4.01	1.28±0.266	
9,10-DiHOME	CYPe	7.93±0.828	6.11±1.04	7.31±0.885	4.86±0.796	
12,13-EpOME	CYPe	8.05±1.53	6.13±1.26	17.5±10.9	4.61±0.669	
12,13-DiHOME	CYPe	4.08±0.418	3.58±0.711	3.63±0.744	3.08±0.482	
LA CYPe		22.6±2.06	17.7±3.19	34.0±16.3	13.8±1.78	
9-HODE	LOX	39.6±3.85	41.1±6.52	41.9±16.7	39.8±4.87	
9-oxoODE	LOX	15.8±4.74	10.7±2.36	25.8±19.8	10.3±3.16	
13-HODE	LOX	37.1±3.59	35.8±6.10	40.1±16.7	31.0±3.95	
13-oxoODE	LOX	15.3±3.45	13.7±2.31	19.7±12.0	11.5±2.48	
(9,10,13- & 9,12,13-) triHOME	LOX	14.6±2.58	9.20±1.42	18.0±9.26	9.00±1.60	
LA LOX		122±16.7	110±16.9	146±74.3	102±14.5	
LA total		145±16.6	128±19.0	180±90.4	115±15.0	
GLA oxylipins						

13-HOTrE-γ	LOX	0.509±0.0634	0.802±0.174	0.349±0.130	0.480±0.0797
DGLA oxylipins					
TXB1	COX	4.95±0.446	3.27±0.548	4.82±0.399	4.83±0.813
15-HETrE	LOX	1.09±0.136	0.780±0.104	1.22±0.330	1.02±0.184
8-HETrE	LOX	0.601±0.104	0.387±0.0367	0.502±0.226	0.436±0.0789
DGLA LOX		1.69±0.237	1.17±0.136	1.72±0.554	1.45±0.250
DGLA total		6.64±0.660	4.43±0.672	6.54±0.711	6.29±1.00
AA oxylipins					
PGD2	COX	10.4±1.81	4.88±0.740	8.15±0.811	7.40±1.26
11β-PGF2α	COX	33.6±7.03	16.2±2.55	24.5±2.99	23.8±2.92
PGE2	COX	6.45±1.09	2.80±0.489	4.96±0.585	4.42±0.708
PGB2	COX	0.786±0.137	0.256±0.069	0.470±0.0816	0.624±0.268
11β-PGE2	COX	2.97±0.470	1.33±0.220	2.41±0.310	2.14±0.316
15k-PGE2	COX	1.12±0.276	1.13±0.217	1.28±0.379	1.29±0.438
6k-PGF1α	COX	0.0965±0.0120	0.0845±0.0204	0.281±0.201	0.119±0.0288
PGF2α	COX	5.54±0.795	2.60±0.436	4.38±0.284	3.98±0.646
TXB2	COX	230±20.7	144±26.1	216±19.8	223±38.5
12-HHTrE	COX	81.8±9.89	45.8±9.45	74.2±5.95	72.8±11.8

AA COX		373±39.7	219±38.5	337±28.8	339±54.2
5,6-EpETrE	CYPe	2.38±0.439	1.72±0.566	2.64±1.19	1.10±0.163
5,6-DiHETrE	CYPe	0.653±0.161	0.256±0.0390	0.418±0.0749	0.249±0.0369
8,9-DiHETrE	CYPe	0.223±0.0335	0.168±0.0178	0.170±0.048	0.185±0.0468
11,12-DiHETrE	CYPe	0.246±0.0337	0.194±0.0136	0.217±0.0627	0.187±0.0294
14,15-EpETrE	CYPe	0.410±0.0623	0.273±0.0574	0.684±0.441	0.197±0.0380
14,15-DiHETrE	CYPe	0.389±0.0557	0.276±0.0158	0.309±0.0898	0.280±0.0319
AA CYPe		4.31±0.629	2.88±0.638	4.44±1.87	2.20±0.289
17-HETE	CYPh	0.0349±0.00736	0.0311±0.00257	0.0428±0.0189	0.0333±0.00705
18-HETE	CYPh	0.0642±0.00739	0.0730±0.00938	0.0738±0.0222	0.067±0.0125
20-COOH-AA	CYPh	5.96±0.947	12.8±1.60	6.39±1.44	8.63±1.25
AA CYPh		6.05±0.950	12.9±1.60	6.51±1.48	8.73±1.25
5-HETE	LOX	8.52±2.16	4.79±0.477	7.51±3.14	4.62±0.953
5-oxoETE	LOX	19.0±8.02	7.82±0.938	15.3±8.44	9.05±2.58
8-HETE	LOX	8.31±2.00	6.99±0.995	6.56±2.60	6.47±0.747
11-HETE	LOX	32.6±3.57	20.5±4.13	28.6±4.40	28.1±5.38
12-HETE	LOX	1009±128	787±121	599±68.3	885±163
12-oxoETE	LOX	616±113	431±64.1	461±168	412±71.3
tetranor 12-HETE	LOX	2.07±0.304	2.27±0.567	1.14±0.150	1.65±0.436

15-HETE	LOX	14.5±2.34	9.30±1.37	14.1±3.00	11.6±1.45	
15-oxoETE	LOX	2.06±0.767	0.916±0.0979	1.78±0.853	1.02±0.237	
6t-LTB4	LOX	23.8±10.2	8.58±1.94	15.9±9.27	6.07±1.36	
AA LOX		1736±236	1279±163	1150±241	1365±220	
AA total		2119±272	1514±197	1498±246	1716±258	
ALA oxylipins						
9-HOTrE	LOX	0.434±0.0528^{B}	0.414±0.0843^{B}	2.83±1.28^{A}	1.63±0.303^{A}	<0.001^{ALA}
9-oxoOTrE	LOX	0.342±0.116^{B}	0.146±0.0509^{B}	2.15±1.17^{A}	0.807±0.209^{A}	<0.001^{ALA}
13-HOTrE	LOX	0.606±0.0708^{B}	0.570±0.0865^{B}	2.68±1.17^{A}	1.99±0.438^{A}	<0.001^{ALA}
ALA total		1.38±0.220^{B}	1.13±0.207^{B}	7.66±3.62^{A}	4.43±0.830^{A}	<0.001^{ALA}
EPA oxylipins						
18-HEPE	CYPh	<LOQ^{b}	<LOQ^{b}	0.228±0.11^{a}	0.195±0.11^{a}	0.006^{KW}
9-HEPE	LOX	0.188±0.0521^{b}	0.159±0.0517^{b}	1.25±0.174^{a}	1.81±0.404^{a}	<0.001^{KW}
12-HEPE	LOX	10.8±1.32^{b}	8.01±1.45^{b}	41.6±5.19^{a}	57.1±15.1^{a}	<0.001^{KW}
15-HEPE	LOX	0.0449±0.00801^{b}	<LOQ^{b}	0.368±0.150^{a}	0.273±0.0960^{a}	0.006^{KW}
EPA LOX		11.0±1.34^{B}	8.20±1.47^{B}	43.2±5.34^{A}	59.2±15.6^{A}	<0.001^{ALA}
EPA total		11.0±1.34^{B}	8.20±1.47^{B}	43.4±5.37^{A}	59.3±15.6^{A}	<0.001^{ALA}

DHA oxylipins						
16,17-DiHDoPE	CYPe	0.00803±0.00267	0.0140±0.00182	0.0267±0.0103	0.0239±0.00312	
20-HDoHE	CYPh	1.02±0.262	1.11±0.137	2.64±1.26	1.71±0.477	
7-HDoHE	LOX	0.211±0.0841	0.246±0.0397	0.832±0.517	0.375±0.129	
10-HDoHE	LOX	1.10±0.174^{B}	0.788±0.140^{B}	1.82±0.643^{A}	1.98±0.539^{A}	0.049^{ALA}
13-HDoHE	LOX	2.17±0.364^{B}	1.83±0.353^{B}	4.89±1.71^{A}	3.79±0.876^{A}	0.049^{ALA}
14-HDoHE	LOX	11.8±1.61	10.7±2.55	16.3±3.96	27.3±8.11	
16-HDoHE	LOX	0.483±0.119	0.333±0.0342	1.39±0.714	0.703±0.148	
17-HDoHE	LOX	4.28±0.772	3.87±0.494	10.5±4.70	7.08±1.36	
DHA LOX		20.0±2.87	17.8±3.38	35.7±12.1	41.2±10.8	
DHA total		21±3.11^{B}	18.9±3.5^{B}	38.3±13.3^{A}	42.9±10.9^{A}	0.031^{ALA}
COX total		378±40.1	222±39.1	342±29.2	344±55.0	
CYPe total		26.9±2.30	20.6±3.31	38.5±18.1	16.1±1.81	
CYPh total		7.11±0.980	14.1±1.68	9.37±2.82	10.6±1.55	
LOX total		1893±256	1419±172	1384±330	1574±249	
n-3		33.4±3.97^{B}	28.3±4.68^{B}	89.4±19.3^{A}	107±26.7^{A}	<0.001^{ALA}
n-6		2271±289	1647±202	1684±331	1838±263	

Total	2074±275	1532±183	1558±349	1722±261

Values mean ± standard error. Superscript uppercase letters indicate a main-effect group difference of diet or treatment. Superscript lowercase letters indicate interaction-effect group differences by Tukey's post-hoc test or pairwise comparison of groups using Dunn's test. Adjusted p-values < 0.05 are listed, with ^{ALA} indicating a main-effect of dietary ALA, ^{2M} indicating a main-effect of 2-MCPD treatment, ^{INT} indicating an ALA x 2-MCPD interaction-effect, and ^{KW} indicating pairwise comparison using the Kruskal-Wallis test was used. P-values were adjusted by the Benjamini-Hochberg procedure. P-values of the oxylipin totals were adjusted separately by category such that the comparisons were independent.

6. Study C: Supplemental Tables

Study C: Supplemental Table 1. Characteristics of healthy control patients included in the plasma oxylipins analysis.

	Control n=44
Age	59.7 (10.9)
Sex (Male)	24 (54.5%)
Height (cm)	167 (9.84)
Weight (kg)	86.3 (22.9)
BSA (m^2)	1.99 (0.294)
BMI	30.9 (7.68)
Hypertension	19 (43.2%)
History of Smoking	9 (20.5%)
Current	5 (11.4%)
Previous	4 (9.09%)
Never	35 (79.5%)
Medication	
ACE inhibitors or ARBs	8 (18.2%)
ASA	6 (13.6%)
Betablocker	8 (18.2%)
Statin	7 (15.9%)
Coronary artery bypass graft	0 (0%)
Coronary artery disease	1 (2.27%)
Diabetes	
Type 1	0 (0%)
Type 2	8 (18.2%)
Dyslipidemia	10 (22.7%)
Chronic renal failure	1 (2.27%)

End-stage renal disease on hemodialysis	0 (0%)
Family history of cardiovascular disease	4 (9.09%)
History of congestive heart failure	3 (6.82%)
History of peripheral vascular disease	1 (2.27%)
ST-elevation myocardial infarction	0 (0%)
Non-ST-elevation myocardial infarction	0 (0%)
NYHA Classification	
Class I	28 (50.9%)
Class II	8 (14.6%)
Class III	1 (1.82%)
Class IV	0 (0%)
Obstructive valvular heart disease	5 (9.09%)
Percutaneous coronary intervention	2 (3.64%)
History of Smoking	14 (25.5%)
Current	7 (12.7%)
Previous	7 (12.7%)
Never	41 (74.5%)
Stroke	3 (5.45%)

Continuous variables are given as mean (standard deviation) and categorical variables are given as count (proportion), Abbreviations: ACE, angiotensin-converting enzyme; ARBs, angiotensin II receptor blockers; ASA, Acetylsalicylic Acid; BMI, body mass index; BSA, body surface area; NYHA, New York Heart Association.

Study C: Supplemental Table 2. The complete list of deuterated internal standards and oxylipins scanned for.

Analyte	Q1 Mass (Da)	Q3 Mass (Da)	t_R (min)	LLOD (ng)	ULOD (ng)
Internal standards					
(d4) 6k-PGF1α	373	167	5.66	-	-
(d4) TXB2	373	173	6.97	-	-
(d4) PGF2α	357	197	7.55	-	-
(d4) PGE2	355	275	7.70	-	-
(d4) PGD2	355	275	8.08	-	-
(d4) 8-iso-PGF2αIII	357	197	6.81	-	-
(d4) 15d-PGJ2	319	203	14.72	-	-
(d4) dhk-PGF2α	357	295	8.95	-	-
(d4) LTB4	339	197	12.34	-	-
(d8) 5-HETE	327	116	17.33	-	-
(d8) 12-HETE	327	184	16.64	-	-
(d8) 15-HETE	327	226	16.11	-	-
(d6) 20-HETE	325	281	15.14	-	-
(d11) 8,9-DiHETrE	348	127	15.02	-	-
(d11) 11,12-DiHETrE	348	167	14.41	-	-
(d11) 14,15-DiHETrE	348	207	13.67	-	-
(d4) 9-HODE	299	172	16.03	-	-
(d4) 13-HODE	299	198	15.87	-	-
(d7) 5-oxoETE	323	279	17.74	-	-
(d5) RvD1	380	141	8.81	-	-
(d4) 9,10-diHOME	317	203	13.42	-	-
(d4) 12,13-diHOME	317	185	12.84	-	-
Oxylipins					
PGD2	351	271	8.12	0.00138	8.89

15d-PGD2	333	271	12.24	0.000395	8.89
dhk-PGD2	351	207	9.50	0.000395	8.89
15k-PGD2	349	235	8.95	-	-
PGJ2	333	189	10.17	0.000395	8.89
15d-PGJ2	315	203	14.74	0.00484	8.89
11β-PGF2α	353	335	7.01	0.00484	8.89
11β-dhk-PGF2α	353	113	8.47	0.00484	8.89
2,3-dinor-11β-PGF2α	325	227	5.94	0.00484	8.89
PGK2	349	249	8.84	0.00138	8.89
PGE2	351	271	7.71	0.00138	8.89
PGA2	333	271	10.00	0.000395	8.89
PGB2	333	271	10.25	0.00138	8.89
bicyclo-PGE2	333	175	10.86	0.00484	8.89
dhk-PGE2	351	207	8.72	0.0169	8.89
11β-PGE2	351	271	7.75	0.0169	8.89
15k-PGE2	349	235	8.09	0.00138	8.89
6k-PGF1α	369	245	5.68	0.00138	8.89
2,3-dinor-6k-PGF1α	341.2	261	6.90	-	-
6k-PGE1	367	331	5.95	0.000395	2.54
6,15-dk-dh-PGF1α	369	267	6.90	0.0169	8.89
PGF2α	353	193	7.56	0.000395	8.89
dh-PGF2α	355	283	8.25	-	-
dhk-PGF2α	353	291	8.97	0.000113	8.89
15k-PGF2α	351	219	8.02	0.00138	8.89
TXB2	369	169	6.94	0.00138	2.54
2,3-dinor-TXB2	341	137	5.92	0.00484	8.89
11d-TXB2	367	305	7.84	0.000395	8.89
12-HHTrE	279	217	13.82	0.00138	8.89
PGD1	353	235	8.03	0.000395	2.54
PGK1	351	251	9.09	0.00138	8.89
PGE1	353	235	7.90	0.000395	8.89

15k-PGE1	351.2	237	8.40	0.000395	2.54
PGF1α	355	293	7.54	0.000395	8.89
15k-PGF1α	353	221	8.19	0.000395	8.89
TXB1	371	171	6.60	0.00138	2.54
dihomo-PGD2	379	299	10.03	-	-
dihomo-15d-PGD2	361	299	14.31	-	-
dihomo-PGJ2	361	299	12.76	-	-
dihomo-PGE2	379	299	9.70	-	-
dihomo-PGF2α	381	337	9.50	0.00138	8.89
PGD3	349	269	7.09	0.00484	8.89
PGE3	349	269	6.75	0.00484	8.89
Δ17-6k-PGF1α	367	163	4.98	0.000113	8.89
PGF3α	351	193	6.54	0.00138	8.89
TXB3	367	169	6.03	0.00138	2.54
9-HODE	295	171	16.11	0.000113	8.89
9-oxoODE	293	185	16.38	0.00484	8.89
13-HODE	295	195	15.94	0.000113	8.89
13-oxoODE	293	167	16.06	0.00484	8.89
9,10,13-triHOME	329	171	7.65	0.000113	8.89
9,12,13-triHOME	329	211	7.53	0.000113	8.89
13-HOTrE-γ	293	193	15.08	0.00138	8.89
5-HETrE	321	205	18.91	0.00138	8.89
8-HETrE	321	157	17.30	0.000395	8.89
15-HETrE	321	221	16.88	0.000395	8.89
5-HETE	319	115	17.46	0.000113	8.89
5-oxoETE	317	203	17.84	0.000113	8.89
5,15-diHETE	335	201	11.92	0.00138	8.89
8-HETE	319	155	16.76	0.000395	8.89
9-HETE	319	123	17.06	0.00138	8.89
11-HETE	319	167	16.54	0.000395	8.89
12-HETE	319	135	16.72	0.00138	8.89

12-oxoETE	317	153	16.76	0.0169	8.89
tetranor-12-HETE	265	109	13.72	0.000113	8.89
15-HETE	319	175	16.17	0.00138	8.89
15-oxoETE	317	113	16.30	0.000113	8.89
8,15-diHETE	335	235	11.34	0.00484	8.89
6t-LTB4	335	195	11.96	0.00138	8.89
6t, 12-epi-LTB4	335	195	12.08	0.000395	8.89
5,6-diHETE	335	115	15.72	0.000395	8.89
LTB4	335	195	12.40	0.000395	8.89
12-oxo-LTB4	333	179	13.08	0.000395	8.89
20oh-LTB4	351	195	5.92	0.00138	8.89
20cooh-LTB4	365	195	5.77	0.00484	8.89
12-epi-LTB4	335	195	12.42	0.000395	8.89
LTC4	624	272	12.50	0.00138	8.89
LTD4	495	177	9.60	0.00138	8.89
LTE4	438	333	11.47	0.000395	8.89
14,15-LTC4 (EXC4)	624	272	7.80	-	-
14,15-LTD4 (EXD4)	495	177	11.34	-	-
14,15-LTE4 (EXE4)	438	333	9.30	-	-
6(R)-LXA4	351	217	8.85	0.00138	8.89
6(S)-LXA4	351	115	9.11	0.000395	8.89
15(R)-LXA4	351	165	8.85	-	-
LXB4	351	221	7.87	0.00138	8.89
HXA3	335	195	14.80	-	-
HXB3	335	183	15.00	-	-
15-oxoEDE	321	223	17.99	0.00138	8.89
9-HOTrE	293	171	14.68	0.00138	8.89
9-oxoOTrE	291	185	15.17	0.000113	8.89
13-HOTrE	293.4	195	14.75	0.00138	8.89
13-oxoOTrE	291	247	15.00	0.207	8.89
LXA5	349	215	7.82	0.00138	8.89

RvE1	349	195	5.84	0.000395	8.89
5-HEPE	317	115	16.04	0.00138	8.89
8-HEPE	317	155	15.50	0.00138	8.89
9-HEPE	317	149	15.67	0.00138	8.89
11-HEPE	317	167	15.28	0.000395	8.89
12-HEPE	317	179	15.47	0.00138	8.89
15-HEPE	317	219	15.16	0.0592	8.89
RvD1	375	141	8.93	0.000113	8.89
RvD2	375	175	8.04	0.00484	8.89
RvD5	359.2	199	11.78	0.000395	8.89
PD1	359	153	11.15	-	-
15t-PD1	359	153	11.40	-	-
4-HDoHE	343	101	17.77	0.00138	8.89
7-HDoHE	343	141	16.92	0.000395	8.89
8-HDoHE	343	109	17.06	0.00138	8.89
10-HDoHE	343	153	16.53	0.000113	8.89
11-HDoHE	343	149	16.70	0.00138	8.89
13-HDoHE	343	221	16.34	0.00138	8.89
14-HDoHE	343	205	16.45	0.00138	8.89
16-HDoHE	343	233	16.14	0.000395	8.89
17-HDoHE	343	245	16.24	0.0169	8.89
10(S),17(S)-DiHDoHE (PDX)	359	153	11.57	0.00138	8.89
4k-DHA	341	297	18.10	0.00138	8.89
17k-DHA	341	297	16.43	0.0169	8.89
7(R)-Maresin-1	359	177	11.79	0.00138	8.89
17k-DPA	343	247	16.99	0.00484	8.89
9,10-EpOME	295	171	17.55	0.000395	8.89
9,10-diHOME	313	201	13.48	0.000395	8.89
12,13-EpOME	295	195	17.29	0.00138	8.89
12,13-diHOME	313	183	12.92	0.000113	8.89
5,6-EpETrE	319	191	18.33	0.000395	8.89

5,6-DiHETrE	337	145	15.91	0.00138	8.89
8,9-EpETrE	319	155	18.05	0.00138	8.89
8,9-DiHETrE	337	127	15.13	0.00138	8.89
11,12-EpETrE	319	167	17.78	0.00138	8.89
11,12-DiHETrE	337	167	14.50	0.00138	8.89
14,15-EpETrE	319	175	17.33	0.00484	8.89
14,15-DiHETrE	337	207	13.77	0.000113	8.89
9,10-EpODE	293	171	16.40	-	-
9,10-diHODE	311	201	11.88	-	-
12,13-EpODE	293	183	16.30	0.000395	8.89
12,13-diHODE	311	183	11.40	0.000113	8.89
15,16-EpODE	293	235	16.00	-	-
15,16-diHODE	311	223	11.53	-	-
14,15-EpETE	317	207	16.39	0.000113	8.89
14,15-diHETE	335	207	12.31	0.00484	8.89
17,18-EpETE	317	259	16.00	0.00138	8.89
17,18-diHETE	335	247	11.76	0.00484	8.89
16,17-EpDoPE	343	193	17.58	0.0169	8.89
16,17-DiHoDPE	361	233	14.14	0.000395	8.89
19,20-EpDoPE	343	241	17.09	0.00484	8.89
19,20-DiHDoPE	361	229	13.62	0.00484	8.89
16-HETE	319	189	15.62	0.000395	8.89
17-HETE	319	247	15.51	0.00138	8.89
18-HETE	319	261	15.40	0.00138	8.89
19-HETE	319	231	15.03	0.0592	8.89
20-HETE	319	245	15.17	0.00138	8.89
20cooh-AA	333	271	14.80	0.00484	8.89
18-HEPE	317	215	14.66	0.00138	8.89
20-HDoHE	343	241	15.88	0.00484	8.89
2,3-dinor 8-iso-PGF2α	325	237	5.55	0.00138	8.89
8-iso-15k-PGF2β	351	219	7.28	0.0169	8.89

5-iso-PGF2αVI	353	115	7.44	0.000395	8.89
8-iso-PGF2αIII	353	193	6.81	0.00484	8.89
8-iso-PGF3α	351	307	5.82	-	-
9-Nitrooleate	326	168	19.44	-	-
10-Nitrooleate	326	169	19.44	-	-
15d-PGA2	315	271	15.31	0.0592	8.89

LLOD and ULOD values were determined using 40 µL on the column of standards in MS grade water: acetonitrile: acetic acid (70:30:0.02; v/v/v). Abbreviations: AA, arachidonic acid; DHA, docosahexaenoic acid; DiHDoPE, dihydroxy-docosapentaenoic acid; DiHETE, dihydroxy-eicosatetraenoic acid; DiHETrE, dihydroxy-eicosatrienoic acid; DiHODE, dihydroxy-octadienoic acid; DiHOME, dihydroxy-octadecaenoic acid; DPA, docosapentaenoic acid; EpDoPE, epoxy-docosapentaenoic acid; EpETE, epoxy-eicosatetraenoic acid; EpETrE, epoxy-eicosatrienoic acid; EpODE, epoxy-octadecadienoic acid; EpOME, epoxy-octadecaenoic acid; HDoHE, hydroxy-docosahexaenoic acid; HEPE, hydroxy-eicosapentaenoic acid; HETE, hydroxy-eicosatetraenoic acid; HETrE, hydroxy-eicosatrienoic acid; HHTrE, hydroxyheptadecatrienoic acid; HODE, hydroxy-octadecadienoic acid; HOTrE, hydroxy-octadecatrienoic acid; HX, hepoxilin; LA, linoleic acid; LLOD, lower limit of detection; LT, leukotriene; LX, lipoxin; oxoEDE, oxo-eicosadienoic acid; oxoETE, oxo-eicosatetraenoic acid; oxoODE, oxo-octadecadienoic acid; oxoOTrE, oxo-octadecatrienoic acid; P, protectin; PG, prostaglandin; Rv, resolvin; triHOME, trihydroxy-octadecenoic acid; TX, thromboxane; ULOD, upper limit of detection.

Study C: Supplemental Table 3. Aortic valve leaflet oxylipins by aortic valve stenosis severity group determined by patient transvalvular mean pressure gradient.

Aortic Valve Leaflet Oxylipins (µg/g protein)						
Oxylipin	Enz	Mild n=15	Moderate n=39	Severe n=45	*P* value	Adjusted *P* values
LA oxylipins						
9,10-diHOME	CYP	0.107±0.0461	0.156±0.0266	0.197±0.0292	0.060	>0.99
12,13-diHOME	CYP	0.119±0.0580[b]	0.207±0.0363[ab]	0.232±0.0387[a]	0.041	>0.99
LA CYP total		0.226±0.104[b]	0.363±0.0615[ab]	0.429±0.0672[a]	0.023	0.14
9-HODE	LOX	70.2±42.9[b]	121±14.8[a]	174±29.8[a]	<0.001	0.002
9-oxoODE	LOX	26.7±7.84[b]	55.6±7.63[a]	66.3±10.8[a]	0.001	0.049
13-HODE	LOX	77.8±53.1[b]	122±15.2[a]	183±32.4[a]	<0.001	0.002
13-oxoODE	LOX	57.8±24.5[b]	125±17.6[a]	178±38.7[a]	<0.001	0.008
(9,10,13- & 9,12,13-) triHOME	LOX	1.22±0.656[b]	2.33±0.325[a]	2.69±0.434[a]	<0.001	0.023
LA LOX total		234±128[b]	426±52.4[a]	604±106[a]	<0.001	<0.001
LA total		234±128[b]	426±52.4[a]	604±106[a]	<0.001	<0.001
GLA oxylipins						
13-HOTrE-γ	LOX	0.304±0.152[b]	0.936±0.116[a]	1.12±0.168[a]	<0.001	<0.001

DGLA oxylipins						
8-HETrE	LOX	1.87±1.22[b]	3.25±0.378[a]	4.91±0.653[a]	<0.001	<0.001
15-HETrE	LOX	0.727±0.479[b]	1.10±0.134[a]	1.58±0.196[a]	<0.001	<0.001
DGLA total		2.59±1.70[b]	4.35±0.505[a]	6.49±0.842[a]	<0.001	<0.001
AA oxylipins						
PGE2	COX	0.156±0.0337[b]	0.528±0.197[ab]	1.06±0.310[a]	<0.001	0.010
12-HHTrE	COX	3.18±0.693[b]	7.49±1.89[ab]	13.6±2.68[a]	0.001	0.051
PGB2	COX	9.94±5.48[b]	22.6±2.74[a]	28.9±3.38[a]	<0.001	<0.001
PGF2α	COX	0.865±0.311[b]	2.30±0.360[ab]	2.99±0.315[a]	0.001	0.048
TXB2	COX	0.314±0.0938[b]	0.613±0.132[b]	1.16±0.191[a]	<0.001	<0.001
6k-PGF1α	COX	3.01±0.613[b]	5.67±1.08[a]	9.87±1.63[a]	<0.001	<0.001
AA COX		17.5±6.24[b]	39.2±5.25[a]	57.5±5.56[a]	<0.001	<0.001
14,15-diHETrE	CYP	0.117±0.0558[ab]	0.165±0.0150[a]	0.205±0.0197[a]	<0.001	0.008
5-HETE	LOX	45.6±26.8[b]	110±14.7[a]	154±19.8[a]	<0.001	<0.001
8-HETE	LOX	8.44±3.41[b]	20.9±2.33[a]	29.2±3.42[a]	<0.001	<0.001
11-HETE	LOX	4.95±2.41[b]	11.9±1.40[a]	16.4±2.34[a]	<0.001	<0.001
12-HETE	LOX	3.19±1.22[b]	7.95±0.900[a]	11.0±1.21[a]	<0.001	<0.001

15-HETE	LOX	7.02±3.36[b]	17.8±1.99[a]	24.0±2.87[a]	<0.001	<0.001
15-oxoETE	LOX	2.46±0.660[b]	5.71±0.770[a]	6.08±0.602[a]	<0.001	0.010
8,15-diHETE	LOX	2.16±1.23[b]	5.37±0.646[a]	7.50±1.10[a]	<0.001	<0.001
AA LOX		73.8±38.7[b]	180±21.5[a]	248±30.2[a]	<0.001	<0.001
5-iso PGF2α VI	Non-Enz	0.967±0.523[b]	1.99±0.309[a]	2.26±0.295	<0.001	0.007
AA total		92.4±45.2[b]	221±25.5[a]	308±33.3[a]	<0.001	<0.001
ALA oxylipins						
9-HOTrE	LOX	0.463±0.350[b]	1.05±0.177[a]	1.43±0.220[a]	<0.001	0.007
13-HOTrE	LOX	4.73±3.26[b]	8.74±1.22[a]	10.8±1.66[a]	<0.001	0.003
ALA total		5.19±3.61[b]	9.79±1.39[a]	12.2±1.87[a]	<0.001	<0.001
EPA oxylipins						
18-HEPE	CYP	0.319±0.136[b]	1.42±0.205[a]	1.74±0.211[a]	<0.001	<0.001
5-HEPE	LOX	18.9±10.1[b]	71.2±10.9[a]	90.7±13.1[a]	<0.001	<0.001
12-HEPE	LOX	0.288±0.0877[b]	1.13±0.165[a]	1.38±0.150[a]	<0.001	<0.001
15-HEPE	LOX	0.283±0.123[b]	1.04±0.137[a]	1.24±0.137[a]	<0.001	<0.001
EPA LOX		19.5±10.3[b]	73.3±11.1[a]	93.3±13.3[a]	<0.001	<0.001

EPA total		19.8±10.4[b]	74.8±11.3[a]	95.0±13.5[a]	<0.001	<0.001
DHA oxylipins						
20-HDoHE	CYP	1.32±0.720[b]	3.02±0.395[a]	4.29±0.516[a]	<0.001	<0.001
					<0.001	<0.001
13-HDoHE	LOX	2.70±1.35[b]	6.65±0.839[a]	9.03±1.04[a]	<0.001	<0.001
14-HDoHE	LOX	0.707±0.360[b]	1.60±0.197[a]	2.33±0.239[a]	<0.001	<0.001
16-HDoHE	LOX	0.876±0.470[b]	1.92±0.248[a]	2.79±0.321[a]	<0.001	<0.001
17-HDoHE	LOX	2.44±1.34[b]	5.48±0.721[a]	7.70±0.830[a]	<0.001	<0.001
DHA LOX		6.72±3.51[b]	15.7±1.98[a]	21.8±2.41[a]	<0.001	<0.001
DHA total		8.04±4.23[b]	18.7±2.37[a]	26.1±2.92[a]	<0.001	<0.001
COX total		17.5±6.24[b]	39.2±5.25[a]	57.5±5.56[a]	<0.001	<0.001
CYP total		1.97±1.01[b]	4.±0.433[a]	4.97±0.610[a]	<0.001	<0.001
LOX total		342±185[b]	710±79.9[a]	987±143[a]	<0.001	<0.001
Total oxylipins		362±192[b]	756±84.0[a]	1053±146[a]	<0.001	-

Values are mean ± standard error. Adjusted *P* values are calculated using the Bonferroni correction for multiple comparisons, with the PUFA totals, Enzyme totals, and PUFA-Enzyme totals calculated separately. AA, arachidonic acid; ALA, α-linolenic acid;

COX, cyclooxygenase; CYP, cytochrome P450; DGLA, dihomo-γ-linolenic acid; diHETE, dihydroxy-eicosatetraenoic acid; diHETrE, dihydroxy-eicosatrienoic acid; diHOME, dihydroxy-octadecaenoic acid; DHA, docosahexaenoic acid; Enz, enzymatic pathway; GLA, γ-linolenic acid; HDoHE, hydroxy-docosahexaenoic acid; HEPE, hydroxy-eicosapentaenoic acid; HETE, hydroxy-eicosatetraenoic acid; HETrE, hydroxy-eicosatrienoic acid; HHTrE, hydroxyheptadecatrienoic acid; HODE, hydroxy-octadecadienoic acid; HOTrE, hydroxy-octadecatrienoic acid; k, keto; LA, linoleic acid; LOX, lipoxygenase; Non-Enz, non-enzymatically produced; oxoETE, oxo-eicosatetraenoic acid; oxoODE, oxo-octadecadienoic acid; PG, prostaglandin; triHOME, trihydroxy-octadecenoic acid (9,10,13-triHOME & 9,12,13-triHOME peaks could not be separated); TX, thromboxane.

Study C: Supplemental Table 4. Aortic Valve Oxylipins by patient ASA use.

Aortic Valve Leaflet Oxylipins (µg/g protein)					
Oxylipin	Enz	No ASA n=74	ASA n=25	*P* value	Adjusted *P* value
LA oxylipins					
9,10-diHOME	CYP	0.173±0.0227	0.182±0.0369	0.82	>0.99
12,13-diHOME	CYP	0.213±0.0305	0.223±0.0476	0.59	>0.99
LA CYP total		0.386±0.0527	0.405±0.0822	0.54	>0.99
9-HODE	LOX	141±21.2	153±28.8	0.58	>0.99
9-oxoODE	LOX	60.2±8.20	54.6±7.03	0.76	>0.99
13-HODE	LOX	146±22.6	163±35.4	0.53	>0.99
13-oxoODE	LOX	150±27.4	134±19.8	0.38	>0.99
(9,10,13- & 9,12,13-) triHOME	LOX	2.43±0.328	2.48±0.472	0.78	>0.99
LA LOX total		499±75.2	507±88.3	0.57	>0.99
LA total		500±75.3	507±88.3	0.57	>0.99
GLA oxylipins					
13-HOTrE-γ	LOX	0.949±0.122	1.04±0.169	0.68	>0.99
DGLA oxylipins					

8-HETrE	LOX	3.49±0.464	5.21±0.830	0.083	>0.99
15-HETrE	LOX	1.20±0.149	1.64±0.291	0.14	>0.99
DGLA total		4.69±0.607	6.85±1.11	0.089	0.53
AA oxylipins					
PGE2	COX	0.61±0.172	0.731±0.253	0.22	>0.99
12-HHTrE	COX	8.17±1.48	12.4±3.44	0.28	>0.99
PGB2	COX	23.4±2.70	28.1±3.69	0.25	>0.99
PGF2α	COX	2.18±0.229	3.20±0.538	0.13	>0.99
TXB2	COX	0.758±0.119	0.984±0.254	0.55	>0.99
6k-PGF1α	COX	6.81±1.02	8.13±2.04	0.43	>0.99
AA COX		42.0±4.14	53.5±7.86	0.20	>0.99
14,15-diHETrE	CYP	0.169±0.0151	0.219±0.0339	0.13	>0.99
5-HETE	LOX	115±14.2	157±24.9	0.17	>0.99
8-HETE	LOX	22.1±2.52	28.1±3.56	0.18	>0.99
11-HETE	LOX	12.9±1.70	15.2±2.13	0.30	>0.99
12-HETE	LOX	8.25±0.886	10.2±1.30	0.19	>0.99
15-HETE	LOX	18.6±2.15	22.9±2.99	0.22	>0.99
15-oxoETE	LOX	5.47±0.572	5.77±0.659	0.56	>0.99

8,15-diHETE	LOX	5.96±0.804	6.67±0.960	0.33	>0.99
AA LOX		188±22.1	246±35.4	0.18	>0.99
5-iso PGF2α VI	Non-Enz	1.97±0.238	2.32±0.429	0.36	>0.99
AA total		232±25.2	302±40.1	0.16	0.96
ALA oxylipins					
9-HOTrE	LOX	1.13±0.166	1.36±0.280	0.37	>0.99
13-HOTrE	LOX	9.25±1.23	10.3±2.26	0.68	>0.99
ALA total		10.4±1.39	11.7±2.52	0.65	>0.99
EPA oxylipins					
18-HEPE	CYP	1.33±0.152	1.83±0.313	0.21	>0.99
5-HEPE	LOX	67.0±8.16	99.6±20.3	0.19	>0.99
12-HEPE	LOX	1.04±0.105	1.44±0.258	0.21	>0.99
15-HEPE	LOX	0.966±0.100	1.31±0.213	0.21	>0.99
EPA LOX		69.0±8.35	102±20.7	0.19	>0.99
EPA total		70.4±8.48	104±21.0	0.19	>0.99

DHA oxylipins					
20-HDoHE	CYP	2.89±0.342	5.11±0.719	0.017	0.62
13-HDoHE	LOX	6.51±0.73	9.94±1.43	0.061	>0.99
14-HDoHE	LOX	1.60±0.169	2.57±0.346	0.025	0.88
16-HDoHE	LOX	1.94±0.228	3.09±0.430	0.036	>0.99
17-HDoHE	LOX	5.42±0.598	8.59±1.23	0.048	>0.99
DHA LOX		15.5±1.71	24.2±3.42	0.048	0.29
DHA total		18.4±2.05	29.3±4.13	0.040	0.24
COX total		42.0±4.14	53.5±7.86	0.20	0.60
CYP total		4.77±0.529	7.57±1.07	0.040	0.12
LOX total		788±102	899±139	0.39	>0.99
Total oxylipins		837±106	962±145	0.36	-

Values are mean ± standard error. Adjusted *P* values are calculated using the Bonferroni correction for multiple comparisons, with the PUFA totals, Enzyme totals, and PUFA-Enzyme totals calculated separately. AA, arachidonic acid; ALA, α-linolenic acid; COX, cyclooxygenase; CYP, cytochrome P450; DGLA, dihomo-γ-linolenic acid; diHETE, dihydroxy-eicosatetraenoic acid; diHETrE, dihydroxy-eicosatrienoic acid; diHOME, dihydroxy-octadecaenoic acid; DHA, docosahexaenoic acid; Enz, enzymatic pathway; GLA,

γ-linolenic acid; HDoHE, hydroxy-docosahexaenoic acid; HEPE, hydroxy-eicosapentaenoic acid; HETE, hydroxy-eicosatetraenoic acid; HETrE, hydroxy-eicosatrienoic acid; HHTrE, hydroxyheptadecatrienoic acid; HODE, hydroxy-octadecadienoic acid; HOTrE, hydroxy-octadecatrienoic acid; k, keto; LA, linoleic acid; LOX, lipoxygenase; Non-Enz, non-enzymatic production; oxoETE, oxo-eicosatetraenoic acid; oxoODE, oxo-octadecadienoic acid; PG, prostaglandin; triHOME, trihydroxy-octadecenoic acid (9,10,13-triHOME & 9,12,13-triHOME peaks could not be separated); TX, thromboxane.

Study C: Supplemental Table 5. Plasma oxylipins by aortic valve stenosis severity determined by patient transvalvular mean pressure gradient.

Oxylipin	Enzyme	Plasma Oxylipins (ng/ml) Control n=44	Mild n=5	Moderate n=27	Severe n=31	*P* value	Adjusted *P* value
LA oxylipins							
9-HODE	LOX	7.75±0.659[b]	16.7±3.37[a]	17.4±1.44[a]	20.7±1.62[a]	<0.001	<0.001
9-oxoODE	LOX	0.993±0.101[b]	4.62±0.663[a]	7.63±1.44[a]	6.77±0.681[a]	<0.001	<0.001
13-HODE	LOX	3.43±0.256[b]	7.97±1.65[a]	7.61±0.545[a]	9.38±0.635[a]	<0.001	<0.001
13-oxoODE	LOX	0.444±0.0649[b]	5.15±0.559[a]	7.70±1.28[a]	9.54±1.46[a]	<0.001	<0.001
(9,10,13- & 9,12,13-) triHOME	LOX	4.39±0.396[a]	0.175±0.0349[b]	0.216±0.0185[b]	0.316±0.0353[b]	<0.001	<0.001
LA total		17.0±1.20[b]	34.6±5.99[a]	40.6±4.05[a]	46.7±4.09[a]	<0.001	<0.001
GLA oxylipins							
13-HOTrE-γ	LOX	9.45±0.705[a]	0.0979±0.0267[b]	0.156±0.0212[b]	0.152±0.0137[b]	<0.001	<0.001
DGLA oxylipins							
8-HETrE	LOX	0.347±0.0431[a]	0.120±0.0385[b]	0.144±0.0194[ab]	0.135±0.0106[ab]	<0.001	<0.001
15-HETrE	LOX	0.190±0.0203	0.0886±0.0194	0.149±0.0106	0.141±0.0103	0.24	>0.99

DGLA total		0.537±0.0546[a]	0.208±0.0570[b]	0.292±0.0280[ab]	0.276±0.0196[ab]	<0.001	0.002
AA oxylipins							
5-HETE	LOX	0.917±0.233[b]	0.984±0.266[ab]	1.17±0.111[a]	1.25±0.0849	<0.001	<0.001
8-HETE	LOX	23.2±1.46[a]	0.381±0.115[b]	0.537±0.0700[b]	0.482±0.0347[b]	<0.001	<0.001
11-HETE	LOX	0.264±0.0356	0.126±0.0279	0.165±0.0142	0.161±0.0151	0.14	3.98
12-HETE	LOX	0.255±0.0492[b]	4.18±2.25[a]	6.33±1.06[a]	7.41±1.30[a]	<0.001	<0.001
tetranor 12-HETE	LOX	0.659±0.0637[b]	0.252±0.0921[a]	0.303±0.0575[a]	0.270±0.0317[a]	<0.001	<0.001
15-HETE	LOX	0.472±0.0539[b]	0.560±0.157[ab]	0.817±0.108[ab]	1.04±0.204[a]	<0.001	<0.001
AA total		25.7±1.67[a]	6.48±2.70[b]	9.32±1.13[b]	10.6±1.38[b]	<0.001	<0.001
ALA oxylipins							
9-HOTrE	LOX	0.393±0.0288[b]	2.82±0.782[a]	2.99±0.274[a]	3.70±0.316[a]	<0.001	<0.001
9-oxoOTrE	LOX	1.73±0.184[a]	0.613±0.106[b]	1.10±0.168[ab]	1.16±0.153[ab]	0.005	0.14
13-HOTrE	LOX	0.302±0.0434[b]	1.21±0.341[a]	1.38±0.121[a]	1.71±0.143[a]	<0.001	<0.001
ALA total		2.43±0.233[b]	4.64±1.21[a]	5.48±0.480[a]	6.58±0.567[a]	<0.001	<0.001
EPA oxylipins							
5-HEPE	LOX	0.733±0.0781[a]	0.287±0.0769[b]	0.448±0.0986[ab]	0.489±0.0516[ab]	0.010	0.28

12-HEPE	LOX	0.727±0.0624[a]	0.915±0.396[a]	1.85±0.305[a]	3.23±0.660[a]	0.012	0.34
15-HEPE	LOX	0.176±0.0156	0.0824±0.0164	0.149±0.0119	0.177±0.0229	0.31	>0.99
EPA total		1.64±0.124[ab]	1.28±0.459[b]	2.45±0.322[ab]	3.89±0.705[a]	0.042	0.25
DPA oxylipins							
17k-DPA	LOX	0.435±0.0653[b]	6.78±1.97[a]	13.2±1.46[a]	12.4±1.26[a]	<0.001	<0.001
DHA oxylipins							
4-HDoHE	LOX	0.229±0.0239[b]	0.574±0.131[a]	0.770±0.0639[a]	0.958±0.112[a]	<0.001	<0.001
7-HDoHE	LOX	0.313±0.0600[b]	0.263±0.0499[ab]	0.377±0.0414[a]	0.377±0.0364[a]	0.004	0.11
8-HDoHE	LOX	0.384±0.0791[b]	0.368±0.104[ab]	0.480±0.0411[a]	0.567±0.0561[a]	<0.001	<0.001
10-HDoHE	LOX	1.15±0.182[a]	0.165±0.0537[b]	0.269±0.0310[b]	0.316±0.0401[b]	<0.001	<0.001
11-HDoHE	LOX	5.23±0.645[a]	0.230±0.0752[c]	0.353±0.0391[bc]	0.455±0.0590[b]	<0.001	<0.001
14-HDoHE	LOX	1.65±0.277[a]	1.92±0.825[a]	4.02±0.694[a]	5.34±0.912[a]	0.007	0.20
16-HDoHE	LOX	0.549±0.0842[a]	0.0994±0.0425[b]	0.207±0.0348[ab]	0.269±0.0444[ab]	<0.001	0.001
17-HDoHE	LOX	1.81±0.123[a]	0.377±0.113[c]	0.619±0.0572[bc]	0.715±0.0745[b]	<0.001	<0.001
DHA total		11.3±1.05[a]	4.00±1.28[b]	7.09±0.845[ab]	8.99±1.22[ab]	0.002	0.011
Total oxylipins		68.5±4.22[ab]	58.1±11.7[b]	78.6±5.46[ab]	89.6±7.04[a]	0.019	-

Values are mean ± standard error. Adjusted *P* values are calculated using the Bonferroni correction for multiple comparisons, with the PUFA totals calculated separately. AA, arachidonic acid; ALA, α-linolenic acid; DGLA, dihomo-γ-linolenic acid; DHA, docosahexaenoic acid; DPA, docosapentaenoic acid; GLA, γ-linolenic acid; HDoHE, hydroxy-docosahexaenoic acid; HEPE, hydroxy-eicosapentaenoic acid; HETE, hydroxy-eicosatetraenoic acid; HETrE, hydroxy-eicosatrienoic acid; HODE, hydroxy-octadecadienoic acid; HOTrE, hydroxy-octadecatrienoic acid; LA, linoleic acid; LOX, lipoxygenase; oxoODE, oxo-octadecadienoic acid; oxoOTrE, oxo-octadecatrienoic acid; triHOME, trihydroxy-octadecenoic acid (9,10,13- triHOME & 9,12,13-triHOME peaks could not be separated).

Study C: Supplemental Table 6. Aortic valve leaflet oxylipins grouped by patient aortic valve stenosis severity (transvalvular mean pressure gradient) and sex.

Aortic Valve Leaflet Oxylipins Sex x MPG-Severity (µg/g protein)							
Oxylipin	Enz	Female-Mild n=3	Female-Moderate n=16	Female-severe n=12	Male-mild n=12	Male-moderate n=23	Male-severe n=33
LA oxylipins							
9,10-diHOME	CYP	0.0294±0.0120	0.214±0.0574	0.226±0.0732	0.127±0.0567	0.116±0.0182	0.187±0.0303
12,13-diHOME	CYP	0.0295±0.0274	0.262±0.0770	0.279±0.0954	0.141±0.0714	0.169±0.0298	0.215±0.0404
LA CYP total	CYP	0.0589±0.0394	0.476±0.134	0.505±0.166	0.268±0.128	0.285±0.0442	0.402±0.0702
9-HODE	LOX	7.50±1.57	134±26.3	267±88.7	85.9±53.1	112±17.6	140±23.5
9-oxoODE	LOX	8.62±4.47	69.9±15.8	87.5±19.4	31.2±9.36	45.6±6.41	58.6±12.8
13-HODE	LOX	5.12±1.05	139±27.5	281±93.1	95.9±65.8	110±17.4	147±27.2
13-oxoODE	LOX	12.3±6.71	149±35.4	253±97.2	69.2±29.9	108±16.7	150±39.3
(9,10,13- & 9,12,13-) triHOME	LOX	0.182±0.0589	2.87±0.658	3.53±1.16	1.48±0.808	1.95±0.299	2.39±0.419
LA LOX total	LOX	33.7±13.4	496±99.8	892±296	284±158	377±55.3	499±93.2
LA total		33.8±13.4	496±99.9	893±297	284±158	377±55.3	499±93.3

GLA oxylipins							
13-HOTrE-γ	LOX	0.0421±0.000588	0.952±0.177	1.66±0.347	0.370±0.187	0.924±0.156	0.930±0.183
DGLA oxylipins							
8-HETrE	LOX	0.176±0.0219	3.35±0.571	7.19±1.73	2.29±1.51	3.18±0.514	4.08±0.587
15-HETrE	LOX	0.0729±0.0287	1.21±0.222	2.27±0.502	0.891±0.594	1.02±0.170	1.33±0.182
DGLA total		0.249±0.0454	4.56±0.773	9.47±2.21	3.18±2.11	4.2±0.679	5.41±0.763
AA oxylipins							
PGE2	COX	0.0728±0.0275	0.296±0.095	0.425±0.0714	0.177±0.0397	0.690±0.326	1.29±0.416
12-HHTrE	COX	2.15±1.27	5.97±1.96	6.34±0.957	3.43±0.813	8.55±2.93	16.2±3.55
PGB2	COX	0.365±0.218	21.4±3.82	40.3±8.06	12.3±6.72	23.5±3.87	24.7±3.36
PGF2α	COX	0.363±0.147	1.91±0.454	2.61±0.378	0.99±0.381	2.57±0.522	3.13±0.407
TXB2	COX	0.170±0.119	0.465±0.125	0.674±0.0870	0.35±0.113	0.716±0.207	1.34±0.253
6k-PGF1α	COX	2.49±1.71	5.00±1.40	5.36±1.05	3.14±0.676	6.14±1.56	11.5±2.13
AA COX		5.61±3.26	35.1±6.75	55.7±7.66	20.4±7.58	42.1±7.62	58.2±7.11
14,15-diHETrE	CYP	0.0369±0.000429	0.161±0.0222	0.257±0.047	0.137±0.0691	0.167±0.0206	0.186±0.0202
5-HETE	LOX	3.27±0.749	86.4±13.0	219±43.1	56.2±33.1	127±22.8	130±20.9
8-HETE	LOX	1.55±0.332	20.2±3.08	40.2±8.28	10.2±4.14	21.3±3.37	25.2±3.39

11-HETE	LOX	0.929±0.159	11.6±2.02	22.9±4.93	5.96±2.96	12.2±1.95	14.1±2.56
12-HETE	LOX	0.636±0.0798	7.53±1.21	14.3±2.69	3.83±1.47	8.24±1.29	9.85±1.29
15-HETE	LOX	1.09±0.0869	17.1±2.74	34.1±7.01	8.50±4.12	18.4±2.84	20.3±2.78
15-oxoETE	LOX	1.36±0.565	6.71±1.54	7.09±1.00	2.73±0.803	5.01±0.746	5.71±0.733
8,15-diHETE	LOX	0.176±0.0755	5.12±0.968	10.7±2.77	2.65±1.51	5.54±0.880	6.33±1.07
AA LOX		9.01±1.32	155±22.5	349±66.4	90.1±47.6	197±32.9	212±31.7
5-iso PGF2α VI	Non-Enz	0.0873±0.0201	1.73±0.331	3.04±0.570	1.19±0.642	2.17±0.473	1.98±0.336
AA total		14.7±4.57	192±28.1	408±73.4	112±55.4	242±38.6	272±35.4
ALA oxylipins							
9-HOTrE	LOX	<LOQ	1.32±0.301	2.12±0.512	0.578±0.435	0.861±0.211	1.18±0.225
13-HOTrE	LOX	0.249±0.0464	10.7±2.15	14.9±3.80	5.85±4.04	7.37±1.41	9.28±1.76
ALA total		0.249±0.0464	12.0±2.43	17.0±4.29	6.42±4.47	8.23±1.61	10.5±1.98
EPA oxylipins							
18-HEPE	CYP	0.0808±0.00566	1.44±0.252	2.55±0.550	0.378±0.167	1.40±0.305	1.44±0.188
5-HEPE	LOX	1.81±0.389	60.1±11.2	140±37.8	23.2±12.4	78.9±16.7	72.8±10.2

12-HEPE	LOX	0.111±0.00177	1.09±0.193	1.83±0.392	0.333±0.107	1.15±0.249	1.22±0.142
15-HEPE	LOX	0.0591±0.0128	1.08±0.168	1.73±0.351	0.339±0.150	1.01±0.205	1.06±0.127
EPA LOX		1.98±0.375	62.3±11.5	143±38.5	23.8±12.6	81.0±17.1	75.1±10.4
EPA total		2.06±0.380	63.7±11.7	146±39.0	24.2±12.8	82.4±17.4	76.6±10.6
DHA oxylipins							
20-HDoHE	CYP	0.193±0.0242	2.62±0.421	6.27±1.48	1.60±0.889	3.30±0.603	3.57±0.408
13-HDoHE	LOX	0.488±0.0765	5.98±0.856	13.1±3.01	3.25±1.66	7.12±1.30	7.56±0.804
14-HDoHE	LOX	0.121±0.0247	1.46±0.215	3.20±0.646	0.854±0.443	1.71±0.301	2.01±0.207
16-HDoHE	LOX	0.116±0.0189	1.69±0.279	4.04±0.898	1.07±0.579	2.08±0.375	2.33±0.261
17-HDoHE	LOX	0.365±0.0371	4.90±0.844	10.9±2.38	2.95±1.65	5.87±1.08	6.55±0.655
DHA LOX	LOX	1.09±0.0688	14.0±2.15	31.2±6.91	8.13±4.33	16.8±3.03	18.5±1.90
DHA total		1.28±0.0501	16.7±2.55	37.4±8.38	9.73±5.22	20.1±3.62	22.0±2.29
COX total		5.61±3.26	35.1±6.75	55.7±7.66	20.4±7.58	42.1±7.62	58.2±7.11
CYP total		0.370±0.0453	4.69±0.696	9.59±2.17	2.38±1.24	5.16±0.926	5.6±0.635
LOX total		46.3±14.8	744±130	1443±377	416±228	685±103	821±131
Total oxylipins		52.4±18.1	786±136	1512±387	440±237	735±109	886±135

Values are mean ± standard error. AA, arachidonic acid; ALA, α-linolenic acid; COX, cyclooxygenase; CYP, cytochrome P450; DGLA, dihomo-γ-linolenic acid; diHETE, dihydroxy-eicosatetraenoic acid; diHETrE, dihydroxy-eicosatrienoic acid; diHOME, dihydroxy-octadecaenoic acid; DHA, docosahexaenoic acid; Enz, Enzymatic pathway; GLA, γ-linolenic acid; HDoHE, hydroxy-docosahexaenoic acid; HEPE, hydroxy-eicosapentaenoic acid; HETE, hydroxy-eicosatetraenoic acid; HETrE, hydroxy-eicosatrienoic acid; HHTrE, hydroxyheptadecatrienoic acid; HODE, hydroxy-octadecadienoic acid; HOTrE, hydroxy-octadecatrienoic acid; k, keto; LA, linoleic acid; LOX, lipoxygenase; Non-Enz, non-enzymatic production; oxoETE, oxo-eicosatetraenoic acid; oxoODE, oxo-octadecadienoic acid; PG, prostaglandin; triHOME, trihydroxy-octadecenoic acid (9,10,13- triHOME & 9,12,13-triHOME peaks could not be separated); TX, thromboxane.

Study C: Supplemental Table 7. Plasma oxylipins grouped by patient aortic valve stenosis severity (transvalvular mean pressure gradient) and sex.

		Plasma Oxylipins (ng/ml)							
Oxylipin	Enz	Female-Control n=13	Female-Mild n=1	Female-Moderate n=11	Female-Severe n=22	Male-Control n=18	Male-Mild n=4	Male-Moderate n=16	Male-Severe n=19
LA oxylipins									
9-HODE	LOX	5.53±0.418	23.4	17.4±1.92	20.4±2.13	7.59±0.986	15.0±3.77	17.5±2.10	21±2.53
9-oxoODE	LOX	0.712±0.124	5.20	9.6±3.25	6.97±1.05	0.947±0.153	4.47±0.835	6.28±0.955	6.54±0.849
13-HODE	LOX	3.14±0.254	11.4	7.66±0.738	9.28±0.830	3.41±0.368	7.13±1.83	7.58±0.787	9.49±1.00
13-oxoODE	LOX	0.478±0.0984	5.99	8.93±2.91	9.96±2.30	0.481±0.108	4.94±0.669	6.86±0.900	9.07±1.76
(9,10,13- & 9,12,13-) triHOME	LOX	3.67±0.417	0.200	0.227±0.0334	0.295±0.0481	3.99±0.491	0.168±0.0443	0.208±0.0218	0.340±0.0528
LA total		13.5±0.971	46.2	43.8±8.12	46.9±6.05	16.4±1.67	31.7±6.78	38.4±4.11	46.5±5.54
GLA oxylipins									
13-HOTrE-γ	LOX	9.61±1.05	0.0768	0.171±0.0394	0.158±0.0205	8.77±1.02	0.103±0.0338	0.145±0.0241	0.145±0.0180
DGLA oxylipins									
8-HETrE	LOX	0.352±0.0693	0.106	0.165±0.0462	0.142±0.0131	0.307±0.0659	0.123±0.0495	0.129±0.00942	0.127±0.0172
15-HETrE	LOX	0.160±0.0241	0.0604	0.147±0.0195	0.146±0.0122	0.198±0.0337	0.0957±0.0233	0.150±0.0123	0.134±0.0174
DGLA total		0.512±0.0762	0.167	0.312±0.0644	0.288±0.0245	0.504±0.0872	0.219±0.0724	0.279±0.0193	0.261±0.0319

AA oxylipins									
5-HETE	LOX	0.870±0.482	1.16	1.15±0.182	1.28±0.104	0.739±0.224	0.939±0.338	1.19±0.143	1.22±0.141
8-HETE	LOX	19.6±2.05	0.255	0.604±0.164	0.512±0.0491	23.8±2.43	0.413±0.143	0.491±0.0417	0.448±0.0488
11-HETE	LOX	0.193±0.0387	0.0974	0.166±0.0232	0.161±0.0155	0.222±0.0468	0.134±0.0348	0.165±0.0185	0.162±0.0279
12-HETE	LOX	0.234±0.0749	1.14	6.39±1.63	8.32±2.10	0.204±0.0546	4.94±2.74	6.29±1.43	6.35±1.42
tetranor 12-HETE	LOX	0.496±0.0897	0.393	0.43±0.121	0.281±0.0489	0.650±0.0728	0.217±0.110	0.215±0.0408	0.257±0.0397
15-HETE	LOX	0.473±0.115	0.401	0.871±0.200	0.785±0.0792	0.463±0.0878	0.600±0.196	0.780±0.125	1.33±0.428
AA total		21.9±2.55	3.45	9.6±1.64	11.3±2.18	26.1±2.63	7.24±3.34	9.13±1.58	9.77±1.63
ALA oxylipins									
9-HOTrE	LOX	0.364±0.0460	5.38	3.16±0.348	3.75±0.485	0.393±0.0512	2.18±0.581	2.88±0.403	3.65±0.400
9-oxoOTrE	LOX	1.63±0.217	0.970	1.26±0.357	1.25±0.259	1.76±0.388	0.523±0.0731	0.996±0.149	1.06±0.141
13-HOTrE	LOX	0.250±0.0473	2.23	1.39±0.138	1.67±0.215	0.273±0.0574	0.956±0.293	1.38±0.184	1.77±0.187
ALA total		2.24±0.282	8.58	5.8±0.725	6.66±0.905	2.43±0.464	3.66±0.901	5.26±0.653	6.48±0.659
EPA oxylipins									
5-HEPE	LOX	0.564±0.0935	0.518	0.610±0.223	0.540±0.0790	0.677±0.107	0.23±0.0658	0.337±0.0599	0.431±0.0631
12-HEPE	LOX	0.650±0.124	0.936	2.1±0.551	3.59±1.01	0.694±0.0895	0.910±0.511	1.68±0.358	2.81±0.827
15-HEPE	LOX	0.150±0.0283	0.136	0.144±0.0211	0.171±0.0248	0.173±0.0241	0.069±0.0121	0.152±0.0144	0.184±0.0409
EPA total		1.36±0.196	1.59	2.85±0.575	4.30±1.06	1.54±0.164	1.21±0.584	2.17±0.372	3.42±0.912
DPA oxylipins									
17k-DPA	LOX	0.480±0.0936	13.4	12.4±2.26	14.6±1.78	0.338±0.0778	5.12±1.38	13.8±1.95	9.93±1.64

DHA oxylipins									
4-HDoHE	LOX	0.210±0.0276	0.911	0.735±0.134	0.931±0.153	0.258±0.0386	0.490±0.129	0.794±0.0601	0.990±0.170
7-HDoHE	LOX	0.302±0.0767	0.409	0.364±0.082	0.400±0.0531	0.228±0.0569	0.227±0.0438	0.386±0.0440	0.350±0.0497
8-HDoHE	LOX	0.602±0.262	0.628	0.465±0.0793	0.572±0.0869	0.284±0.0150	0.303±0.104	0.49±0.0453	0.561±0.0699
10-HDoHE	LOX	0.894±0.166	0.273	0.259±0.0483	0.324±0.0515	1.02±0.229	0.138±0.0598	0.276±0.0416	0.307±0.0643
11-HDoHE	LOX	3.81±1.08	0.416	0.369±0.0726	0.482±0.0879	5.02±0.744	0.184±0.0762	0.341±0.0452	0.423±0.0785
14-HDoHE	LOX	1.64±0.339	1.99	3.98±1.04	5.23±1.22	1.44±0.254	1.90±1.06	4.04±0.958	5.45±1.40
16-HDoHE	LOX	0.426±0.0687	0.0995	0.204±0.0518	0.263±0.0609	0.457±0.103	0.0994±0.0549	0.209±0.0481	0.275±0.0666
17-HDoHE	LOX	1.58±0.149	0.741	0.556±0.0824	0.725±0.0974	1.81±0.206	0.286±0.0871	0.662±0.0784	0.703±0.117
DHA total		9.46±1.33	5.47	6.93±1.23	8.93±1.58	10.5±0.905	3.63±1.58	7.20±1.18	9.06±1.93
Total oxylipins		59.1±5.59	78.9	81.9±9.99	93.1±9.54	66.6±5.87	52.9±13.6	76.3±6.37	85.5±10.6

Values are mean ± standard error. AA, arachidonic acid; ALA, α-linolenic acid; DGLA, dihomo-γ-linolenic acid; DHA, docosahexaenoic acid; DPA, docosapentaenoic acid; ENZ, Enzyme; GLA, γ-linolenic acid; HDoHE, hydroxy-docosahexaenoic acid; HEPE, hydroxy-eicosapentaenoic acid; HETE, hydroxy-eicosatetraenoic acid; HETrE, hydroxy-eicosatrienoic acid; HODE, hydroxy-octadecadienoic acid; HOTrE, hydroxy-octadecatrienoic acid; LA, linoleic acid; LOX, lipoxygenase; oxoODE, oxo-octadecadienoic acid; oxoOTrE, oxo-octadecatrienoic acid; triHOME, trihydroxy-octadecenoic acid (9,10,13- triHOME & 9,12,13-triHOME peaks could not be separated).

7. Study C: Supplemental Figures

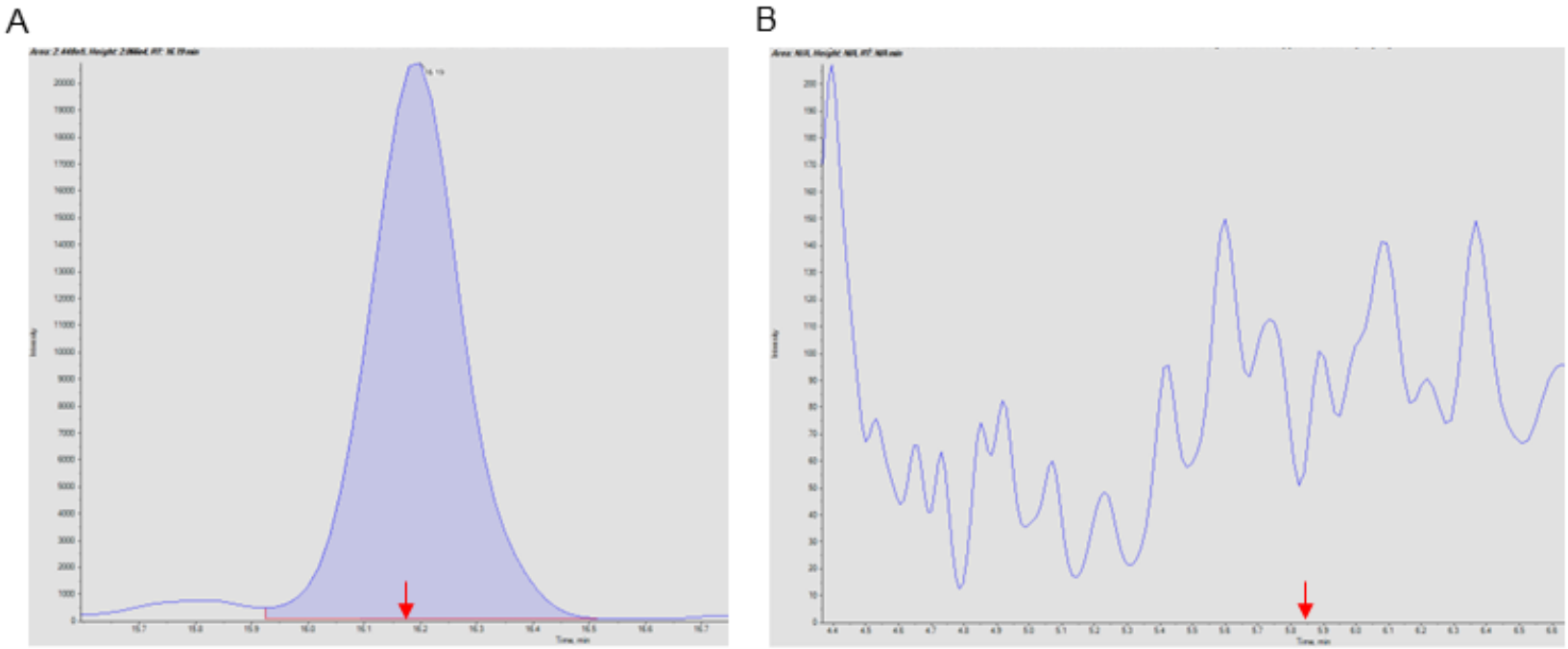

Study C: Supplemental Figure 1. Example chromatograms of oxylipin peak selection.

A) Chromatogram of 15-hydroxy-eicosatetraenoic acid. Peak selected at **e**xpected retention time of 16.17 min exceeds 5-times baseline. **B)** Chromatogram of resolvin E1. Peak not selected at expected retention time of 5.84 min, does not exceed baseline.